Performance Analysis of Wireless Relay Systems

A Thesis Submitted
to the College of Graduate Studies and Research
in Partial Fulfillment of the Requirements
for the Degree of Doctor of Philosophy
in the Department of Electrical and Computer Engineering
University of Saskatchewan

by

Nam H. Vien

Saskatoon, Saskatchewan, Canada

Permission to Use

In presenting this thesis in partial fulfillment of the requirements for a Postgraduate degree from the University of Saskatchewan, it is agreed that the Libraries of this University may make it freely available for inspection. Permission for copying of this thesis in any manner, in whole or in part, for scholarly purposes may be granted by the professors who supervised this thesis work or, in their absence, by the Head of the Department of Electrical and Computer Engineering or the Dean of the College of Graduate Studies and Research at the University of Saskatchewan. Any copying, publication, or use of this thesis, or parts thereof, for financial gain without the written permission of the author is strictly prohibited. Proper recognition shall be given to the author and to the University of Saskatchewan in any scholarly use which may be made of any material in this thesis.

Request for permission to copy or to make any other use of material in this thesis in whole or in part should be addressed to:

Head of the Department of Electrical and Computer Engineering
57 Campus Drive
University of Saskatchewan
Saskatoon, Saskatchewan, Canada
S7N 5A9

Acknowledgments

This dissertation would not be possible without the help and support of many people during my graduate studies in Saskatoon. A few words mentioned here cannot adequately express my appreciation.

First and foremost, I would like to express my deepest gratitude toward my supervisor, Professor Ha Nguyen, for his criticism, patience, invaluable support and guidance throughout my research program at the University of Saskatchewan. Professor Ha Nguyen was always there to support, to guide and to help with his influential leadership, great source of knowledge and research enthusiasm. It has truly been my honor and rewarding experience to work under the supervision of Professor Ha Nguyen.

I would also like to thank my co-supervisor, Professor Le-Ngoc from McGill University for his involvement in my research work. He has always been available to support me.

I would like to extend my gratitude to Professors Eric Salt, Aryan Saadat Mehr, Fang Wu from the University of Saskatchewan, and Professor Julian Cheng from the University of British Columbia for serving in my doctoral committee. Their insightful advice and comments have improved the quality of this dissertation. Special thanks also go to Professor Eric Salt for the many technical and non-technical discussions during my studies in Saskatoon. Undoubtedly, I have benefited tremendously from not only his broad and deep knowledge of research and life but also his charming style, demonstrated integrity and enthusiasm.

It has been my great pleasure to work with all of my lab-mates: Son Hoang, Son Nguyen, Tung, Ha, Zohreh, Simin, Duy, and Quang in our Communications Theories Research Group (CTRG). With them, my time in the Ph.D. program is more enjoyable and interesting.

As always, my deepest love and gratitude go to all of my family members, espe-

cially Mom and Dad, for their unconditional love, care and support in every endeavor of my life. I would also thank my beloved wife and daughter for their love, support and encouragement. Furthermore, I wish to thank my Mom-in-law for her stay with us and great care of our little angel. Without her help, this dissertation would not have been existed.

Finally, I gratefully acknowledge Natural Sciences and Engineering Research Council (NSERC) and the Department of Electrical and Computer Engineering at the University of Saskatchewan for their financial supports of my studies.

Abstract

There has been phenomenal interest in applying space-time coding techniques in wireless communications in the last two decades. In general, the benefit of applying space-time codes in multiple-input, multiple-output (MIMO) wireless channels is an increase in transmission reliability or system throughput (capacity). However, such a benefit cannot be obtained in some wireless systems where size or other constraints preclude the use of multiple antennas. As such, wireless relay communications has recently been proposed as a means to provide spatial diversity in the face of this limitation. In this approach, some users or relay nodes assist the transmission of other users' information. This dissertation contributes to the advancement of wireless relay communications by investigating the performance of various relaying signal processing methods under different practical fading environments. In particular, it examines two main relaying methods, namely decode-and-forward (DF) and amplify-and-forward (AF).

For DF, the focus is on the diversity analysis of relaying systems under various practical protocols when detection error at relays is taken into account. In order to effectively mitigate the phenomenon of error propagation, the smart relaying technique proposed by Wang et al. in [R1] is adopted. First, diversity analysis of a single-relay system under the scenario that only the relay is allowed to transmit in the second time slot (called Protocol II) is carried out. For Nakagami and Hoyt generalized fading channels, analytical and numerical results are provided to demonstrate that the system always obtains the maximal diversity when binary phase shift keying (BPSK) modulation is used. Second, a novel and low-complexity relaying system is proposed when smart relaying and equal gain combing (EGC) techniques are combined. In the proposed system, the destination requires only the phases of the channel state information in order to detect the transmitted signals. For the single-relay system with M-ary PSK modulation, it is shown that the system can achieve the maximal diversity under Nakagami and Hoyt fading channels. For the K-relay system, simulation results suggest that the maximal diversity can also be achieved. Finally, the

diversity analysis for a smart relaying system under the scenario when both the source and relay are permitted to transmit in the second time slot (referred to as Protocol I) is presented. It is shown that Protocol I can achieve the same diversity order as Protocol II for the case of 1 relay. In addition, the diversity is very robust to the quality of the feedback channel as well as the accuracy of the quantization of the power scaling implemented at the relay.

For AF, the dissertation considers a fixed-gain multiple-relay system with maximal ratio combining (MRC) detection at the destination under Nakagami fading channels. Different from the smart relaying for DF, all the channel state information is assumed to be available at the destination in order to perform MRC for any number of antennas. Upperbound and lowerbound on the system performance are then derived. Based on the bounds, it is shown that the system can achieve the maximal diversity. Furthermore, the tightness of the upperbound is demonstrated via simulation results. With only the statistics of all the channels available at the destination, a novel power allocation (PA) is then proposed. The proposed PA shows significant performance gain over the conventional equal PA.

Table of Contents

List of Tables

List of Figures

List of Abbreviations

AF	Amplify-and-Forward
AWGN	Additive White Gaussian Noise
BEP	Bit Error Probability
BPSK	Binary Phase Shift Keying
CDMA	Code-Division Multiple Access
CSI	Channel State Information
dB	Decibel
DF	Decode-and-Forward
DSTC	Distributed Space Time Coding
EGC	Equal Gain Combing
EPA	Equal Power Allocation
i.i.d.	Independent and Identically Distributed
ISI	Inter-Symbol Interference
LOS	Line-of-Sight
MGF	Moment Generating Function
MIMO	Multiple-Input Multiple-Output
MISO	Multiple-Input Single-Output
ML	Maximum-Likelihood
MRC	Maximal Ratio Combining

OFDM	Orthogonal-Frequency Division Multiplexing
OPA	Optimal Power Allocation
PA	Power Allocation
pdf	Probability Density Function
PEP	Pairwise Error Probability
QAM	Quadrature Amplitude Modulation
QoS	Quality of Service
RV	Random Variable
SC	Selection Combining
SEP	Symbol Error Probability
SISO	Single-Input Single-Output
SNR	Signal-to-Noise Ratio
STC	Space Time Coding

1. Introduction and Organization of The Dissertation

1.1 Introduction

Over the last decades, the high demand for wireless applications has influenced significant development of wireless communications technologies. Some obvious examples include the latest generations of cellular voice, data networks and more recently ad-hoc networks for wireless computers, home and personal networking, etc.. These networks provide a freedom for users to roam and communicate from anywhere at anytime. The next generation broadband wireless communications systems are expected to offer wireless multimedia services such as high speed Internet access, multimedia message services (MMS) with higher Quality of Service (QoS) requirements, and mobile computing. However, the design of the robust wireless systems that provide the performance necessary to support the emerging applications still faces tough technical challenges, especially the fundamental performance limits of the systems and practical methods to approach the limits. This has increased the effort, both in research and industry, in the study and implementation of wireless communications to meet these expectations.

A fundamental aspect of wireless communications is the poor reliability of the wireless channels. The problem is attributed to the phenomenon of *fading*, which is caused by the reception of different versions of the source signal which propagate through different paths. The paths result from scattering, reflection and diffraction of the transmitted energy by objects, such as buildings, trees, etc., in the environ-

ment [R2–R6][1]. The signals coming from different paths cause interference and attenuation to each other. These effects may cause a significant power reduction of the received signals which severely degrades the performance of the wireless transmission. Advanced transmission/reception techniques are therefore needed to lessen the impairments of the wireless channels. One of the most effective techniques is to exploit *diversity*, i.e., to supply the receiver with multiple versions of the the source signals that are independently affected by the fading environment [R2, R5, R6]. Depending on the domain used to provide the replicas of the source signal, diversity techniques are generally classified into time, spatial and frequency diversity [R2].

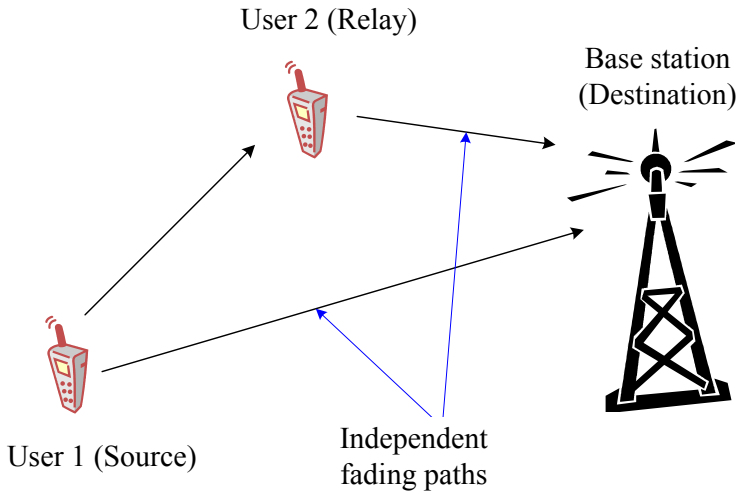

Figure 1.1 Wireless relay communications.

The most popular form of diversity is spatial diversity, which is achieved by employing multiple transmit and/or receive antennas since it does not suffer from bandwidth penalty. The multiple copies of the transmitted signals are properly processed at the destination to improve the overall performance of the wireless systems [R2, R4, R6]. Unfortunately, spatial diversity is not practical in many wireless communications systems due to size, complexity and other constrains which prevent the use of multiple transmit antennas in a single device. An important example on

[1]Since this dissertation is in the manuscript style, there are two sets of references. One set, identified with letter R, is for the main writing. The other set, identified with letter P, is for each included manuscript.

wireless applications is the cellular network. In this network, it is clearly not feasible to implement multiple antennas on the user mobile unit in order to exploit the transmit diversity for the uplink transmission. Recently, performing relay communications is emerging as an attractive diversity solution due to its potential of providing spatial diversity without the need of having collocated antenna array [R7, R8]. The key idea in relay communications can be explained in Fig. 1.1, which shows a simple wireless system with 3 nodes, i.e., user 1 (the source), user 2 (the relay) and a base station (the destination). User 1 tries to transmit to the base station with the help of User 2. User 1 has only one transmit antenna and therefore cannot create spatial diversity by itself. However, due to the broadcasting nature of the wireless transmission, User 2 can receive the transmitted signal from User 1 and then tries to assist the transmission of User 1 by sending a version of the received signal to the base station. Because the two versions of the source signal experience independent fading paths, spatial diversity might be obtained in such a system.

In relay communications, time, frequency and power resources are shared by the source and the relay to transmit the source information to the destination. In general, signal transmission in a single-relay system proposed in the literature is carried out in two time slots. In the first time slot, the source broadcasts its information to both the relay and the destination. During the second time slot, the relay forwards the information to the destination. The source can either keep silent or continue to transmit in the second time slot [R9]. The destination combines the received signals in certain ways in order to effectively decode the information. Typically, time shared by the source and the relay might reduce the transmission rate of the source [R10, R11]. On the other hand, the source gains spatial diversity benefitted from cooperating with the relay [R12, R13]. Furthermore, the performance depends on a number of factors that should be taken into account in the design of a wireless relay network. These factors include the type of signal processing methods employed at the relay, e.g., decode-and-forward and amplify-and-forward, power allocation, channel coding, etc. [R14–R19].

Motivated by the above discussions, this dissertation focuses on various techniques that can improve the performance of wireless relaying systems. In particular, the dissertation is concerned with the performance analysis of the systems and how to utilize the systems' resources, e.g., time, frequency, power, etc., effectively in order to improve the error performance. The motivations and contributions of the research will be given in more detail in each individual chapter.

1.2 Organization of the Dissertation

This dissertation is organized in a manuscript-style. As such, the main content and contributions include published, accepted or submitted manuscripts. There is one chapter, namely Chapter 2, which presents some relevant background and knowledge such as wireless communications, diversity combining techniques and relay communications that are useful for the understanding of the techniques described in the included manuscripts. In what follows, a brief introduction to each manuscript is given. Note that in each chapter the included manuscript is prefaced by a brief connecting text indicating its relationship to this dissertation as a whole.

The first manuscript included in Chapter 3 considers a decode-and-forward smart relaying system proposed by Wang et al. in [R1] under Nakagami and Hoyt generalized fading channels. First, the manuscript reviews the relaying system model when combined with the smart relaying technique. It then provides diversity analysis of the system under two generalized fading channels when the imperfect detection at the relay is taken into account. For the binary phase shift keying (BPSK) modulation, the manuscript shows that the system under these fading channels can always achieve the maximal diversity. Simulation results are also presented to validate the theoretical results.

The second manuscript included in Chapter 4 studies a relaying system that combines the smart relaying technique with equal gain combining (EGC) at the destination in order to reduce the system complexity. Diversity analysis is conducted for the case of M-ary PSK under Nakagami and Hoyt fading channels. Although only

the phases of channel state information (CSI) are required at the destination, the manuscript shows that the maximal diversity can always be achieved in the proposed system with one relay. Simulation results are then provided and they are consistent with analytical results. For the most general case when there are K relays, simulation results also suggest that the maximal diversity can be obtained.

The manuscripts in Chapters 3 and 4 are restricted to Protocol II [R9] wherein only the relay-to-destination transmission is allowed during the second time slot in single-relay systems. Relaxing the above assumption, the manuscript in Chapter 5 investigates a smart relaying system under Protocol I wherein both the relay and source are permitted to send their signals in the second time slot. When the statistical information of the relay-to-destination is available at the relay, the manuscript shows that the system can achieve the diversity order of 2 for BPSK and quadrature PSK (QPSK) under Rayleigh fading channels. For the more general case when higher-order rectangular quadrature amplitude modulation (QAM) constellation is used, an upperbound is provided to assist the diversity analysis. Simulation results are finally presented and discussed. The results also indicate that with smart relaying in decode-and-forward, Protocol I offers performance improvement over Protocol II.

The last manuscript in Chapter 6 is concerned with a fixed-gain amplify-and-forward multiple-relay system under Nakagami fading channels. Performance upperbound and lowerbound on error performance are provided to demonstrate the achievable diversity of the system. Based on the upperbound, the manuscript presents a novel power allocation. The proposed power allocation illustrates significant gains over equal power allocation as predicted by the upperbound.

Chapter 7 concludes this dissertation by summarizing the contributions and suggesting potential directions for future work.

2. Background and System Model

This chapter reviews some important background on wireless fading channels, diversity techniques, fundamental concepts of relay communications and a general framework of a single-relay system integrated with several key signal processing methods. The purpose of this chapter is to familiarize the readers with the field of the study and lay out the foundation for the rest of this dissertation.

2.1 Wireless Channels

Wireless channel modeling is the first concept that needs to be addressed before presenting performance analysis and design of a relay communication system. Different wireless system design decisions depend on various properties of the fading channels that have a direct impact on the quality of wireless transmissions.

One of the main properties of wireless channels is the fact that there are many different propagation paths between the transmitter and receiver. The existence of many paths leads to different copies of the same transmitted signal at the receiver. Each path experiences different attenuation and time delay. As a result, the accumulation of all the received signals introduces a multiplicative noise for the wireless channels. As depicted in Fig. 2.1, there are different types of paths in a typical wireless channel.

If there are no obstacles between the transmitter and receiver, the signal travels along a straight line between the two. The corresponding received signal is called the line-of-sight (LOS) signal or ray and usually the strongest and dominant one. The LOS signal is preferable as it can be easily predicted and its varying strength is just

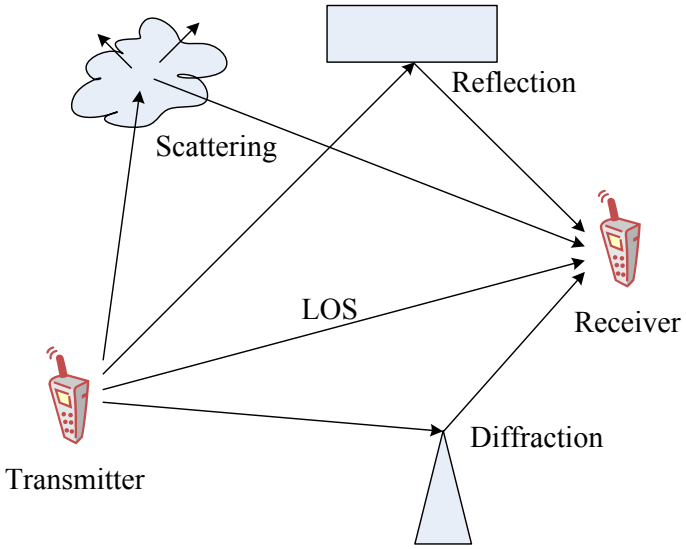

Figure 2.1 An example of different paths in a wireless channel.

a function of the distance and not many other factors. In general, the strength of the wave decreases as the distance between the transmitter and receiver increases.

Besides LOS, an electromagnetic wave can propagate over other paths from a transmitter to a receiver. The first way is through reflection. It occurs when an electromagnetic wave hits objects, e.g., walls, buildings, etc., that are much larger than the wavelength, and may reflect into various directions. The other way of wireless propagation is through diffraction. The phenomenon happens when the wave reaches irregular surfaces like sharp edges. The last type is known as scattering where there is a large number of objects much smaller than the wavelength in the transmission path from the transmitter and receiver. Going through the objects, a propagation wave is then reflected off in multiple different directions.

The above mechanisms behind the electromagnetic wave propagation and their combinations affect many characteristics of the received signal in wireless channels. For example, the power of the received signal can be affected in different ways. In general, there are two aspects of signal power variation that require separate treatments. One aspect is called attenuation, path loss or sometime large-scale fading, which corresponds to the characterization of signal strength over large transmitter-receiver

separation distances (several hundreds or thousands of meters) or the time-average behavior of the signal. The other aspect characterizes the rapid fluctuation of the received signal strength over very short transmission distances (a few wavelengths) or short time periods (on the order of seconds). It is called small-scale fading or just fading.

As small-scale fading is one of the most challenging issues in designing reliable and efficient wireless networks, it is of interest to focus on the small-scale fading within the scope of this dissertation. In what follows, we discuss models that explain the behavior of small-scale fading.

Small-scale fading, or equivalent fading, happens due to the interference between two or more versions of the transmitted signal which arrive at the receiver at slightly different times. The signals, called multipath waves, combine together at the receiver to create a combined signal whose amplitude and phase can vary largely, depending on the distribution of the intensity and relative propagation time of the waves and the bandwidth of the transmitted signal. The rapid fluctuation of the amplitude of a combined signal over a short period of time, corresponding to a short transmission distance, is such that the large-scale fading effects might be ignored. Due to the randomness of multipath effects and fading, it is necessary to use different statistical arguments to model the wireless channel. Next, we define the (discrete-time) baseband model for the (single antenna) wireless link and discuss the most important statistical models for fading proposed in the literature.

2.1.1 Input-output Model of Wireless Channels

In typical wireless applications, the continuous-time signals are transmitted at carrier frequencies, normally at the order of GHz. However, most of the processing, such as coding/decoding, modulation/demodulation, etc, is actually carried out at the baseband, i.e., frequency range around 0 Hz. At the transmitter side, the signal is up-converted to the carrier frequency before being sent via the antenna in the final stage of operation. Similarly, at the receiver side, the radio-frequency (RF) signal is

first down-converted to the baseband before any further processing. Therefore from the communication system design point of view, it is often conceptually convenient to model the radio signal as discrete-time signal centered at 0Hz, i.e., baseband signal [R2, R20]. The convenience of the baseband-equivalent models is due to the fact that they suppress the issues related to frequency up- and down-conversion.

First, one needs to consider a generic continuous-time single-input single-output (SISO) transmission over a fading channel before understanding its equivalent discrete-time baseband input-output model. Given the input signal $s(t)$, which is assumed to be bandlimited to W Hz, the continuous-time input-output model of a wireless channel can be mathematically represented as [R2]

$$y(t) = \sum_i a_i(t)s(t - \tau_i(t)) + z(t), \tag{2.1}$$

where $a_i(t)$ and $\tau_i(t)$ are the overall attenuation and propagation delay at time t on path i. The noise $z(t)$ is assumed to be zero-mean additive white Gaussian with power spectral density $N_0/2$ (watts/Hz). The signal $s(t)$ represents the transmitted signal, whose energy is E_s over the duration of T seconds. The assumption is valid when interference by other users in wireless networks is considered insignificant and therefore ignored in the system design. In practice, the attenuations and propagation delays vary slowly over frequency. However, as data transmission is primarily carried out over bands that are narrow relative to the carrier frequency, it is reasonable to assume that $a_i(t)$ and $\tau_i(t)$ do not depend on frequency f. Therefore, the impulse response $h(t, \tau)$ of the linear model in (2.1) at time t to an impulse transmitted at time $(t - \tau)$ can be described as follows:

$$h(t, \tau) = \sum_i a_i(t)\delta(\tau - \tau_i(t)), \tag{2.2}$$

where $\delta(\cdot)$ is the Dirac delta function.

By applying sampling theorem, an useful discrete-time baseband input-output model of (2.1) can be given as [R13, R20]:

$$y[n] = \sum_l a_l[n]s[n - l] + z[n], \tag{2.3}$$

where $z[n]$ represents additive white Gaussian noise (AWGN) and is modeled as a circularly symmetric complex Gaussian random variable (RV), $\mathcal{CN}(0, N_0)$, i.e., the real and imaginary parts of $z[n]$ are zero-mean independent and identically distributed (i.i.d.) Gaussian RVs with variances $N_0/2$ (volt^2).[1] The lth complex channel filter tap at time n is denoted by $a_l[n]$. The value of the filter tap is a function of mainly the gains $a_i(t)$ of the propagation paths whose delays $\tau_i(t)$ are close to l/W.

An important characteristic of a multipath channel is the time delay spread that it causes to the received signal. This delay spread equals the time duration between the arrival of the first received signal component and the last signal component. More precisely, the delay spread is calculated as $T_d = \max_{i,j} |\tau_i(t) - \tau_j(t)|$. Due to the delay spread, a transmitted signal of duration T, or equivalently, multiplicative inverse of the signal bandwidth W, will result in a received signal of duration $(T + T_d)$. Therefore, the duration of the received signal might be significantly increased. The distortion of the received signal as shown in Fig. 2.2 might interfere with subsequently transmitted signals. This effect is called intersymbol interference (ISI).

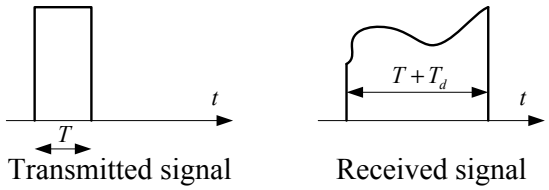

Figure 2.2 ISI phenomenon.

If the delay spread is considerably less than the signal duration, i.e., $T_d \ll T$, there is little time spreading in the received signal. Therefore, the interference is negligible. In this situation, all the multipath components are received roughly during one signal duration. As a result, a single filter tap is sufficient to represent the channel model in (2.3) as

$$y[n] = a[n]s[n] + z[n]. \tag{2.4}$$

[1]Note that the power spectral density of $z(t)$ in (2.1) is also $N_0/2$ but in the unit of watts/Hz.

This model is suitable to describe narrowband transmission and the wireless fading channel is called as *frequency non-selective* or *flat fading* channel. Also, it is necessary to define the bandwidth of the channel in order to compare it with the signal bandwidth W. Generally, the channel *coherent bandwidth*, over which the channel possesses a constant gain, is approximated by a reciprocal of the delay spread T_d, i.e., $W_c = 1/T_d$. Equivalent to what mentioned above, in a flat fading channel, the channel coherent bandwidth W_c is much larger than the signal bandwidth W.

On the other hand, when the delay spread is much larger than the signal duration, i.e., $T_d \gg T$, or equivalently, $W_c \ll W$ in the frequency domain, the channel is said to be *frequency selective* and it has to be represented by multiple taps as shown in (2.3). It is worthy noting that flat or frequency selective property of a channel depends on the signal duration as well as the channel characteristics.

Another important characteristic of a fading channel is its time-varying nature. This time variation is because either the transmitter or receiver is moving, and therefore the location of reflectors in the transmission path will change over time. Whether the channel can be categorized as *fast* or *slow* fading depends on both the application and the channel. In other words, the channel is considered to be slow fading if its channel impulse response varies at the rate much slower than the transmitted signal and the channels is assumed to be static over one or several signal durations. In contrast, when the channel impulse response changes quickly within a signal duration, the channel is considered to be fast fading.

2.1.2 Statistical Models for Fading

So far, we have modeled the fading channels by discrete-time baseband input-output relations as in (2.3) or (2.4). As discussed, the main characteristic of the multipath channels is that the amplitude of the channel coefficient is a RV. This randomness is because of the multipath and arbitrary locations of objects in the propagation environment. Therefore, statistical models are necessary to study the behavior of the amplitude and power of the received signal. In what follows, we

discuss some of the most important models in the literature.

The most popular statistical model for the fading channel is Rayleigh. It is based on the assumption that there is a large number of statistically and independently paths with random amplitudes and all the delays are within a single tap duration. Each channel coefficient $a[n]$ is a sum of independent circularly symmetric RVs. Based on this assumption, the probability density function (pdf) for the magnitude, $|a[n]|$, converges toward the Rayleigh distribution. The pdf of the channel fading magnitude is given as follows [R21]:

$$p_{|a[n]|}(x) = \frac{2x}{\Omega} \exp\left(-\frac{x^2}{\Omega}\right), \tag{2.5}$$

where the average fading power is $E\{|a[n]|^2\} = \Omega$. The received signal-to-noise-ratio, $\gamma = (E_s/N_0)|a[n]|^2$, is therefore exponentially distributed with density

$$p_\gamma(\gamma) = \frac{1}{\bar{\gamma}} \exp\left(-\frac{\gamma}{\bar{\gamma}}\right), \tag{2.6}$$

where $\bar{\gamma} = \Omega E_s/N_0$ is the mean value of γ.

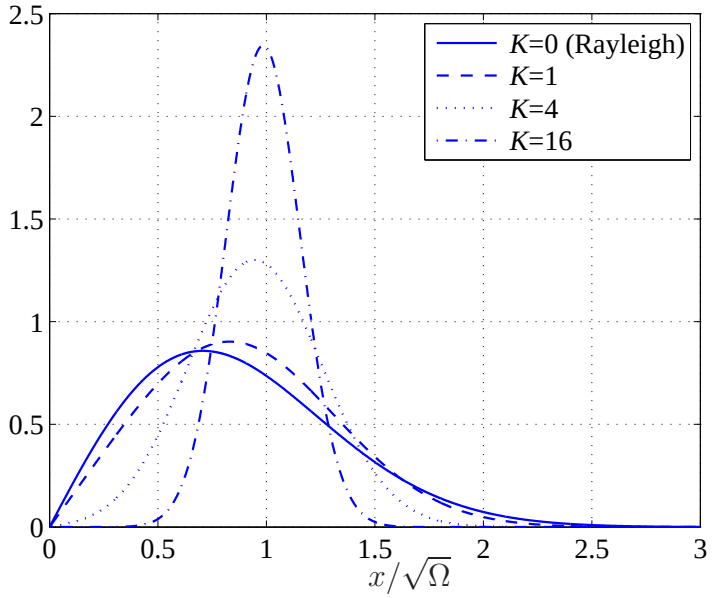

Figure 2.3 Rician distribution.

In the case that propagation paths contain a strong direct LOS component and other random weaker components, Rician fading channel model is applicable (Fig.

2.3). Here the pdf of the channel's magnitude is defined as

$$p_{|a[n]|}(x) = \frac{2(1+K)x}{\Omega} \exp\left[-K - \frac{(1+K)x^2}{\Omega}\right] I_0\left(2x\sqrt{\frac{K(1+K)}{\Omega}}\right), \tag{2.7}$$

where $I_0(\cdot)$ is the zeroth-order modified Bessel function of the first kind and is given as [R22]

$$I_0(z) = \frac{1}{\pi}\int_0^{\pi} \exp(z\cos(\phi))d\phi \approx \begin{cases} \frac{\exp(z)}{\sqrt{2\pi z}}, & z \gg 1, \\ 1 + \frac{z^2}{4}, & z \ll 1. \end{cases} \tag{2.8}$$

The Rician K factor accounts for the ratio of the power in the LOS component to the non LOS (NLOS) components. The case $K = 0$ corresponds to Rayleigh fading whereas $K = \infty$ gives an AWGN channel. The received signal-to-noise ratio (SNR), γ, follows a distribution given as [R21]

$$p_{\gamma}(\gamma) = \frac{(1+K)}{\bar{\gamma}} \exp\left[-K - \frac{(1+K)\gamma}{\bar{\gamma}}\right] I_0\left(2\sqrt{\frac{K(1+K)\gamma}{\bar{\gamma}}}\right). \tag{2.9}$$

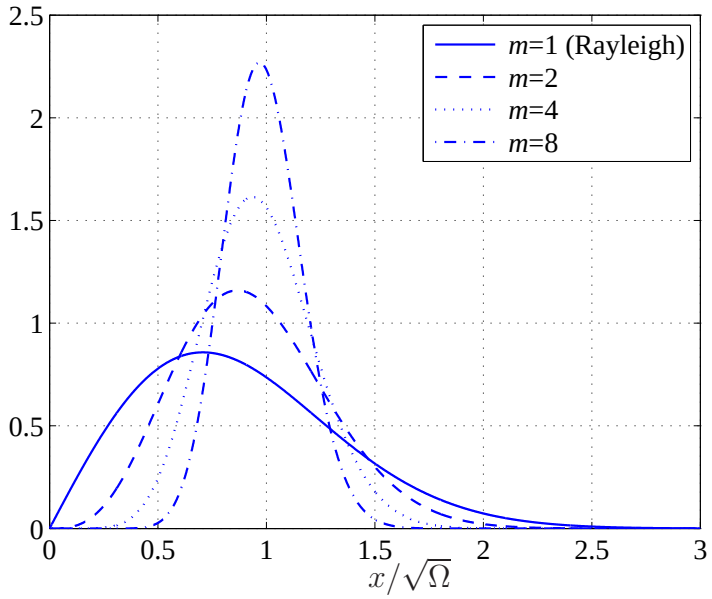

Figure 2.4 Nakagami-m distribution.

The next fading model is Nakagami-m, which is mainly applied in environments where the size of clusters of scatters is comparable to the signal wavelength [R4, R6].

For this fading model, the channel's magnitude follows the following distribution:

$$p_{|a[n]|}(x) = \frac{2m^m x^{2m-1}}{\Omega^m \Gamma(m)} \exp\left(-\frac{mx^2}{\Omega}\right), \tag{2.10}$$

where m is the Nakagami-m fading parameter which ranges from 1/2 to ∞. The gamma function, $\Gamma(\cdot)$, is given as [R22]

$$\Gamma(m) = \int_0^\infty t^{m-1} \exp(-t) dt \tag{2.11}$$

$$= (m-1)! \qquad \text{for } m \text{ integer.} \tag{2.12}$$

The received SNR is distributed according to a gamma distribution, given by [R21]

$$p_\gamma(\gamma) = \frac{m^m \gamma^{m-1}}{\bar{\gamma}^m \Gamma(m)} \exp\left(-\frac{m\gamma}{\bar{\gamma}}\right). \tag{2.13}$$

The Nakagami-m fading model can cover a wide range of many other fading models considered in the literature by adjusting its fading parameter m (Fig. 2.4). For instance, it includes the one-sided Gaussian (the worst-case fading) and the Rayleigh fading models as special cases when $m = 1/2$ and $m = 1$, respectively. Also, the fading channel approaches an AWGN channel when $m \to \infty$.

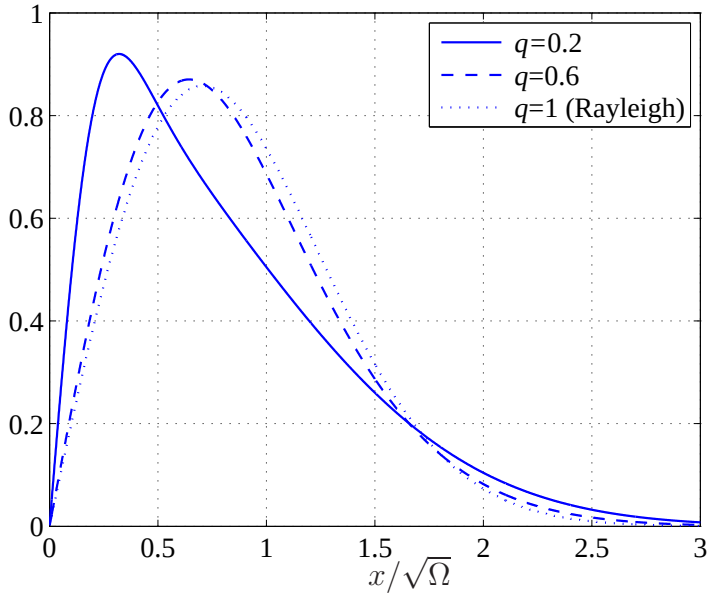

Figure 2.5 Hoyt distribution.

The last commonly used statistical model is Hoyt or Nakagami-q, where q is the Hoyt fading parameter which ranges from 0 (the one-sided Gaussian fading) to 1 (the

Rayleigh fading) (Fig. 2.5). The model is typically used when wireless transmission takes place in the LOS or satellite links subject to strong ionospheric scintillation [R21]. The channel's magnitude is distributed according to

$$p_{|a[n]|}(x) = \frac{(1+q^2)x}{q\Omega} \exp\left[-\frac{(1+q^2)^2x^2}{4q^2\Omega}\right] I_0\left(\frac{(1-q^4)x^2}{4q^2\Omega}\right). \tag{2.14}$$

It can be shown that the received SNR has the following distribution [R21]:

$$p_\gamma(\gamma) = \frac{1+q^2}{2q\bar{\gamma}} \exp\left[-\frac{(1+q^2)^2\gamma}{4q^2\bar{\gamma}}\right] I_0\left(\frac{(1-q^4)\gamma}{4q^2\bar{\gamma}}\right). \tag{2.15}$$

Unlike the wired channels which are typically affected only by AWGN, the performance of a wireless communication system is mainly governed by fading channels. As can be seen in Figs. 2.3, 2.4 and 2.5, there are high probabilities of having small channel gains (which correspond to those values near the origin) and such high probabilities are mainly responsible for the degradation of the system performance. For all of the above fading channels, smaller fading parameters, i.e., small K, m and q, imply more severe fading, whereas larger fading parameters mean relatively mild fading. For the cases of Rician and Nakagami-m fading, the wireless channels approach the AWGN channel when the corresponding fading parameters go to infinity. In this situation, the channel gain density functions shrink toward a delta function at the value of one or equivalently, the channel gain is no longer a random value but a fixed value. Fig. 2.6 shows the error performance of an AWGN channel and a Rayleigh fading channel when BPSK modulation is used. As shown in Fig. 2.6, the AWGN channel is clearly more favorable than the Rayleigh channel.

Due to the poor performance experienced with wireless channels, there have been significant efforts to compensate for the error and distortion introduced by the multipath fading. The main techniques include forward error correction, adaptive equalization and diversity. In practice, all of these techniques can be combined to combat fading. In this dissertation, we focus on the diversity techniques. Some major diversity techniques for wireless communications are introduced in the next section.

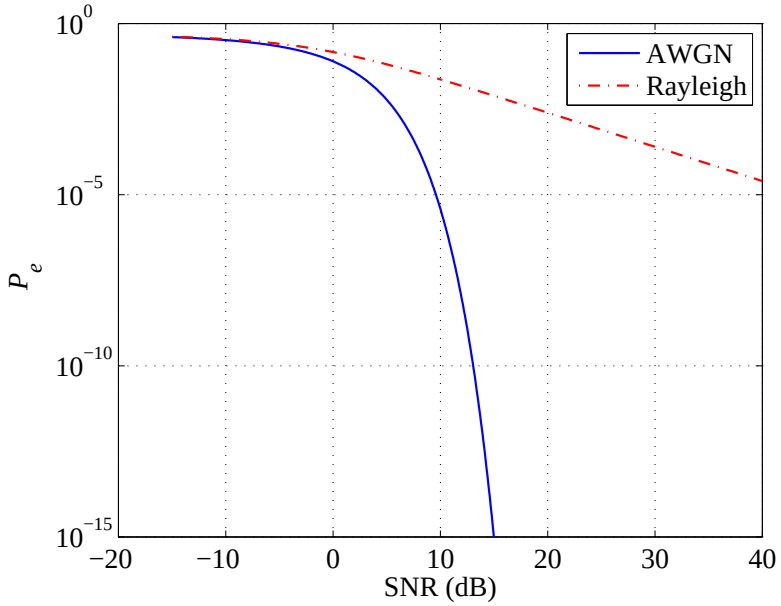

Figure 2.6 Performance comparison for BPSK under AWGN and Rayleigh fading channels.

2.2 Diversity Techniques in Wireless Channels

The received signal of the fading channel model in (2.3) might suffer from sudden declines in the power. Due to the destructive addition of multipath signals in the propagation environment, the channel coefficients sometimes drop dramatically in magnitude. When it happens, the channel is said to be in deep fade in which any communication scheme will likely suffer from errors. A natural solution is to provide replicas of the transmitted signal through multiple signal paths, each of which fades independently. Since each replica experiences a different channel effect, the probability of all copies simultaneously in deep fade is reduced dramatically. If all the copies of the transmitted signal can be combined appropriately at the destination, the severity of fading is greatly overcome and hence the reliability of the transmission is ensured. This technique is called *diversity* and it can significantly improve the performance over fading channels.

To quantify the effectiveness of the diversity technique, the relationship between the average received SNR, $\bar{\gamma}$, and the error probability, denoted by $P_e(\bar{\gamma})$, is intro-

duced. A tractable definition of the diversity order (diversity gain) is [R6]:

$$G_d = -\lim_{\bar{\gamma}\to\infty} \frac{\log(P_e(\bar{\gamma}))}{\log(\bar{\gamma})}, \tag{2.16}$$

where $P_e(\bar{\gamma})$ is the error probability at an average SNR of $\bar{\gamma}$. Basically, the diversity order is equal to the decaying exponent of the error probability curve with respect to the average received SNR, in a logarithm to logarithm scale, as the average received SNR tends to infinity. For example, a diversity order of 2 means that $P_e(\bar{\gamma})$ drops by 2 orders of magnitude (100 times) whenever the SNR increases by 10dB in the high SNR region. In general, the larger the diversity order is, the steeper the slope of the error performance curves becomes, hence, the more reliable the communications system is. If properly designed, a wireless communications system can achieve diversity order up to the number of diversity paths, what can be referred to as the maximal diversity order [R2]. Important diversity techniques that have been studied extensively in the literature are [R2, R6]:

- time diversity, e.g., channel coding and interleaving;
- spatial diversity, e.g., multiple-input multiple-output systems;
- frequency diversity, e.g., orthogonal frequency division multiplexing.

The above diversity techniques as well as their applications in wireless communications are discussed in more detail in the following.

2.2.1 Time Diversity

Time diversity can be achieved by transmitting the same information over different time slots. Time diversity is often used with error control coding and time interleaving. Coded information is dispersed over time in different periods of the coherent time so that different parts of codewords can experience independent fades. Naturally, the simplest form of coding in time diversity is *repetition coding*, in which the signal is repeated exactly the same over a number of time intervals [R2]. To

guarantee that the coded symbols are affected by independent or almost independent channel gains, the codewords should be interleaved (see Fig. 2.7). The repetition coding offers the maximal diversity but suffers from the loss of coding gain (which is defined as the difference between the SNR levels required by the uncoded and coded systems to achieve the same error performance level). This is because the repetition-based system simply repeats the same symbol over different time slots and therefore does not utilize all the degrees of freedom. More efficient coding can be used with time diversity to attain both the maximal diversity and the coding gain [R23].

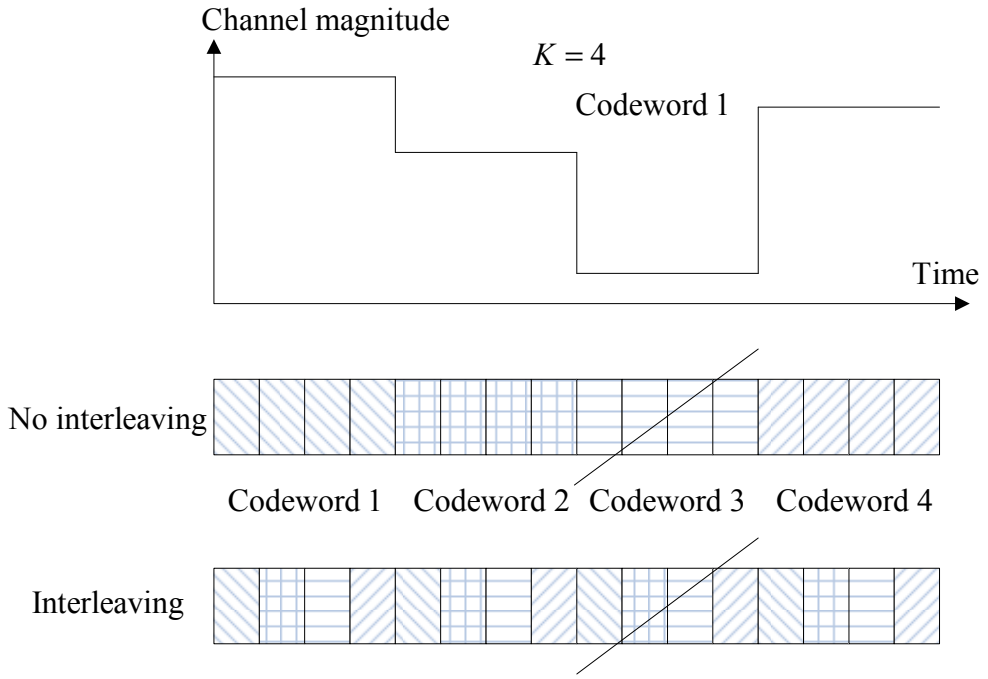

Figure 2.7 The effect of interleaving in time diversity technique [R2]. With interleaving, the whole codewords are less likely in deep fades than without interleaving.

In slow fading environments, the coherent time is large. Therefore, the time diversity technique has a huge delay since the destination has to wait to receive every part of the codewords. Therefore this technique might not be suitable for some delay-sensitive applications, e.g., voice transmissions [R5].

2.2.2 Spatial Diversity

One technique to exploit diversity that may not suffer from the time delay (or equivalently, bandwidth deficiency) which is unavoidable in the system using time diversity technique is antenna diversity or space diversity. The technique is realized by placing multiple antennas at the transmitter and/or the receiver [R2, R24]. The multiple antennas are physically separated by a sufficient distance to make the individual received signals uncorrelated. The separation requirement depends on the frequency, the antenna height as well as the propagation environment. To achieve the uncorrelation property, an antenna separation of a few wavelengths is usually enough.

Depending on whether multiple antennas are used for reception or transmission or both, space diversity can be classified into three categories (see Fig. 2.8): receive diversity (single-input multiple-output, SIMO, channel), transmit diversity (multiple-input single-output, MISO, channel) or transmit and receive diversity (multiple-input multiple-output, MIMO, channel). In the receive diversity, multiple antennas are used at the receiver to gather independent replicas of the transmitted signals without an increase in the transmit signal power or bandwidth. In the transmit diversity, multiple antennas are employed at the transmitter. The source messages are precoded at the transmitter and then spread across multiple antennas. The last type of diversity is the combined version of the transmit diversity and the receive diversity, in which multiple antennas are employed at both the transmitter and receiver sides.

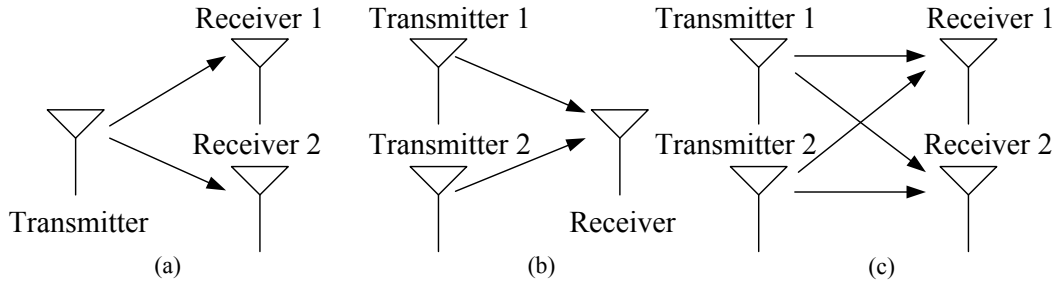

Figure 2.8 (a) SIMO; (b) MISO; (c) MIMO.

Receive Diversity

In receive diversity, the independent paths associated with multiple receive antennas are combined at the receiver. For example, consider a flat fading system with 1 transmit antenna and K receive antennas. Given the transmitted signal $s[n]$ with average symbol energy of E_s, the K received signals are

$$y_k[n] = a_k[n]s[n] + z_k[n], \quad k = 1, \ldots, K, \tag{2.17}$$

where $a_k[n]$ represents the fading channel coefficient from the transmitter to the kth receive antenna at the receiver and $z_k[n]$ models AWGN with one-sided power spectral density of N_0. Let $\mathbf{y}[n] = [y_1[n], \ldots, y_K[n]]^T$, $\mathbf{a}[n] = [a_1[n], \ldots, a_K[n]]^T$ and $\mathbf{z}[n] = [z_1[n], \ldots, z_K[n]]^T$ where $[\cdot]^T$ denotes transpose operation. Then (2.17) can be equivalently written as

$$\mathbf{y}[n] = \mathbf{a}[n]s[n] + \mathbf{z}[n]. \tag{2.18}$$

Performance of communication systems employing the receive diversity technique depends on how the multiple signal copies are combined at the receiver. There are several ways of combining the received signals which vary in complexity and overall performance. According to the levels of channel state information (CSI) available at the receiver, there are three main combining methods, namely maximal-ratio combining (MRC), equal-gain combining (EGC) and selection combining (SC) [R21, R25].

Maximal Ratio Combining

In this method, each individual received signal must be co-phased, weighted with its respective amplitude and then added up. The method is called optimum combining (regardless of the fading statistics) in the sense that it maximizes the received signal-to-noise ratio, γ, of the system under Gaussian noise. The maximal SNR is equal to the sum of all the instantaneous SNRs of the individual signals, i.e.,

$$\gamma = ||\mathbf{a}[n]||\bar{\bar{\gamma}}, \tag{2.19}$$

where $\bar{\bar{\gamma}} = E_s/N_0$ (note that the mean value of γ is $\bar{\gamma} = \Omega E_s/N_0$) and $||\mathbf{a}[n]|| = \sum_{k=1}^{K} |a_k[n]|^2$. However, the performance advantage comes at the expense of high

complexity since all the fading channel parameters need to be available at the receiver [R21].

Equal Gain Combining

As mentioned, MRC requires the knowledge of the time-varying channel coefficients including amplitudes and phases of all branches. A suboptimal method, called equal-gain combining (EGC) with coherent detection, is an attractive alternative since it does not require the channel amplitude estimation. Hence, the implementation complexity relative to the optimal MRC is reduced. In this method, all the received signals are co-phased and simply added together. The received SNR in this method can be calculated as

$$\gamma = \frac{1}{K}\left(\sum_{k=1}^{K}\sqrt{|a_k[n]|^2\bar{\bar{\gamma}}}\right)^2 \tag{2.20}$$

Furthermore, the performance of EGC is only marginally inferior to that of the optimal MRC [R25].

Selection Combining

Selection combining is even a simpler diversity combining method. In this approach, the receiver picks up the signal with the highest SNR (or equivalently, with the strongest incoming path assuming equal noise power in all branches) for detection. The output of the SC combining is computed as

$$\gamma = \left(\max_k |a_k[n]|^2\right)\bar{\bar{\gamma}} \tag{2.21}$$

Moreover, since the output of the SC detector involves only one of the branches, SC can be employed with differentially coherent and noncoherent modulation techniques [R21]. In practice, the signal branch with the highest sum of signal and noise power is often used as it is more difficult to measure the SNR.

Transmit Diversity

Transmit diversity has recently been studied extensively as an effective method to overcome the detrimental effects in wireless communications. Transmit diversity

can reduce the required signal processing effort of the receiver, which leads to a lower systems' complexity, power consumption and cost [R5,R6,R26–R28]. Moreover, when incorporated with receive diversity, transmit diversity further improves the system performance. Different from receive diversity, it is more difficult to exploit spatial diversity with transmit diversity. This is because a careful design of the transmitted signals is required at the transmitter in order to distinguish the received signals at the receiver and exploit diversity since the transmitted signals are spread out to all transmit antennas; and the transmitter does not generally have the instantaneous CSI (unless the information is fed back from the receiver to the transmitter). To deal with these difficulties, a number of the transmit diversity schemes have been proposed in the literature [R29, R30]. An equivalent approach to realize transmit diversity is to view coding, modulation and multiple transmission as one signal processing module [R27]. Such an approach for multiple transmit antennas is called *space-time coding*. In particular, the transmitted signals are spread over both spatial and temporal dimensions, which introduces correlations over the transmitted signals.

In what follows, we discuss one of the particularly simple and yet elegant space-time codes to gain some insight into how a space-time coding system works. It is the very well-known Alamouti scheme, originally designed for 2 transmit antennas [R26]. The generalization to more than 2 antennas can be done under some restrictions [R6,R27]. The Alamouti scheme works over two consecutive symbol time slots under the assumption that channel coefficients are constant during that period, i.e., n and $(n+1)$ time slots. During the nth time slot, two signals $s_1[n]$ and $s_2[n]$ are transmitted simultaneously from antenna one and antenna two, respectively. In the $(n+1)$th time slot, signals $-s_2^*[n]$ and $s_1^*[n]$ are respectively sent from antenna one and antenna two, where $(\cdot)^*$ is complex conjugate operation. Denote the channel coefficients from antenna one and antenna two to the receiver by $a_1[n]$ and $a_2[n]$, respectively. The input-output relation can be then written in matrix form as:

$$\left[\begin{array}{cc} y[n] & y[n+1] \end{array}\right] = \left[\begin{array}{cc} a_1[n] & a_2[n] \end{array}\right] \left[\begin{array}{cc} s_1[n] & -s_2^*[n] \\ s_2[n] & s_1^*[n] \end{array}\right] + \left[\begin{array}{cc} z[n] & z[n+1] \end{array}\right], \quad (2.22)$$

or

$$\underbrace{\begin{bmatrix} y[n] \\ y^*[n+1] \end{bmatrix}}_{\mathbf{y}[n]} = \underbrace{\begin{bmatrix} a_1[n] & a_2[n] \\ a_2^*[n] & -a_1^*[n] \end{bmatrix}}_{\mathbf{A}[n]} \underbrace{\begin{bmatrix} s_1[n] \\ s_2[n] \end{bmatrix}}_{\mathbf{s}[n]} + \underbrace{\begin{bmatrix} z[n] \\ z^*[n+1] \end{bmatrix}}_{\mathbf{z}[n]}, \tag{2.23}$$

where $y[n]$ and $z[n]$ are, respectively, the received signal and AWGN with one-sided power spectral density of N_0 at the receiver in the nth time slot.

It can be noted that the columns of the square matrix $\mathbf{A}[n]$ are orthogonal, i.e., $\mathbf{A}^H[n]\mathbf{A}[n] = ||\mathbf{a}[n]||\mathbf{I}_2$ where $(\cdot)^H$ denotes conjugate transpose (i.e., Hermitian) operation, $\mathbf{a}[n] = [a_1[n] \quad a_2[n]]^T$ and $\mathbf{I}_n$ is a identity matrix of size n. Therefore, one can effectively decouple the two-symbol transmissions into two separate, orthogonal and scalar one-symbol transmissions as follows.

$$r_i[n] = ||\mathbf{a}[n]|| \cdot s_i[n] + \tilde{z}_i[n], \quad i = 1, 2, \tag{2.24}$$

where $\mathbf{r}[n] = [r_1[n] \quad r_2[n]]^T = \mathbf{A}^H\mathbf{y}[n]$ and $\tilde{\mathbf{z}}[n] = [\tilde{z}_1[n] \quad \tilde{z}_2[n]]^T = \mathbf{A}^H\mathbf{z}[n]$. Since $\tilde{\mathbf{z}}[n]$ is a complex Gaussian noise vector with zero mean and covariance matrix $E[\tilde{\mathbf{z}}[n]\tilde{\mathbf{z}}^H[n]] = ||\mathbf{a}[n]||N_0\mathbf{I}_2$, it follows that $\tilde{z}_i[n] \sim \mathcal{CN}(0, N_0)$ and $\tilde{z}_1[n]$, $\tilde{z}_2[n]$ are independent. Thus, the received SNR is given by

$$\gamma_i = ||\mathbf{a}[n]||\bar{\gamma}. \tag{2.25}$$

The above received SNR is identical to that of receive diversity with 2 receive antennas and MRC (see Eq. (2.19)). Therefore, the Alamouti scheme obtains the maximal diversity order of 2 for a two-antenna transmit system.

2.2.3 Frequency Diversity

In the frequency diversity technique, a number of different frequencies are employed to transmit the same signal. The carrier frequencies should be separated by more than the coherent bandwidth of the channel in order to achieve frequency diversity. In this way, different copies of the signal undergo independent fades. In wireless communications, the copies of the transmitted signals are often supplied to

the receiver in the form of frequency redundancy introduced by one of the following three common approaches.

Single-carrier Transmission with Equalization

Single-carrier modulation can alleviate the ISI problems, but the time domain complexity is proportional to the delay spread in a conventional adaptive decision-feedback equalizer (DFE) or linear equalizer. Generally speaking, a DFE can perform better (in the sense of lower mean square error and bit error rate) than a linear equalizer in wireless communications [R31]. This is because the multipath fading can lead to severe nulls in channel frequency response, which would result in a noise enhancement problem for linear equalizers. The optimal maximum-likelihood (ML) detection of the transmitted signals is typically realized with the Viterbi algorithm. However, its complexity is too high unless the impulse response is truncated. In contrast, linear equalizers have a lower complexity since they attempt to demodulate the current signal while linearly canceling the interference from other signals.

Direct-sequence Spread Spectrum

In this approach, the transmitted signals occupy a bandwidth that far exceeds the minimum requirement to send the information. The bandwidth spread is carried out by means of a code which is independent of the data. A synchronized reception is employed at the receiver for despreading and data recovery [R32, R33]. The receiver structure is simplified substantially since the data rate is very low and ISI can be considered negligible. Moreover, this approach can offer the capability of multiple user random access communications which was first commercialized in the IS-95 code-division multiple access (CDMA) system [R32].

Multi-carrier Systems

The basic idea of multi–carrier systems is to divide the available spectrum into various subcarriers [R34,R35]. By making all subcarriers narrowband, the transmitted signals undergo almost flat fading, which makes equalization process very simple. To

attain high spectral efficiency, the subcarriers are overlapping but orthogonal, which leads to the name of orthogonal-frequency division multiplexing (OFDM).

2.3 Relay Communications

Although spatial diversity techniques can provide impressive performance in wireless transmission, the requirement of collocated-antenna array might not be practical in some wireless applications (e.g., those with size and complexity constraints) [R13, R20]. In such cases, relay communications can be an alternative solution. In fact, relay communications has been seriously considered for cellular, wireless ad hoc and sensor networks. This section provides an introduction to some of the most important relay protocols in point-to-point wireless communications. The main relay protocols and signal processing methods are described. At the end, an input-output system model for a system with one relay is introduced.

2.3.1 Relay Protocols

Consider a general relay network in which multiple relays are used to help signal transmission from a source to a destination. In general, the relays can assist the transmission with one of the following 3 main approaches (see Fig. 2.9): repetition-based, selection and distributed space time coding (DSTC). In the first approach, system resources are shared and the relays transmit in orthogonal channels. The repetition-based approach can offer the maximum spatial diversity which is equal to the number of relays. However, the approach is spectrally inefficient since the number of required channels cannot be less than the number of relays. This requirement is particularly infeasible in large-scale relay systems. Recently, the selection approach is introduced to solve this problem in wireless relay systems (see [R36, R37] and references therein). The idea behind selection relaying is to choose the "best" relay in order to help the direct source-destination link. The overall transmission is divided into two time slots. During the first time slot, the source broadcasts a signal/codeword to all the relays and destination. The destination must know all the participating

channel fading gains in order to choose the "best" relay; and then indicates the chosen candidate via a low rate feedback channel. In the second time slot, only the selected relay forwards the received signal/codeword to the destination. As a result, the system spectral efficiency is significantly improved. In the last approach, the idea of space time coding (STC) for collocated MIMO systems is applied into the scenario of multiple-relay networks (known as DSTC), wherein a codeword is spread over time and all the relays. While this approach is able to offer the diversity order up to the number of relays, it requires symbol-level synchronization of collaborating relays and large overhead during the set-up phase [R38–R40].

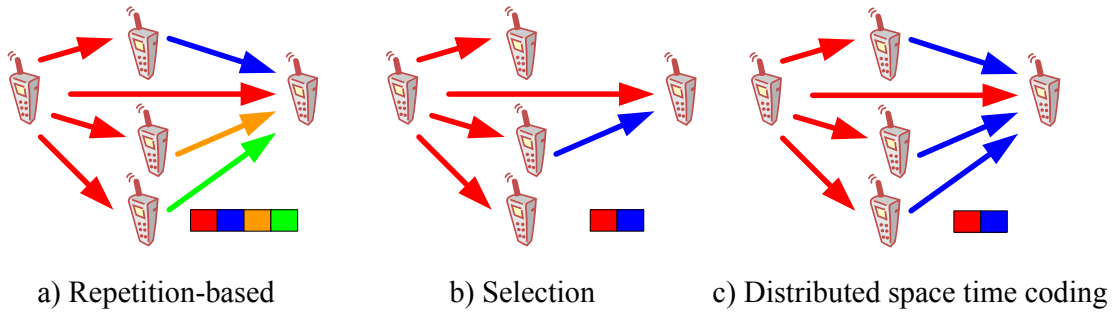

Figure 2.9 Three approaches in multiple-relay networks.

In the specific case of a single–relay system with three nodes, i.e., the source S, the relay R and the destination D, there are three possible protocols, called Protocols I, II and III, that can be used to assist the source–destination communication [R7].

Protocol I: The source broadcasts to both the relay and destination during the first time slot. In the second time slot, both the source and relay communicate with the destination.

Protocol II: The source broadcasts to the relay and destination in the first time slot. The relay communicates with the destination while the source keeps silent during the second time slot.

Protocol III: The source communicates only with the relay in the first time slot. Both the source and relay transmit their messages to the destination in the second time slot.

2.3.2 Relay Signal Processing

There are two major processing methods at the relay which are widely considered in the literature. One is amplify–and–forward (AF) and the other is decode–and–forward (DF) [R12, R13].

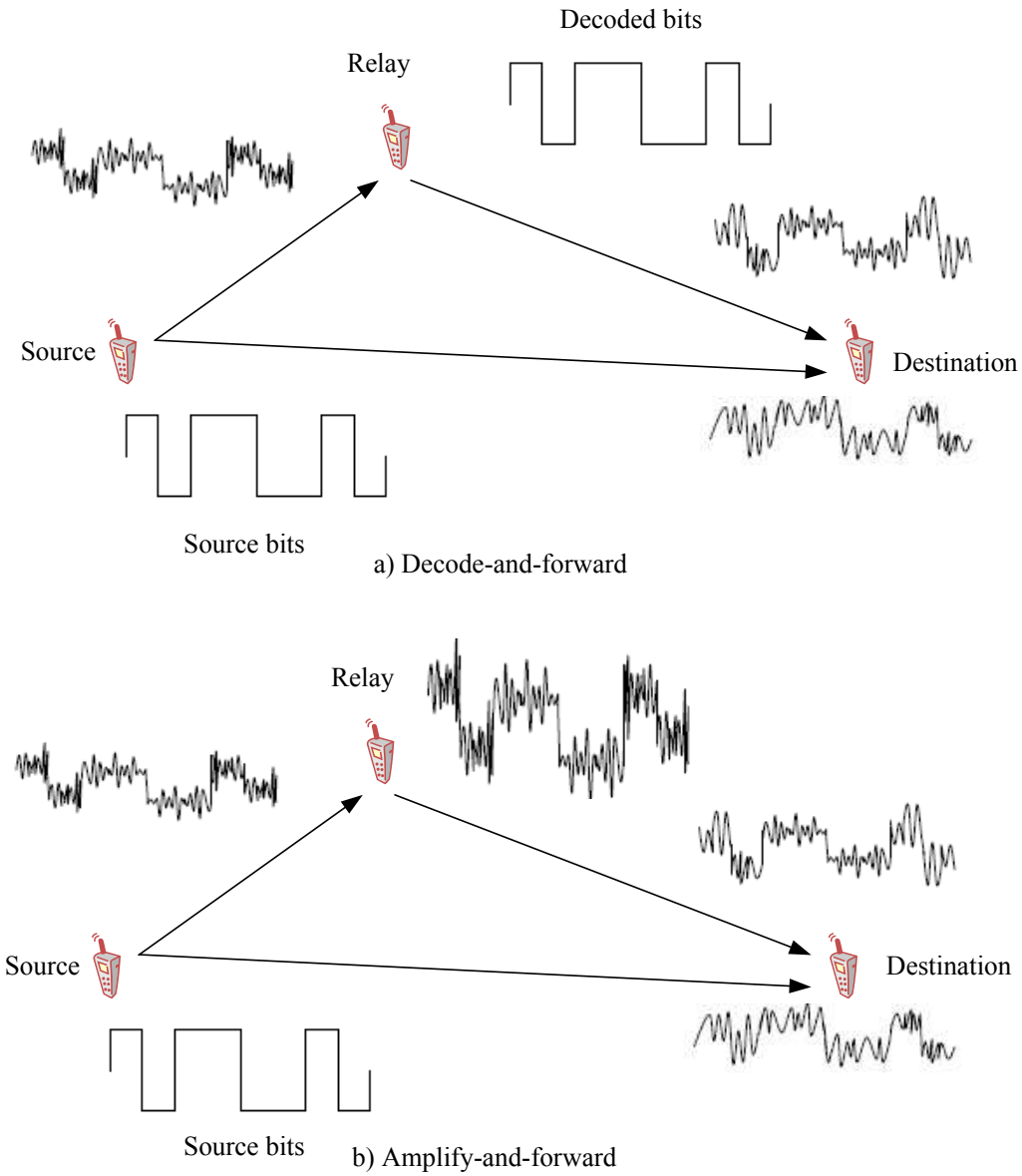

Figure 2.10 Amplify–and–forward and decode–and–forward signal processing methods.

As illustrated in Fig. 2.10a, in DF, the relay decodes the source symbol before re-transmitting to the destination. In order to obtain the maximal diversity order

for the single-relay system, the relay should be able to know whether or not it has decoded correctly and then adaptively transmit the decoded signal based on the obtained knowledge. Such an ability can be realized through some sophisticated mechanisms done at the relay, e.g., the use of error detecting codes [R17] or smart relaying technique [R1,R7,R17] or appropriate SNR thresholds at the relay [R41,R42]. If the relay always blindly forwards the decoded signals, the system performance will be limited by errors at the relay since they propagate to the destination. How to avoid error propagation by using adaptive techniques at the relay(s) in DF is one of the main objectives of this dissertation.

For AF, as depicted in Fig. 2.10b, the relay receives the transmitted signal from the source and sends a scaled version of it to the destination. There are two ways to limit the transmit power at the relay(s), namely with a varying or fixed gain [R15,R43]. In order to maintain the constant transmit power at the relays at all times, the varying-gain relaying scheme requires the knowledge of the instantaneous source-relay channel coefficients at the corresponding relays. As an alternative, the fixed-gain relaying scheme has been proposed in order to reduce the system complexity while still maintaining the long-term average transmit power at each relay [R15, R44]. The AF method does not suffer from the error propagation problem as the DF method because there is no hard-decision operation on the received signal at the relay. However, noise accumulates with the desired signal along the transmission path. In order to effectively combine the received signals at the destination in coherent reception, e.g., employing MRC at the destination, it requires that all the participating channel coefficients must be available at the destination. This requirement results in an increase in the system complexity of the AF method [R9]. Performance of an AF system depends on many factors such as fading environments or power allocated to the source and relays or availability of the channel state information at the source. To understand the performance of an AF system and how to improve the performance is the other objective of this dissertation.

In what follows, input-output models for a single-relay system in Protocol II[2] are presented. The models also include two main signal processing methods at the relay, i.e., DF and AF, which shall be extensively investigated in subsequent chapters.

2.4 Single-relay System Model

Consider a single-relay system which consists of a source S, a relay R and a destination D as depicted in Fig. 2.11. All nodes are equipped with single-antenna transmitter and receiver. The source message is transmitted from S to D with the help of R. The half duplex transmission is adopted so that R is not allowed to transmit and receive simultaneously. The transmission follows Protocol II and is carried out in 2 time slots. During the first time slot, the source signal s is broadcasted from S to R and D. The relay signal processing at R can be either DF or AF. For DF, R decodes the source signal and re-transmits the decoded signal to D. For AF, R amplifies the signal from S (without decoding them) with a fixed power gain [R9] and then forwards the amplified signal to D. After receiving two copies of the source signal, D can detect the source signal by performing a combining technique such as MRC or EGC. Note that, in practice, it is advantage to implement EGC for modulation constellations having equal energy symbols, e.g., M-ary phase shift keying (M-PSK). Otherwise, with constellations of unequal energy symbols, e.g., quadrature amplitude modulation (QAM), the instantaneous channel gain magnitudes of all paths are required at D in order to compute the optimal symbol detection rule, thus eliminating the advantage of avoiding channel magnitude estimation in EGC [R45, R46]. In this dissertation, M-PSK is adopted when the EGC technique is used.

The fading environment is assumed to be frequency-flat. All the channel coefficients involved, i.e., a_{SR}, a_{RD} and a_{SD}, are assumed to represent independent fading with mean-square values Ω_{SR}, Ω_{RD} and Ω_{SD}, respectively. It means the received SNR of the PQ link is equal to $\gamma_{\mathrm{PQ}} = \bar{\gamma}|a_{\mathrm{PQ}}|^2$, $\mathrm{PQ} \in \{\mathrm{SR}, \mathrm{RD}, \mathrm{SD}\}$ with $\bar{\gamma} = E_s/N_0$,

[2]Models for Protocol I and III are quite straightforward extensions of that for Protocol II. Therefore they are omitted here for simplicity.

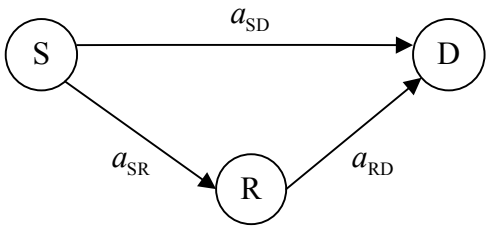

Figure 2.11 A single-relay system.

where N_0 is one-sided power spectral density of additive white Gaussian noise at each receiving node. The average SNR of the PQ link, denoted by $\bar{\gamma}_{\mathrm{PQ}}$, is equal to $\bar{\gamma}\Omega_{\mathrm{PQ}}$.

Depending on the considered fading environment, the magnitude of the channel coefficient, $|a_{\mathrm{PQ}}|$, follows the Rayleigh, Rician, Nakagami-m or Hoyt distribution. In the first time slot, the received signal at R, y_{SR}, and at D, y_{SD}, are respectively given as

$$y_{\mathrm{SR}} = a_{\mathrm{SR}}s + z_{\mathrm{SR}} \tag{2.26}$$

$$y_{\mathrm{SD}} = a_{\mathrm{SD}}s + z_{\mathrm{SD}}, \tag{2.27}$$

where z_{SR} and z_{SD} represent AWGN samples and are modeled as independent and identically distributed (i.i.d) $\mathcal{CN}(0, N_0)$ random variables.

In the second time slot, depending on the relay signal processing method under consideration, R forwards either the decoded or amplified signal to D. In what follows, input-output model descriptions for DF and AF are given.

2.4.1 Decode-and-Forward Processing

In this relaying signal processing method, R decodes the received signal from S by using the coherent ML detector, which chooses the symbol $\hat{s}$ that maximizes the conditional pdf of the received signal. The equivalent detection rule is

$$\hat{s} = \arg\min_{s\in\mathcal{S}} \left\{ \left| a_{\mathrm{SR}}^{*} y_{\mathrm{SR}} - |a_{\mathrm{SR}}|^2 s \right|^2 \right\}, \tag{2.28}$$

where $\mathcal{S}$ is the underlying constellation with size $M = |\mathcal{S}|$.

In non-adaptive forwarding strategies, R re-sends all the decoded signals with

maximal power even when they are not correct [R17,R47–R49]. Not only it wastes the power but also causes error propagation, which then degrades the error performance. On the other hand, the smart relaying technique, introduced in [R1], adapts to the SR channel qualities by transmitting to D a scaled version of $\hat{s}$ with the transmit power amplification factor α_1 given by [R1]:

$$\alpha_1 = \frac{\min(\gamma_{\mathrm{SR}}, \bar{\gamma}_{\mathrm{RD}})}{\bar{\gamma}_{\mathrm{RD}}} \leq 1. \tag{2.29}$$

To establish α_1 as in (2.29), the system needs a feedback channel from D to R to convey the average SNR, $\bar{\gamma}_{\mathrm{RD}}$. The advantages of choosing α_1 as in (2.29), are twofold. First, it saves the total transmitted power since α_1 is always less than or equal to 1. Furthermore, the adaptive transmission scheme at R helps to maintain the maximal diversity order of the DF relay network even when error propagation at R is taken into account.

The received signal, y_{RD}, at the destination in time slot 2 is given as

$$y_{\mathrm{RD}} = \sqrt{\alpha_1} a_{\mathrm{RD}} \hat{s} + z_{\mathrm{RD}}, \tag{2.30}$$

where z_{RD} is $\mathcal{CN}(0, N_0)$, which represents AWGN at D.

After receiving all the signals, D needs to detect the transmitted signal by some detection rules. As shown in [R1], the maximum likelihood detector is prohibitively complex for high-order constellations, e.g., QAM. In addition, it requires the SR channel information available at D, which increases the system complexity. In the case that D has no SR channel information nor detection performance of S–R link, it is reasonable to assume that the SR link is perfect. This assumption simplifies the optimal detector to [R1]

$$s' = \arg\min_{s \in \mathcal{S}} \left\{ \left| \left(w_{\mathrm{SD}} y_{\mathrm{SD}} + w_{\mathrm{RD}} y_{\mathrm{RD}} \right) - \left(w_{\mathrm{SD}} a_{\mathrm{SD}} + w_{\mathrm{RD}} a_{\mathrm{RD}} \right) s \right|^2 \right\}, \tag{2.31}$$

where $w_{\mathrm{SD}} = a_{\mathrm{SD}}^*$ and $w_{\mathrm{RD}} = a_{\mathrm{RD}}^*$. As the detection rule in (2.31) has the similar form as the naive MRC that does not apply any smart relaying technique, we call the proposed detection rule Smart MRC.

The other detection rule considered in this dissertation is called Smart EGC when we combine the smart relaying technique with equal gain combining (EGC) at D. For Smart EGC, $w_{\mathrm{SD}} = \exp(-j\phi_{\mathrm{SD}})$ and $w_{\mathrm{RD}} = \exp(-j\phi_{\mathrm{RD}})$, where ϕ_{SD} and ϕ_{RD} are the phases of the SD and RD channel coefficients, respectively. The equivalent detection rule for Smart EGC then becomes

$$s' = \arg\max_{s\in\mathcal{S}} \left\{ \mathrm{Re}\left[\Big(\exp(-j\phi_{\mathrm{SD}}) y_{\mathrm{SD}} + \exp(-j\phi_{\mathrm{RD}}) y_{\mathrm{RD}} \Big) s^* \right] \right\}. \tag{2.32}$$

It should be pointed out that to apply Smart EGC, D only needs to collect the channel coefficients' phases, i.e., ϕ_{SD} and ϕ_{RD}. On the other hand, Smart MRC needs to know all the RD channel information. In addition, it also has to measure the power scaling factor, i.e., α_1, to implement MRC at D. Therefore, the complexity of Smart MRC is much higher than that of Smart EGC scheme.

2.5 Amplify-and-Forward Processing

For AF with a fixed-gain relay, R places a fixed gain to the received signal, regardless of the fading amplitude of the channel in the first phase in order to limit the average transmitted power at R. The received signal, y_{RD}, at D in the second time slot is

$$y_{\mathrm{RD}} = G a_{\mathrm{RD}} (a_{\mathrm{SR}} s + z_{\mathrm{SR}}) + z_{\mathrm{RD}}. \tag{2.33}$$

The fixed gain G can be expressed as [R9]:

$$G^2 = \frac{\bar{\gamma}}{\bar{\gamma}_{\mathrm{SR}} + 1}, \tag{2.34}$$

which means that the average SNR at R is maintained at $\bar{\gamma}$. Because of the noise accumulation via the indirect path SRD, the noise variance (power) contributed through that path at D is $N_0(G^2|a_{\mathrm{RD}}|^2 + 1)$. Obviously, the noise components via the direct path, SD, in the first time slot and the indirect path through R have different variances. Before performing detection at D, the received signal through R is normalized to yield

$$\tilde{y}_{\mathrm{RD}} = \frac{G a_{\mathrm{RD}} a_{\mathrm{SR}}}{\sqrt{G^2 |a_{\mathrm{RD}}|^2 + 1}} s + \tilde{z}_{\mathrm{SRD}}, \tag{2.35}$$

where $\tilde{y}_{\mathrm{RD}} = y_{\mathrm{RD}}/\sqrt{G^2|a_{\mathrm{RD}}|^2+1}$ and $\tilde{z}_{\mathrm{SRD}} = (Ga_{\mathrm{RD}}z_{\mathrm{SR}} + z_{\mathrm{RD}})/\sqrt{G^2|a_{\mathrm{RD}}|^2+1} \sim \mathcal{CN}(0, N_0)$.

Similar to the case of DF, the normalized received signal through R along with the one from the direct path are then coherently combined at D for the detection of the source symbol as

$$s' = \arg\min_{s\in\mathcal{S}} \left\{ \left| \Big(w_{\mathrm{SD}} y_{\mathrm{SD}} + w_{\mathrm{RD}} y_{\mathrm{RD}} \Big) - \Big(w_{\mathrm{SD}} a_{\mathrm{SD}} + w_{\mathrm{RD}} a_{\mathrm{RD}} \Big) s \right|^2 \right\}. \tag{2.36}$$

For AF, the optimal ML detection coincides with MRC where $w_{\mathrm{SD}} = a^*_{\mathrm{SD}}$ and $w_{\mathrm{RD}} = Ga^*_{\mathrm{RD}}a^*_{\mathrm{SR}}\big/\sqrt{G^2|a_{\mathrm{RD}}|^2+1}$. The corresponding SNR at the output of the detector is

$$\gamma = \gamma_{\mathrm{SD}} + \frac{G^2\gamma_{\mathrm{SR}}\gamma_{\mathrm{RD}}}{\Big(\bar{\gamma} + G^2\gamma_{\mathrm{RD}}\Big)}. \tag{2.37}$$

An important remark about this detection is that it requires all the channel information, i.e., a_{SD}, a_{SR} and a_{RD}, available at D in order to combine the incoming signals effectively.

For EGC, the received signals are equally combined as

$$s' = \arg\max_{s\in\mathcal{S}} \left\{ \mathrm{Re}\Big[\Big(\exp(-j\phi_{\mathrm{SD}}) y_{\mathrm{SD}} + \exp[-j(\phi_{\mathrm{SR}} + \phi_{\mathrm{RD}})] \tilde{y}_{\mathrm{RD}} \Big) s^* \Big] \right\}, \tag{2.38}$$

where ϕ_{SD}, ϕ_{SR} and ϕ_{RD} are the phases of the SD, SR and SR channel coefficients, respectively. The SNR at the output of the EGC detector is calculated as

$$\gamma = \frac{1}{2}\left(\sqrt{\gamma_{\mathrm{SD}}} + \sqrt{\frac{G^2\gamma_{\mathrm{SR}}\gamma_{\mathrm{RD}}}{\bar{\gamma} + G^2\gamma_{\mathrm{RD}}}} \right)^2. \tag{2.39}$$

In order to apply (2.38) to detect the source signal, D needs to know all $\{a_{\mathrm{RD}}\}_{k=1}^{K}$ to normalize the received noise power. In addition, only ϕ_{SD} and ϕ_{SR} are also required at D. Therefore, the system complexity is much reduced.

The next chapter will present the first paper which investigates performance of the DF smart relaying system with Nakagami-m and Hoyt fading environments in Protocol II.

3. Diversity Analysis of Smart Relaying over Nakagami and Hoyt Generalized Fading Channels

Published as:

N. H. Vien, H. H. Nguyen, and T. Le-Ngoc, "Diversity analysis of smart relaying over Nakagami and Hoyt generalised fading channels," *IET Commun.*, vol. 3, pp. 1778–1789, November 2009.[1]

In the previous chapter, some relevant background and a system model for wireless relay communications have been presented. It was pointed out that for the first relaying signal processing method of interest, DF, the phenomenon of error propagation at the relays(s) causes performance degradation of the system. In order to mitigate error propagation, an effective technique adopted in this dissertation is smart relaying. In particular, the traditional MRC detection is employed at the destination, D, and an adaptive weighted coefficient is placed at the relay, R. The system is referred to as Smart MRC. It was shown in [R1] that the approach can always obtain the maximal diversity order of 2 for the single-relay system under Rayleigh fading channels under Protocol II. Also, what was learnt from Chapter 2 is that Nakagami and Hoyt distributions are generalized distributions which can be used to model different fading environments. In fact, the two distributions include the Rayleigh and one-sided Gaussian distributions as special cases. Due to the importance of Nakagami and Hoyt generalized fading channel models, the manuscript included in this chapter

[1]This paper is included with the expressed permission of the journal's publisher.

studies the performance in terms of diversity orders of Smart MRC under these two generalized fading channel models.

The system model in this chapter follows exactly the system model for DF in Section 2.4, except that only the MRC detection rule, is implemented at D. For this system with BPSK modulation, the maximal diversity order under Nakagami generalized fading channels is shown to be $m_{\mathrm{SD}} + \min\{m_{\mathrm{SR}}, m_{\mathrm{RD}}\}$. In particular, it was proved that the diversity order contributed by the dual-hop S-R-D is solely determined by the more severe faded link, i.e., $\min\{m_{\mathrm{SR}}, m_{\mathrm{RD}}\}$. For Hoyt generalized fading channels, the paper shows that the system can always achieve the maximal diversity order of 2 and the diversity order does not depend on the fading parameters, i.e., q_{SR}, q_{SD} and q_{RD}. To verify the analytical results, computer simulations are also presented and they are in line with the theoretical analysis.

Diversity Analysis of Smart Relaying over Nakagami and Hoyt Generalized Fading Channels

Nam H. Vien*, *Student Member, IEEE* and Ha H. Nguyen, *Senior Member, IEEE*, Tho Le-Ngoc, *Fellow, IEEE*

Abstract

Signal transmission with the help of relay(s) in wireless networks can achieve spatial diversity without the need of having multiple antennas at the source and/or destination. Among various signal processing techniques proposed for the relays, the adaptive decode–and–forward (DF) relaying strategy, recently proposed by Wang et al. and generally referred to as *smart* relaying, has been shown to achieve the *maximal* spatial diversity even when imperfect detection is committed at the relays. The work by Wang et al., however, only considers Rayleigh fading channels. This paper extends the diversity analysis of the smart relaying technique to the important Nakagami and Hoyt generalized fading channels. Performance analysis proves that, at high signal–to–noise ratio (SNR), the *maximal* diversity order achieved by the smart relaying system under the Nakagami channel is $m_{\rm SD} + \min\{m_{\rm SR}, m_{\rm RD}\}$, where $m_{\rm SR}$, $m_{\rm RD}$ and $m_{\rm SD}$ are the fading figures of the source–relay (S–R), relay–destination (R–D) and source–destination (S–D) links. Under the Hoyt fading channel, the diversity order is 2. The obtained results on the diversity order are shown to be insensitive to the quality of the R–D feedback channel.

Index terms

Cooperative communications, smart relaying, adaptive transmission, decode–and–forward, diversity order, Nakagami fading, Hoyt fading, maximal ratio combiner.

3.1 Introductions

In wireless networks, deploying relays to assist communication between the source and destination is continuing to attract a lot of research interests due to its ability to

---

Nam H. Vien (*contact author) and Ha H. Nguyen are with the Department of Electrical & Computer Engineering, University of Saskatchewan, 57 Campus Dr., Saskatoon, SK, Canada S7N 5A9. Emails: nam.vien@usask.ca, ha.nguyen@usask.ca.

Tho Le-Ngoc is with the Department of Electrical & Computer Engineering, McGill University, 3480 University St., Montreal, Quebec, Canada H3A 2A7. Email: tho@ece.mcgill.ca.

provide spatial diversity without the need of having multiple antennas at the source and/or destination [P1–P8]. In this approach, a source transmits messages to a destination with the aid of relays. The source along with the relays, creates a virtual antenna array. If properly designed, relaying can achieve a diversity order up to the number of diversity paths, what can be referred to as full diversity [P5]. Therefore, a network with M relays can potentially provide a diversity order of $M + 1$.

In [P4], several low–complexity relaying strategies are proposed and studied, including fixed relaying, selection relaying and incremental relaying. Moreover in each of these relaying strategies the relays can either amplify–and–forward (AF) or decode–and–forward (DF) the received signals. For the AF protocol, when the instantaneous channel state information (CSI) is not available at the receivers, fulfilling the relays' power constraints greatly complicates the demodulation as well as its performance analysis [P6, P9]. With the DF protocol, the power constraints are easily satisfied. Moreover, compared to AF, DF can be combined with coding techniques and it is also easier to incorporate into network protocols [P10–P13]. It should be noted, however, that integrating channel coding into the DF protocol considerably complicates the systems as compared to the uncoded DF considered in this paper. In particular, this paper is confined to symbol–by–symbol demodulation and retransmission.

For uncoded systems, the authors in [P5, P14] proved that relaying with AF can obtain the full diversity with the maximum likelihood (ML) demodulation. For relaying with DF, the full diversity can also be achieved with binary–phase–shift–keying (BPSK) and the optimal ML coherent demodulation [P2]. However, the ML demodulation becomes prohibitively complex for high–order constellations. To reduce the complexity, one can use the maximum ratio combiner (MRC) to demodulate the received signals. Unfortunately, MRC can offer the full diversity only for the perfect source–relay (S–R) link due to the error propagation at the relay [P15]. To improve the performance of MRC, λ–MRC and piecewise–linear (PL) combiner were proposed in [P2] and [P6], respectively. Numerical results in [P2] illustrate that the λ–MRC's performance is close to that of the ML demodulation when BPSK is used. However,

it cannot be assured whether the λ–MRC offers the full diversity since the parameter λ is not analytically specified. In [P6], the PL combiner was derived for noncoherent and coherent demodulations with the assumption that the average S–R bit error probability (BEP) is available at the destination. But again, this fact is only established for BPSK modulation.

More recently, an elegant demodulation method, called cooperative–MRC (C–MRC), was proposed in [P16]. It was shown in [P16] that the C–MRC's performance is close to that of the optimal ML demodulation for BPSK and it can obtain the full diversity *regardless* of the underlying constellation. The main idea behind the C–MRC method is that the BEP of the cascaded source–relay–destination (S–R–D) channel can be considered as a BEP of an *equivalent* additive white Gaussian noise (AWGN) channel. The equivalent channel is realizable under the assumption that the instantaneous S–R signal–to–noise ratio (SNR) is available at the destination. By using the C–MRC, the available channel information is efficiently utilized at the destination to achieve the full diversity. An adaptive weighted coefficient is imposed on the S–R–D link by the C–MRC at the destination, depending on the relative qualities of the S–R and R–D links.

An equivalence of the relaying system that employs C–MRC at the destination is a system that implements the traditional MRC at the destination and places the adaptive weighted coefficient at the relay. The latter system, referred to as the *smart* relaying system [P17–P19], only requires that the characteristic of the R–D link is available at the relay. It was shown that the technique can always achieve the maximal diversity of 2 for the simple relaying system with three nodes, i.e., S, R and D. The analysis on achievable diversity order of the smart relaying was also recently presented in [P20] for a more general relaying protocol[2] in which both the source and relay simultaneously transmit to the destination during the second time slot [P21].

[2]The relaying protocol investigated in [P17–P19] consists of two time slots, where the source broadcasts its messages to the relay and the destination in the first time slot while only the relay transmits to the destination during the second time slot.

In particular, [P20] shows that the smart relaying can not only achieve the diversity order of 2 for a 3-node network, but also offer a performance gain over the relaying protocol considered in [P17–P19].

The diversity analysis of the smart relaying systems in [P17–P20] however only applies to Rayleigh fading channels. Since Nakagami and Hoyt distributions have been shown to provide excellent fits to experimental fading channel measurements for land, mobile, terrestrial and satellite communications [P22–P24], it is important to study the performance of relaying systems under these fading channel models [P22–P26]. Moreover, because the Rayleigh distribution can be considered as a special case of the Nakagami or Hoyt distribution, the performance analysis for Nakagami or Hoyt fading is a more general and powerful framework. Due to the importance of Nakagami and Hoyt fading channel models, the main objective of this paper is therefore to obtain the diversity analysis of the smart relaying systems under these channel models. For a system with three nodes, i.e., S, R and D, and with BPSK modulation, it is shown that the maximal diversity order is $m_{\mathrm{SD}} + \min\{m_{\mathrm{SR}}, m_{\mathrm{RD}}\}$ under Nakagami generalized fading channels. For Hoyt generalized fading channels, the maximal diversity order is always 2 and does not depend on the channel parameters, i.e., q_{SR}, q_{SD} and q_{RD}. It should be pointed out that our analysis can be straightforwardly extended to quadrature phase shift keying (QPSK) modulation. Furthermore, the analysis can be easily generalized to higher–order constellations, e.g., quadrature amplitude modulation (QAM), or to the multiple–relay systems by using the same techniques in [P19]. Due to space limit, these extensions are not treated in this paper.

The remaining of this paper is organized as follows. Section 3.2 describes the system model and signal processing in smart relaying. The diversity analysis for Nakagami and Hoyt generalized fading channels is investigated in Section 3.3. In Section 3.4, the analytical results are thoroughly verified by computer simulation. Finally, conclusions are given in Section 3.5.

Notation: $(\cdot)^*$ denotes complex conjugate, $\mathrm{Re}(x)$ takes the real part of complex number x. The Q-function is defined as $Q(x) = (1/\sqrt{2\pi}) \int_x^\infty \exp(-t^2/2)dt$. A random

variable (RV) $X \sim \text{Gamma}(n, \bar{\gamma})$ if its pdf is given as $p_X(x) = x^{n-1}/[\Gamma(n)\bar{\gamma}^n] \exp(-x/\bar{\gamma})$, where $\Gamma(z) = \int_0^\infty \exp(-t)t^{z-1}dt$ is the gamma function.

3.2 System Model

Consider a simple relaying system with three nodes, i.e., the source S, the relay R and the destination D, as in Fig. 5.1. In the first time slot, the source broadcasts its signal s, to both the relay and the destination. In the second time slot, the relay, after decoding the received signal from the source, re–sends a scaled version of the decoded signal $\hat{s}$ to the destination. The source keeps silent during the second time slot. Frequency–flat fading channels are assumed throughout the paper, where the perfect channel state information (CSI) is only available at the receiver and not at the transmitter. The perfect CSI means that the relay knows the channel state of the S–R link and the destination knows the channel states of the S–D and the R–D links. Let a_{SR}, a_{RD} and a_{SD} denote the channel coefficients of the S–R, R–D and S–D links, respectively. Different from [P19], the magnitudes of these coefficients are not modeled by the conventional Rayleigh distribution but by the Nakagami or Hoyt distribution, with mean–square values Ω_{SR}, Ω_{RD} and Ω_{SD}, respectively.

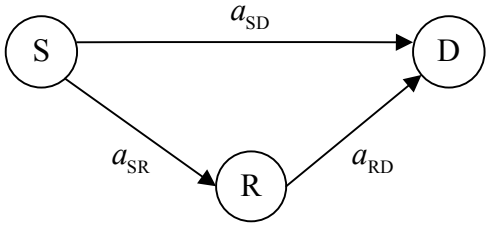

Figure 3.1 A simple relaying system with 3 nodes.

During the first time slot, the source broadcasts the signal s with an average power E_s to both the relay and destination. The received signals at the relay and destination are

$$y_{\text{R}}[1] = a_{\text{SR}}s + z_{\text{R}}[1], \tag{3.1}$$

$$y_{\text{D}}[1] = a_{\text{SD}}s + z_{\text{D}}[1], \tag{3.2}$$

where $z_{\mathrm{R}}[1]$ and $z_{\mathrm{D}}[1]$ represent AWGN and are modeled as independent and identically distributed (i.i.d) circularly symmetric complex Gaussian random variables (RVs) of variance N_0.

The relay decodes the received signal from the source by using the coherent ML detector. This means that the relay chooses the symbol $\hat{s}$ that maximizes the conditional density function of the received signal as follows

$$\hat{s} = \arg\max_{s\in\mathbf{S}} \left\{ \frac{1}{\pi N_0} \exp\left[\frac{-\left|y_{\mathrm{R}}[1] - a_{\mathrm{SR}} s\right|^2}{N_0} \right] \right\} = \arg\min_{s\in\mathbf{S}} \left\{ \left|y_{\mathrm{R}}[1] - a_{\mathrm{SR}} s\right|^2 \right\} \tag{3.3}$$

$$= \arg\min_{s\in\mathbf{S}} \left\{ \left| a_{\mathrm{SR}}^* y_{\mathrm{R}}[1] - |a_{\mathrm{SR}}|^2 s \right|^2 \right\}. \tag{3.4}$$

Different from other relaying options [P2, P4, P15, P16] where the re–transmitted symbol power is fixed in the second time slot, here, similar to [P19], the relay adapts to the S–R channel quality by transmitting to the destination a scaled version of $\hat{s}$ with the following transmit power gain α_1:

$$\alpha_1 = \frac{\min(\gamma_{\mathrm{SR}}, \theta\bar{\gamma}_{\mathrm{RD}})}{\theta\bar{\gamma}_{\mathrm{RD}}} \leq 1. \tag{3.5}$$

Denote the instantaneous signal–to–noise ratios (SNRs) of the S–R, R–D and S–D links by $\gamma_{\mathrm{SR}} := |a_{\mathrm{SR}}|^2\bar{\gamma}$, $\gamma_{\mathrm{RD}} := |a_{\mathrm{RD}}|^2\bar{\gamma}$ and $\gamma_{\mathrm{SD}} := |a_{\mathrm{SD}}|^2\bar{\gamma}$, respectively, where $\bar{\gamma} = E_s/N_0$. Similarly, the average SNRs of the S–R, R–D and S–D links are given as $\bar{\gamma}_{\mathrm{SR}} := \Omega_{\mathrm{SR}}\bar{\gamma}$, $\bar{\gamma}_{\mathrm{RD}} := \Omega_{\mathrm{RD}}\bar{\gamma}$ and $\bar{\gamma}_{\mathrm{SD}} := \Omega_{\mathrm{SD}}\bar{\gamma}$. The rationale in choosing α_1 as in (3.5) is that α_1 prescribes relay information at full power whenever the S–R link is reliable, i.e., $\gamma_{\mathrm{SR}} > \theta\bar{\gamma}_{\mathrm{RD}}$, otherwise, it scales the power down (even to zero) in order to lessen the error propagation underwent in the R–D link. The constant θ describes the imperfection in the feedback channel, e.g., $\theta = 1$ for the perfect feedback.

During the second time slot, the relay transmits the signal $\hat{s}$ with power $\alpha_1 E_s$ to the destination. The received signal $y_{\mathrm{D}}[2]$ at the destination is given by

$$y_{\mathrm{D}}[2] = \sqrt{\alpha_1} a_{\mathrm{RD}} \hat{s} + z_{\mathrm{D}}[2], \tag{3.6}$$

where $z_{\mathrm{D}}[2]$ is a circularly symmetric complex Gaussian random variable of variance N_0.

Having received two signals from S and R in the first and second time slots, respectively, D needs to combine them to make the decision on the transmitted signal s. Obviously the complexity and performance of the system depend largely on the amount of the channel information available at the destination and, accordingly, on how detection is performed. If the S–R link channel information is also available at the destination, the maximum likelihood (ML) detector can be carried out. The use of the ML detector, while achieving the best error performance, increases the system's complexity due to the need of having the instantaneous S–R channel information at the destination. Furthermore, the performance analysis of the ML detector is only viable only through numerical simulations [P19]. On the other hand, when the destination has no S–R channel information (as considered in our system model), it is common to assume that the S–R link is perfect. This assumption simplifies the optimal detector at the destination to

$$s^{'} = \arg\min_{s\in\mathbf{S}} \left\{ \left| a_{\mathrm{SD}}^{*} y_{\mathrm{D}}[1] + w_{\mathrm{RD}} y_{\mathrm{D}}[2] - \left(|a_{\mathrm{SD}}|^2 + |w_{\mathrm{RD}}|^2 \right) s \right|^2 \right\}, \tag{3.7}$$

where the weighted coefficient w_{RD} is

$$w_{\mathrm{RD}} = \sqrt{\alpha_1} a_{\mathrm{RD}}^{*}. \tag{3.8}$$

Note that the detection in (3.7) only requires the destination to know the S–D channel information, i.e., a_{SD}, and the equivalent R–D link state, i.e., $\sqrt{\alpha_1} a_{\mathrm{RD}}$.

Based on the system model laid out in this section, analysis of the diversity order of the symbol error probability of the detector in (3.7) shall be carried out in the next section. Note that the diversity order is defined as the decaying factor of the error probability curves in a log-log scale [P27].

3.3 Diversity Analysis

It is obvious that the error performance of the detection rule in (3.7) depends on whether the relay makes a a decision error under the ML detection rule in (3.4). When BPSK modulation is employed, there are two possibilities of the decoded signal at R, namely, $\hat{s} = s$ or $\hat{s} = -s$ with the corresponding probabilities $[1 - Q(\sqrt{2\gamma_{\mathrm{SR}}})]$ or

$Q(\sqrt{2\gamma_{\rm SR}})$. Due to the symmetry of BPSK, the overall error performance of the smart relaying is the same, regardless of whether $s=\sqrt{E_s}$ or $s=-\sqrt{E_s}$ was transmitted. Therefore, without loss of generality, only the case that $s=\sqrt{E_s}$ needs to be examined in the following analysis.

When R makes a correct decision, i.e., $\hat{s}=s$ is made at R, the probability of making an error at D is equal to the probability of the following event:

$$-\Big(|a_{\rm SD}|^2+|w_{\rm RD}|^2\Big)\sqrt{E_s}\geq {\rm Re}\{a_{\rm SD}^* z_{\rm D}[1]+w_{\rm RD}z_{\rm D}[2]\}. \tag{3.9}$$

Replacing $w_{\rm RD}$ by $\sqrt{\alpha_1}a_{\rm RD}^*$ as in (3.8), the probability of the event in (3.9) can be evaluated as

$$\Pr\{\text{error}|\hat{s}=s\}=Q\left[\sqrt{2\left(\gamma_{\rm SD}+\alpha_1\gamma_{\rm RD}\right)}\right]. \tag{3.10}$$

On the other hand, when R commits an error detection, the event of making an error at D is

$$-\Big(\Big|a_{\rm SD}\Big|^2-\alpha_1\Big|a_{\rm RD}\Big|^2\Big)\sqrt{E_s}\geq {\rm Re}\Big\{a_{\rm SD}^* z_{\rm D}[1]+w_{\rm RD}z_{\rm D}[2]\Big\}. \tag{3.11}$$

The probability of the event in (3.11) is then computed as

$$\Pr\Big\{\text{error}|\hat{s}=-s\Big\}=Q\left[\frac{\sqrt{2}\left(\gamma_{\rm SD}-\alpha_1\gamma_{\rm RD}\right)}{\sqrt{\gamma_{\rm SD}+\alpha_1\gamma_{\rm RD}}}\right]. \tag{3.12}$$

Combining (3.10) and (3.12) results in the following overall conditional BEP $P_b(\gamma_{\rm SR},\gamma_{\rm RD},\gamma_{\rm SD})$ [P19, eq. (17)]:

$$P_b(\gamma_{\rm SR},\gamma_{\rm RD},\gamma_{\rm SD})=P_1(\gamma_{\rm SR},\gamma_{\rm RD},\gamma_{\rm SD})+P_2(\gamma_{\rm SR},\gamma_{\rm RD},\gamma_{\rm SD}), \tag{3.13}$$

where

$$P_1(\gamma_{\rm SR},\gamma_{\rm RD},\gamma_{\rm SD})=\left[1-Q\left(\sqrt{2\gamma_{\rm SR}}\right)\right]Q\left[\sqrt{2\left(\gamma_{\rm SD}+\alpha_1\gamma_{\rm RD}\right)}\right], \tag{3.14}$$

$$P_2(\gamma_{\rm SR},\gamma_{\rm RD},\gamma_{\rm SD})=Q\left(\sqrt{2\gamma_{\rm SR}}\right)Q\left[\frac{\sqrt{2}\left(\gamma_{\rm SD}-\alpha_1\gamma_{\rm RD}\right)}{\sqrt{\gamma_{\rm SD}+\alpha_1\gamma_{\rm RD}}}\right]. \tag{3.15}$$

The overall error performance is obtained by taking the expectation over all the channel gain variables, i.e., $(\gamma_{\rm SR},\gamma_{\rm RD},\gamma_{\rm SD})$. The following subsections compute such overall error performance for Nakagami and Hoyt fading channels, which is not available in [P19].

3.3.1 Nakagami Fading Channels

For Nakagami fading, the pdfs[3] $p^{(N)}_{\gamma_{\rm SR}}(\gamma_{\rm SR})$, $p^{(N)}_{\gamma_{\rm RD}}(\gamma_{\rm RD})$ and $p^{(N)}_{\gamma_{\rm SD}}(\gamma_{\rm SD})$ of the instantaneous SNRs of the S–R, R–D and S–D links can be respectively written as [P28]

$$p^{(N)}_{\gamma_{\rm SR}}(\gamma_{\rm SR}) = \frac{m_{\rm SR}^{m_{\rm SR}}\gamma_{\rm SR}^{m_{\rm SR}-1}}{\bar{\gamma}_{\rm SR}^{m_{\rm SR}}\Gamma(m_{\rm SR})}\exp\left(-\frac{m_{\rm SR}\gamma_{\rm SR}}{\bar{\gamma}_{\rm SR}}\right), \tag{3.16}$$

$$p^{(N)}_{\gamma_{\rm RD}}(\gamma_{\rm RD}) = \frac{m_{\rm RD}^{m_{\rm RD}}\gamma_{\rm RD}^{m_{\rm RD}-1}}{\bar{\gamma}_{\rm RD}^{m_{\rm RD}}\Gamma(m_{\rm RD})}\exp\left(-\frac{m_{\rm RD}\gamma_{\rm RD}}{\bar{\gamma}_{\rm RD}}\right), \tag{3.17}$$

$$p^{(N)}_{\gamma_{\rm SD}}(\gamma_{\rm SD}) = \frac{m_{\rm SD}^{m_{\rm SD}}\gamma_{\rm SD}^{m_{\rm SD}-1}}{\bar{\gamma}_{\rm SD}^{m_{\rm SD}}\Gamma(m_{\rm SD})}\exp\left(-\frac{m_{\rm SD}\gamma_{\rm SD}}{\bar{\gamma}_{\rm SD}}\right), \tag{3.18}$$

where $m_{\rm SR}$, $m_{\rm RD}$ and $m_{\rm SD}$ are the fading figures of the S–R, R–D and S–D links, respectively.

In order to average $P_b(\gamma_{\rm SR}, \gamma_{\rm RD}, \gamma_{\rm SD})$ over RVs $\gamma_{\rm SR}$, $\gamma_{\rm RD}$ and $\gamma_{\rm SD}$, the following lemma from [P12] is useful.

Lemma 1 ([P12])**.** *Consider the error probability $P_e(\gamma_c, \gamma_e, \eta_c, \eta_e)$ satisfying*

$$P_e(\gamma_c, \gamma_e, \eta_c, \eta_e) \leq \kappa_1 \exp(-\kappa_2\gamma_e) Q\left[\frac{\sqrt{2}(\kappa_3\gamma_c\eta_c - \kappa_4\gamma_e\eta_e)}{\sqrt{\kappa_3\gamma_c\eta_c + \kappa_4\gamma_e\eta_e}}\right], \tag{3.19}$$

for some finite constants κ_1, κ_2, κ_3, κ_4 and γ_c, η_c, γ_e and η_e are nonnegative RVs and independent of each other; $\gamma_c \sim$ Gamma$(n_c, \bar{\gamma})$ and $\gamma_e \sim$ Gamma$(n_e, \bar{\gamma})$. If the pdfs $p(\eta_c)$ and $p(\eta_e)$ do not depend on $\bar{\gamma}$, the expectation of $P_e(\gamma_c, \gamma_e, \eta_c, \eta_e)$ over γ_c, η_c, γ_e and η_e is bounded as

$$P_e \leq (k\bar{\gamma})^{-(n_c+n_e)}, \tag{3.20}$$

where $k = E[k(\eta_c, \eta_e)] \geq 0$ is a constant and does not depend on $\bar{\gamma}$.

Proof: See [P12, Appendix B].

The diversity order of the smart relaying under Nakagami fading channels is stated in the next proposition, whose proof is completed with the aid of Lemma 1.

[3]Hereafter, the superscripts (N) and (H) refer to Nakagami and Hoyt fading channels, respectively.

Proposition 1. *For Nakagami fading channels and BPSK modulation, the average probability* $P_b^{(N)} = E[P_b(\gamma_{SR}, \gamma_{RD}, \gamma_{SD})]$ *is upperbounded as* $P_b^{(N)} \leq I^{(N)}$*, where* $I^{(N)}$ *decays with an exponent equal to* $m_{SD} + \min\{m_{SR}, m_{RD}\}$*, i.e.,*

$$P_b^{(N)} \leq I^{(N)} \bar{\gamma} \overset{\bar{\gamma}\to\infty}{\approx} (k^{(N)}\bar{\gamma})^{-(m_{SD}+\min\{m_{SR},m_{RD}\})}, \tag{3.21}$$

where $k^{(N)}$ *is a nonnegative constant that depends on* $(\Omega_{SR}, \Omega_{RD}, \Omega_{SD})$*.*

Proof: To ease the analysis, the first conditional probability $P_1^{(N)}(\gamma_{\rm SR}, \gamma_{\rm RD}, \gamma_{\rm SD})$ can be bounded as

$$P_1^{(N)}(\gamma_{\rm SR}, \gamma_{\rm RD}, \gamma_{\rm SD}) \leq Q\left[\sqrt{2\left(\gamma_{\rm SD} + \alpha_1\gamma_{\rm RD}\right)}\right], \tag{3.22}$$

where the inequality in (3.22) comes from the fact that $\left[1 - Q\left(\sqrt{2\gamma_{\rm SR}}\right)\right] \leq 1$.

In order to apply Lemma 1 to bound $P_1^{(N)}$, rewrite the right–hand–side (RHS) of (3.22) as

$$P_1^{(N)}(\gamma_{\rm SR}, \gamma_{\rm RD}, \gamma_{\rm SD}) \leq Q\left[\sqrt{2}\sqrt{\frac{m_{\rm SD}}{\Omega_{\rm SD}}\frac{\Omega_{\rm SD}\gamma_{\rm SD}}{m_{\rm SD}} + \frac{m_{\rm RD}\alpha_1}{\Omega_{\rm RD}}\frac{\Omega_{\rm RD}\gamma_{\rm RD}}{m_{\rm RD}}}\right] \tag{3.23}$$

$$= Q\left[\sqrt{2}\sqrt{\frac{m_{\rm SD}}{\Omega_{\rm SD}}\hat{\gamma}_{\rm SD} + \frac{\alpha_1 m_{\rm RD}}{\Omega_{\rm RD}}\hat{\gamma}_{\rm RD}}\right], \tag{3.24}$$

where $\hat{\gamma}_{\rm SD} = (\Omega_{\rm SD}\gamma_{\rm SD}/m_{\rm SD})$ and $\hat{\gamma}_{\rm RD} = (\Omega_{\rm RD}\gamma_{\rm RD}/m_{\rm RD})$. It is easily to verify that $\hat{\gamma}_{\rm SD} \sim \text{Gamma}(m_{\rm SD}, \bar{\gamma})$ and $\hat{\gamma}_{\rm RD} \sim \text{Gamma}(m_{\rm RD}, \bar{\gamma})$, i.e.,

$$p_{\hat{\gamma}_{\rm SD}}(\hat{\gamma}_{\rm SD}) = \frac{\hat{\gamma}_{\rm SD}^{m_{\rm SD}-1}}{\bar{\gamma}^{m_{\rm SD}}\Gamma(m_{\rm SD})}\exp\left(-\frac{\hat{\gamma}_{\rm SD}}{\bar{\gamma}}\right) \tag{3.25}$$

$$p_{\hat{\gamma}_{\rm RD}}(\hat{\gamma}_{\rm RD}) = \frac{\hat{\gamma}_{\rm RD}^{m_{\rm RD}-1}}{\bar{\gamma}^{m_{\rm RD}}\Gamma(m_{\rm RD})}\exp\left(-\frac{\hat{\gamma}_{\rm RD}}{\bar{\gamma}}\right). \tag{3.26}$$

Define the RV $\eta = \min\{m_{\rm SD}/\Omega_{\rm SD}, \alpha_1 m_{\rm RD}/\Omega_{\rm RD}\}$. Since the function $Q(x)$ is a monotonically decreasing function, $P_1^{(N)}(\gamma_{\rm SR}, \gamma_{\rm RD}, \gamma_{\rm SD})$ can be bounded as follows

$$P_1^{(N)}(\gamma_{\rm SR}, \gamma_{\rm RD}, \gamma_{\rm SD}) \leq Q\left[\sqrt{2}\sqrt{\eta(\hat{\gamma}_{\rm SD} + \hat{\gamma}_{\rm RD})}\right]. \tag{3.27}$$

The pdf of α_1 does not depend on $\bar{\gamma}$ as it is given by

$$p_{\alpha_1}(\alpha_1) = \begin{cases} \frac{m_{\mathrm{SR}}\alpha_1^{m_{\mathrm{SR}}-1}}{\Gamma(m_{\mathrm{SR}})}\left(\frac{\Omega_{\mathrm{RD}}}{\Omega_{\mathrm{SR}}}\right)^{m_{\mathrm{SR}}}\exp\left(-\frac{m_{\mathrm{SR}}\Omega_{\mathrm{RD}}\alpha_1}{\Omega_{\mathrm{SR}}}\right), & \Pr(\gamma_{\mathrm{SR}} \le \bar{\gamma}_{\mathrm{RD}}) = \frac{\gamma(m_{\mathrm{SR}}, m_{\mathrm{SR}}\Omega_{\mathrm{RD}}/\Omega_{\mathrm{SR}})}{\Gamma(m_{\mathrm{SR}})} \\ 1 & \Pr(\gamma_{\mathrm{SR}} > \bar{\gamma}_{\mathrm{RD}}) = 1 - \frac{\gamma(m_{\mathrm{SR}}, m_{\mathrm{SR}}\Omega_{\mathrm{RD}}/\Omega_{\mathrm{SR}})}{\Gamma(m_{\mathrm{SR}})} \end{cases}, \tag{3.28}$$

where $\gamma(\alpha, x) = \int_0^x \exp(-t)t^{(\alpha-1)}dt$ is the incomplete gamma function [P29]. Since the RV η is a function of α_1, the pdf of η does not depend on $\bar{\gamma}$ either. Then Lemma 1 can be applied to (3.27) by setting $\kappa_1 = 1$, $\kappa_2 = \kappa_4 = 0$, $\kappa_3 = 1$, $\eta_c = \eta$ and $\gamma_c = (\hat{\gamma}_{\mathrm{SD}} + \hat{\gamma}_{\mathrm{RD}}) \sim \mathrm{Gamma}(m_{\mathrm{SD}} + m_{\mathrm{RD}}, \bar{\gamma})$, which gives

$$P_1^{(N)} \le (k_1^{(N)}\bar{\gamma})^{-(m_{\mathrm{SD}}+m_{\mathrm{RD}})}, \tag{3.29}$$

where $k_1^{(N)}$ is a nonnegative constant and does not depend on $\bar{\gamma}$.

The next task is to find the upperbound on the second probability $P_2^{(N)}$. To this end, one can bound the conditional probability $P_2^{(N)}(\gamma_{\mathrm{SR}}, \gamma_{\mathrm{RD}}, \gamma_{\mathrm{SD}})$ as follows:

$$P_2^{(N)}(\gamma_{\mathrm{SR}}, \gamma_{\mathrm{RD}}, \gamma_{\mathrm{SD}}) \le (1/2)\exp(-\gamma_{\mathrm{SR}})Q\left[\frac{\sqrt{2}\left(\gamma_{\mathrm{SD}} - \alpha_1\gamma_{\mathrm{RD}}\right)}{\sqrt{\gamma_{\mathrm{SD}} + \alpha_1\gamma_{\mathrm{RD}}}}\right] \tag{3.30}$$

$$\le (1/2)\exp(-\gamma_{\mathrm{SR}})Q\left[\frac{\sqrt{2}\left(\gamma_{\mathrm{SD}} - \frac{\gamma_{\mathrm{SR}}\gamma_{\mathrm{RD}}}{\theta\bar{\gamma}_{\mathrm{RD}}}\right)}{\sqrt{\gamma_{\mathrm{SD}} + \frac{\gamma_{\mathrm{SR}}\gamma_{\mathrm{RD}}}{\theta\bar{\gamma}_{\mathrm{RD}}}}}\right], \tag{3.31}$$

where the first inequality in (3.30) comes from the Chernoff bound, i.e., $Q(x) \le (1/2)\exp(-x^2/2)$, $x \ge 0$, and the second one in (3.31) follows from the fact that $\alpha_1 \le \gamma_{\mathrm{SR}}/(\theta\bar{\gamma}_{\mathrm{RD}})$.

Following the same steps as done with $P_1^{(N)}(\gamma_{\mathrm{SR}}, \gamma_{\mathrm{RD}}, \gamma_{\mathrm{SD}})$, one can rewrite (3.31) as follows

$$P_2^{(N)}(\gamma_{\mathrm{SR}}, \gamma_{\mathrm{RD}}, \gamma_{\mathrm{SD}}) \le (1/2)\exp\left(-\frac{m_{\mathrm{SR}}}{\Omega_{\mathrm{SR}}}\frac{\Omega_{\mathrm{SR}}\gamma_{\mathrm{SR}}}{m_{\mathrm{SR}}}\right) Q\left[\frac{\sqrt{2}\left(\frac{m_{\mathrm{SD}}}{\Omega_{\mathrm{SD}}}\frac{\Omega_{\mathrm{SD}}\gamma_{\mathrm{SD}}}{m_{\mathrm{SD}}} - \frac{m_{\mathrm{SR}}}{\theta\Omega_{\mathrm{SR}}}\frac{\Omega_{\mathrm{SR}}\gamma_{\mathrm{SR}}}{m_{\mathrm{SR}}}\tilde{\gamma}_{\mathrm{RD}}\right)}{\sqrt{\frac{m_{\mathrm{SD}}}{\Omega_{\mathrm{SD}}}\frac{\Omega_{\mathrm{SD}}\gamma_{\mathrm{SD}}}{m_{\mathrm{SD}}} + \frac{m_{\mathrm{SR}}}{\theta\Omega_{\mathrm{SR}}}\frac{\Omega_{\mathrm{SR}}\gamma_{\mathrm{SR}}}{m_{\mathrm{SR}}}\tilde{\gamma}_{\mathrm{RD}}}}\right] \tag{3.32}$$

$$=(1/2)\exp\left(-\frac{m_{\mathrm{SR}}}{\Omega_{\mathrm{SR}}}\hat{\gamma}_{\mathrm{SR}}\right) Q\left[\frac{\sqrt{2}\left(\frac{m_{\mathrm{SD}}}{\Omega_{\mathrm{SD}}}\hat{\gamma}_{\mathrm{SD}} - \frac{m_{\mathrm{SR}}}{\theta\Omega_{\mathrm{SR}}}\hat{\gamma}_{\mathrm{SR}}\tilde{\gamma}_{\mathrm{RD}}\right)}{\sqrt{\frac{m_{\mathrm{SD}}}{\Omega_{\mathrm{SD}}}\hat{\gamma}_{\mathrm{SD}} + \frac{m_{\mathrm{SR}}}{\theta\Omega_{\mathrm{SR}}}\hat{\gamma}_{\mathrm{SR}}\tilde{\gamma}_{\mathrm{RD}}}}\right], \tag{3.33}$$

where $\tilde{\gamma}_{\mathrm{RD}} = \gamma_{\mathrm{RD}}/\bar{\gamma}_{\mathrm{RD}}$ and its pdf can be written as

$$p_{\tilde{\gamma}_{\mathrm{RD}}}(\tilde{\gamma}_{\mathrm{RD}}) = \frac{m_{\mathrm{RD}}\tilde{\gamma}_{\mathrm{RD}}^{m_{\mathrm{RD}}-1}}{\Gamma(m_{\mathrm{RD}})}\exp(-m_{\mathrm{RD}}\tilde{\gamma}_{\mathrm{RD}}). \tag{3.34}$$

Note that the pdf $p_{\tilde{\gamma}_{\mathrm{RD}}}(\tilde{\gamma}_{\mathrm{RD}})$ does not depend on $\bar{\gamma}$. The RV $\hat{\gamma}_{\mathrm{SD}} \sim \mathrm{Gamma}(m_{\mathrm{SD}}, \bar{\gamma})$ and its pdf is given in (3.25). Similarly, the RV $\hat{\gamma}_{\mathrm{SR}} \sim \mathrm{Gamma}(m_{\mathrm{SR}}, \bar{\gamma})$ and its pdf is given as follows

$$p_{\hat{\gamma}_{\mathrm{SR}}}(\hat{\gamma}_{\mathrm{SR}}) = \frac{\hat{\gamma}_{\mathrm{SR}}^{m_{\mathrm{SR}}-1}}{\bar{\gamma}^{m_{\mathrm{SR}}}\Gamma(m_{\mathrm{SR}})}\exp\left(-\frac{\hat{\gamma}_{\mathrm{SR}}}{\bar{\gamma}}\right). \tag{3.35}$$

As before, Lemma 1 can be applied to the RHS of (3.33) by setting $\kappa_1 = 1/2$, $\kappa_2 = m_{\mathrm{SR}}/\Omega_{\mathrm{SR}}$, $\kappa_3 = m_{\mathrm{SD}}/\Omega_{\mathrm{SD}}$, $\kappa_4 = m_{\mathrm{SR}}/(\theta\Omega_{\mathrm{SR}})$, $\eta_c = 1$, $\gamma_c = \hat{\gamma}_{\mathrm{SD}}$, $\eta_e = \tilde{\gamma}_{\mathrm{RD}}$ and $\gamma_e = \hat{\gamma}_{\mathrm{SR}}$, which results in the following upperbound on $P_2^{(N)}$:

$$P_2^{(N)} \leq (k_2^{(N)}\bar{\gamma})^{-(m_{\mathrm{SD}}+m_{\mathrm{SR}})}, \tag{3.36}$$

where $k_2^{(N)}$ is a nonnegative constant that does not depend on $\bar{\gamma}$.

Finally, combining (3.29) and (3.36) completes the proof of Proposition 1.

From Proposition 1, it can be concluded that the diversity order contributed by the dual–hop S–R–D link is equal to the minimum of m_{SR} and m_{RD}. It means that the resulting diversity of the S–R–D link is solely determined by the more severely faded link. It should be noted that the same phenomenon in Nakagami fading channels is also observed and proved in the context of AF relaying systems [P14, P30].

3.3.2 Hoyt Fading Channels

For Hoyt fading channels, the pdfs of the S–R, R–D and S–D link SNRs are given as follows [P22]

$$p_{\gamma_{\mathrm{SR}}}^{(H)}(\gamma_{\mathrm{SR}}) = \frac{1+q_{\mathrm{SR}}^2}{2q_{\mathrm{SR}}\bar{\gamma}_{\mathrm{SR}}}\exp\left[-\frac{(1+q_{\mathrm{SR}}^2)^2\gamma_{\mathrm{SR}}}{4q_{\mathrm{SR}}^2\bar{\gamma}_{\mathrm{SR}}}\right]I_0\left[\frac{(1-q_{\mathrm{SR}}^4)\gamma_{\mathrm{SR}}}{4q_{\mathrm{SR}}^2\bar{\gamma}_{\mathrm{SR}}}\right], \tag{3.37}$$

$$p_{\gamma_{\mathrm{RD}}}^{(H)}(\gamma_{\mathrm{RD}}) = \frac{1+q_{\mathrm{RD}}^2}{2q_{\mathrm{RD}}\bar{\gamma}_{\mathrm{RD}}}\exp\left[-\frac{(1+q_{\mathrm{RD}}^2)^2\gamma_{\mathrm{RD}}}{4q_{\mathrm{RD}}^2\bar{\gamma}_{\mathrm{RD}}}\right]I_0\left[\frac{(1-q_{\mathrm{RD}}^4)\gamma_{\mathrm{RD}}}{4q_{\mathrm{RD}}^2\bar{\gamma}_{\mathrm{RD}}}\right], \tag{3.38}$$

$$p_{\gamma_{\mathrm{SD}}}^{(H)}(\gamma_{\mathrm{SD}}) = \frac{1+q_{\mathrm{SD}}^2}{2q_{\mathrm{SD}}\bar{\gamma}_{\mathrm{SD}}}\exp\left[-\frac{(1+q_{\mathrm{SD}}^2)^2\gamma_{\mathrm{SD}}}{4q_{\mathrm{SD}}^2\bar{\gamma}_{\mathrm{SD}}}\right]I_0\left[\frac{(1-q_{\mathrm{SD}}^4)\gamma_{\mathrm{SD}}}{4q_{\mathrm{SD}}^2\bar{\gamma}_{\mathrm{SD}}}\right], \tag{3.39}$$

where the coefficients $q_{\rm SR}$, $q_{\rm RD}$ and $q_{\rm SD} \in (0, 1]$ and $I_0(x)$ is the zeroth–order modified Bessel function of the first kind. The Hoyt distribution spans the range from one–sided Gaussian fading ($q = 0$) to Rayleigh fading ($q = 1$).

To calculate the maximal diversity order of the smart relaying systems, one needs to take the expectation of (3.13) over all the channel variables with their pdfs given in (3.37), (3.38) and (3.39). The main difficulty of such calculation is mostly due to the existence of function $I_0(x)$ in the pdfs of the Hoyt RVs. However, as far as the diversity order of smart relaying is concerned, one can safely upperbound the Hoyt distributions as long as the decaying factors of the bounds (i.e., the diversity orders) are preserved. Fortunately, the following upperbound on the νth–order modified Bessel function of the first kind, $I_\nu(x)$, is helpful in this regard [P31]:

$$I_\nu(x) < x^\nu 2^\nu \Gamma(\nu + 1) \exp(x). \tag{3.40}$$

For the special case of zeroth–order function, i.e., $\nu = 0$, the bound is $I_0(x) < \exp(x)$. Thus, the pdfs of SNRs $\gamma_{\rm SR}$, $\gamma_{\rm RD}$ and $\gamma_{\rm SD}$ can be respectively bounded as

$$p^{(H)}_{\gamma_{\rm SR}}(\gamma_{\rm SR}) < \frac{a_{\rm SR}}{\bar{\gamma}_{\rm SR}} \exp\left[-\frac{b_{\rm SR}\gamma_{\rm SR}}{\bar{\gamma}_{\rm SR}}\right] = \tilde{p}_{\gamma_{\rm SR}}(\gamma_{\rm SR}), \tag{3.41}$$

$$p^{(H)}_{\gamma_{\rm RD}}(\gamma_{\rm RD}) < \frac{a_{\rm RD}}{\bar{\gamma}_{\rm RD}} \exp\left[-\frac{b_{\rm RD}\gamma_{\rm RD}}{\bar{\gamma}_{\rm RD}}\right] = \tilde{p}_{\gamma_{\rm RD}}(\gamma_{\rm RD}), \tag{3.42}$$

$$p^{(H)}_{\gamma_{\rm SD}}(\gamma_{\rm SD}) < \frac{a_{\rm SD}}{\bar{\gamma}_{\rm SD}} \exp\left[-\frac{b_{\rm SD}\gamma_{\rm SD}}{\bar{\gamma}_{\rm SD}}\right] = \tilde{p}_{\gamma_{\rm SD}}(\gamma_{\rm SD}), \tag{3.43}$$

where $a_{\rm SR} = (1 + q^2_{\rm SR})/(2q_{\rm SR})$, $a_{\rm RD} = (1 + q^2_{\rm RD})/(2q_{\rm RD})$ and $a_{\rm SD} = (1 + q^2_{\rm SD})/(2q_{\rm SD})$. Similarly, $b_{\rm SR} = (1 + q^2_{\rm SR})/2$, $b_{\rm RD} = (1 + q^2_{\rm RD})/2$ and $b_{\rm SD} = (1 + q^2_{\rm SD})/2$.

The overall probability $P_b^{(H)}$ can now be bounded as follows:

$$P_b^{(H)} < \int_0^\infty \int_0^\infty \int_0^\infty P_b(\gamma_{\rm SR}, \gamma_{\rm RD}, \gamma_{\rm SD}) \tilde{p}_{\gamma_{\rm SR}}(\gamma_{\rm SR}) \tilde{p}_{\gamma_{\rm RD}}(\gamma_{\rm RD}) \tilde{p}_{\gamma_{\rm SD}}(\gamma_{\rm SD}) d\gamma_{\rm SR} d\gamma_{\rm RD} d\gamma_{\rm SD} \tag{3.44}$$

$$= P_1^{(H)} + P_2^{(H)}, \tag{3.45}$$

where $P_b(\gamma_{\rm SR}, \gamma_{\rm RD}, \gamma_{\rm SD})$ is given in (3.13). The probabilities $P_1^{(H)}$ and $P_2^{(H)}$ are defined

as

$$P_1^{(H)} = \int_0^\infty \int_0^\infty \int_0^\infty P_1^{(H)}(\gamma_{\rm SR}, \gamma_{\rm RD}, \gamma_{\rm SD}) \tilde{p}_{\gamma_{\rm SR}}(\gamma_{\rm SR}) \tilde{p}_{\gamma_{\rm RD}}(\gamma_{\rm RD}) \tilde{p}_{\gamma_{\rm SD}}(\gamma_{\rm SD}) d\gamma_{\rm SR} d\gamma_{\rm RD} d\gamma_{\rm SD}, \tag{3.46}$$

$$P_2^{(H)} = \int_0^\infty \int_0^\infty \int_0^\infty P_2^{(H)}(\gamma_{\rm SR}, \gamma_{\rm RD}, \gamma_{\rm SD}) \tilde{p}_{\gamma_{\rm SR}}(\gamma_{\rm SR}) \tilde{p}_{\gamma_{\rm RD}}(\gamma_{\rm RD}) \tilde{p}_{\gamma_{\rm SD}}(\gamma_{\rm SD}) d\gamma_{\rm SR} d\gamma_{\rm RD} d\gamma_{\rm SD}, \tag{3.47}$$

where $P_1^{(H)}(\gamma_{\rm SR}, \gamma_{\rm RD}, \gamma_{\rm SD})$ and $P_2^{(H)}(\gamma_{\rm SR}, \gamma_{\rm RD}, \gamma_{\rm SD})$ are specified in (3.14) and (3.15), respectively.

The next two propositions establish the diversity order 2 of both $P_1^{(H)}$ and $P_2^{(H)}$.

Proposition 2. *For Hoyt fading channels and BPSK modulation, the average probability $P_1^{(H)}$ can be upperbounded as $P_1^{(H)} \leq I_1^{(H)}$, where $I_1^{(H)}$ decays with an exponent equal to two, i.e.,*

$$P_1^{(H)} \leq I_1^{(H)} \bar{\gamma} \to \infty \approx (k_1^{(H)} \bar{\gamma})^{-2}, \tag{3.48}$$

where $k_1^{(H)}$ is a nonnegative constant that depends on $(\Omega_{SR}, \Omega_{RD}, \Omega_{SD})$.

Proof: See Appendix 3.A.

Proposition 3. *For Hoyt fading channels and BPSK modulation, the average probability $P_2^{(H)}$ can be upperbounded as $P_2^{(H)} \leq I_2^{(H)}$, where $I_2^{(H)}$ decays with an exponent equal to two, i.e.,*

$$P_2^{(H)} \leq I_2^{(H)} \bar{\gamma} \to \infty \approx (k_2^{(H)} \bar{\gamma})^{-2}, \tag{3.49}$$

where $k_2^{(H)}$ is a nonnegative constant that depends on $(\Omega_{SR}, \Omega_{SD})$.

Proof: See Appendix 3.B.

Propositions 1 and 2 therefore demonstrate that the smart relaying systems under Hoyt fading channels can always achieve the maximal diversity of 2. Since Rayleigh fading is a special case of Hoyt fading when $q = 1$, all the corresponding analytical results done in [P19] are colligated by Propositions 1 and 2.

3.4 Numerical Results

Numerical results of the bit error probabilities for the smart relaying systems when BPSK modulation is employed are presented in this section to verify the diversity order analysis carried out in the previous section. Three possible settings for practical SNRs, i.e., S is close to R, R is close to D and the three nodes are equidistant, are studied. Let $(\bar{\gamma}_{\rm SR}, \bar{\gamma}_{\rm RD}, \bar{\gamma}_{\rm SD})$ denote the average SNRs of the S–R, R–D and S–D links, respectively. The three settings mentioned above are assumed to correspond to the following three cases: $(\bar{\gamma}_{\rm SR}, \bar{\gamma}_{\rm RD}, \bar{\gamma}_{\rm SD}) = (\bar{\gamma}+10{\rm dB}, \bar{\gamma}, \bar{\gamma})$, $(\bar{\gamma}, \bar{\gamma}+10{\rm dB}, \bar{\gamma})$ and $(\bar{\gamma}, \bar{\gamma}, \bar{\gamma})$, where $\bar{\gamma} = E_s/N_0$.

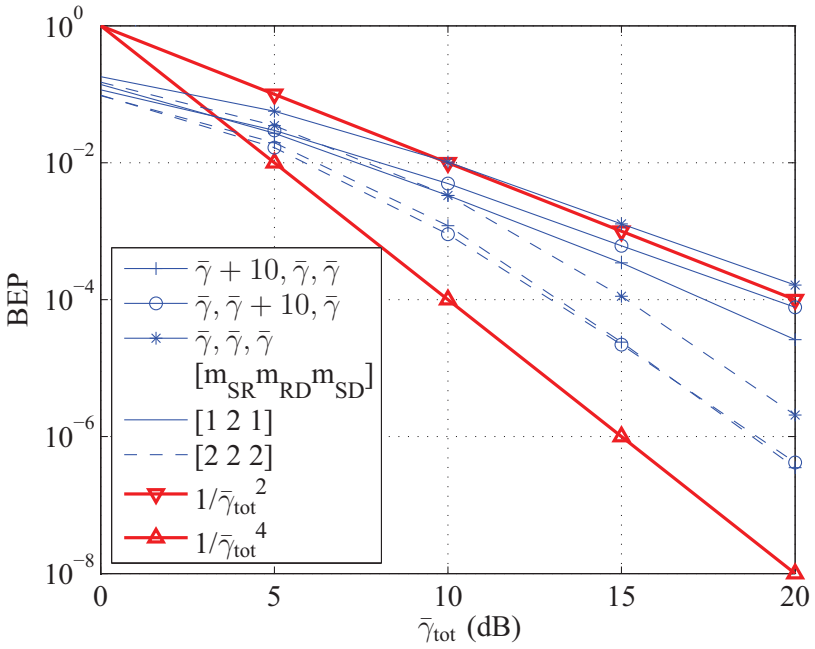

Figure 3.2 Performance of BPSK over Nakagami fading channels under different SNR triples.

For a fair comparison among different schemes, the total power used in all schemes is fixed to be

$$\bar{\gamma}_{\rm tot} = \bar{\gamma}[1 + E(\alpha_1)], \tag{3.50}$$

where $E(\alpha_1)$ is the average power scaling at the relay. For Nakagami fading channels,

$E^{(N)}(\alpha_1)$ is found to be

$$E^{(N)}(\alpha_1) = 1 + \frac{\Omega_{\mathrm{SR}}\gamma\left(m_{\mathrm{SR}}+1, \frac{\theta\Omega_{\mathrm{RD}}m_{\mathrm{SR}}}{\Omega_{\mathrm{SR}}}\right)}{\theta\Omega_{\mathrm{RD}}m_{\mathrm{SR}}\Gamma(m_{\mathrm{SR}})} - \frac{\gamma\left(m_{\mathrm{SR}}, \frac{\theta\Omega_{\mathrm{RD}}m_{\mathrm{SR}}}{\Omega_{\mathrm{SR}}}\right)}{\Gamma(m_{\mathrm{SR}})}. \tag{3.51}$$

For Hoyt fading channels, the closed–form expression of $E^{(H)}(\alpha_1)$ is not available and $E^{(H)}(\alpha_1)$ is computed numerically. Furthermore the numerical results are obtained with different channel realizations for each setting as well as for each total power consumption specified in (3.50). At least 300 bit errors are counted for each total power value.

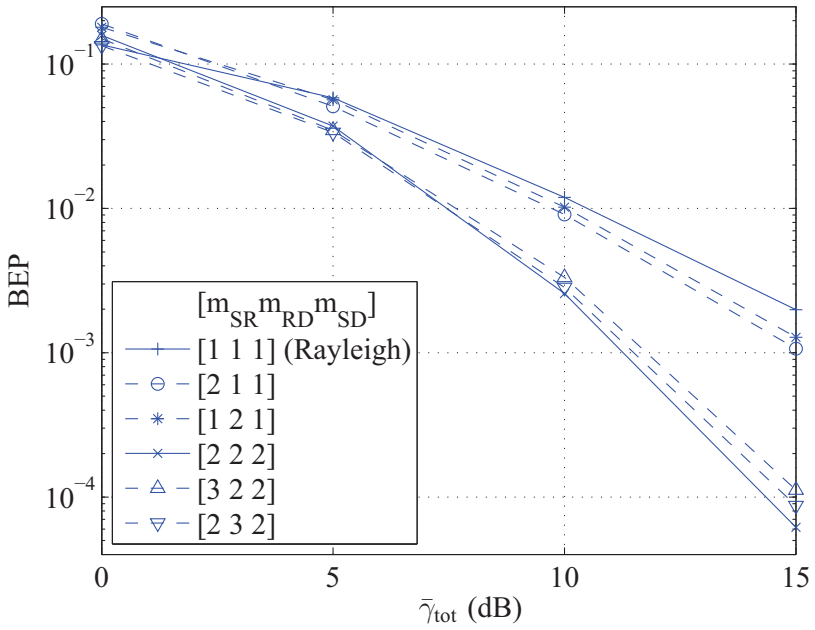

Figure 3.3 Performance of BPSK over Nakagami fading channels with equidistant relaying.

For Nakagami channels, Fig. 3.2 examines the obtainable diversity orders for two cases of $[m_{\mathrm{SR}}\ m_{\mathrm{RD}}\ m_{\mathrm{SD}}] = [1\ 2\ 1]$ and $[m_{\mathrm{SR}}\ m_{\mathrm{RD}}\ m_{\mathrm{SD}}] = [2\ 2\ 2]$. In order to show the achievable diversity orders more clearly, two curves of $1/\bar{\gamma}_{\mathrm{tot}}^2$ and $1/\bar{\gamma}_{\mathrm{tot}}^4$ are also included in Fig. 3.2. Since the two curves have the diversity orders of 2 and 4 (measured in the log-log scale), respectively, they can be used as references. It can be observed from Fig. 3.2 that, as predicted by the analysis in previous section, the smart relaying systems achieve the maximal diversity orders of 2 and 4 for the

two cases of $[m_{\mathrm{SR}}\ m_{\mathrm{RD}}\ m_{\mathrm{SD}}] = [1\ 2\ 1]$ and $[m_{\mathrm{SR}}\ m_{\mathrm{RD}}\ m_{\mathrm{SD}}] = [2\ 2\ 2]$, respectively. Moreover, observe that when $\bar{\gamma}_{\mathrm{SR}}$ or $\bar{\gamma}_{\mathrm{RD}}$ is 10dB higher than the other channel SNRs, the error performance improves compared to the equidistant case. In particular, more than 1dB improvement is realized when $[m_{\mathrm{SR}}\ m_{\mathrm{RD}}\ m_{\mathrm{SD}}] = [1\ 2\ 1]$ and about 2dB is possible when $[m_{\mathrm{SR}}\ m_{\mathrm{RD}}\ m_{\mathrm{SD}}] = [2\ 2\ 2]$. The results in Fig. 3.2 shows that smart relaying can work very effectively wherever the relay is placed, but for simplicity the results presented in Fig. 3.3 are confined to the equidistant case.

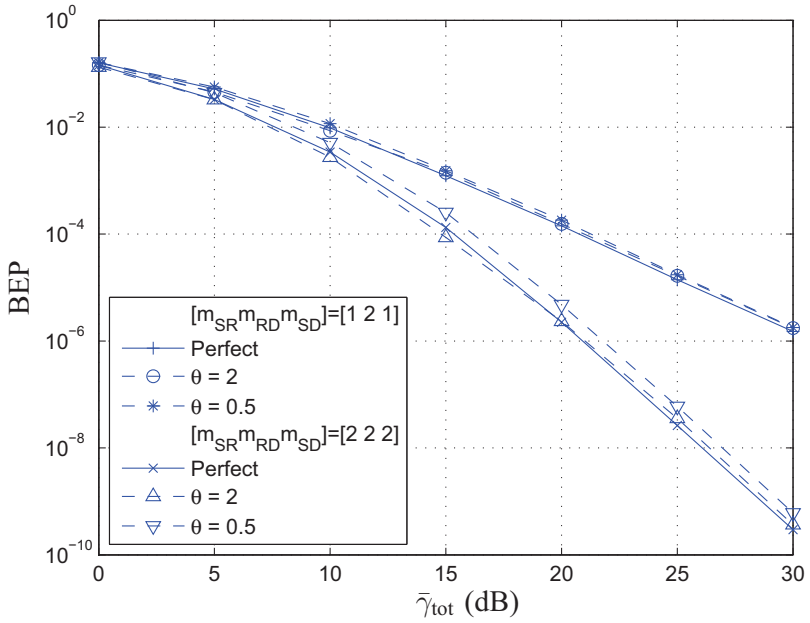

Figure 3.4 Performance of BPSK over Nakagami fading channels under equidistant relaying and different feedback channel conditions.

Similar to Fig. 3.2, Fig. 3.3 verifies that the diversity order achieved by smart relaying is equal to $m_{\mathrm{SD}} + \min\{m_{\mathrm{SR}}, m_{\mathrm{RD}}\}$. In particular, results plotted for the cases of $[m_{\mathrm{SR}}\ m_{\mathrm{RD}}\ m_{\mathrm{SD}}] = [1\ 1\ 1]$, $[m_{\mathrm{SR}}\ m_{\mathrm{RD}}\ m_{\mathrm{SD}}] = [2\ 1\ 1]$ and $[m_{\mathrm{SR}}\ m_{\mathrm{RD}}\ m_{\mathrm{SD}}] = [1\ 2\ 1]$ all exhibit the diversity order of 2. Note also that the result for the case of $[m_{\mathrm{SR}}\ m_{\mathrm{RD}}\ m_{\mathrm{SD}}] = [1\ 1\ 1]$ agrees with that reported in [P19] for Rayleigh fading channels. Similarly, the BEP curves corresponding to $[m_{\mathrm{SR}}\ m_{\mathrm{RD}}\ m_{\mathrm{SD}}] = [2\ 2\ 2]$, $[m_{\mathrm{SR}}\ m_{\mathrm{RD}}\ m_{\mathrm{SD}}] = [3\ 2\ 2]$ and $[m_{\mathrm{SR}}\ m_{\mathrm{RD}}\ m_{\mathrm{SD}}] = [2\ 3\ 2]$ all have the decaying factor of 4.

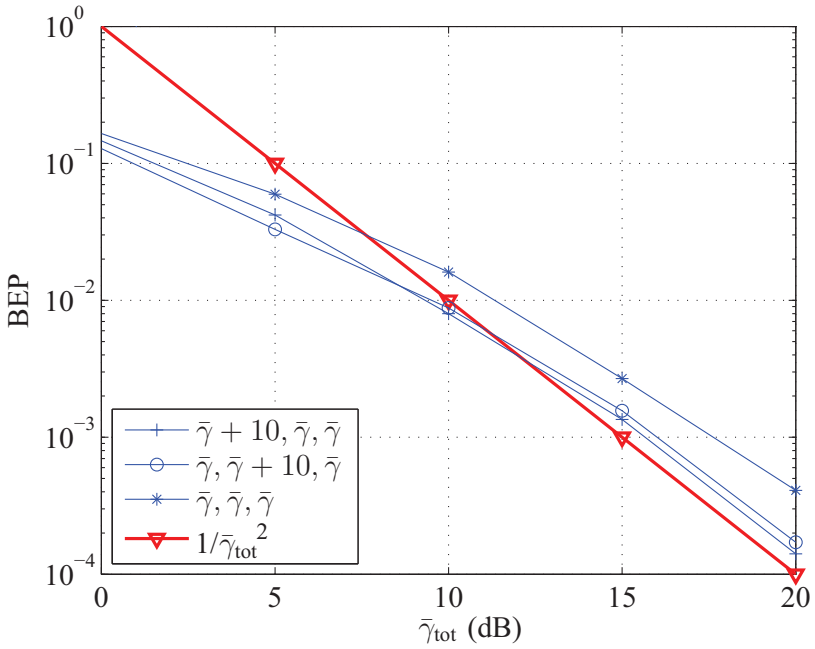

Figure 3.5 Performance of BPSK over Hoyt fading channels under different SNR triples and $q = 0.5$.

Fig. 3.4 investigates the effect of the feedback channel quality on the performance of the smart relaying systems under Nakagami channels. As shown in Fig. 3.4, regardless of the quality of the feedback link, the achievable diversity orders are 2 and 4 when $[m_{\text{SR}}\ m_{\text{RD}}\ m_{\text{SD}}] = [1\ 2\ 1]$ and $[m_{\text{SR}}\ m_{\text{RD}}\ m_{\text{SD}}] = [2\ 2\ 2]$, respectively. A close examination of the figure reveals that, although having a perfect feedback channel yields the best error performance, the performance loss due to the imperfect feedback channel is very small.

For Hoyt fading channels, Fig. 3.5 illustrates that the smart relaying system provides the diversity order of 2 when all the links are identical, i.e., $q_{\text{SR}} = q_{\text{RD}} = q_{\text{SD}} = 0.5$. In addition, performance of the systems when $(\bar{\gamma}_{\text{SR}}, \bar{\gamma}_{\text{RD}}, \bar{\gamma}_{\text{SD}}) = (\bar{\gamma} + 10\text{dB}, \bar{\gamma}, \bar{\gamma})$ or $(\bar{\gamma}, \bar{\gamma} + 10\text{dB}, \bar{\gamma})$ is better than the one in the symmetric setting. In particular, the improvement is about 2dB at the BEP level of $= 10^{-3}$.

Fig. 3.6 examines the obtainable diversity orders of the smart relaying system under different Hoyt fading parameters and for the case of equidistant relaying. As shown in Fig. 3.6, the BEP curves decrease with the decaying factor of 2, which

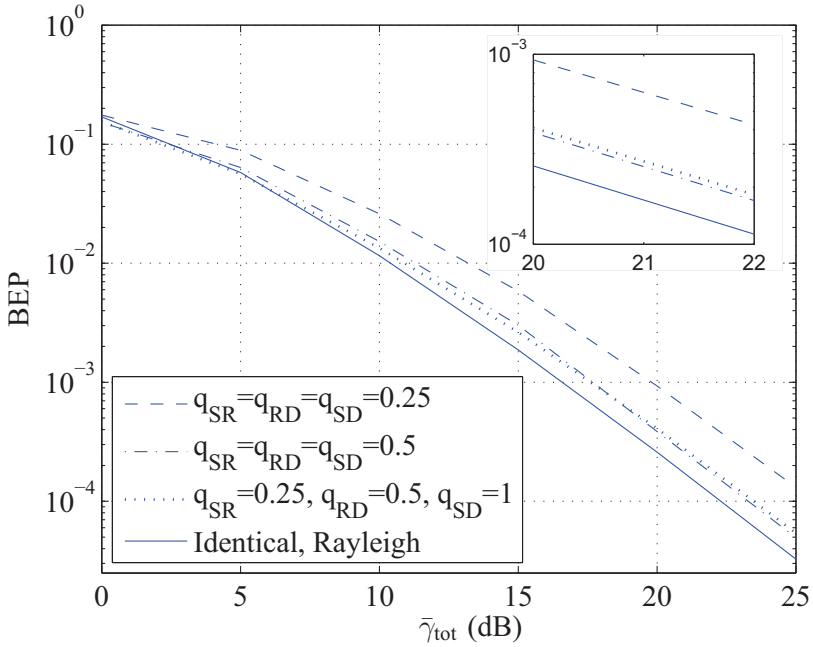

Figure 3.6 Performance of BPSK over Hoyt fading channels under equidistant relaying and different channel parameters.

agrees with the analysis made in Section 3.3. Fig. 3.6 also demonstrates that the obtained results is valid for the generalized and not–necessary–identical link parameters. Furthermore, the special case of $q_{\mathrm{SR}} = q_{\mathrm{RD}} = q_{\mathrm{SD}} = 1$ (i.e., Rayleigh fading) outperforms all the other cases. This is also expected since Rayleigh fading is the most favorable fading condition described by the Hoyt fading family.

Finally, Fig. 3.7 shows that the smart relaying systems are also very robust to the feedback channel quality in Hoyt fading environment. For the two cases of $\theta = 2$ and $\theta = 0.5$, the system attains the diversity order of 2 when $q_{\mathrm{SR}} = q_{\mathrm{RD}} = q_{\mathrm{SD}} = 0.5$.

3.5 Conclusions

This paper performed diversity analysis of smart relaying technique under the important Nakagami and Hoyt generalized fading channels for uncoded DF relaying systems when BPSK modulations is used. For Nakagami channels, it was proved that the attainable diversity order is $m_{\mathrm{SD}} + \min\{m_{\mathrm{SR}}, m_{\mathrm{RD}}\}$. For Hoyt channels, the diversity order is 2 and independent of the channel parameter q. As Rayleigh

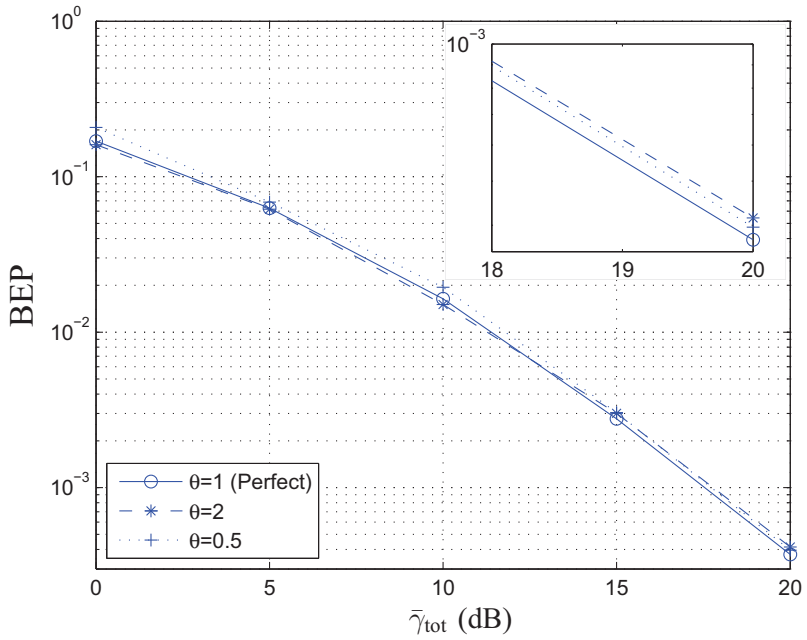

Figure 3.7 Performance of BPSK over Hoyt fading channels under equidistant relaying, $q = 0.5$ and different feedback channel conditions.

distribution is a special case of Nakagami or Hoyt distribution, all the corresponding analytical results reported in [P19] are subsumed in our analysis. Extensive numerical results were presented for the two types of fading and they all are in good agreement with the obtained analysis.

3.A Proof of Proposition 1

Using the Chernoff bound, $P_1^{(H)}$ can be bounded as follows

$$P_1^{(H)} \leq \frac{1}{2}\int_0^\infty \frac{a_{\text{SD}}}{\bar{\gamma}_{\text{SD}}} \exp\left[-\left(1+\frac{b_{\text{SD}}}{\bar{\gamma}_{\text{SD}}}\right)\gamma_{\text{SD}}\right] d\gamma_{\text{SD}} \times \int_0^\infty \int_0^\infty \frac{a_{\text{SR}}a_{\text{RD}}}{\bar{\gamma}_{\text{SR}}\bar{\gamma}_{\text{RD}}} \exp\left(-\frac{b_{\text{SR}}\gamma_{\text{SR}}}{\bar{\gamma}_{\text{SR}}}\right) \exp\left(-\frac{b_{\text{RD}}\gamma_{\text{RD}}}{\bar{\gamma}_{\text{RD}}}\right) \exp(-\alpha_1\gamma_{\text{RD}}) d\gamma_{\text{RD}} d\gamma_{\text{SR}} \tag{3.52}$$

$$= \frac{a_{\text{SR}}a_{\text{SD}}a_{\text{RD}}}{2\bar{\gamma}_{\text{SR}}\bar{\gamma}_{\text{SD}}\bar{\gamma}_{\text{RD}}(b_{\text{SD}}/\bar{\gamma}_{\text{SD}}+1)} \int_0^\infty \frac{1}{(b_{\text{RD}}/\bar{\gamma}_{\text{RD}}+\alpha_1)} \exp\left(-\frac{b_{\text{SR}}\gamma_{\text{SR}}}{\bar{\gamma}_{\text{SR}}}\right) d\gamma_{\text{SR}}. \tag{3.53}$$

Substituting α_1 in (3.5) to (3.53) leads to

$$P_1^{(H)} \leq \frac{a_{\mathrm{SR}}a_{\mathrm{SD}}a_{\mathrm{RD}}}{2\bar{\gamma}_{\mathrm{SR}}\bar{\gamma}_{\mathrm{SD}}\bar{\gamma}_{\mathrm{RD}}(b_{\mathrm{SD}}/\bar{\gamma}_{\mathrm{SD}}+1)}\Bigg[\int_0^{\theta\bar{\gamma}_{\mathrm{RD}}}\frac{\theta\bar{\gamma}_{\mathrm{RD}}}{(\theta b_{\mathrm{RD}}+\gamma_{\mathrm{SR}})}\exp\left(-\frac{b_{\mathrm{SR}}\gamma_{\mathrm{SR}}}{\bar{\gamma}_{\mathrm{SR}}}\right)d\gamma_{\mathrm{SR}} + \int_{\theta\bar{\gamma}_{\mathrm{RD}}}^{\infty}\frac{1}{(b_{\mathrm{RD}}/\bar{\gamma}_{\mathrm{RD}}+1)}\exp\left(-\frac{b_{\mathrm{SR}}\gamma_{\mathrm{SR}}}{\bar{\gamma}_{\mathrm{SR}}}\right)d\gamma_{\mathrm{SR}}\Bigg] \tag{3.54}$$

Using the fact that $\int_0^a f(x)dx \leq \int_0^\infty f(x)dx$ for $a \geq 0$ and $f(x) \geq 0$ for $x \in [0,\infty\}$, (3.54) is bounded as

$$P_1^{(H)} \leq \frac{a_{\mathrm{SR}}a_{\mathrm{SD}}a_{\mathrm{RD}}}{2\bar{\gamma}_{\mathrm{SR}}\bar{\gamma}_{\mathrm{SD}}\bar{\gamma}_{\mathrm{RD}}(b_{\mathrm{SD}}/\bar{\gamma}_{\mathrm{SD}}+1)}\Bigg[\int_0^{\infty}\frac{\theta\bar{\gamma}_{\mathrm{RD}}}{(\theta b_{\mathrm{RD}}+\gamma_{\mathrm{SR}})}\exp\left(-\frac{b_{\mathrm{SR}}\gamma_{\mathrm{SR}}}{\bar{\gamma}_{\mathrm{SR}}}\right)d\gamma_{\mathrm{SR}} + \int_{\theta\bar{\gamma}_{\mathrm{RD}}}^{\infty}\frac{1}{(b_{\mathrm{RD}}/\bar{\gamma}_{\mathrm{RD}}+1)}\exp\left(-\frac{b_{\mathrm{SR}}\gamma_{\mathrm{SR}}}{\bar{\gamma}_{\mathrm{SR}}}\right)d\gamma_{\mathrm{SR}}\Bigg]. \tag{3.55}$$

Applying [P29, pp. 341, Eq. (3.352.4)] to (3.55) results in

$$P_1^{(H)} \leq \frac{a_{\mathrm{SR}}a_{\mathrm{SD}}a_{\mathrm{RD}}}{2\bar{\gamma}_{\mathrm{SR}}\bar{\gamma}_{\mathrm{SD}}\bar{\gamma}_{\mathrm{RD}}(b_{\mathrm{SD}}/\bar{\gamma}_{\mathrm{SD}}+1)}\Bigg[-\theta\bar{\gamma}_{\mathrm{RD}}\exp\left(\frac{\theta b_{\mathrm{SR}}b_{\mathrm{RD}}}{\bar{\gamma}_{\mathrm{SR}}}\right)\mathrm{Ei}\left(-\frac{\theta b_{\mathrm{SR}}b_{\mathrm{RD}}}{\bar{\gamma}_{\mathrm{SR}}}\right) + \frac{\bar{\gamma}_{\mathrm{SR}}}{b_{\mathrm{SR}}(b_{\mathrm{RD}}/\bar{\gamma}_{\mathrm{RD}}+1)}\exp\left(-\frac{\theta b_{\mathrm{SR}}\bar{\gamma}_{\mathrm{RD}}}{\bar{\gamma}_{\mathrm{SR}}}\right)\Bigg] \tag{3.56}$$

$$\leq \frac{a_{\mathrm{SR}}a_{\mathrm{SD}}a_{\mathrm{RD}}}{2\bar{\gamma}_{\mathrm{SR}}\bar{\gamma}_{\mathrm{SD}}\bar{\gamma}_{\mathrm{RD}}(b_{\mathrm{SD}}/\bar{\gamma}_{\mathrm{SD}}+1)}\left[\theta\bar{\gamma}_{\mathrm{RD}}\ln\left(1+\frac{\bar{\gamma}_{\mathrm{SR}}}{\theta b_{\mathrm{SR}}b_{\mathrm{RD}}}\right)+\frac{\bar{\gamma}_{\mathrm{SR}}\exp\left(-\frac{\theta b_{\mathrm{SR}}\bar{\gamma}_{\mathrm{RD}}}{\bar{\gamma}_{\mathrm{SR}}}\right)}{b_{\mathrm{SR}}(b_{\mathrm{RD}}/\bar{\gamma}_{\mathrm{RD}}+1)}\right], \tag{3.57}$$

where the inequality (3.57) follows from the property $-\exp(x)\mathrm{Ei}(-x) \leq \ln(1+1/x)$, for $x \geq 0$ [P32, Eq. (5.1.20)]. Here $\mathrm{Ei}(x)$ is the exponential integral function, defined as [P29, pp. 883, Eq. 8.211.1]

$$\mathrm{Ei}(x) = -\int_{-x}^{\infty}\frac{\exp(-t)}{t}dt, \quad x < 0.$$

Upon defining $(\bar{\gamma}_{\mathrm{SR}}, \bar{\gamma}_{\mathrm{RD}}, \bar{\gamma}_{\mathrm{SD}}) = (\Omega_{\mathrm{SR}}\bar{\gamma}, \Omega_{\mathrm{RD}}\bar{\gamma}, \Omega_{\mathrm{SD}}\bar{\gamma})$, where three constants $(\Omega_{\mathrm{SR}}, \Omega_{\mathrm{RD}}, \Omega_{\mathrm{SD}})$ depend on specific systems, one can easily see that

$$P_1^{(H)} \leq I_1^{(H)}\bar{\gamma}\overset{\bar{\gamma}\to\infty}{\approx}(k_1^{(H)}\bar{\gamma})^{-2}, \tag{3.58}$$

where $k_1^{(H)}$ is a nonnegative constant that depends on $(\Omega_{\mathrm{SR}}, \Omega_{\mathrm{RD}}, \Omega_{\mathrm{SD}})$. Therefore, (3.58) proves Proposition 1.

3.B Proof of Proposition 2

First the conditional probability $P_2^{(H)}(\gamma_{\rm SR}, \gamma_{\rm RD}, \gamma_{\rm SD})$ can be upperbounded as follows:

$$P_2^{(H)}(\gamma_{\rm SR}, \gamma_{\rm RD}, \gamma_{\rm SD}) \leq Q\left(\sqrt{2\gamma_{\rm SR}}\right) Q\left[\frac{\sqrt{2}\left(\gamma_{\rm SD} - \alpha_2\gamma_{\rm RD}\right)}{\sqrt{\gamma_{\rm SD} + \alpha_2\gamma_{\rm RD}}}\right], \tag{3.59}$$

where

$$\alpha_2 = \frac{\gamma_{\rm SR}}{\theta\bar{\gamma}_{\rm RD}} \geq \frac{\min(\gamma_{\rm SR}, \theta\bar{\gamma}_{\rm RD})}{\theta\bar{\gamma}_{\rm RD}} = \alpha_1. \tag{3.60}$$

With the aid of (3.59), the average probability $P_2^{(H)}$ is bounded as

$$P_2^{(H)} \leq P_A + P_B, \tag{3.61}$$

where

$$P_A = \int_0^\infty \int_0^\infty \int_0^{\alpha_2\gamma_{\rm RD}} Q(\sqrt{2\gamma_{\rm SR}})\tilde{p}_{\gamma_{\rm SD}}(\gamma_{\rm SD})\tilde{p}_{\gamma_{\rm RD}}(\gamma_{\rm RD})\tilde{p}_{\gamma_{\rm SR}}(\gamma_{\rm SR})d\gamma_{\rm SD}d\gamma_{\rm RD}d\gamma_{\rm SR} \tag{3.62}$$

$$P_B = \int_0^\infty \int_0^\infty \int_{\alpha_2\gamma_{\rm RD}}^\infty Q(\sqrt{2\gamma_{\rm SR}})Q\left[\frac{\sqrt{2}\left(\gamma_{\rm SD} - \alpha_2\gamma_{\rm RD}\right)}{\sqrt{\gamma_{\rm SD} + \alpha_2\gamma_{\rm RD}}}\right] \tilde{p}_{\gamma_{\rm SD}}(\gamma_{\rm SD})\tilde{p}_{\gamma_{\rm RD}}(\gamma_{\rm RD})\tilde{p}_{\gamma_{\rm SR}}(\gamma_{\rm SR})d\gamma_{\rm SD}d\gamma_{\rm RD}d\gamma_{\rm SR}. \tag{3.63}$$

For probability P_A, applying the Chernoff bound to (3.62) gives

$$P_A \leq \frac{1}{2}\int_0^\infty \int_0^\infty \int_0^{\alpha_2\gamma_{\rm RD}} \exp(-\gamma_{\rm SR})\tilde{p}_{\gamma_{\rm SD}}(\gamma_{\rm SD})\tilde{p}_{\gamma_{\rm RD}}(\gamma_{\rm RD})\tilde{p}_{\gamma_{\rm SR}}(\gamma_{\rm SR})d\gamma_{\rm SD}d\gamma_{\rm RD}d\gamma_{\rm SR}. \tag{3.64}$$

The RHS of (3.64) can be averaged over the RV $\gamma_{\rm SD}$ first, then $\gamma_{\rm RD}$ and finally $\gamma_{\rm SR}$.

$$P_A \leq \frac{a_{\rm SD}}{2\bar{\gamma}_{\rm SD}} \int_0^\infty \int_0^\infty \left[\int_0^{\alpha_2\gamma_{\rm RD}} \exp(-\gamma_{\rm SR}) \exp\left(-\frac{b_{\rm SD}\gamma_{\rm SD}}{\bar{\gamma}_{\rm SD}}\right) d\gamma_{\rm SD}\right] \tilde{p}_{\gamma_{\rm RD}}(\gamma_{\rm RD})\tilde{p}_{\gamma_{\rm SR}}(\gamma_{\rm SR})d\gamma_{\rm RD}d\gamma_{\rm SR} \tag{3.65}$$

$$= I_{21} - I_{22}, \tag{3.66}$$

where

$$I_{21} = \frac{a_{\rm SD}a_{\rm RD}a_{\rm SR}}{2b_{\rm SD}b_{\rm RD}\bar{\gamma}_{\rm SR}\left(\frac{b_{\rm SR}}{\bar{\gamma}_{\rm SR}}+1\right)}, \tag{3.67}$$

$$I_{22} = \frac{a_{\rm SD}a_{\rm RD}a_{\rm SR}}{2b_{\rm SD}\bar{\gamma}_{\rm RD}\bar{\gamma}_{\rm SR}}\int_0^\infty \frac{1}{\left(\frac{b_{\rm RD}}{\bar{\gamma}_{\rm RD}}+\frac{b_{\rm SD}\gamma_{\rm SR}}{\theta\bar{\gamma}_{\rm RD}\bar{\gamma}_{\rm SD}}\right)}\exp\left[-\left(\frac{b_{\rm SR}}{\bar{\gamma}_{\rm SR}}+1\right)\gamma_{\rm SR}\right]d\gamma_{\rm SR}. \tag{3.68}$$

Applying [P29, pp. 341, Eq. (3.352.4)] to (3.68) gives

$$I_{22} \approx \frac{a_{\rm SD}a_{\rm RD}a_{\rm SR}}{2b_{\rm SD}b_{\rm RD}\bar{\gamma}_{\rm SR}\left(\frac{b_{\rm SR}}{\bar{\gamma}_{\rm SR}}+1\right)}\left[1-\frac{1}{\left(\frac{b_{\rm SR}}{\bar{\gamma}_{\rm SR}}+1\right)\frac{b_{\rm RD}\theta\bar{\gamma}_{\rm SD}}{b_{\rm SD}}}\right], \tag{3.69}$$

where the approximation (3.69) is obtained with the help of [P29, pp. 885, Eq. (8.215)].

Replacing (3.67) and (3.69) into (3.66), one can upperbound P_A as

$$P_A \le \frac{a_{\rm SD}a_{\rm RD}a_{\rm SR}}{2b_{\rm RD}^2\theta\bar{\gamma}_{\rm SD}\bar{\gamma}_{\rm SR}\left(\frac{b_{\rm SR}}{\bar{\gamma}_{\rm SR}}+1\right)^2} \overset{\bar{\gamma}\to\infty}{\approx} (k_A\bar{\gamma})^{-2}, \tag{3.70}$$

where the nonnegative constant k_A depends on $(\Omega_{\rm SR}, \Omega_{\rm SD})$.

For the second probability P_B, its upperbound can be calculated as

$$\begin{aligned} P_B \le \frac{1}{4}\int_0^\infty\int_0^\infty\int_{\alpha_2\gamma_{\rm RD}}^\infty \exp(-\gamma_{\rm SR})\exp\left[-\frac{\left(\gamma_{\rm SD}-\alpha_2\gamma_{\rm RD}\right)^2}{\gamma_{\rm SD}+\alpha_2\gamma_{\rm RD}}\right] \\ \times \tilde{p}_{\gamma_{\rm SD}}(\gamma_{\rm SD})\tilde{p}_{\gamma_{\rm RD}}(\gamma_{\rm RD})\tilde{p}_{\gamma_{\rm SR}}(\gamma_{\rm SR})d\gamma_{\rm SD}d\gamma_{\rm RD}d\gamma_{\rm SR}, \end{aligned} \tag{3.71}$$

where the Chernoff bound is applied to (3.71). The Cauchy-Schwarz inequality[4], i.e., $x+y \ge 2\sqrt{xy}$, for x, $y \ge 0$, is used to bound (3.71) as

$$\begin{aligned} P_B &\le \frac{1}{4}\int_0^\infty\int_0^\infty\int_{\alpha_2\gamma_{\rm RD}}^\infty \exp(-\gamma_{\rm SR})\exp\left[-\left(\gamma_{\rm SD}+\alpha_2\gamma_{\rm RD}-2\sqrt{\alpha_2\gamma_{\rm RD}\gamma_{\rm SD}}\right)\right] \\ &\quad\times \tilde{p}_{\gamma_{\rm SD}}(\gamma_{\rm SD})\tilde{p}_{\gamma_{\rm RD}}(\gamma_{\rm RD})\tilde{p}_{\gamma_{\rm SR}}(\gamma_{\rm SR})d\gamma_{\rm SD}d\gamma_{\rm RD}d\gamma_{\rm SR} \end{aligned} \tag{3.72}$$

$$\begin{aligned} &\le \frac{1}{4}\int_0^\infty\int_0^\infty\int_0^\infty \exp(-\gamma_{\rm SR})\exp\left[-\left(\gamma_{\rm SD}+\alpha_2\gamma_{\rm RD}-2\sqrt{\alpha_2\gamma_{\rm RD}\gamma_{\rm SD}}\right)\right] \\ &\quad\times \tilde{p}_{\gamma_{\rm SD}}(\gamma_{\rm SD})\tilde{p}_{\gamma_{\rm RD}}(\gamma_{\rm RD})\tilde{p}_{\gamma_{\rm SR}}(\gamma_{\rm SR})d\gamma_{\rm SD}d\gamma_{\rm RD}d\gamma_{\rm SR} \end{aligned} \tag{3.73}$$

[4]The Cauchy-Schwarz inequality states that for two vectors $\mathbf{u}$ and $\mathbf{v}$, one has $\langle\mathbf{u},\mathbf{v}\rangle \le \|\mathbf{u}\|\|\mathbf{v}\|$. Taking $\mathbf{u} = [\sqrt{x}, \sqrt{y}]$, $\mathbf{v} = [1,1]$ yields the inequality. However the inequality $x+y \ge 2\sqrt{xy}$, for x, $y \ge 0$, is better recognized as the arithmetic and geometric (AM-GM) bound.

where the inequality (3.73) comes from the fact that $\int_a^\infty f(x)dx \leq \int_0^\infty f(x)dx$, $f(x) \geq 0\ \forall x \in [0,\infty\}$, and $a \geq 0$.

Define $I_3(\gamma_{\mathrm{RD}}, \gamma_{\mathrm{SR}}, \gamma_{\mathrm{RD}})$ as the integrand function in (3.73). In the next steps, $I_3(\gamma_{\mathrm{RD}}, \gamma_{\mathrm{SR}}, \gamma_{\mathrm{RD}})$ is averaged over γ_{SD}, then γ_{RD} and finally γ_{SR}. First, $I_3(\gamma_{\mathrm{SR}}, \gamma_{\mathrm{RD}})$ can be calculated as

$$I_3(\gamma_{\mathrm{SR}}, \gamma_{\mathrm{RD}}) = \frac{1}{4}\exp(-\gamma_{\mathrm{SR}})\tilde{p}_{\gamma_{\mathrm{RD}}}(\gamma_{\mathrm{RD}})\tilde{p}_{\gamma_{\mathrm{SR}}}(\gamma_{\mathrm{SR}})\int_0^\infty \frac{a_{\mathrm{SD}}}{\bar{\gamma}_{\mathrm{SD}}} \times \exp\left[-\left(\sqrt{\left(1+\frac{b_{\mathrm{SD}}}{\bar{\gamma}_{\mathrm{SD}}}\right)\gamma_{\mathrm{SD}}} - \sqrt{\frac{\alpha_2\gamma_{\mathrm{RD}}}{\left(1+\frac{b_{\mathrm{SD}}}{\bar{\gamma}_{\mathrm{SD}}}\right)}}\right)^2 - \frac{b_{\mathrm{SD}}\alpha_2\gamma_{\mathrm{RD}}}{\left(1+\frac{b_{\mathrm{SD}}}{\bar{\gamma}_{\mathrm{SD}}}\right)}\right] d\gamma_{\mathrm{SD}}. \tag{3.74}$$

For simplicity, let $\beta_1 = (1 + b_{\mathrm{SD}}/\bar{\gamma}_{\mathrm{SD}})$. Then $I_3(\gamma_{\mathrm{SR}}, \gamma_{\mathrm{RD}})$ can be evaluated by changing the variable γ_{SD} to the new variable $u = \sqrt{\beta_1\gamma_{\mathrm{SD}}} - \sqrt{\alpha_2\gamma_{\mathrm{RD}}/\beta_1}$. After some manipulations, (3.74) becomes

$$\begin{aligned} I_3(\gamma_{\mathrm{SR}}, \gamma_{\mathrm{RD}}) \leq{}& \frac{a_{\mathrm{SD}}}{2\beta_1\bar{\gamma}_{\mathrm{SD}}}\exp(-\gamma_{\mathrm{SR}})\tilde{p}_{\gamma_{\mathrm{RD}}}(\gamma_{\mathrm{RD}})\tilde{p}_{\gamma_{\mathrm{SR}}}(\gamma_{\mathrm{SR}})\exp\left(-\frac{b_{\mathrm{SD}}\alpha_2\gamma_{\mathrm{RD}}}{b_{\mathrm{SD}}+\bar{\gamma}_{\mathrm{SD}}}\right) \\ &\times\left[\frac{1}{2}\exp(-\alpha_2\gamma_{\mathrm{RD}}/\beta_1) + \sqrt{\pi}\sqrt{\alpha_2\gamma_{\mathrm{RD}}/\beta_1}\right], \end{aligned} \tag{3.75}$$

where (3.75) is derived with the help of the property $\int_{-a}^\infty \exp(-u^2)du \leq \sqrt{\pi}$, for $a \geq 0$.

With (3.75), the probability P_B can be bounded as

$$P_B \leq I_{31} + I_{32}. \tag{3.76}$$

where

$$I_{31} = \frac{a_{\mathrm{SD}}a_{\mathrm{RD}}}{2\beta_1\bar{\gamma}_{\mathrm{SD}}\bar{\gamma}_{\mathrm{RD}}}\int_0^\infty \exp(-\gamma_{\mathrm{SR}})\tilde{p}_{\gamma_{\mathrm{SR}}}(\gamma_{\mathrm{SR}}) \left\{\int_0^\infty \exp\left[-\left(\frac{b_{\mathrm{RD}}}{\bar{\gamma}_{\mathrm{RD}}} + \frac{\gamma_{\mathrm{SR}}}{\theta\bar{\gamma}_{\mathrm{RD}}}\right)\gamma_{\mathrm{RD}}\right] d\gamma_{\mathrm{SD}}\right\} d\gamma_{\mathrm{SR}} \tag{3.77}$$

$$I_{32} = \frac{\sqrt{\pi}a_{\mathrm{SD}}a_{\mathrm{RD}}}{2\beta_1\bar{\gamma}_{\mathrm{SD}}\bar{\gamma}_{\mathrm{RD}}}\int_0^\infty \exp(-\gamma_{\mathrm{SR}})\tilde{p}_{\gamma_{\mathrm{SR}}}(\gamma_{\mathrm{SR}}) \times\left\{\int_0^\infty \exp\left[-\left(\frac{b_{\mathrm{RD}}}{\bar{\gamma}_{\mathrm{RD}}} + \frac{b_{\mathrm{SD}}\gamma_{\mathrm{SR}}}{\theta\bar{\gamma}_{\mathrm{RD}}(b_{\mathrm{SD}}+\bar{\gamma}_{\mathrm{SD}})}\right)\gamma_{\mathrm{RD}}\right]\sqrt{\frac{\gamma_{\mathrm{SR}}\gamma_{\mathrm{RD}}}{\beta_1\theta\bar{\gamma}_{\mathrm{RD}}}}d\gamma_{\mathrm{SD}}\right\} d\gamma_{\mathrm{SR}}. \tag{3.78}$$

The integral I_{31} can be computed as follows

$$I_{31} = -\frac{a_{\mathrm{SD}}a_{\mathrm{RD}}a_{\mathrm{SR}}\theta}{2\bar{\gamma}_{\mathrm{SR}}(b_{\mathrm{SD}}+\bar{\gamma}_{\mathrm{SD}})}\exp\left[\left(1+\frac{b_{\mathrm{SR}}}{\bar{\gamma}_{\mathrm{SR}}}\right)\theta b_{\mathrm{RD}}\right]\mathrm{Ei}\left[-\left(1+\frac{b_{\mathrm{SR}}}{\bar{\gamma}_{\mathrm{SR}}}\right)\theta b_{\mathrm{RD}}\right], \tag{3.79}$$

where [P29, pp. 341, Eq. (3.352.4)] is applied to (3.79). The integral I_{32} is bounded as

$$I_{32} \leq \frac{\sqrt{\pi} a_{\mathrm{SD}} a_{\mathrm{RD}} a_{\mathrm{SR}} \Gamma^2(1.5) \sqrt{\bar{\gamma}_{\mathrm{SD}}}}{2\beta_1^{1.5} b_{\mathrm{RD}}^{1.5} \sqrt{\theta} \bar{\gamma}_{\mathrm{SR}} (b_{\mathrm{SD}} + \bar{\gamma}_{\mathrm{SD}})^{1.5}}, \tag{3.80}$$

where (3.80) is derived with the help of [P29, pp. 346, Eq. (381.4)].

By substituting (3.79) and (3.80) into (3.76), one can conclude that the second probability P_B is inversely proportional to the order 2 of the average SNR $\bar{\gamma}$, i.e.,

$$P_B \leq I_{31} + I_{32} \overset{\bar{\gamma} \to \infty}{\approx} (k_B \bar{\gamma})^{-2}, \tag{3.81}$$

where the nonnegative constant k_B depends on $(\Omega_{\mathrm{SR}}, \Omega_{\mathrm{SD}})$.

Finally, applying (3.70) and (3.81) into (3.61) completes the proof of Proposition 2.

REFERENCES

[P1] A. Sendonaris, E. Erkip, and B. Aazhang, "User cooperation diversity – part 1: System description," *IEEE Trans. Commun.*, vol. 51, pp. 1927 – 1938, Nov. 2003.

[P2] A. Sendonaris, E. Erkip, and B. Aazhang, "User cooperation diversity – part 2: Implementation aspects and performance analysis," *IEEE Trans. Commun.*, vol. 51, pp. 1939 – 1948, Nov. 2003.

[P3] J. N. Laneman and G. W. Wornell, "Distributed space–time–coded protocol for exploiting cooperative diversity," *IEEE Trans. Inform. Theory*, vol. 49, pp. 2415 – 2425, Oct. 2003.

[P4] J. N. Laneman, D. N. C. Tse, and G. W. Wornell, "Cooperative diversity in the wireles networks: Efficient protocols and outage behavior," *IEEE Trans. Inform. Theory*, vol. 49, pp. 3062 – 3080, Dec. 2004.

[P5] A. Ribeiro, X. Cai, and G. Giannakis, "Symbol error probabilities for general

cooperative links," *IEEE Trans. on Wireless Commun.*, vol. 4, pp. 1264–1273, May 2005.

[P6] D. Chen and J. N. Laneman, "Modulation and demodulation for cooperative diversity in wireless systems," *IEEE Trans. on Wireless Commun.*, vol. 5, pp. 1785–1794, July 2006.

[P7] S. Ikki and M. Ahmed, "Performance analysis of cooperative diversity wireless networks over Nakagami-m fading channel," *IEEE Commun. Letters*, vol. 11, pp. 334–336, April 2007.

[P8] L.-L. Yang and H.-H. Chen, "Error probability of digital communications using relay diversity over Nakagami-m fading channels," *IEEE Trans. on Wireless Commun.*, vol. 7, pp. 1806–1811, May 2008.

[P9] M. O. Hasna and M.-S. Alouini, "A performance study of dual–hop transmissions with fixed gain relays," in *Proc. IEEE ICASSP*, vol. 4, pp. IV–189–92, 2003.

[P10] S. Yiu, R. Schober, and L. Lampe, "Distributed space-time block coding," *IEEE Trans. Commun.*, vol. 54, pp. 1195 – 1206, July 2006.

[P11] P. A. Anghel and M. Kaveh, "Distributed space–time cooperative system with regenerative relays," *IEEE Trans. on Wireless Commun.*, vol. 5, pp. 3130 – 3141, Nov. 2006.

[P12] T. Wang and G. B. Giannakis, "Complex field network coding for multiuser cooperative communications," *IEEE J. Select. Areas in Commun.*, vol. 26, pp. 561 – 571, Apr. 2008.

[P13] A. Cano, T. Wang, A. Ribeiro, and G. B. Giannakis, "Link–Adaptive Distributed Coding for Multisource Cooperation," *Euraship Journal on Advances in Signal Processing*, vol. 2008, Article ID 352796, 12 pages, 2008. doi:10.1155/2008/352796.

[P14] Y. Song, M. Sarkar, and H. Shin, "Cooperative diversity with blind relays in Nakagami-m fading channels: MRC analysis," *Proc. IEEE Veh. Technol. Conf.*, pp. 1196–1200, May 2008.

[P15] J. Adeane, M. R. D. Rodrigues, and I. J. Wassell, "Characterisation of the performance of cooperative networks in Ricean fading channels," in *Proceedings of the International Conference on Telecommunications*, (Cape Town, South Africa), May 2005.

[P16] T. Wang, A. Cano, G. B. Giannakis, and J. N. Laneman, "High–performance cooperative demodulation with decode–and–forward relays," *IEEE Trans. Commun.*, vol. 55, pp. 1427–1438, July 2007.

[P17] T. Wang, R. Wang, and G. B. Giannakis, "Smart regenerative relays for link–adaptive cooperative communications," in *40th Annual Conference on Information Sciences and Systems*, pp. 1038–1043, Mar. 2006.

[P18] T. Wang, A. Cano, and G. B. Giannakis, "Link–adaptive cooperative communications without channel state information," in *Proc. IEEE Military Commun. Conf.*, pp. 1–7, Oct. 2006.

[P19] T. Wang, G. Giannakis, and R. Wang, "Smart regenerative relays for link-adaptive cooperative communications," *IEEE Trans. Commun.*, vol. 56, pp. 1950–1960, Nov. 2008.

[P20] N. H. Vien, H. H. Nguyen, and T. Le-Ngoc, "Diversity analysis of smart relaying," to appear in *IEEE Trans. Veh. Technol.*

[P21] R. U. Nabar, H. Bolcskei, and F. W. Kneubhler, "Fading relay channels: performance limits and space–time signal design," *IEEE J. Select. Areas in Commun.*, vol. 22, pp. 1099 – 1109, Aug. 2004.

[P22] M. K. Simon and M.-S. Alouini, *Digital Communication over Fading Channels.* Wiley-IEEE Press, 2th ed., 2004.

[P23] D. A. Zogas, G. K. Karagiannidis, and S. A. Kotsopoulos, "Equal gain combining over Nakagami–n (Rice) and Nakagami–q (Hoyt) generalized fading channels," *IEEE Trans. on Wireless Commun.*, vol. 4, pp. 374 – 379, Mar. 2005.

[P24] R. Radaydeh and M. Matalgah, "Non-coherent improved-gain diversity reception of binary orthogonal signals in Nakagami-q (Hoyt) mobile channels," *Communications, IET*, vol. 2, no. 2, pp. 372 – 379, Feb. 2008.

[P25] G. K. Karagiannidis, "Performance bounds of multihop wireless communications with blind relays over generalized fading channels," *IEEE Trans. on Wireless Commun.*, vol. 5, pp. 498 – 503, Mar. 2006.

[P26] C. D. Iskander and P. T. Mathiopoulos, "Exact performance analysis of dual-branch coherent equal–gain combining in Nakagami–m, Rician, and Hoyt fading," *IEEE Trans. Veh. Technol.*, vol. 57, pp. 921 – 931, Mar. 2008.

[P27] J. N. Laneman, *Cooperative Diversity in Wireless Network: Algorithms and Architectures*. PhD thesis, MIT, Cambridge, MA, 2002.

[P28] J. G. Proakis, *Digital Communications*. McGraw-Hill, 4th ed., 2001.

[P29] L. S. Gradshteyn and L. M. Ryzhik, *Tables of Integrals, Series and Products*. Academic Press, 7th ed., 2007.

[P30] Y. Li and S. Kishore, "Asymptotic analysis of amplify–and–forward relaying in Nakagami-m fading environments," *IEEE Trans. on Wireless Commun.*, pp. 4256 – 4262, Dec. 2007.

[P31] C. M. Joshi and S. K. Bissu, "Some inequalities of Bessel and modified Bessel functions," *Journal of the Australian Mathematical Society*, vol. 50, no. 2, pp. 333 – 342, 1991.

[P32] M. Abramowitz and I. A. Stegun, *Handbook of Mathematical Functions With Formulas, Graphs, and Mathematical Tables*. U.S. Department of Commerce, 1972.

4. Performance Analysis of Smart Relaying with Equal Gain Combining

N. H. Vien, H. H. Nguyen, and T. Le-Ngoc, "Performance analysis of smart relaying with equal gain combining," *submitted to Springer Wireless Personal Communications*.

In the manuscript of Chapter 3, performance analysis of the smart relaying systems under Protocol II and Nakagami and Hoyt fading channel models has been presented. The manuscript shows that the systems can effectively mitigate the error propagation phenomenon in DF and successfully achieve the maximal diversity under these channel models. It should be noted that in achieving the maximal diversity, the manuscript in Chapter 3 assumes that the destination has perfect knowledge of channel state information of the source-to-destination and relay-to-destination links in order to perform the MRC-like detection rule as in (3.7). As discussed in Chapter 2, equal gain combining (EGC) can be used as an alternative to MRC since it achieves performance comparable to MRC but with a simpler implementation. Specifically, each signal path is weighted with the same factor, irrespective of the channel fading amplitude. However, co-phasing all the signal paths is still required to avoid signal cancellation. Due to the advantages of EGC, the manuscript included in this chapter proposes a novel and low-complexity relaying system, called Smart EGC, by integrating EGC with smart relaying for DF under Nakagami and Hoyt fading channels. The performance of the proposed Smart EGC is also analyzed.

As mentioned with EGC, only the channel coefficients' phases are required at the destination and therefore the system complexity is reduced when compared to that

of Smart MRC in Chapter 3. For a single-relay system with M-PSK modulation, it is proved that under Nakagami and Hoyt fading channels, Smart EGC can always achieve the maximal diversity orders of $2m$ and 2, respectively. For the most general case when there are K relays, numerical results suggest that the proposed Smart EGC can also attain the corresponding maximal diversity orders of $m(K+1)$ and $(K+1)$ for these fading channels.

Performance Analysis of Smart Relaying with Equal Gain Combining

Nam H. Vien*, *Student Member, IEEE* and Ha H. Nguyen, *Senior Member, IEEE*, Tho Le-Ngoc, *Fellow, IEEE*

Abstract

Relaying communications has been proposed as a way to provide spatial diversity. In general, one is interested in a relaying system that can achieve the maximal diversity order with a low system complexity. One enabling technique is equal gain combining (EGC) and its application in relaying systems is the main focus of this paper. In particular, the techniques of EGC and smart relaying are combined in the decode-and-forward (DF) processing method. It is shown that for a system with one relay and M-ary phase-shift-keying (M-PSK) modulation, maximal diversity orders of $2m$ and 2 are achieved over Nakagami-m and Hoyt fading environments, respectively. With K relays, simulation results suggest that the corresponding diversity orders are $m(K+1)$ and $(K+1)$.

Index terms

Relaying communications, adaptive transmission, decode-and-forward, diversity order, equal gain combining, Nakagami-m fading, Hoyt fading.

4.1 Introduction

Recently, relaying communications has drawn much attention due to its ability to exploit spatial diversity while avoiding the need of co-located antenna arrays (see, for example [P1–P4] and [P5]). If properly designed, the system can achieve a diversity order up to the number of diversity paths, what can be referred to as the *maximal* diversity order [P6]. To exploit such inherent spatial diversity, some signal processing

Nam H. Vien (*contact author) and Ha H. Nguyen are with the Department of Electrical & Computer Engineering, University of Saskatchewan, 57 Campus Dr., Saskatoon, SK, Canada S7N 5A9. Emails: nam.vien@usask.ca, ha.nguyen@usask.ca.

Tho Le-Ngoc is with the Department of Electrical & Computer Engineering, McGill University, 3480 University St., Montreal, Quebec, Canada H3A 2A7. Email: tho@ece.mcgill.ca.

methods have been proposed in the literature, e.g., decode-and-forward (DF) and amplify-and-forward (AF) [P3]. For DF, a relay (R) decodes the source signals before resending them to the destination (D). On the other hand, for AF, R simply amplifies the received signals without decoding them and forwards the amplified versions to D.

For DF, the maximal diversity with binary-phase-shift-keying (BPSK) modulation can be achieved with the maximal likelihood (ML) coherent demodulation [P2]. However, the ML demodulation becomes prohibitively complex for high-order constellations. To reduce the complexity, many sub-optimum detection schemes were proposed. For example, the cooperative-MRC (C-MRC) is shown in [P6] to perform close to that of the optimal ML demodulation for BPSK and it can obtain the maximal diversity *regardless* of the underlying constellations. An equivalence of the relaying system with C-MRC at D is the smart relaying scheme described in [P7–P9], where the transmission power at R is scaled by an adaptive weighting coefficient. In [P10], SC technique was incorporated into C-MRC as well as smart relaying in order to increase the bandwidth efficiency.

It should be pointed out that, in achieving the maximal diversity, the works in [P2, P6, P11–P13] assume that D has a perfect knowledge of the channel state information (CSI) of all the channel links, namely the source-destination (SD), source-relay (SR) and relay-destination (RD) links. The overall complexity also increases in proportion to the number of relays. For the proposed schemes in [P7–P10], which can be referred to as Smart MRC, the system complexity is reduced but the schemes still require CSI of the SD and RD links at D. It is well-known that alternative combining techniques such as equal gain combining (EGC) are often used in practice because the system complexity is decreased when compared to that of MRC scheme [P14]. In deed, the EGC scheme weights each branch with an equal gain before combining and therefore does not requires the estimation of the fading amplitudes.

Motivated by the above discussions, in this paper, a novel and low-complexity, repetition-based relaying system is proposed by integrating EGC technique with DF to achieve the maximal diversity. In particular, smart relaying and EGC are com-

bined, which result in a Smart EGC scheme. As Nakagami and Hoyt fading models[1] is shown to excellently match experimental fading channel measurements in wireless communications [P14–P17], it is important to study the performance of Smart EGC under these fading models and it is one of the main objective of the paper. With the average signal-to-noise ratio (SNR) of the RD link available at R via a low-rate feedback channel, it is proved that under Nakagami-m and Hoyt fading, Smart EGC can obtain the maximal diversity orders of $2m$ and 2, respectively, for any M-PSK modulation when there is one relay. For a higher number of relays, i.e., $K > 1$, simulation results suggest that the achievable diversity orders are $m(K+1)$ and $(K+1)$, respectively.

The rest of the paper is organized as follows. Section 6.2 describes the system model where the proposed Smart EGC scheme is also presented. The diversity analysis for Smart EGC scheme under Nakagami-m and Hoyt fading is carried out in Section 6.3. Simulation results and conclusions are given in Sections 6.4 and 6.5, respectively.

4.2 System Model

Consider a simple relaying system with a source S, a relay R, and a destination D. All nodes are equipped with single-antenna transmitter and receiver. Information is sent from S to D with the help of R. The system is half-duplex, in which R cannot transmit and receive at the same time. Transmission to D is carried out in 2 time slots. In the first time slot, S broadcasts its signal s to R and D. The relay R decodes the received signal from S and resends the decoded one to D during the second time slot. After receiving 2 versions of the source signal, D detects the source signal by performing equal gain combining (EGC). In order to implement EGC when only the channel coefficients' phases are available at D, M-ary phase-shift-keying (M-PSK)

[1]In fact, Nakagami and Hoyt fading channel models include the well-known Rayleigh fading channel model as a special case, i.e., $m = 1$ or $q = 1$, where m and q are respectively the fading parameters of Nakagami and Hoyt fading channel models.

modulation, which has equal symbol energy of E_s, is adopted in this paper.

Frequency-flat slow fading is assumed throughout the paper. All the channel coefficients, namely $a_{\rm SR}$, $a_{\rm RD}$ and $a_{\rm SD}$, are assumed to represent independent Nakagami-m or Hoyt fading channels with mean-square values $\Omega_{\rm SR}$, $\Omega_{\rm RD}$ and $\Omega_{\rm SD}$, respectively. Let $\gamma_{\rm PQ} = \bar{\gamma}|a_{\rm PQ}|^2$, where PQ $\in \{\rm SR, RD, SD\}$ and $\bar{\gamma} = E_s/N_0$, be the received SNR of the PQ link. For Nakagami fading[2], the probability density function (pdf) of $\gamma_{\rm PQ}$, i.e., $p^{(N)}_{\gamma_{\rm PQ}}(\gamma_{\rm PQ})$, is given as [P18]

$$p^{(N)}_{\gamma_{\rm PQ}}(\gamma_{\rm PQ}) = m^m \gamma_{\rm PQ}^{m-1} \exp\left(-m\gamma_{\rm PQ}/\bar{\gamma}_{\rm PQ}\right) / (\bar{\gamma}^m_{\rm PQ}\Gamma(m)), \tag{4.1}$$

where m is the fading parameter and assumed to be an integer. The average SNR of the PQ link, denoted by $\bar{\gamma}_{\rm PQ}$, is equal to $\bar{\gamma}\Omega_{\rm PQ}$. For Hoyt fading, the pdf of $\gamma_{\rm PQ}$, i.e., $p^{(H)}_{\gamma_{\rm PQ}}(\gamma_{\rm PQ})$, is as follows [P18].

$$p^{(H)}_{\gamma_{\rm PQ}}(\gamma_{\rm PQ}) = (1+q^2)/(2q\bar{\gamma}_{\rm PQ}) \exp\left[-(1+q^2)^2\gamma_{\rm PQ}/(4q^2\bar{\gamma}_{\rm PQ})\right] I_0\left[(1-q^4)\gamma_{\rm PQ}/(4q^2\bar{\gamma}_{\rm PQ})\right], \tag{4.2}$$

where the fading parameter $q \in (0, 1]$ and $I_0(x)$ is zeroth-order modified Bessel function of the first kind. The Hoyt fading spans from the worst one-sided Gaussian fading ($q = 0$) to Rayleigh fading ($q = 1$).

In the first time slot, the received signals at R, $y_{\rm SR}$, and at D, $y_{\rm SD}$, are respectively given as

$$y_{\rm SR} = a_{\rm SR}s + z_{\rm SR}, \tag{4.3}$$

$$y_{\rm SD} = a_{\rm SD}s + z_{\rm SD}, \tag{4.4}$$

where $z_{\rm SR}$ and $z_{\rm SD}$ represent additive white Gaussian noise (AWGN) and are modeled as independent and identically distributed (i.i.d) circularly symmetric complex Gaussian random variables of variance N_0, i.e., $\mathcal{CN}(0, N_0)$. As mentioned before, the information symbol s is drawn from an M-PSK constellation with symbol energy of E_s.

[2]Hereafter, the superscripts (N) and (H) refer to Nakagami and Hoyt fading, respectively.

In the second time slot, R forwards the decoded signal to D. The decoding at R is carried out with the coherent maximal likelihood (ML) criterion as follows:

$$\hat{s} = \arg\min_{s\in\mathcal{S}} \left\{ \left| a_{\mathrm{SR}}^{*} y_{\mathrm{SR}} - |a_{\mathrm{SR}}|^{2} s \right|^{2} \right\}, \tag{4.5}$$

where $\mathcal{S}$ denotes the M-PSK constellation with size $M = |\mathcal{S}|$ and a_{SR}^{*} is the complex conjugate of a_{SR}.

In non-adaptive forwarding strategies, R resends the decoded signal with maximal power even when it is not correct [P2,P3,P6,P19]. Not only this wastes the power but also introduces error propagation, which then degrades the overall error performance. On the other hand, the smart relaying technique, which is adopted in this paper, adapts to the SR channel quality by transmitting to D a scaled version of $\hat{s}$ with the transmit power amplification factors α given by [P8]

$$\alpha = \min(\gamma_{\mathrm{SR}}, \bar{\gamma}_{\mathrm{RD}})/\bar{\gamma}_{\mathrm{RD}} \leq 1. \tag{4.6}$$

To establish α as in (4.6), the system needs a pilot feedback channel from D to R to convey the average SNR $\bar{\gamma}_{\mathrm{RD}}$. The advantages of choosing α as in (4.6), respectively, are twofold. First, it saves the total transmitted power since α is always less than or equal to 1. Furthermore, as shall be seen later, the adaptive transmission scheme at R helps to maintain the maximal diversity order of the system even when error propagation at R is taken into account.

The received signal, y_{RD}, at D in the second time slot is

$$y_{\mathrm{RD}} = \sqrt{\alpha} a_{\mathrm{RD}} \hat{s} + z_{\mathrm{RD}}, \tag{4.7}$$

where z_{RD} is $\mathcal{CN}(0, N_0)$, which represents AWGN at D.

Regarding the combining technique at D, besides maximal ratio combining (MRC) and selection combining (SC), equal gain combining (EGC) is an attractive alternative since it does not need the estimation of the channel amplitudes. Therefore, its complexity is reduced [P18]. When EGC technique is used, the detection rule at D is as follows:

$$s' = \arg\max_{s\in\mathcal{S}} \left\{ \mathrm{Re}\left[\left(\exp(-j\phi_{\mathrm{SD}}) y_{\mathrm{SD}} + \exp(-j\phi_{\mathrm{RD}}) y_{\mathrm{RD}} \right) s^{*} \right] \right\}, \tag{4.8}$$

where ϕ_{SD} and ϕ_{RD} are the phases of the SD and RD channel coefficients, respectively, and $\mathrm{Re}(x)$ takes the real part of complex number x. Note that, to apply Smart EGC, D only needs to collect the channel coefficients' phases, i.e., ϕ_{SD} and ϕ_{RD}. On the other hand, Smart MRC in [P8] needs to know all the SD and RD channel state information. In addition, it also has to measure the power scaling factor, i.e., α, to implement MRC at D. For Smart SC in [P10], although the scheme can improve the system spectral efficiency, D also has to obtain all the instantaneous received SNRs before deciding the best path in the sense of maximizing the received SNR [P10, Sec. IV]. This means that D in Smart SC has to know the same amount of channel information as in Smart MRC. Moreover, D also needs to broadcast a private message through a pilot channel to all the relays to indicate the chosen candidate, i.e., the $\bar{k}$th relay, which involves the transmission during the second time slot. Therefore, the complexity of both Smart EGC and Smart SC is higher than that of the proposed Smart EGC.

4.3 Diversity Analysis

4.3.1 Nakagami Fading Channels

With M-PSK modulation, the transmitted signal by S in the first time slot is $s = s_l = \sqrt{E_s}\exp(j2\pi(l-1)/M)$, $l = 1, \ldots, M$. The decoded signal at R, $\hat{s}$, can be either s_l or s_n, $n = 1, \ldots, M$, $n \neq l$, with probability $[1 - P_s^{(\mathrm{SR})}(\gamma_{\mathrm{SR}})]$ or $P_s^{(\mathrm{SR})}(\gamma_{\mathrm{SR}})$, respectively. Here, $P_s^{(\mathrm{SR})}(\gamma_{\mathrm{SR}})$ is the symbol error probability (SEP) at R during the first time slot, which can be well approximated as follows [P20, Eq. 5.2-61]:

$$P_s^{(\mathrm{SR})}(\gamma_{\mathrm{SR}}) \approx 2Q\left(\sqrt{2\gamma_{\mathrm{SR}}}\sin\left(\pi/M\right)\right). \tag{4.9}$$

The overall SEP $P_s^{(N)}$ at D is then given in terms of two probabilities as follows:

$$P_s^{(N)} = P_{s,1}^{(N)} + P_{s,2}^{(N)}, \tag{4.10}$$

where $P_{s,1}^{(N)}$ and $P_{s,2}^{(N)}$ correspond to the probabilities of the events that R makes correct and wrong decoding decisions, respectively. Our target is to show that in both possibilities of decoding at R, Smart EGC still enjoys the diversity order of $2m$.

When R correctly decoded, the corresponding probability $P_{s,1}^{(N)}$ can be bounded by the union bound as follows:

$$P_{s,1}^{(N)} \leq E\Big\{(1-P_s^{(\mathrm{SR})}(\gamma_{\mathrm{SR}}))\sum_{l=1}^{M}\sum_{\substack{n=1\\n\neq l}}^{M} P(s_l \to s_n|\hat{s}=s_l,\gamma_{\mathrm{SR}},\gamma_{\mathrm{RD}},\gamma_{\mathrm{SD}})\Big\} \tag{4.11}$$

$$\leq E\Big\{\sum_{l=1}^{M}\sum_{(n=1,n\neq l)}^{M} P(s_l \to s_n|\hat{s}=s_l,\gamma_{\mathrm{SR}},\gamma_{\mathrm{RD}},\gamma_{\mathrm{SD}})\Big\}, \tag{4.12}$$

where $E\{X\}$ denotes the expectation, and $P(s_l \to s_n|\hat{s}=s_l,\gamma_{\mathrm{SR}},\gamma_{\mathrm{RD}},\gamma_{\mathrm{SD}})$ is the conditional pairwise error probability (PEP) of decoding to s_n at D while s_l was actually transmitted from both S and R (correctly decoding at R). The inequality in (4.12) comes from the fact that $(1-P_s^{(\mathrm{SR})}(\gamma_{\mathrm{SR}})) \leq 1$. The conditional PEP $P(s_l \to s_n|\hat{s}=s_l,\gamma_{\mathrm{SR}},\gamma_{\mathrm{RD}},\gamma_{\mathrm{SD}})$ is the probability of the following event:

$$\mathrm{Re}\Big\{\Big[(|a_{\mathrm{SD}}|+\sqrt{\alpha}\,|a_{\mathrm{RD}}|)s_l+z\Big]s_n^*\Big\} \geq \mathrm{Re}\Big\{\Big[(|a_{\mathrm{SD}}|+\sqrt{\alpha}\,|a_{\mathrm{RD}}|)s_l+z\Big]s_l^*\Big\}$$

$$\sqrt{E_s}\left(|a_{\mathrm{SD}}|+\sqrt{\alpha}\,|a_{\mathrm{RD}}|\right)\left(\cos\left[\frac{2\pi(l-n)}{M}\right]-1\right) \geq$$

$$\mathrm{Re}\Big\{z\Big[\exp\Big(-\frac{j2\pi l}{M}\Big)-\exp\Big(-\frac{j2\pi n}{M}\Big)\Big]\Big\}, \tag{4.13}$$

where $z=[\exp(-j\phi_{\mathrm{SD}})z_{\mathrm{SD}}+\exp(-j\phi_{\mathrm{RD}})z_{\mathrm{RD}}] \sim \mathcal{CN}(0,2N_0)$, is the equivalent noise at the output of the detector.

The probability of the event in (4.13) can be found to be

$$P(s_l \to s_n|\hat{s}=s_l,\gamma_{\mathrm{SR}},\gamma_{\mathrm{RD}},\gamma_{\mathrm{SD}}) = Q\left(\sqrt{\beta(l,n)}\,(\sqrt{\gamma_{\mathrm{SD}}}+\sqrt{\alpha\gamma_{\mathrm{RD}}})\right), \tag{4.14}$$

where $\beta(l,n)=[1-\cos(2\pi(l-n)/M)]/2$.

To evaluate the diversity order of $P_{s,1}^{(N)}$, one can use the following proposition, which establishes an upperbound on $E\{P(s_l \to s_n|\hat{s}=s_l,\gamma_{\mathrm{SR}},\gamma_{\mathrm{RD}},\gamma_{\mathrm{SD}})\}$.

Proposition 1. *For the system with one relay, M-PSK modulation and Nakagami-m fading, the average pairwise error probability* $E\{P(s_l \to s_n|\hat{s}=s_l,\gamma_{SR},\gamma_{RD},\gamma_{SD})\}$, $n \neq l$, *is upperbounded as*

$$E\{P(s_l \to s_n|\hat{s}=s_l,\gamma_{SR},\gamma_{RD},\gamma_{SD})\} \overset{\bar{\gamma}\to\infty}{\leq} (k_1^{(N)}\bar{\gamma})^{-2m}, \tag{4.15}$$

where the conditional PEP $P(s_l \to s_n|\hat{s}=s_l,\gamma_{SR},\gamma_{RD},\gamma_{SD})$ *is given in* (4.14). *The constant* $k_1^{(N)}$ *is nonnegative and depends on* $(\Omega_{SR},\Omega_{RD},\Omega_{SD})$, l, n *and the fading parameter* m.

Proof: See Appendix 4.A.

Thus, by applying Proposition 1 to the right hand side (RHS) of (4.12), it can be concluded that $P_{s,1}^{(N)}$ has the diversity order of $2m$. Such a result is well expected since the relaying system acts as a co-located antenna array and the associated symbol error probability decays with an exponent of $2m$.

For the case that a wrong decision was made at R, the union bound is used to bound $P_{s,2}^{(N)}$ as

$$P_{s,2}^{(N)} \leq E\Big\{ P_{\mathrm{SR}}^{s}(\gamma_{\mathrm{SR}}) \sum_{l=1}^{M} \sum_{(n=1,n\neq l)}^{M} \sum_{(t=1,t\neq l)}^{M} P(s_l \to s_n|\hat{s}=s_t,\gamma_{\mathrm{SR}},\gamma_{\mathrm{RD}},\gamma_{\mathrm{SD}}) \Big\}, \quad (4.16)$$

where $P(s_l \to s_n|\hat{s}=s_t,\gamma_{\mathrm{SR}},\gamma_{\mathrm{RD}},\gamma_{\mathrm{SD}})$ is the conditional PEP of decoding to s_n at D while s_l and $\hat{s}=s_t \neq s_l$ were transmitted at S and R during the first and second time slots, respectively.

The conditional PEP $P(s_l \to s_n|\hat{s}=s_t,\gamma_{\mathrm{SR}},\gamma_{\mathrm{RD}},\gamma_{\mathrm{SD}})$ is equal to the probability of the following event:

$$\begin{aligned}
&\mathrm{Re}\Big\{ \big(|a_{\mathrm{SD}}|\, s_l + \sqrt{\alpha}\,|a_{\mathrm{RD}}|\, s_t + z \big) s_n^* \Big\} \geq \mathrm{Re}\Big\{ \big(|a_{\mathrm{SD}}|\, s_l + \sqrt{\alpha}\,|a_{\mathrm{RD}}|\, s_t + z \big) s_l^* \Big\} \\
&\sqrt{E_s}\,|a_{\mathrm{SD}}| \left(\cos\left[\frac{2\pi(l-n)}{M}\right] - 1 \right) + \sqrt{E_s}\sqrt{\alpha}\,|a_{\mathrm{RD}}| \left(\cos\left[\frac{2\pi(t-n)}{M}\right] - \cos\left[\frac{2\pi(t-l)}{M}\right] \right) \\
&\qquad \geq \mathrm{Re}\Big\{ z \Big[\exp\Big(-\frac{j2\pi(l-1)}{M} \Big) - \exp\Big(-\frac{j2\pi(n-1)}{M} \Big) \Big] \Big\}. \qquad (4.17)
\end{aligned}$$

The conditional probability $P(s_l \to s_n|\hat{s}=s_t,\gamma_{\mathrm{SR}},\gamma_{\mathrm{RD}},\gamma_{\mathrm{SD}})$ can be written in a closed-form expression as

$$P(s_l \to s_n|\hat{s}=s_t,\gamma_{\mathrm{SR}},\gamma_{\mathrm{RD}},\gamma_{\mathrm{SD}}) = Q\left(\eta_{\mathrm{SD}}(l,n)\sqrt{\gamma_{\mathrm{SD}}} + \zeta_{\mathrm{RD}}(l,n,t)\sqrt{\alpha\gamma_{\mathrm{RD}}} \right), \quad (4.18)$$

where

$$\eta_{\mathrm{SD}}(l,n) = \sqrt{\Big(1 - \cos\Big[2\pi(l-n)/M\Big]\Big)/2},$$

$$\zeta_{\mathrm{RD}}(l,n,t) = \left(\cos\left[2\pi(t-l)/M\right] - \cos\left[2\pi(t-n)/M\right]\right) \Big/ \sqrt{2\left(1 - \cos\Big[2\pi(l-n)/M\Big]\right)}.$$

It should be noted that $\eta_{\mathrm{SD}}(l,n) > 0$ and $\zeta_{\mathrm{RD}}(l,n,t) \neq 0$ since $l \neq n$ and $l \neq t$.

When $\zeta_{\mathrm{RD}}(l,n,t) > 0$, the conditional probability $P(s_l \to s_n|\hat{s} = s_t, \gamma_{\mathrm{SR}}, \gamma_{\mathrm{RD}}, \gamma_{\mathrm{SD}})$ has the same form with $P(s_l \to s_n|\hat{s} = s_l, \gamma_{\mathrm{SR}}, \gamma_{\mathrm{RD}}, \gamma_{\mathrm{SD}})$ given in (4.14), except some scaling factors. Since the product $P_s^{(\mathrm{SR})}(\gamma_{\mathrm{SR}})P(s_l \to s_n|\hat{s} = s_t, \gamma_{\mathrm{SR}}, \gamma_{\mathrm{RD}}, \gamma_{\mathrm{SD}})$ can be upperbounded by $P(s_l \to s_n|\hat{s} = s_t, \gamma_{\mathrm{SR}}, \gamma_{\mathrm{RD}}, \gamma_{\mathrm{SD}})$, Proposition 1 can still be applied for $E\{P_s^{(\mathrm{SR})}(\gamma_{\mathrm{SR}})P(s_l \to s_n|\hat{s} = s_t, \gamma_{\mathrm{SR}}, \gamma_{\mathrm{RD}}, \gamma_{\mathrm{SD}})\}$. Therefore, one can conclude that when $\zeta_{\mathrm{RD}}(l,n,t) > 0$, $E\{P_s^{(\mathrm{SR})}(\gamma_{\mathrm{SR}})P(s_l \to s_n|\hat{s} = s_t, \gamma_{\mathrm{SR}}, \gamma_{\mathrm{RD}}, \gamma_{\mathrm{SD}})\}$ has the diversity order of $2m$.

Our remaining task is to find the diversity order of $E\{P_{(\mathrm{SR})}^{s}(\gamma_{\mathrm{SR}})P(s_l \to s_n|\hat{s} = s_t, \gamma_{\mathrm{SR}}, \gamma_{\mathrm{RD}}, \gamma_{\mathrm{SD}})\}$ when $\zeta_{\mathrm{RD}}(l,n,t) < 0$. The order can be asserted with the help of the following proposition.

Proposition 2. *For the system with one relay, M-PSK modulation and Nakagami-m fading,* $E\{P_s^{(SR)}(\gamma_{SR})P(s_l \to s_n|\hat{s} = s_t, \gamma_{SR}, \gamma_{RD}, \gamma_{SD})\}$, $l \neq n$, $l \neq t$ *and* $\zeta_{RD}(l,n,t) < 0$*, is upperbounded as*

$$E\{P_s^{(SR)}(\gamma_{SR})P(s_l \to s_n|\hat{s} = s_t, \gamma_{SR}, \gamma_{RD}, \gamma_{SD})\} \overset{\bar{\gamma}\to\infty}{\leq} \left(k_2^{(N)}\bar{\gamma}\right)^{-2m}, \tag{4.19}$$

where the conditional probabilities $P_s^{(SR)}(\gamma_{SR})$ *and* $P(s_l \to s_n|\hat{s} = s_t, \gamma_{SR}, \gamma_{RD}, \gamma_{SD})\}$ *are given in* (4.9) *and* (4.18)*, respectively. The constant* $k_2^{(N)}$ *is nonnegative and depends on* $(\Omega_{SR}, \Omega_{SD})$*,* l*,* n*,* t *and the fading parameter* m*.*

Proof: See Appendix 4.B.

To conclude, for either $\zeta_{\mathrm{RD}}(l,n,t) > 0$ or $\zeta_{\mathrm{RD}}(l,n,t) < 0$, the diversity order of $E\{P_s^{(\mathrm{SR})}(\gamma_{\mathrm{SR}})P(s_l \to s_n|\hat{s} = s_t, \gamma_{\mathrm{SR}}, \gamma_{\mathrm{RD}}, \gamma_{\mathrm{SD}})\}$ is $2m$. Therefore, $P_{s,2}^{(N)}$ can achieve the diversity order of $2m$.

Combining the achievable diversity order of $P_{s,1}^{(N)}$ and $P_{s,2}^{(N)}$, it can be concluded that Smart EGC can achieve the maximal diversity order of $2m$ for any M-PSK constellations.

For the general case with K relays and M-PSK modulation, it is conjectured that

the diversity order of Smart EGC is bounded by $m(K+1)$. This is supported by simulation results in Section 6.4.

4.3.2 Hoyt Fading Channels

For Hoyt fading channels, the pdfs of the received SNRs are given in (4.2). The following proposition establishes the decaying exponent for the single-relay system with M-PSK modulation.

Proposition 3. *For the system with one relay, M-PSK modulation and Hoyt fading, the average symbol error probability $P_s^{(H)}$ is upperbounded as*

$$P_s^{(H)} \overset{\bar{\gamma}\to\infty}{\leq} \left(k^{(H)}\bar{\gamma}\right)^{-2}, \tag{4.20}$$

where the constant $k^{(H)}$ is nonnegative and depends on $(\Omega_{SR}, \Omega_{RD}, \Omega_{SD})$, l, n, t and the fading parameter q.

Proof: See Appendix 4.C.

For the most general case when there are K relays and M-PSK modulations, simulation results also suggest that the proposed Smart EGC can attain the maximal diversity order, i.e., $(K+1)$.

4.4 Simulation Results

Simulation results of the BEPs for the relaying systems under consideration are presented in this section. For the simple system with one relay, i.e., $K=1$, three possible settings for practical SNRs, i.e., R is close to S, R is close to D and the three nodes are equidistant, are studied. Let $(\bar{\gamma}_{\mathrm{SR}}, \bar{\gamma}_{\mathrm{RD}}, \bar{\gamma}_{\mathrm{SD}})$ denote the average SNRs of the SR, RD and SD links, respectively. The three settings mentioned above are assumed to correspond to the following three cases: $(\bar{\gamma}_{\mathrm{SR}}, \bar{\gamma}_{\mathrm{RD}}, \bar{\gamma}_{\mathrm{SD}}) = (\bar{\gamma}+10\mathrm{dB}, \bar{\gamma}, \bar{\gamma})$, $(\bar{\gamma}, \bar{\gamma}+10\mathrm{dB}, \bar{\gamma})$ and $(\bar{\gamma}, \bar{\gamma}, \bar{\gamma})$, where $\bar{\gamma} = E_s/N_0$. When there are more than 1 relay, i.e., $K>1$, for simplicity, only the case that $\bar{\gamma}_{\mathrm{SR}_1} = \ldots = \bar{\gamma}_{\mathrm{SR}_K} = \bar{\gamma}_{\mathrm{R}_1\mathrm{D}} = \ldots = \bar{\gamma}_{\mathrm{R}_K\mathrm{D}} = \bar{\gamma}_{\mathrm{SD}} = \bar{\gamma}$ is studied.

For a fair comparison among different schemes, the total power used in all schemes is fixed at $\bar{\gamma}_{\text{tot}} = \bar{\gamma}\,[1 + E\{\alpha\}]$, where $E\{\alpha\}$ is the average power scaling at R. For Nakagami-m fading channels, $E\{\alpha\}$ is found to be

$$E\{\alpha\} = 1 + \frac{\Omega_{\text{SR}}\gamma\,(m+1, \Omega_{\text{RD}}m/\Omega_{\text{SR}})}{(\Omega_{\text{RD}}m\Gamma(m))} - \frac{\gamma\,(m, \Omega_{\text{RD}}m/\Omega_{\text{SR}})}{\Gamma(m)}, \tag{4.21}$$

where $\Gamma(x)$ represents the gamma function, i.e., $\Gamma(x) = \int_0^\infty \exp(-t)t^{x-1}dt$, $\text{Re}(x) > 0$. The incomplete gamma function is denoted by $\gamma(\alpha, x)$, i.e., $\gamma(\alpha, x) = \int_0^x \exp(-t)t^{\alpha-1}dt$, $\text{Re}(\alpha) > 0$. For Hoyt fading, the close-form expression of $E\{\alpha\}$ is not available, but it can be computed numerically, e.g., by Monte Carlo method.

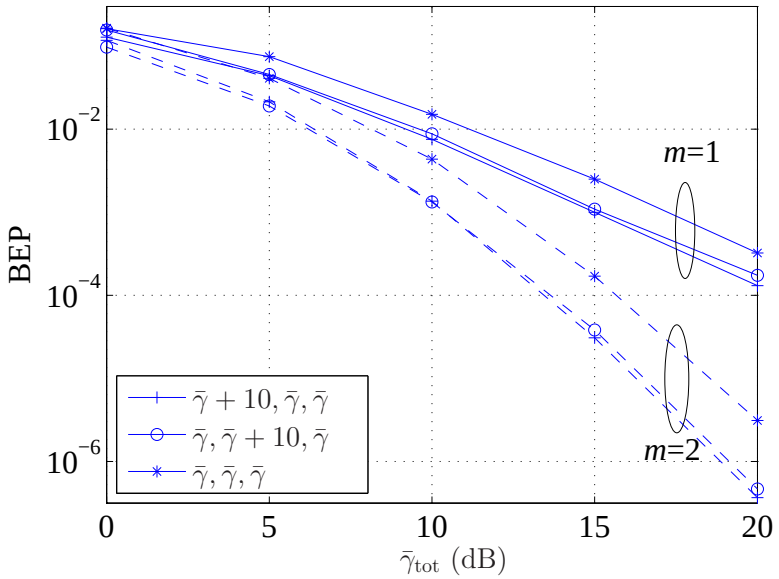

Figure 4.1 Performance of Smart EGC with BPSK under Nakagami-m fading: Different SNR triples and one relay.

For the system with one relay, BPSK modulation and Nakagami-m fading, Fig. 4.1 demonstrates that Smart EGC, when R is close to S or D, can offer SNR gains of 1 and 2 dB over the equidistant case for $m = 1$ (Rayleigh) and $m = 2$, respectively. More importantly, the maximal diversity orders of 2 ($m = 1$) and 4 ($m = 2$), are achieved in all three settings, which agree with the analysis.

Fig. 4.2 shows similar results under the same settings as those of Fig. 4.1 except that 8-PSK modulation is now used. It can be seen that the maximal diversity order

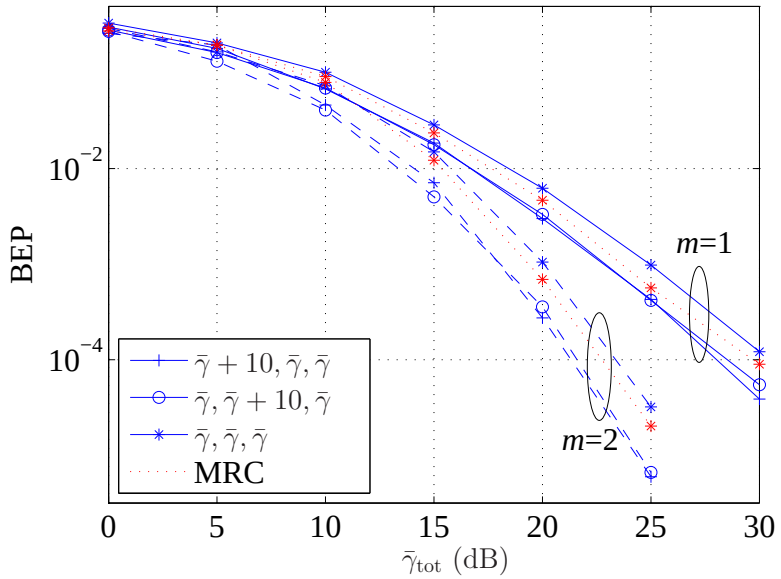

Figure 4.2 Performance of Smart EGC with 8-PSK under Nakagami-m fading: Different SNR triples and one relay.

of $2m$ can always be achieved by Smart EGC. In addition, among the three cases considered, the performance of the equidistant one is the worst. For comparison, the performance of Smart MRC [P8] is also included in Fig. 4.2 when three nodes are equidistant, i.e., $(\bar{\gamma}_{\text{SR}}, \bar{\gamma}_{\text{RD}}, \bar{\gamma}_{\text{SD}}) = (\bar{\gamma}, \bar{\gamma}, \bar{\gamma})$. It is observed that the proposed system looses only 0.5dB in SNR at BEP $= 10^{-4}$ for $m = 1$ and 2 when compared to Smart MRC. The lost is reasonable given the fact that only the phase information is required at D in Smart EGC.

Fig. 4.3 shows the performance of the system with two relays and Nakagami-m fading. The performance of Smart MRC and Smart SC are also included in order to demonstrate the benefit of the proposed Smart EGC. To have a fair comparison in terms of spectral efficiency, e.g., 2 bps/Hz, the modulation is adjusted between quadrature phase-shift keying (QPSK) and 8-PSK. The results in Fig. 4.3 support our conjecture that the achieved diversity order of Smart EGC is $m(K+1)$. Moreover, the performance loss of Smart EGC when compared to Smart MRC is very small for both cases of $m = 1$ and $m = 2$. As shown in Fig. 4.3, Smart SC offers performance improvements over Smart MRC and Smart EGC. However, the gains come with an

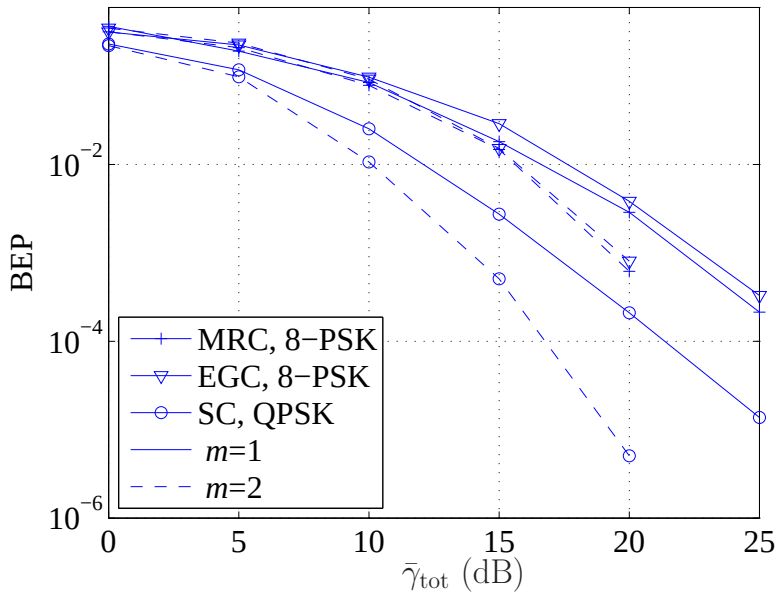

Figure 4.3 Performance of Smart MRC and Smart EGC with 8-PSK; and Smart SC with QPSK under Nakagami-m fading: Equidistant case, two relays and 2 bps/Hz.

increase in the system complexity as mentioned in Section 6.2.

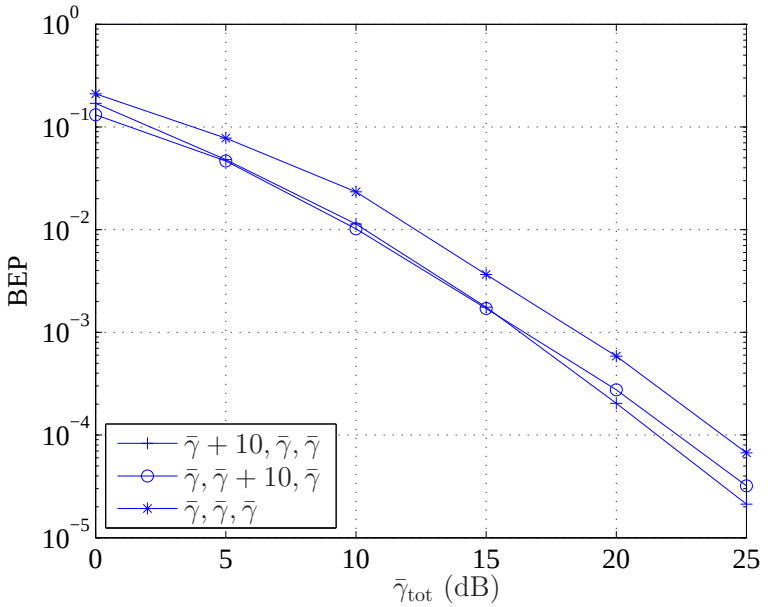

Figure 4.4 Performance of Smart EGC with BPSK under Hoyt fading: Different SNR triples, one relay and $q = 0.5$.

For Hoyt fading with the fading parameter $q = 0.5$, Fig. 4.4 considers the performance of the system with one relay and BPSK modulation. Fig. 4.4 shows that the maximal diversity order of 2 is achieved for all three settings, which agrees with the analysis. Similar to the system under Nakagami-m fading, Smart EGC under Hoyt fading performs better when R is close to S or D than the equidistant case.

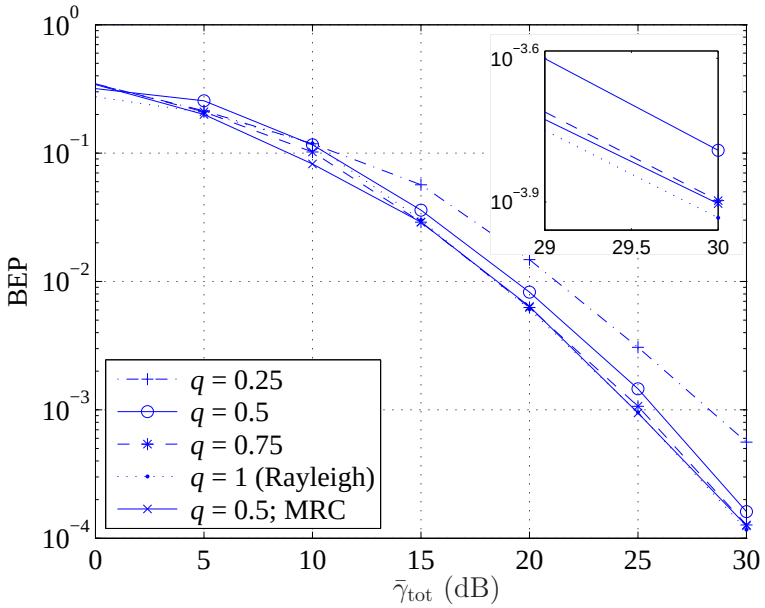

Figure 4.5 Performance of Smart EGC and Smart MRC with 8-PSK under Hoyt fading: Equidistant case and one relay.

Fig. 4.5 investigates the effects of varying the fading parameter q on the system performance. 8-PSK modulation is now used. As expected, when the fading parameter q decreases, the system becomes deteriorates. More importantly, agreed with the analysis, the system always achieves the maximal diversity of 2, regardless of the values of q. The performance of Smart MRC when $q = 0.5$ is also included in Fig. 4.5. Again, it can be seen that Smart EGC only experiences a small loss of about 0.5dB at BEP $= 10^{-3}$ when compared to Smart MRC.

For the system with two relays and $q = 0.5$, Fig. 4.6 supports our conjecture that the obtained diversity order of the system is $(K + 1)$. Similar to the case of Nakagami-m fading, Smart SC can offer performance improvement over Smart MRC and Smart EGC at the expense of increased system complexity.

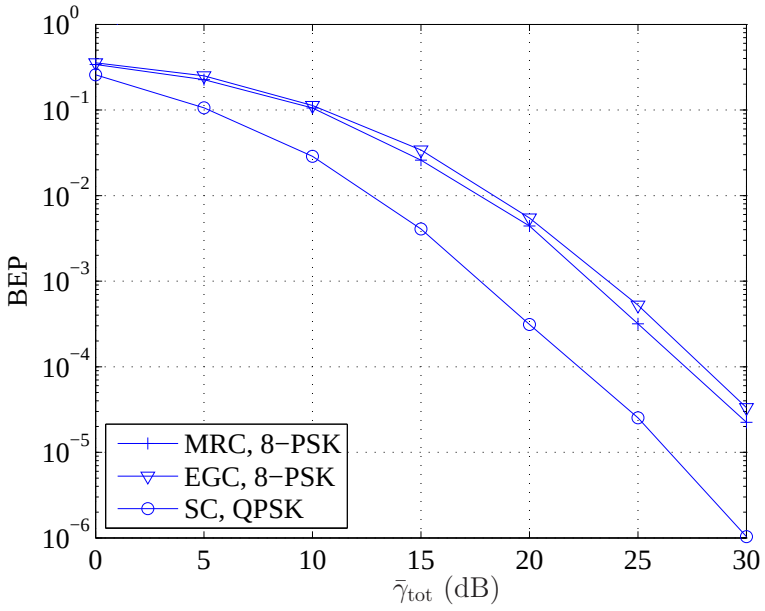

Figure 4.6 Performance of Smart MRC and Smart EGC with 8-PSK; and Smart SC with QPSK under Hoyt fading: Equidistant case, two relays and $q = 0.5$.

4.5 Conclusions

A novel and low-complexity relaying system was proposed by integrating EGC technique with DF relay processing method. The maximal diversity orders over Nakagami-m and Hoyt fading were proved to be $2m$ and 2, respectively, for the system with 1 relay and M-PSK. When the system has more relays, diversity orders of $m(K+1)$ and $(K+1)$ were respectively observed by computer simulations. Simulation results also revealed that the performance of Smart EGC is quite close to that of Smart MRC while the system complexity of Smart EGC is considerably lower.

4.A Proof of Proposition 1

The average pairwise error probability $E\{P(s_l \to s_n|\hat{s}=s_l,\gamma_{\rm SR},\gamma_{\rm RD},\gamma_{\rm SD})\}$ can be upperbounded as

$$\begin{aligned}
&E\{P(s_l \to s_n|\hat{s}=s_l,\gamma_{\rm SR},\gamma_{\rm RD},\gamma_{\rm SD})\}\\
&\leq \frac{1}{2}\int_0^\infty\int_0^\infty\int_0^\infty \exp\left[-\frac{\beta(l,n)}{2}(\sqrt{\gamma_{\rm SD}}+\sqrt{\alpha\gamma_{\rm RD}})^2\right]\\
&\quad p_{\gamma_{\rm RD}}(\gamma_{\rm RD})p_{\gamma_{\rm SR}}(\gamma_{\rm SR})p_{\gamma_{\rm SD}}(\gamma_{\rm SD})d\gamma_{\rm RD}d\gamma_{\rm SR}d\gamma_{\rm SD} \qquad (4.22)\\
&\leq \frac{1}{2}\underbrace{\int_0^\infty \exp\left(-\frac{\beta(l,n)\gamma_{\rm SD}}{2}\right)p_{\gamma_{\rm SD}}(\gamma_{\rm SD})d\gamma_{\rm SD}}_{I_{11}^{(N)}}\\
&\quad \underbrace{\int_0^\infty\int_0^\infty \exp\left(-\frac{\beta(l,n)\alpha\gamma_{\rm RD}}{2}\right)p_{\gamma_{\rm RD}}(\gamma_{\rm RD})p_{\gamma_{\rm SR}}(\gamma_{\rm SR})d\gamma_{\rm RD}d\gamma_{\rm SR}}_{I_{12}^{(N)}}, \qquad (4.23)
\end{aligned}$$

where the first inequality follows from the Chernoff bound, i.e., $Q(x)\leq (1/2)\exp(-x^2/2)$, $x\geq 0$.

The first integral $I_{11}^{(N)}$ can be evaluated as

$$\begin{aligned}
I_{11}^{(N)} &= \int_0^\infty \exp\left(-\frac{\beta(l,n)\gamma_{\rm SD}}{2}\right)\frac{m^m\gamma_{\rm SD}^{m-1}}{\bar{\gamma}_{\rm SD}^m\Gamma(m)}\exp\left(-\frac{m\gamma_{\rm SD}}{\bar{\gamma}_{\rm SD}}\right)d\gamma_{\rm SD}\\
&= \frac{m^m}{\left(\frac{\beta(l,n)}{2}+\frac{m}{\bar{\gamma}_{\rm SD}}\right)^m\bar{\gamma}_{\rm SD}^m}. \qquad (4.24)
\end{aligned}$$

The second integral $I_{12}^{(N)}$ can be computed and bounded as

$$\begin{aligned}
I_{12}^{(N)} &= \frac{m^{2m}}{\bar{\gamma}_{\rm SR}^m\bar{\gamma}_{\rm RD}^m\Gamma(m)}\int_0^\infty \frac{\gamma_{\rm SR}^{m-1}\exp\left(-\frac{m\gamma_{\rm SR}}{\bar{\gamma}_{\rm SR}}\right)}{\left(\frac{\beta(l,n)\alpha}{2}+\frac{m}{\bar{\gamma}_{\rm RD}}\right)^m}d\gamma_{\rm SR}\\
&\leq \frac{m^{2m}}{\bar{\gamma}_{\rm SR}^m\bar{\gamma}_{\rm RD}^m\Gamma(m)}\Bigg\{\int_0^{\bar{\gamma}_{\rm RD}}\left(\frac{2\bar{\gamma}_{\rm RD}}{\beta(l,n)}\right)^m\frac{\exp\left(-\frac{m\gamma_{\rm SR}}{\bar{\gamma}_{\rm SR}}\right)}{(\gamma_{\rm SR}+\frac{2m}{\beta(l,n)})^m}d\gamma_{\rm SR}+\frac{1}{\left(\frac{\beta(l,n)}{2}+\frac{m}{\bar{\gamma}_{\rm RD}}\right)^m}\\
&\left(\frac{m}{\bar{\gamma}_{\rm SR}}\right)^{-m}\Gamma\left(m,\frac{m\bar{\gamma}_{\rm RD}}{\bar{\gamma}_{\rm SR}}\right)\Bigg\} \qquad (4.25)\\
&= \frac{m^{2m}}{\bar{\gamma}_{\rm SR}^m\bar{\gamma}_{\rm RD}^m\Gamma(m)}\Bigg\{\left(\frac{2\bar{\gamma}_{\rm RD}}{\beta(l,n)}\right)^m\exp\left(\frac{2m^2}{\beta(l,n)\bar{\gamma}_{\rm SR}}\right)\Bigg[E_1\left(\frac{2m^2}{\beta(l,n)\bar{\gamma}_{\rm SR}}\right)\\
&- E_1\left(\frac{2m^2}{\beta(l,n)\bar{\gamma}_{\rm SR}}+\frac{m\bar{\gamma}_{\rm RD}}{\bar{\gamma}_{\rm SR}}\right)\Bigg]+\frac{1}{\left(\frac{\beta(l,n)}{2}+\frac{m}{\bar{\gamma}_{\rm RD}}\right)^m}\left(\frac{m}{\bar{\gamma}_{\rm SR}}\right)^{-m}\Gamma\left(m,\frac{m\bar{\gamma}_{\rm RD}}{\bar{\gamma}_{\rm SR}}\right)\Bigg\}, \qquad (4.26)
\end{aligned}$$

where the inequality is derived with the aid of [P21, Eq. (3.351.2)]. The notation $E_1(x)$ is used to denote the exponential integral, i.e., $E_1(x) = \int_x^\infty (\exp(-t)/t)dt$. Following the fact that $\mathrm{E}_1(x) > 0$, $x \geq 0$, and the property $\exp(x)\mathrm{E}_1(x) \leq \ln(1+1/x)$, for $x \geq 0$ [P22, Eq. (5.1.20)], the RHS of (4.26) can be upperbounded as

$$\begin{aligned} I_{12}^{(N)} \leq & \frac{m^{2m}}{\bar{\gamma}_{\mathrm{SR}}^m \bar{\gamma}_{\mathrm{RD}}^m \Gamma(m)} \Bigg\{ \left(\frac{2\bar{\gamma}_{\mathrm{RD}}}{\beta(l,n)} \right)^m \ln \left(1 + \frac{\beta(l,n)\bar{\gamma}_{\mathrm{SR}}^m}{2m^2} \right) \\ & + \frac{1}{\left(\frac{\beta(l,n)}{2} + \frac{m}{\bar{\gamma}_{\mathrm{RD}}} \right)^m} \left(\frac{m}{\bar{\gamma}_{\mathrm{SR}}} \right)^{-m} \Gamma \left(m, \frac{m\bar{\gamma}_{\mathrm{RD}}}{\bar{\gamma}_{\mathrm{SR}}} \right) \Bigg\}. \end{aligned} \tag{4.27}$$

Substituting (4.24) and (4.27) to (4.23) proves Proposition 1.

4.B Proof of Proposition 2

The term $E\{P_{\mathrm{SR}}^s(\gamma_{\mathrm{SR}})P(s_l \to s_n|\hat{s} = s_t, \gamma_{\mathrm{SR}}, \gamma_{\mathrm{RD}}, \gamma_{\mathrm{SD}})\}$, $l \neq n$, $l \neq t$ and $\zeta_{\mathrm{RD}}(l,n,t) < 0$, can be upperbounded as follows:

$$E\{P_{\mathrm{SR}}^s(\gamma_{\mathrm{SR}})P(s_l \to s_n|\hat{s} = s_t, \gamma_{\mathrm{SR}}, \gamma_{\mathrm{RD}}, \gamma_{\mathrm{SD}})\} \leq P_A^{(N)} + P_B^{(N)}, \tag{4.28}$$

where

$$\begin{aligned} P_A^{(N)} = & \int_0^\infty \int_0^\infty \int_0^{\frac{\zeta_{\mathrm{RD}}^2(l,n,t)}{\eta_{\mathrm{SD}}^2(l,n)}\hat{\alpha}\gamma_{\mathrm{RD}}} \exp\left(-\sin^2\left(\frac{\pi}{M}\right)\gamma_{\mathrm{SR}} \right) \\ & p_{\gamma_{\mathrm{SD}}}(\gamma_{\mathrm{SD}}) p_{\gamma_{\mathrm{SR}}}(\gamma_{\mathrm{SR}}) p_{\gamma_{\mathrm{RD}}}(\gamma_{\mathrm{RD}}) d\gamma_{\mathrm{SD}} d\gamma_{\mathrm{SR}} d\gamma_{\mathrm{RD}} \end{aligned} \tag{4.29}$$

$$\begin{aligned} P_B^{(N)} = & \int_0^\infty \int_0^\infty \int_{\frac{\zeta_{\mathrm{RD}}^2(l,n,t)}{\eta_{\mathrm{SD}}^2(l,n)}\hat{\alpha}\gamma_{\mathrm{RD}}}^\infty \frac{1}{2} \exp\left[-\frac{1}{2} \left(\eta_{\mathrm{SD}}(l,n)\sqrt{\gamma_{\mathrm{SD}}} - |\zeta_{\mathrm{RD}}(l,n,t)|\sqrt{\hat{\alpha}\gamma_{\mathrm{RD}}} \right)^2 \right] \\ & \times \exp\left(-\sin^2\left(\frac{\pi}{M}\right)\gamma_{\mathrm{SR}} \right) p_{\gamma_{\mathrm{SD}}}(\gamma_{\mathrm{SD}}) p_{\gamma_{\mathrm{SR}}}(\gamma_{\mathrm{SR}}) p_{\gamma_{\mathrm{RD}}}(\gamma_{\mathrm{RD}}) d\gamma_{\mathrm{SD}} d\gamma_{\mathrm{SR}} d\gamma_{\mathrm{RD}}. \end{aligned} \tag{4.30}$$

Note that the inequality (4.28) comes from the Chernoff bound and the fact that $\alpha \leq \hat{\alpha} = \gamma_{\mathrm{SR}}/\bar{\gamma}_{\mathrm{RD}}$.

The probability $P_A^{(N)}$ can be bounded as

$$\begin{aligned}
P_A^{(N)} \leq & \int_0^\infty \int_0^\infty \left[\int_0^{\frac{\zeta_{\mathrm{RD}}^2(l,n,t)}{\eta_{\mathrm{SD}}^2(l,n)}\hat{\alpha}\gamma_{\mathrm{RD}}} \frac{m^m \left(\frac{\zeta_{\mathrm{RD}}^2(l,n,t)}{\eta_{\mathrm{SD}}^2(l,n)}\hat{\alpha}\gamma_{\mathrm{RD}}\right)^{m-1}}{\bar{\gamma}_{\mathrm{SD}}^m \Gamma(m)} \exp\left(-\frac{m\gamma_{\mathrm{SD}}}{\bar{\gamma}_{\mathrm{SD}}}\right) d\gamma_{\mathrm{SD}} \right] \\
& \exp\left(-\sin^2\left(\frac{\pi}{M}\right)\gamma_{\mathrm{SR}}\right) p_{\gamma_{\mathrm{SR}}}(\gamma_{\mathrm{SR}}) p_{\gamma_{\mathrm{RD}}}(\gamma_{\mathrm{RD}}) d\gamma_{\mathrm{SR}} d\gamma_{\mathrm{RD}} \\
= & \left[\frac{\zeta_{\mathrm{RD}}^2(l,n,t)}{\eta_{\mathrm{SD}}^2(l,n)}\right]^{m-1} \frac{m^{3m-1}}{\Gamma^3(m)\bar{\gamma}_{\mathrm{SD}}^{m-1}\bar{\gamma}_{\mathrm{RD}}^{2m-1}\bar{\gamma}_{\mathrm{SR}}^m} \int_0^\infty \int_0^\infty (\gamma_{\mathrm{SR}}\gamma_{\mathrm{RD}})^{2m-2} \exp\left(-\sin^2\left(\frac{\pi}{M}\right)\gamma_{\mathrm{SR}}\right) \\
& \times \left[1 - \exp\left(-\frac{\zeta_{\mathrm{RD}}^2(l,n,t)}{\eta_{\mathrm{SD}}^2(l,n)} \frac{m\gamma_{\mathrm{SR}}\gamma_{\mathrm{RD}}}{\bar{\gamma}_{\mathrm{SD}}\bar{\gamma}_{\mathrm{RD}}}\right)\right] \exp\left(-\frac{m\gamma_{\mathrm{SR}}}{\bar{\gamma}_{\mathrm{SR}}}\right) \exp\left(-\frac{m\gamma_{\mathrm{RD}}}{\bar{\gamma}_{\mathrm{RD}}}\right) d\gamma_{\mathrm{SR}} d\gamma_{\mathrm{RD}} \\
= & \left[\frac{\zeta_{\mathrm{RD}}^2(l,n,t)}{\eta_{\mathrm{SD}}^2(l,n)}\right]^{m-1} \frac{m^{3m-1}}{\Gamma^3(m)\bar{\gamma}_{\mathrm{SD}}^{m-1}\bar{\gamma}_{\mathrm{RD}}^{2m-1}\bar{\gamma}_{\mathrm{SR}}^m} \int_0^\infty \gamma_{\mathrm{RD}}^{2m-2} \exp\left(-\frac{m\gamma_{\mathrm{RD}}}{\bar{\gamma}_{\mathrm{RD}}}\right) \\
& \times \left[\frac{\Gamma(2m-1)}{\left(\sin^2\left(\frac{\pi}{M}\right) + \frac{m}{\bar{\gamma}_{\mathrm{SR}}}\right)^{2m-1}} - \frac{\Gamma(2m-1)}{\left(\sin^2\left(\frac{\pi}{M}\right) + \frac{m}{\bar{\gamma}_{\mathrm{SR}}} + \frac{\zeta_{\mathrm{RD}}^2(l,n,t)}{\eta_{\mathrm{SD}}^2(l,n)}\frac{m\gamma_{\mathrm{RD}}}{\bar{\gamma}_{\mathrm{RD}}}\right)^{2m-1}}\right] d\gamma_{\mathrm{RD}}, \quad (4.31)
\end{aligned}$$

where (4.31) comes from [P21, Eq. (3.381.4)]. Using the factor theorem, the RHS of (4.31) can be calculated as

$$\begin{aligned}
P_A^{(N)} \leq & \left[\frac{\zeta_{\mathrm{RD}}^2(l,n,t)}{\eta_{\mathrm{SD}}^2(l,n)}\right]^{m-1} \frac{m^{3m}\Gamma(2m-1)}{\Gamma^3(m)\bar{\gamma}_{\mathrm{SD}}^m\bar{\gamma}_{\mathrm{RD}}^{2m-1}\bar{\gamma}_{\mathrm{SR}}^m} \sum_{n=0}^{2m-2} \frac{1}{\left(\sin^2\left(\frac{\pi}{M}\right) + \frac{m}{\bar{\gamma}_{\mathrm{SR}}}\right)^{n+1}} \\
& \times \int_0^\infty \frac{\gamma_{\mathrm{RD}}^{2m-2} \exp\left(-m\gamma_{\mathrm{RD}}/\bar{\gamma}_{\mathrm{RD}}\right) d\gamma_{\mathrm{RD}}}{\left(\sin^2\left(\frac{\pi}{M}\right) + \frac{m}{\bar{\gamma}_{\mathrm{SR}}} + \frac{\zeta_{\mathrm{RD}}^2(l,n,t)}{\eta_{\mathrm{SD}}^2(l,n)}\frac{m\gamma_{\mathrm{RD}}}{\bar{\gamma}_{\mathrm{RD}}}\right)^{2m-1-n}} \\
\leq & \left[\frac{\zeta_{\mathrm{RD}}^2(l,n,t)}{\eta_{\mathrm{SD}}^2(l,n)}\right]^{m-1} \frac{m^m(m-1)\Gamma(2m)\Gamma(2m-1)}{\left(\sin^2\left(\frac{\pi}{M}\right) + \frac{m}{\bar{\gamma}_{\mathrm{SR}}}\right)^{2m} \bar{\gamma}_{\mathrm{SD}}^m\bar{\gamma}_{\mathrm{SR}}^m}. \quad (4.32)
\end{aligned}$$

The probability $P_B^{(N)}$ can be bounded as follows:

$$\begin{aligned}
P_B^{(N)} \leq & \frac{m^m}{2\Gamma(m)\bar{\gamma}_{\mathrm{SD}}^m} \int_0^\infty \int_0^\infty \Bigg\{ \int_{\frac{\zeta_{\mathrm{RD}}^2(l,n,t)}{\eta_{\mathrm{SD}}^2(l,n)}\hat{\alpha}\gamma_{\mathrm{RD}}}^\infty \\
& \times \exp\left[-\frac{1}{2}\left(\eta_{\mathrm{SD}}(l,n)\sqrt{\gamma_{\mathrm{SD}}} - |\zeta_{\mathrm{RD}}(l,n,t)|\sqrt{\hat{\alpha}\gamma_{\mathrm{RD}}}\right)^2\right] \\
& \times \gamma_{\mathrm{SD}}^{m-1} d\gamma_{\mathrm{SD}} \Bigg\} \exp\left(-\sin^2\left(\frac{\pi}{M}\right)\gamma_{\mathrm{SR}}\right) p_{\gamma_{\mathrm{SR}}}(\gamma_{\mathrm{SR}}) p_{\gamma_{\mathrm{RD}}}(\gamma_{\mathrm{RD}}) d\gamma_{\mathrm{SR}} d\gamma_{\mathrm{RD}}, \quad (4.33)
\end{aligned}$$

where the property $\exp(-m\gamma_{\mathrm{SD}}/\bar{\gamma}_{\mathrm{SD}}) \leq 1$ has been used. Changing the variable γ_{SD}

to $u = \left(\eta_{\mathrm{SD}}(l,n)\sqrt{\gamma_{\mathrm{SD}}} - |\zeta_{\mathrm{RD}}(l,n,t)|\sqrt{\hat{\alpha}\gamma_{\mathrm{RD}}}\right)$, the RHS of (4.33) is computed as

$$\begin{aligned}
P_B^{(N)} \leq & \frac{m^m}{\eta_{\mathrm{SD}}^{2m-4}(l,n)\Gamma(m)\bar{\gamma}_{\mathrm{SD}}^m}\int_0^\infty\int_0^\infty\Big[\int_0^\infty \exp(-u^2/2)\Big(u+|\zeta_{\mathrm{RD}}(l,n,t)|\sqrt{\hat{\alpha}\gamma_{\mathrm{RD}}}\Big)^{2m-1}du\Big] \\
& \times \exp\left(-\sin^2\left(\frac{\pi}{M}\right)\gamma_{\mathrm{SR}}\right)p_{\gamma_{\mathrm{SR}}}(\gamma_{\mathrm{SR}})p_{\gamma_{\mathrm{RD}}}(\gamma_{\mathrm{RD}})d\gamma_{\mathrm{SR}}d\gamma_{\mathrm{RD}} \\
\leq & \frac{m^m}{\eta_{\mathrm{SD}}^{2m-4}(l,n)\Gamma(m)\bar{\gamma}_{\mathrm{SD}}^m}\int_0^\infty\int_0^\infty\Big[\sum_{n=0}^{2m-1}\binom{2m-1}{n}(\zeta_{\mathrm{RD}}^2(l,n,t)\hat{\alpha}\gamma_{\mathrm{RD}})^{\frac{2m-1-n}{2}} \\
& \times \int_0^\infty u^n\exp(-u^2/2)du\Big]\exp\left(-\sin^2\left(\frac{\pi}{M}\right)\gamma_{\mathrm{SR}}\right)p_{\gamma_{\mathrm{SR}}}(\gamma_{\mathrm{SR}})p_{\gamma_{\mathrm{RD}}}(\gamma_{\mathrm{RD}})d\gamma_{\mathrm{SR}}d\gamma_{\mathrm{RD}}.
\end{aligned} \tag{4.34}$$

With the help of [P21, Eq. (3.478.1)], the RHS of (4.34) can be derived as

$$\begin{aligned}
P_B^{(N)} \leq & \frac{m^m}{\eta_{\mathrm{SD}}^{2m-4}(l,n)\Gamma(m)\bar{\gamma}_{\mathrm{SD}}^m}\int_0^\infty\int_0^\infty\Big[\sum_{n=0}^{2m-1}\binom{2m-1}{n}(\zeta_{\mathrm{RD}}^2(l,n,t)\hat{\alpha}\gamma_{\mathrm{RD}})^{\frac{2m-1-n}{2}}2^{(n+1)/2} \\
& \times\Gamma\left(\frac{n+1}{2}\right)\Big]\exp\left(-\sin^2\left(\frac{\pi}{M}\right)\gamma_{\mathrm{SR}}\right)p_{\gamma_{\mathrm{SR}}}(\gamma_{\mathrm{SR}})p_{\gamma_{\mathrm{RD}}}(\gamma_{\mathrm{RD}})d\gamma_{\mathrm{SR}}d\gamma_{\mathrm{RD}} \\
= & \frac{m^m}{\eta_{\mathrm{SD}}^{2m-4}(l,n)\Gamma(m)\bar{\gamma}_{\mathrm{SD}}^m}\sum_{n=0}^{2m-1}\binom{2m-1}{n}\frac{2^{(n+1)/2}\Gamma[(n+1)/2]|\zeta_{\mathrm{RD}}(l,n,t)|^{2m-1-n}}{\bar{\gamma}_{\mathrm{RD}}^{(2m-1-n)/2}} \\
& \underbrace{\int_0^\infty\gamma_{\mathrm{SR}}^{(2m-1-n)/2}\exp\left(-\sin^2\left(\frac{\pi}{M}\right)\gamma_{\mathrm{SR}}\right)p_{\gamma_{\mathrm{SR}}}(\gamma_{\mathrm{SR}})d\gamma_{\mathrm{SR}}}_{I_{2,n}^{(N)}}\underbrace{\int_0^\infty\gamma_{\mathrm{RD}}^{(2m-1-n)/2}p_{\gamma_{\mathrm{RD}}}(\gamma_{\mathrm{RD}})d\gamma_{\mathrm{RD}}}_{I_{3,n}^{(N)}}.
\end{aligned} \tag{4.35}$$

The integrals $I_{2,n}^{(N)}$ and $I_{3,n}^{(N)}$ are computed as follows:

$$\begin{aligned}
I_{2,n}^{(N)} = & \frac{m^m}{\Gamma(m)\bar{\gamma}_{\mathrm{SR}}^m}\int_0^\infty\gamma_{\mathrm{SR}}^{(2m-1-n)/2}\gamma_{\mathrm{SR}}^{m-1}\exp\Big[-\Big(\sin^2\left(\frac{\pi}{M}\right)+\frac{m}{\bar{\gamma}_{\mathrm{SR}}}\Big)\gamma_{\mathrm{SR}}\Big]d\gamma_{\mathrm{SR}} \\
= & m^m\Gamma\left[\frac{4m-1-n}{2}\right]\Big/\Big[\Gamma(m)\bar{\gamma}_{\mathrm{SR}}^m\Big(\sin^2\left(\frac{\pi}{M}\right)+m/\bar{\gamma}_{\mathrm{SR}}\Big)^{\frac{4m-1-n}{2}}\Big] \qquad (4.36) \\
I_{3,n}^{(N)} = & \frac{m^m}{\Gamma(m)\bar{\gamma}_{\mathrm{RD}}^m}\int_0^\infty\gamma_{\mathrm{RD}}^{(2m-1-n)/2}\gamma_{\mathrm{RD}}^{m-1}\exp\Big(-\frac{m\gamma_{\mathrm{RD}}}{\bar{\gamma}_{\mathrm{RD}}}\Big)d\gamma_{\mathrm{RD}} \\
= & \frac{m^m\Gamma\left[\frac{4m-1-n}{2}\right]}{\Gamma(m)}\Big(\frac{\bar{\gamma}_{\mathrm{RD}}}{m}\Big)^{\frac{2m-1-n}{2}}, \qquad (4.37)
\end{aligned}$$

where (4.36) and (4.37) come from [P21, Eq. (3.384.1)]. Substituting (4.36) and (4.37) to (4.35) yields the following upperbound on $P_B^{(N)}$:

$$P_B^{(N)} \leq \frac{m^{3m}}{\eta_{\mathrm{SD}}^{2m-4}(l,n)\Gamma^3(m)\bar{\gamma}_{\mathrm{SR}}^m\bar{\gamma}_{\mathrm{SD}}^m}\sum_{n=0}^{2m-1}\binom{2m-1}{n}\frac{2^{\frac{(n+1)}{2}}\Gamma[\frac{(n+1)}{2}]\Gamma^2\left[\frac{4m-1-n}{2}\right]}{m^{\frac{2m-1-n}{2}}\Big(\sin^2\left(\frac{\pi}{M}\right)+\frac{m}{\bar{\gamma}_{\mathrm{SR}}}\Big)^{\frac{4m-1-n}{2}}}. \tag{4.38}$$

Substituting (4.32) and (4.38) to (4.28) proves Proposition 2 when $\bar{\gamma} \to \infty$.

4.C Proof of Proposition 3

To perform diversity analysis for the systems under Hoyt fading, one needs to average $P_s^{(H)}(\gamma_{\mathrm{SR}}, \gamma_{\mathrm{RD}}, \gamma_{\mathrm{SD}})$ over all RVs, which now have their pdfs given in (4.2). The existence of function $I_0(x)$ makes the analysis intractable. Fortunately, one can utilize the following upperbound on the modified Bessel function of the first kind, $I_\nu(x)$, in order to overcome the difficulty [P23].

$$I_\nu(x) < x^\nu 2^\nu \Gamma(\nu+1)\exp(x). \tag{4.39}$$

For the special case of zeroth-order function, i.e., $\nu = 0$, the bound simplifies to $I_0(x) < \exp(x)$. Therefore, the pdf of SNR γ_{PQ}, $\mathrm{PQ} \in \{\mathrm{SR}, \mathrm{RD}, \mathrm{SD}\}$, can be bounded as

$$p_{\gamma_{\mathrm{PQ}}}^{(H)}(\gamma_{\mathrm{PQ}}) < (a/\bar{\gamma}_{\mathrm{PQ}}) \exp\left[-b\gamma_{\mathrm{PQ}}/\bar{\gamma}_{\mathrm{PQ}}\right] = \tilde{p}_{\gamma_{\mathrm{PQ}}}(\gamma_{\mathrm{PQ}}). \tag{4.40}$$

where $a = (1+q^2)/(2q)$ and $b = (1+q^2)/2$.

By using the same procedure as done for Nakagami fading in (4.23) and the bound in (4.40), the average pairwise error probability can be bounded as follows:

$$E\{P(s_l \to s_n | \hat{s} = s_l, \gamma_{\mathrm{SR}}, \gamma_{\mathrm{RD}}, \gamma_{\mathrm{SD}})\} < 0.5 I_{11}^{(H)} I_{12}^{(H)}, \tag{4.41}$$

where

$$I_{11}^{(H)} = \int_0^\infty \exp\left(-\frac{\beta(l,n)\gamma_{\mathrm{SD}}}{2}\right) \frac{a}{\bar{\gamma}_{\mathrm{SD}}} \exp\left[-\frac{b\gamma_{\mathrm{SD}}}{\bar{\gamma}_{\mathrm{SD}}}\right] d\gamma_{\mathrm{SD}} = \frac{(1+q^2)}{q(1+q^2+\beta(l,n)\bar{\gamma}_{\mathrm{SD}})}, \tag{4.42}$$

$$\begin{aligned} I_{12}^{(H)} =& \int_0^{\bar{\gamma}_{\mathrm{RD}}} \frac{2a}{(\beta(l,n)\gamma_{\mathrm{SR}} + 2b)} \tilde{p}_{\gamma_{SR}}(\gamma_{\mathrm{SR}}) d\gamma_{\mathrm{SR}} + \int_{\bar{\gamma}_{\mathrm{RD}}}^\infty \frac{2a}{(\beta(l,n)\bar{\gamma}_{\mathrm{RD}} + 2b)} \tilde{p}_{\gamma_{SR}}(\gamma_{\mathrm{SR}}) d\gamma_{\mathrm{SR}} \\ \leq& \frac{(1+q^2)^2}{2q^2\beta(l,n)\bar{\gamma}_{\mathrm{SR}}} \ln\left(1 + \frac{\beta(l,n)\bar{\gamma}_{\mathrm{SR}}}{(1+q^2)^2/2}\right) \\ &+ \frac{(1+q^2)}{q^2(\beta(l,n)\bar{\gamma}_{\mathrm{RD}} + 1 + q^2)} \exp\left(-\frac{(1+q^2)\bar{\gamma}_{\mathrm{RD}}}{2\bar{\gamma}_{\mathrm{SR}}}\right). \end{aligned} \tag{4.43}$$

The inequality (4.43) comes with the help of [P22, Eq. (5.1.20)].

Substituting (4.42) and (4.43) into (4.41) and combining (4.41) with (4.12), one can conclude that the probability $P_1^{(H)}$ is inversely proportional to order two of the average SNR $\bar{\gamma}$, i.e.,

$$P_{1s}^{(H)} \overset{\bar{\gamma}\to\infty}{<} \left(k_1^{(H)}\bar{\gamma}\right)^{-2}, \tag{4.44}$$

where the constant $k_1^{(H)}$ is nonnegative and depends on $(\bar{\gamma}_{\mathrm{SR}}, \bar{\gamma}_{\mathrm{RD}}, \bar{\gamma}_{\mathrm{SD}})$, l, n and the fading parameter q.

When the relay wrongly decodes the received message and forwards the error to the destination, the corresponding average probability $E\{P_{\mathrm{SR}}^s(\gamma_{\mathrm{SR}})P(s_l \to s_n|\hat{s} = s_t, \gamma_{\mathrm{SR}}, \gamma_{\mathrm{RD}}, \gamma_{\mathrm{SD}})\}$, $l \neq t$ and $\zeta_{\mathrm{RD}}(l,n,t) < 0$, can be bounded as follows:

$$E\{P_{\mathrm{SR}}^s(\gamma_{\mathrm{SR}})P(s_l \to s_n|\hat{s} = s_t, \gamma_{\mathrm{SR}}, \gamma_{\mathrm{RD}}, \gamma_{\mathrm{SD}})\} < P_A^{(H)} + P_B^{(H)}, \tag{4.45}$$

where

$$\begin{aligned} P_A^{(H)} = &\int_0^\infty \int_0^\infty \int_0^{\frac{\zeta_{\mathrm{RD}}^2(l,n,t)}{\eta_{\mathrm{SD}}^2(l,n)}\hat{\alpha}\gamma_{\mathrm{RD}}} \exp\left(-\sin^2\left(\frac{\pi}{M}\right)\gamma_{\mathrm{SR}}\right) \\ &\tilde{p}_{\gamma_{\mathrm{SD}}}(\gamma_{\mathrm{SD}})\tilde{p}_{\gamma_{\mathrm{SR}}}(\gamma_{\mathrm{SR}})\tilde{p}_{\gamma_{\mathrm{RD}}}(\gamma_{\mathrm{RD}})d\gamma_{\mathrm{SD}}d\gamma_{\mathrm{SR}}d\gamma_{\mathrm{RD}} \end{aligned} \tag{4.46}$$

$$\begin{aligned} P_B^{(H)} = &\int_0^\infty \int_0^\infty \int_{\frac{\zeta_{\mathrm{RD}}^2(l,n,t)}{\eta_{\mathrm{SD}}^2(l,n)}\hat{\alpha}\gamma_{\mathrm{RD}}}^\infty \frac{1}{2}\exp\left[-\frac{1}{2}\left(\eta_{\mathrm{SD}}(l,n)\sqrt{\gamma_{\mathrm{SD}}} - |\zeta_{\mathrm{RD}}(l,n,t)|\sqrt{\hat{\alpha}\gamma_{\mathrm{RD}}}\right)^2\right] \\ &\times \exp\left(-\sin^2\left(\frac{\pi}{M}\right)\gamma_{\mathrm{SR}}\right)\tilde{p}_{\gamma_{\mathrm{SD}}}(\gamma_{\mathrm{SD}})\tilde{p}_{\gamma_{\mathrm{SR}}}(\gamma_{\mathrm{SR}})\tilde{p}_{\gamma_{\mathrm{RD}}}(\gamma_{\mathrm{RD}})d\gamma_{\mathrm{SD}}d\gamma_{\mathrm{SR}}d\gamma_{\mathrm{RD}}. \end{aligned} \tag{4.47}$$

The inequality (4.45) is derived with the help of the Chernoff bound, the fact that $\alpha \leq \hat{\alpha} = \gamma_{\mathrm{SR}}/\bar{\gamma}_{\mathrm{RD}}$ and the bounds on the pdfs of the SNRs $(\gamma_{\mathrm{SR}}, \gamma_{\mathrm{RD}}, \gamma_{\mathrm{SD}})$ given in (4.40).

The first term $P_A^{(H)}$ in (4.45) is evaluated as

$$P_A^{(H)} = \int_0^\infty \int_0^\infty \exp\left(-\sin^2\left(\frac{\pi}{M}\right)\gamma_{\rm SR}\right)\frac{a}{b}\left[1-\exp\left(-\frac{\zeta_{\rm RD}^2(l,n,t)}{\eta_{\rm SD}^2(l,n)}\frac{b\gamma_{\rm SR}\gamma_{\rm RD}}{\bar{\gamma}_{\rm SD}\bar{\gamma}_{\rm RD}}\right)\right]$$

$$\tilde{p}_{\gamma_{\rm SR}}(\gamma_{\rm SR})\tilde{p}_{\gamma_{\rm RD}}(\gamma_{\rm RD})d\gamma_{\rm SR}d\gamma_{\rm RD}$$

$$= \frac{a^3}{b\bar{\gamma}_{\rm SR}\bar{\gamma}_{\rm RD}}\left[\frac{\bar{\gamma}_{\rm RD}}{b\Big(\sin^2\left(\frac{\pi}{M}\right)+\frac{b}{\bar{\gamma}_{\rm SR}}\Big)} - \int_0^\infty \frac{\exp(-b\gamma_{\rm RD}/\bar{\gamma}_{\rm RD})d\gamma_{\rm RD}}{\left(\sin^2\left(\frac{\pi}{M}\right)+\frac{b}{\bar{\gamma}_{\rm SR}}+\frac{\zeta_{\rm RD}^2(l,n,t)}{\eta_{\rm SD}^2(l,n)}\frac{b\gamma_{\rm RD}}{(\bar{\gamma}_{\rm SD}\bar{\gamma}_{\rm RD})}\right)}\right]$$

$$= \frac{a^3}{b\bar{\gamma}_{\rm SR}\bar{\gamma}_{\rm RD}}\Bigg\{\frac{\bar{\gamma}_{\rm RD}}{b\Big(\sin^2\left(\frac{\pi}{M}\right)+\frac{b}{\bar{\gamma}_{\rm SR}}\Big)} - \frac{\bar{\gamma}_{\rm SD}\bar{\gamma}_{\rm RD}}{b}\frac{\eta_{\rm SD}^2(l,n)}{\zeta_{\rm RD}^2(l,n,t)}$$

$$\exp\left[b\bar{\gamma}_{\rm SD}\frac{\eta_{\rm SD}^2(l,n)}{\zeta_{\rm RD}^2(l,n,t)}\left(\frac{\sin^2\left(\frac{\pi}{M}\right)}{b}+\frac{1}{\bar{\gamma}_{\rm SR}}\right)\right]{\rm E}_1\left[b\bar{\gamma}_{\rm SD}\frac{\eta_{\rm SD}^2(l,n)}{\zeta_{\rm RD}^2(l,n,t)}\left(\frac{\sin^2\left(\frac{\pi}{M}\right)}{b}+\frac{1}{\bar{\gamma}_{\rm SR}}\right)\right]\Bigg\}, \tag{4.48}$$

where [P21, Eq. (3.352.4)] is applied to (4.48). One can use [P21, Eq. (8.215)] to approximate $P_A^{(H)}$ as follows:

$$P_A^{(H)} \approx \frac{a^3}{b^2\bar{\gamma}_{\rm SR}\bar{\gamma}_{\rm SD}\Big(\sin^2\left(\frac{\pi}{M}\right)+\frac{b}{\bar{\gamma}_{\rm SR}}\Big)^2} = \frac{(1+q^2)\zeta_{\rm RD}^2(l,n,t)}{4q^3\eta_{\rm SD}^2(l,n)\bar{\gamma}_{\rm SR}\bar{\gamma}_{\rm SD}[\sin^2\left(\frac{\pi}{M}\right)+(1+q^2)/(2\bar{\gamma}_{\rm SR})]^2}, \tag{4.49}$$

The second term $P_B^{(H)}$ can be computed as

$$\begin{aligned}
P_B^{(H)} \leq & \frac{a}{2\eta_{\rm SD}(l,n)\bar{\gamma}_{\rm SD}}\int_0^\infty \tilde{p}_{\gamma_{\rm RD}}(\gamma_{\rm RD})\Bigg[\int_0^\infty\left(1+|\zeta_{\rm RD}(l,n,t)|\sqrt{\frac{\pi\gamma_{\rm SR}\gamma_{\rm RD}}{\bar{\gamma}_{\rm RD}}}\right) \\
& \exp\left(-\sin^2\left(\frac{\pi}{M}\right)\gamma_{\rm SR}\right)\frac{a}{\bar{\gamma}_{\rm SR}}\exp\left(-\frac{b\gamma_{\rm SR}}{\bar{\gamma}_{\rm SR}}\right)d\gamma_{\rm SR}\Bigg]d\gamma_{\rm RD} \\
= & \frac{a}{2\eta_{\rm SD}(l,n)\bar{\gamma}_{\rm SD}}\left[\frac{a^2}{b\bar{\gamma}_{\rm SR}\Big(\sin^2\left(\frac{\pi}{M}\right)+\frac{b}{\bar{\gamma}_{\rm SR}}\Big)}+\frac{a^2\Gamma^2(1.5)\sqrt{\pi}|\zeta_{\rm RD}(l,n,t)|}{\bar{\gamma}_{\rm SR}\Big(\sin^2\left(\frac{\pi}{M}\right)+\frac{b}{\bar{\gamma}_{\rm SR}}\Big)^{1.5}}\right] \\
= & \frac{(1+q^2)^3}{16q^3\eta_{\rm SD}(l,n)\bar{\gamma}_{\rm SR}\bar{\gamma}_{\rm SD}[\sin^2\left(\frac{\pi}{M}\right)+(1+q^2)/(2\bar{\gamma}_{\rm SR})]} \\
& \left[\frac{2}{(1+q^2)}+\frac{\Gamma^2(1.5)\sqrt{\pi}|\zeta_{\rm RD}(l,n,t)|}{\sqrt{[\sin^2\left(\frac{\pi}{M}\right)+(1+q^2)/(2\bar{\gamma}_{\rm SR})]}}\right],
\end{aligned} \tag{4.50}$$

where [P21, Eq. (3.478.1)] is employed in (4.50).

Combining (4.49) and (4.50) into (4.45), one can see that $E\{P_{\rm SR}^s(\gamma_{\rm SR})P(s_l \to s_n|\hat{s}=s_t,\gamma_{\rm SR},\gamma_{\rm RD},\gamma_{\rm SD})\}$ when $l \neq t$ and $\zeta_{\rm RD}(l,n,t) < 0$, decays with the exponent

of 2 at the high SNR, i.e.,

$$E\{P^s_{\mathrm{SR}}(\gamma_{\mathrm{SR}})P(s_l \to s_n|\hat{s}=s_t,\gamma_{\mathrm{SR}},\gamma_{\mathrm{RD}},\gamma_{\mathrm{SD}})\} \overset{\bar{\gamma}\to\infty}{<} \left(k_2^{(H)}\bar{\gamma}\right)^{-2}, \tag{4.51}$$

where $k_2^{(H)}$ is nonnegative and depends on $(\Omega_{\mathrm{SR}}, \Omega_{\mathrm{SD}})$, l, n, t and the fading parameter q.

Finally, combining (4.44) and (4.51) proves Proposition 3.

REFERENCES

[P1] A. Sendonaris, E. Erkip, and B. Aazhang, "User cooperation diversity – part 1: System description," *IEEE Trans. Commun.*, vol. 51, pp. 1927–1938, Nov. 2003.

[P2] A. Sendonaris, E. Erkip, and B. Aazhang, "User cooperation diversity – part 2: Implementation aspects and performance analysis," *IEEE Trans. Commun.*, vol. 51, pp. 1939–1948, Nov. 2003.

[P3] J. N. Laneman, D. N. C. Tse, and G. W. Wornell, "Cooperative diversity in the wireles networks: Efficient protocols and outage behavior," *IEEE Trans. Inform. Theory*, vol. 49, pp. 3062–3080, Dec. 2004.

[P4] D. Michalopoulos and G. Karagiannidis, "Phy-layer fairness in amplify and forward cooperative diversity systems," *IEEE Trans. on Wireless Commun.*, vol. 7, no. 3, pp. 1073–1082, March 2008.

[P5] "Special issue on cooperative communications," *IEEE Trans. on Wireless Commun.*, vol. 7, no. 5, May 2008.

[P6] T. Wang, A. Cano, G. B. Giannakis, and J. N. Laneman, "High–performance cooperative demodulation with decode–and–forward relays," *IEEE Trans. Commun.*, vol. 55, pp. 1427–1438, July 2007.

[P7] T. Wang, R. Wang, and G. B. Giannakis, "Smart regenerative relays for link–adaptive cooperative communications," in *40th Annual Conference on Information Sciences and Systems*, pp. 1038–1043, Mar. 2006.

[P8] T. Wang, G. Giannakis, and R. Wang, "Smart regenerative relays for link-adaptive cooperative communications," *IEEE Trans. Commun.*, vol. 56, pp. 1950–1960, Nov. 2008.

[P9] N. H. Vien, H. H. Nguyen, and T. Le-Ngoc, "Diversity analysis of smart relaying," to appear in *IEEE Trans. Veh. Technol.*

[P10] Z. Yi and I.-M. Kim, "Diversity order analysis of the decode-and-forward cooperative networks with relay selection," *IEEE Trans. on Wireless Commun.*, vol. 7, pp. 1792–1799, May 2008.

[P11] A. Ribeiro, X. Cai, and G. Giannakis, "Symbol error probabilities for general cooperative links," *IEEE Trans. on Wireless Commun.*, vol. 4, pp. 1264–1273, May 2005.

[P12] A. Bletsas, A. Khisti, D. Reed, and A. Lippman, "A simple cooperative diversity method based on network path selection," *IEEE J. Select. Areas in Commun.*, vol. 24, pp. 659–672, March 2006.

[P13] H. Shin and J. Song, "MRC analysis of cooperative diversity with fixed-gain relays in Nakagami-m fading channels," *IEEE Trans. on Wireless Commun.*, vol. 7, pp. 2069–2074, June 2008.

[P14] M. K. Simon and M.-S. Alouini, *Digital Communication over Fading Channels.* Wiley-IEEE Press, 2th ed., 2004.

[P15] G. K. Karagiannidis, "Performance bounds of multihop wireless communications with blind relays over generalized fading channels," *IEEE Trans. on Wireless Commun.*, vol. 5, pp. 498 – 503, Mar. 2006.

[P16] R. Radaydeh and M. Matalgah, "Non-coherent improved-gain diversity reception of binary orthogonal signals in Nakagami-q (Hoyt) mobile channels," *Communications, IET*, vol. 2, no. 2, pp. 372 – 379, Feb. 2008.

[P17] C. D. Iskander and P. T. Mathiopoulos, "Exact performance analysis of dual-branch coherent equal–gain combining in Nakagami–m, Rician, and Hoyt fading," *IEEE Trans. Veh. Technol.*, vol. 57, pp. 921 – 931, Mar. 2008.

[P18] M. K. Simon and M.-S. Alouini, *Digital Communication over Fading Channels*. Wiley-IEEE Press, 2th ed., 2005.

[P19] J. Adeane, M. R. D. Rodrigues, and I. J. Wassell, "Characterisation of the performance of cooperative networks in Ricean fading channels," in *Proc. of the International Conf. on Telecommunications*, (Cape Town, South Africa), May 2005.

[P20] J. G. Proakis, *Digital Communications*. McGraw-Hill, 4th ed., 2001.

[P21] L. S. Gradshteyn and L. M. Ryzhik, *Tables of Integrals, Series and Products*. Academic Press, 7th ed., 2007.

[P22] M. Abramowitz and I. A. Stegun, *Handbook of Mathematical Functions With Formulas, Graphs, and Mathematical Tables*. U.S. Department of Commerce, 1972.

[P23] C. M. Joshi and S. K. Bissu, "Some inequalities of Bessel and modified Bessel functions," *Journal of the Australian Mathematical Society*, vol. 50, no. 2, pp. 333 – 342, 1991.

5. Diversity Analysis of Smart Relaying

Published as:

N. H. Vien, H. H. Nguyen, and T. Le-Ngoc, "Diversity analysis of smart relaying," *IEEE Trans. Veh. Technol.*, vol. 58, pp. 2849–2862, July 2009.[1]

The manuscripts in Chapters 3 and 4 adopt Protocol II in DF single-relay systems and analyze diversity performance of Smart MRC and Smart EGC, respectively. Integrating the smart relaying technique with the DF signal processing method is shown to be an effective approach as it can always offer the maximal diversity in any of the fading channel models of interest. However, the systems in these manuscripts are restricted to Protocol II where only the relay is allowed to transmit during the second time slot. As discussed in Chapter 2, Protocol I is more general than Protocol II. Indeed, Protocol I relaxes the above assumption and also allows the source-to-destination transmission during the second time slot. Therefore Protocol I includes Protocol II as a special case. Due to the importance of Protocol I, the manuscript included in this chapter studies the smart relaying with Protocol I and analyzes the system performance in terms of achievable diversity.

As the source is allowed to transmit in the second time slot, the destination must take the source-to-destination channel gain into account in order to perform the MRC-like detection rule. With the statistic of the relay-to-destination channel available at the relay via a feedback channel, the achievable diversity order of 2 is proved for the system with BPSK and QPSK modulation. For the case of higher-

[1]This paper is included with the expressed permission of the journal's publisher.

order rectangular QAM constellations, the diversity order of 2 is also numerically calculated by using an upperbound on the system performance. A remarkable result is that the smart relaying technique can always offer the diversity order of 2 under any feedback channel condition. Furthermore, the weighted coefficient to scale the transmitted power is quantized in order to reduce the complexity at the relay. It is also shown that the achievable diversity order always equals 2 and does not depend on how precise the quantization is.

Diversity Analysis of Smart Relaying

Nam H. Vien*, *Student Member, IEEE* and Ha H. Nguyen, *Senior Member, IEEE*, Tho Le-Ngoc, *Fellow, IEEE*

Abstract

It has been known that relaying can provide spatial diversity while satisfying the size–limited constraint of the users' devices in wireless communications systems. For the practically attractive decode–and–forward (DF) relaying system with maximal–ratio–combining (MRC) at the destination, spatial diversity is lost except when the source–relay link is reliable. To deal with the problem and inspired by the work of Wang et al., this paper considers and analyzes an adaptive transmission scheme, referred to as smart relaying, when only the average relay–destination (R–D) signal–to–noise ratio (SNR) is available at the relay. In the system under consideration, the source *continuously* transmits the information to the destination. The relay scales its transmitted power adaptively to changes in the channel condition but never exceeds the total power used by the conventional relaying. Performance analysis proves that a diversity order of 2 is always obtained for binary–phase–shift–keying (BPSK) and quadrature–phase–shift–keying (QPSK). The diversity order of 2 is also observed for higher–order rectangular quadrature amplitude modulation (QAM) constellations through numerical results. The result on diversity order does not depend on how perfect the R–D feedback channel and how exact the quantization of the power scaling are. All the corresponding results of Wang et al. are subsumed in our analysis.

Index terms

Cooperative communications, relaying, adaptive transmission, decode–and–forward, diversity order, maximal–ratio–combining.

Manuscript received March 1, 2008 and revised July 10, 2008. This work was supported by an NSERC Strategic Program Grant. The review of this paper was coordinated by Prof. Shuguang Cui.

Nam H. Vien (*contact author) and Ha H. Nguyen are with the Department of Electrical & Computer Engineering, University of Saskatchewan, 57 Campus Dr., Saskatoon, SK, Canada S7N 5A9. Emails: nam.vien@usask.ca, ha.nguyen@usask.ca.

Tho Le-Ngoc is with the Department of Electrical & Computer Engineering, McGill University, 3480 University St., Montreal, Quebec, Canada H3A 2A7. Email: tho@ece.mcgill.ca.

5.1 Introduction

Performing relaying communications in wireless networks is continuing to attract a lot of research interests due to its potential of providing spatial diversity without the need of having co-located antenna array (see, for example, [P1–P6] and [P7]). In this approach, a source transmits the messages to a destination with the aid of relays. Together with the relays, the source creates a virtual antenna array. If properly designed, relaying can achieve diversity order up to the number of diversity paths, what can be referred to as the *maximal* diversity order [P8]. In general, there are three possible protocols, named Protocols I, II and III in [P9], that the relay can assist the source–destination communication.

Protocol I: The source broadcasts to both the relay and the destination during the first time slot. In the second time slot, both the source and the relay communicate with the destination.

Protocol II: The source broadcasts to the relay and destination in the first time slot. The relay communicates with the destination while the source keeps silent during the second time slot.

Protocol III: The source communicates only with the relay in the first time slot. Both the source and the relay transmit their messages to the destination in the second time slot.

Furthermore, there are generally two processing options at the relays: amplify–and–forward (AF) and decode–and–forward (DF). In AF, a relay receives the transmitted signal from the source and sends a scaled version of it to the destination. Unfortunately, AF scheme requires expensive RF chains to mitigate the existing coupling effects. This motivates the digital signal processing, i.e., the DF processing, at the relay in which a relay tries to restore the source waveform before retransmission.

Considering systems with L relays and under Protocol II, the authors in [P10], proved that AF relaying can achieve the full diversity order of $L + 1$ with the max-

imum likelihood (ML) demodulation for different fading channels. For DF relaying, full diversity for binary–phase–shift–keying (BPSK) can also be achieved with the optimal ML coherent demodulation [P2]. However, the ML demodulation becomes prohibitively complex for high–order constellations. To reduce the complexity, one can use the maximum ratio combiner (MRC) to demodulate the received signals. Unfortunately, MRC can offer full diversity only for the perfect source–relay (S–R) link due to the error propagation at the relay [P11]. To improve the performance of MRC, λ–MRC and piecewise–linear (PL) combiner were proposed in [P2] and [P12], respectively. Numerical results in [P2] illustrate that the λ–MRC's performance is close to that of the ML when BPSK is used. However, it cannot be assessed that the λ–MRC offers full diversity since the parameter λ is not analytically specified. In [P12], PL combiner was derived for noncoherent and coherent demodulations with the assumption that the average S–R bit error probability (BEP) is available at the destination. But again, this fact is only established for BPSK.

More recently, an elegant demodulation method, called cooperative–MRC (C–MRC), was proposed in [P8]. It was shown in [P8] that, under Protocol II, the C–MRC's performance is close to that of the optimal ML demodulation for BPSK and it can obtain full diversity *regardless* of the underlying constellation. An equivalence of the relaying system with C–MRC at the destination is a system that implements the traditional MRC at the destination and places the adaptive weighted coefficient at the relay. The latter system, referred to as a *smart* relaying system [P13, P14] requires that the characteristic of the R–D link is available at the relay.

The works in [P13,P14], however, are limited to Protocol II only. Since Protocol I is more general than Protocol II (indeed, Protocol I includes Protocol II as a special case), it is important to study smart relaying with Protocol I and this is the objective of the paper. In particular, the paper considers uncoded DF relaying system with one relay under Protocol I. With the R–D average signal–to–noise ratio (SNR) available at the relay via a low–rate feedback channel, it is proved that the smart relaying always obtains a diversity order of 2 for BPSK and QPSK. For higher–order rect-

angular QAM, the exact diversity analysis appears intractable. Instead, a compact upper bound on the performance is obtained, which can be used to (numerically) determine the *achievable* diversity order of 2 for rectangular QAM as well[2]. The paper also shows that the smart relaying is very robust to the feedback channel quality. In fact, it is shown that the diversity order is two under any feedback channel condition. Furthermore, to reduce the signal processing complexity at the relay, one can use the quantized weighted coefficients to scale the transmitted power [P14]. It is demonstrated that the smart relaying can also achieve a diversity order of 2, regardless of how exact the quantization is. Since Protocol II is a special case of Protocol I, the analysis in this paper subsumes all the corresponding analysis in [P14]. Moreover, results show that Protocol I can offer performance improvement over Protocol II under smart relaying.

The rest of the paper is organized as follows. In Section 5.2, the system model is described where the definitions of soft and hard power scalings are given. The diversity analysis for soft and hard scalings is carried out in Section 5.3. Numerical results and conclusions are given in Sections 5.4 and 5.5, respectively.

Notation: x^* is the complex conjugate of x, $\mathrm{Re}(x)$ takes the real part of complex number x. The Q-function is defined as $Q(x) = (1/\sqrt{2\pi}) \int_x^\infty \exp(-t^2/2)dt$. The circularly symmetric complex Gaussian random variable (RV) with variance σ^2 is denoted by $\mathcal{CN}(0, \sigma^2)$.

5.2 System model

Consider a simple relay network with 3 nodes as shown in Figure 5.1. Data is sent from the source node, S, to the destination node, D, with the aid of the relay node, R. All nodes are equipped with single–antenna transmitter and receiver. The system is half–duplex, in which R cannot transmit and receive simultaneously. Transmission

[2]Though there are 3 independent paths in the network with 1 relay, implying a maximal diversity order of 3, achieving such a maximal diversity order requires precoding at the source [P15], but this is beyond the scope of this paper.

to D is done in two time slots. In the first time slot, S broadcasts its signal, s, to both R and D. In the second time slot, S repeats to transmit the signal s to D, while R, after decoding the received signal from S, transmits the decoded signal $\hat{s}$ to D. Such a transmission protocol over the network belongs to Protocol I described before and it is different from Protocol II considered in [P14].

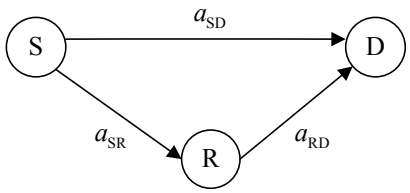

Figure 5.1 A simple relaying system with 3 nodes.

Frequency–flat Rayleigh fading channels are assumed throughout the paper. Furthermore, perfect channel state information (CSI) is only available at the receiver and not at the transmitter. The perfect CSI means that R knows the channel state in the S–R link and D knows the channel states in the S–D and R–D links. Let a_{SR} and a_{RD} denote the channel coefficients of the S–R and R–D links, respectively. Similarly, let a_{SD_1}, a_{SD_2} denote the channel coefficients of the S–D link during time slots 1 and 2, respectively. These coefficients are modeled as independent circularly symmetric complex Gaussian variables with variances σ^2_{SR}, σ^2_{RD} and σ^2_{SD}, respectively.

In the first time slot, S broadcasts the signal s with the average transmitted power $E_s = E\{|s|^2\}$ to both R and D. The received signals at R, $y_{\mathrm{R}}[1]$, and at D, $y_{\mathrm{D}}[1]$ are given as

$$y_{\mathrm{R}}[1] = a_{\mathrm{SR}} s + z_{\mathrm{R}}[1] \tag{5.1}$$

$$y_{\mathrm{D}}[1] = a_{\mathrm{SD}_1} s + z_{\mathrm{D}}[1], \tag{5.2}$$

where $z_{\mathrm{R}}[1]$ and $z_{\mathrm{D}}[1]$ represent additive white Gaussian noise (AWGN) and are modeled as independent and identically distributed (i.i.d) $\mathcal{CN}(0, N_0)$ random variables.

R decodes the received signal from S by using the ML coherent detector, which chooses the symbol $\hat{s}$ that maximizes the conditional probability density function

(pdf) of the received signal. The equivalent detection rule is

$$\hat{s} \;=\; \arg\min_{s\in\mathbf{S}} \left\{ \left| a_{\mathrm{SR}}^{*} y_{\mathrm{R}}[1] - |a_{\mathrm{SR}}|^{2} s \right|^{2} \right\}, \tag{5.3}$$

where $\mathbf{S}$ is the underlying constellation with size $Q = |\mathbf{S}| = 2^{q}$.

5.2.1 Soft–Power Scaling

Different from most models [P2, P4, P8, P11] where the re–transmitted symbol power is fixed in the second time slot, here, similar to [P14], R adapts to the S–R channel quality by transmitting to D a scaled version of $\hat{s}$ with the transmit power amplification factor α given by [P14]

$$\alpha = \frac{\min(\gamma_{\mathrm{SR}}, \gamma_{\mathrm{RD}})}{\gamma_{\mathrm{RD}}} \leq 1. \tag{5.4}$$

In (5.4), the *instantaneous* SNRs of the S–R, R–D and S–D links are defined as $\gamma_{\mathrm{SR}} := |a_{\mathrm{SR}}|^{2}\bar{\gamma}$, $\gamma_{\mathrm{RD}} := |a_{\mathrm{RD}}|^{2}\bar{\gamma}$ and $\gamma_{\mathrm{SD}} := |a_{\mathrm{SD}}|^{2}\bar{\gamma}$, respectively, where $\bar{\gamma} = E_s/N_0$. Similarly, the *average* SNRs of the S–R, R–D and S–D links are $\bar{\gamma}_{\mathrm{SR}} := \sigma_{\mathrm{SR}}^{2}\bar{\gamma}$, $\bar{\gamma}_{\mathrm{RD}} := \sigma_{\mathrm{RD}}^{2}\bar{\gamma}$ and $\bar{\gamma}_{\mathrm{SD}} := \sigma_{\mathrm{SD}}^{2}\bar{\gamma}$, respectively. In choosing α as in (5.4), the information is relayed at full power whenever the S–R link is reliable, i.e., $\gamma_{\mathrm{SR}} > \gamma_{\mathrm{RD}}$. Otherwise, R scales the power down (even to zero) in order to mitigate the error propagation experienced over the R–D link.

It should be pointed out that the computation of α requires the R–D channel information to be sent from D to R. This could be very difficult and impractical for fast-changing channel condition. In such a situation, R can rely on the average R–D channel condition to scale the transmitted signal in the second time slot as follows [P14]:

$$\alpha_1(\theta) \;=\; \frac{\min(\gamma_{\mathrm{SR}}, \theta\bar{\gamma}_{\mathrm{RD}})}{\theta\bar{\gamma}_{\mathrm{RD}}} \tag{5.5}$$

$$\;=\; \begin{cases} 1, & \text{if } \gamma_{\mathrm{SR}} \geq \theta\bar{\gamma}_{\mathrm{RD}} \\ \frac{\gamma_{\mathrm{SR}}}{\theta\bar{\gamma}_{\mathrm{RD}}}, & \text{if } \gamma_{\mathrm{SR}} < \theta\bar{\gamma}_{\mathrm{RD}} \end{cases}, \tag{5.6}$$

where the positive scalar θ represents the imperfectness of the feedback channel from D. The case of perfect feedback channel corresponds to $\theta = 1$. For simplicity, hereafter, $\alpha_1(\theta)$ is simply referred to as α_1. Note also that $\alpha_1 \leq 1$.

The advantages of choosing α and α_1 as in (5.4) and (5.5), respectively, are twofold. First, it saves the total transmitted power since α and α_1 are always less than or equal to 1. Furthermore, as shall be seen later, the adaptive transmission scheme at R helps to maintain the diversity order 2 of the smart relaying even when error propagation at R is taken into account.

Restricting to the simple case of power scaling α_1 at R, the received signal $y_{\mathrm{D}}[2]$ at D in the second time slot is given by

$$y_{\mathrm{D}}[2] = a_{\mathrm{SD}_2} s + \sqrt{\alpha_1} a_{\mathrm{RD}} \hat{s} + z_{\mathrm{D}}[2], \tag{5.7}$$

where $z_{\mathrm{D}}[2]$ is $\mathcal{CN}(0, N_0)$, which represents AWGN at D. Note that during the second time slot, the transmitted signal powers at S and R are E_s and $\alpha_1 E_s$, respectively.

5.2.2 Hard–Power Scaling

Instead of the soft-power scaling $\alpha_1(\theta)$, the transmitted power at R can be scaled by using a quantized version of $\alpha_1(\theta)$ [P14]. This shall reduce the complexity at R. Let $M = 2^{N_q}$ be the number of quantization levels, the hard–power scaling coefficient is given as [P14]:

$$\alpha_q(N_q, \theta) \;=\; \frac{\mathrm{round}[\alpha_1(\theta)(M-1)]}{M-1}, \tag{5.8}$$

where round[$\cdot$] denotes the rounding operation to the nearest integer.

Of particular interest is the case when $N_q = 1$ and $\theta = 2$, in which the quantization coefficient in (5.8) becomes the simple on–off relaying scheme. That is

$$\alpha_{\text{on–off}} = \alpha_q(1,2) = \begin{cases} 1, & \text{if } \gamma_{\mathrm{SR}} \geq \bar{\gamma}_{\mathrm{RD}} \\ 0, & \text{if } \gamma_{\mathrm{SR}} < \bar{\gamma}_{\mathrm{RD}} \end{cases}. \tag{5.9}$$

5.2.3 ML Coherent Detector

In order to compare the performance as well as the complexity of existing demodulation methods, it is necessary to give the ML coherent detector for smart relaying systems. For BPSK, the ML detector is quite simple and it is given by (5.10) [P2],

$$s^{'} = \arg\max_{s\in\mathbf{S}}\Bigg\{\frac{\left(1-P^{b}_{\mathrm{SR}}(\gamma_{\mathrm{SR}})\right)}{\pi N_0}\exp\left[\frac{-|y_{\mathrm{D}}[1]-a_{\mathrm{SD}_1}s|^2}{N_0}-\frac{\left|y_{\mathrm{D}}[2]-(a_{\mathrm{SD}_2}+\sqrt{\alpha_1}a_{\mathrm{RD}})s\right|^2}{N_0}\right]$$
$$+\frac{P^{b}_{\mathrm{SR}}(\gamma_{\mathrm{SR}})}{\pi N_0}\exp\left[-\frac{|y_{\mathrm{D}}[1]-a_{\mathrm{SD}_1}s|^2+\left|y_{\mathrm{D}}[2]-(a_{\mathrm{SD}_2}-\sqrt{\alpha_1}a_{\mathrm{RD}})s\right|^2}{N_0}\right]\Bigg\}, \tag{5.10}$$

where $P^{b}_{\mathrm{SR}}(\gamma_{\mathrm{SR}})$ is the BEP of the S–R link. Note that the ML coherent detector becomes prohibitively complex for higher–order constellations. In addition, even for BPSK, the form of (5.10) makes the performance analysis of the system very difficult, if not impossible.

In the case that D has no S–R channel information nor detection performance of S–R link, it is reasonable to assume that the S–R link is perfect, i.e., $P^{b}_{\mathrm{SR}}(\gamma_{\mathrm{SR}}) = 0$. This assumption simplifies the optimal detector in (5.10) to

$$s^{'} = \arg\min_{s\in\mathbf{S}}\left\{\left|a^{*}_{\mathrm{SD}_1}y_{\mathrm{D}}[1]+w_{\mathrm{RD}}y_{\mathrm{D}}[2]-\left(|a_{\mathrm{SD}_1}|^2+|w_{\mathrm{RD}}|^2\right)s\right|^2\right\}, \tag{5.11}$$

where the weighted coefficient w_{RD} is

$$w_{\mathrm{RD}} = (\sqrt{\alpha_1}a_{\mathrm{RD}}+a_{\mathrm{SD}_2})^{*}. \tag{5.12}$$

It should be pointed out that, in general, the detection rule in (5.11) is not the ML decoding. However, when the S–R link is perfect, (5.11) is the ML decoding rule.

To obtain $s^{'}$, the destination needs to know a_{SD_1}, a_{SD_2} and the equivalent coefficient $\sqrt{\alpha_1}a_{\mathrm{RD}}$. Note that if α_1 is substituted by 1, (5.10) and (5.11) become the ML and the λ–MRC (with $\lambda = 1$) demodulators of the conventional relaying [P2], respectively. Based on the system model presented in this section, performance analysis in terms of diversity order is carried out in the next section.

5.3 Performance analysis

Since the availability of instantaneous R–D information at the relay can be quite impractical, the analysis is confined to soft–power scaling with the amplification factor

α_1 at R. The impact of hard–power scaling with $\alpha_1(N_q, \theta)$ is then investigated. Since Protocol II is a special case of Protocol I when $a_{\mathrm{SD}_2} = 0$, it shall be shown that the analysis done in this section subsumes the analysis for Protocol II in [P14].

5.3.1 Soft–Power Scaling

BPSK

For BPSK, the decoded signal at the relay can be either $\hat{s} = s$ or $\hat{s} = -s$ with probability $\left[1 - P^b_{\mathrm{SR}}(\gamma_{\mathrm{SR}})\right]$ or $P^b_{\mathrm{SR}}(\gamma_{\mathrm{SR}})$, respectively. With BPSK, $s \in \{\sqrt{E_s}, -\sqrt{E_s}\}$. For each value of s, the sufficient statistic at the output of the demodulator is

$$\begin{aligned} y_{\mathrm{D}} &= a^*_{\mathrm{SD}_1} y_{\mathrm{D}}[1] + w_{\mathrm{RD}} y_{\mathrm{D}}[2] \\ &= \begin{cases} \left(|a_{\mathrm{SD}_1}|^2 + w_{\mathrm{RD}}\left(a_{\mathrm{SD}_2} + \sqrt{\alpha_1} a_{\mathrm{RD}}\right)\right) s + z, & \hat{s} = s \\ \left(|a_{\mathrm{SD}_1}|^2 + w_{\mathrm{RD}}\left(a_{\mathrm{SD}_2} - \sqrt{\alpha_1} a_{\mathrm{RD}}\right)\right) s + z, & \hat{s} = -s \end{cases}, \end{aligned} \tag{5.13}$$

where $z = a^*_{\mathrm{SD}_1} z_{\mathrm{D}}[1] + w_{\mathrm{RD}} z_{\mathrm{D}}[2]$ is the equivalent noise at the output of the demodulator.

When $\hat{s} = s$, i.e., the relay makes a correct decision, the probability of making an error at the destination, the same whether $s_0 = \sqrt{E_s}$ or $s_1 = -\sqrt{E_s}$ was transmitted, is equal to the probability of the following event

$$-\left(|a_{\mathrm{SD}_1}|^2 + |w_{\mathrm{RD}}|^2\right)\sqrt{E_s} \geq \mathrm{Re}\left\{a^*_{\mathrm{SD}_1} z_{\mathrm{D}}[1] + w_{\mathrm{RD}} z_{\mathrm{D}}[2]\right\}. \tag{5.14}$$

Since $\mathrm{Re}\left\{a^*_{\mathrm{SD}_1} z_{\mathrm{D}}[1] + w_{\mathrm{RD}} z_{\mathrm{D}}[2]\right\}$ is a real Gaussian RV with zero mean and variance $\sigma^2 = \left(|a_{\mathrm{SD}_1}|^2 + |w_{\mathrm{RD}}|^2\right) N_0/2$, the probability of the event in (5.14) can be calculated as

$$\Pr\{\mathrm{error}|\hat{s} = s\} = Q\left(\sqrt{2\bar{\gamma}\left(|a_{\mathrm{SD}_1}|^2 + |w_{\mathrm{RD}}|^2\right)}\right). \tag{5.15}$$

The conditional BEP $P_1(\gamma_{\mathrm{SR}}, a_{\mathrm{SD}_1}, a_{\mathrm{SD}_2}, a_{\mathrm{RD}})$, provided that $\hat{s} = s$, is then given as

$$P_1(\gamma_{\mathrm{SR}}, a_{\mathrm{SD}_1}, a_{\mathrm{SD}_2}, a_{\mathrm{RD}}) = \left[1 - Q\left(\sqrt{2\gamma_{\mathrm{SR}}}\right)\right] Q\left(\sqrt{2\bar{\gamma}\left(|a_{\mathrm{SD}_1}|^2 + |\sqrt{\alpha_1} a_{\mathrm{RD}} + a_{\mathrm{SD}_2}|^2\right)}\right), \tag{5.16}$$

where $P_{\rm SR}^{b}(\gamma_{\rm SR}) = Q\left(\sqrt{2\gamma_{\rm SR}}\right)$ is the BEP at the relay.

In the case that the relay erroneously decoded, i.e., $\hat{s} = -s$, the event that the destination making an error, when either $\sqrt{E_s}$ or $-\sqrt{E_s}$ was transmitted, is

$$-\Big(\big|a_{\rm SD_1}\big|^2 + \big|a_{\rm SD_2}\big|^2 - \alpha_1\big|a_{\rm RD}\big|^2\Big)\sqrt{E_s} \geq {\rm Re}\Big\{a_{\rm SD_1}^{*} z_{\rm D}[1] + w_{\rm RD} z_{\rm D}[2]\Big\}. \tag{5.17}$$

Similarly, the probability of the above event can be calculated as

$$\Pr\Big\{{\rm error}|\hat{s} = -s\Big\} = Q\left(\frac{\sqrt{2\bar{\gamma}}\left(|a_{\rm SD_1}|^2 + |a_{\rm SD_2}|^2 - \alpha_1|a_{\rm RD}|^2\right)}{\sqrt{|a_{\rm SD_1}|^2 + \left|\sqrt{\alpha_1}a_{\rm RD} + a_{\rm SD_2}\right|^2}}\right). \tag{5.18}$$

Due to the symmetry of BPSK, the conditional BEP $P_2(\gamma_{\rm SR}, a_{\rm SD_1}, a_{\rm SD_2}, a_{\rm RD})$ at the destination in this case is

$$P_2(\gamma_{\rm SR}, a_{\rm SD_1}, a_{\rm SD_2}, a_{\rm RD}) = Q\left(\sqrt{2\gamma_{\rm SR}}\right) Q\left(\frac{\sqrt{2\bar{\gamma}}\left(|a_{\rm SD_1}|^2 + |a_{\rm SD_2}|^2 - \alpha_1|a_{\rm RD}|^2\right)}{\sqrt{|a_{\rm SD_1}|^2 + \left|\sqrt{\alpha_1}a_{\rm RD} + a_{\rm SD_2}\right|^2}}\right). \tag{5.19}$$

Combining (5.16) and (5.19) yields the following overall conditional BEP at D:

$$\begin{aligned} P_b(\gamma_{\rm SR}, a_{\rm SD_1}, a_{\rm SD_2}, a_{\rm RD}) = &\left(1 - Q\left(\sqrt{2\gamma_{\rm SR}}\right)\right) Q\left(\sqrt{2\bar{\gamma}\left(|a_{\rm SD_1}|^2 + |\sqrt{\alpha_1}a_{\rm RD} + a_{\rm SD_2}|^2\right)}\right) + \\ &Q\left(\sqrt{2\gamma_{\rm SR}}\right) Q\left(\frac{\sqrt{2\bar{\gamma}}\left(|a_{\rm SD_1}|^2 + |a_{\rm SD_2}|^2 - \alpha_1|a_{\rm RD}|^2\right)}{\sqrt{|a_{\rm SD_1}|^2 + \left|\sqrt{\alpha_1}a_{\rm RD} + a_{\rm SD_2}\right|^2}}\right). \end{aligned} \tag{5.20}$$

One can easily verify that (5.20) reduces to the corresponding BEP expression, given in [P14, Eq. (17)], for Protocol II when $a_{\rm SD_2}$ is set to 0.

The overall error performance, P_b, is obtained by averaging $P_b(\gamma_{\rm SR}, a_{\rm SD_1}, a_{\rm SD_2}, a_{\rm RD})$ over all the random variables involved, i.e., $\{\gamma_{\rm SR}, a_{\rm SD_1}, a_{\rm SD_2}, a_{\rm RD}\}$. However, the interest here is to see the obtainable diversity of the smart relaying systems, and it can be assessed via an upper bound on P_b, which can be evaluated. Before proceeding further, the unconditional probabilities P_b, P_1 and P_2 are plotted by numerical methods in Fig. 5.2 for two cases of $(\bar{\gamma}_{\rm SR}, \bar{\gamma}_{\rm RD}, \bar{\gamma}_{\rm SD}) = (\bar{\gamma} + 30{\rm dB}, \bar{\gamma}, \bar{\gamma})$ and

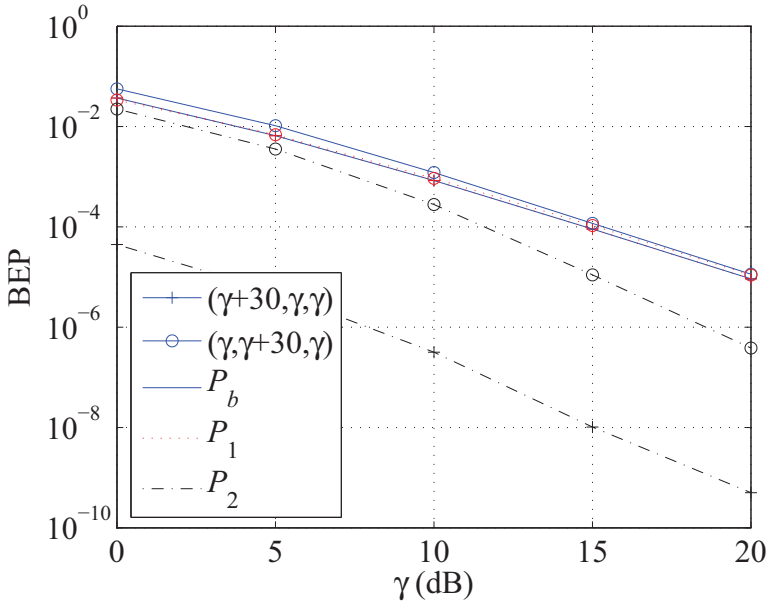

Figure 5.2 BPSK performance obtained with numerical averaging.

$(\bar{\gamma}_{\mathrm{SR}}, \bar{\gamma}_{\mathrm{RD}}, \bar{\gamma}_{\mathrm{SD}}) = (\bar{\gamma}, \bar{\gamma} + 30\mathrm{dB}, \bar{\gamma})$. As shown in Fig. 5.2, P_1 exhibits a diversity order of 2 while P_2 decays more rapidly with a diversity order of 3. Thus, the overall probability P_b is dominated by P_1 and it also exhibits a diversity order of 2. The following analytically establishes such diversity orders of P_1 and P_2 by examining their upperbounds.

Lemma 1. *For soft–power scaling and BPSK modulation, the average probability P_1 is upperbounded as*

$$P_1 \leq \hat{P}_1 \overset{\bar{\gamma}\to\infty}{\approx} (k_1\bar{\gamma})^{-2}, \tag{5.21}$$

where k_1 is a nonnegative constant that depends on $(\sigma_{SR}^2, \sigma_{RD}^2, \sigma_{SD}^2)$.

Proof: See Appendix 5.A.

Lemma 2. *For soft–power scaling and BPSK modulation, the average probability P_2 is upperbounded as*

$$P_2 \leq \hat{P}_2 \overset{\bar{\gamma}\to\infty}{\approx} (k_2\bar{\gamma})^{-3}, \tag{5.22}$$

where k_2 is a nonnegative constant that depends on $(\sigma_{SR}^2, \sigma_{SD}^2)$.

Proof: See Appendix 5.B.

Combining Lemma 1 and Lemma 2, one concludes that, for BPSK, the smart relaying offers a diversity order of 2, i.e.,

$$P_b \overset{\bar{\gamma}\to\infty}{\leq} (k\bar{\gamma})^{-2}, \tag{5.23}$$

where k is a nonnegative constant that depends on $(\sigma^2_{\mathrm{SR}}, \sigma^2_{\mathrm{RD}}, \sigma^2_{\mathrm{SD}})$.

General Rectangular QAM Constellations

Similar to BPSK, the overall symbol error probability (SEP) P_s, can be expressed as a sum of the two terms, denoted by P_1^s and P_2^s. Let $P^s_{\mathrm{SR}}(\gamma_{\mathrm{SR}})$ be the SEP at the relay during the first time slot. For a general two-dimensional $|\mathbf{S}|$–ary modulation, $P^s_{\mathrm{SR}}(\gamma_{\mathrm{SR}})$ can be upperbounded in terms of the Q-function as follows [P10]:

$$P^s_{\mathrm{SR}}(\gamma_{\mathrm{SR}}) \leq (\log_2 |\mathbf{S}|) Q(\sqrt{\mu\gamma_{\mathrm{SR}}}), \tag{5.24}$$

where the constant μ depends on the specific constellation, e.g., $\mu = 2$ for BPSK.

The probability P_1^s is for the case of receiving two identical symbols at the destination, corresponding to probability $(1 - P^s_{\mathrm{SR}}(\gamma_{\mathrm{SR}}))$. On the other hand P_2^s applies to the case of combining two different symbols at the destination, corresponding to probability $P^s_{\mathrm{SR}}(\gamma_{\mathrm{SR}})$. Our objective is to prove that in both cases, the smart relaying enjoys a diversity order of 2.

Consider a general rectangular QAM constellation with the minimum and maximum Euclidean distances $d_{\min}$ and $d_{\max}$. As pointed out in [P8, P14], the analysis in a two–dimensional space can be significantly simplified by invoking the union bound to upper bound P_s as follows:

$$P_s \leq 2P_{s,1D} \leq 2\left(P^s_{1,1D} + P^s_{2,1D}\right), \tag{5.25}$$

where $P_{s,1D}$, $P^s_{1,1D}$ and $P^s_{2,1D}$ correspond to P_s, P_1^s and P_2^s computed in one–dimensional space, respectively. Thus, one needs to calculate the decaying exponents of $P^s_{1,1D}$ and $P^s_{2,1D}$ at high SNR region. The following proposition states the decaying exponent of $P^s_{1,1D}$.

Proposition 1. *For soft–power scaling and general rectangular QAM constellations, the average probability $P^s_{1,1D}$ decays with an exponent of two at high SNR region.*

Proof: See Appendix 5.C.

The conclusion is reasonable since there exist two independent versions of the transmitted symbol arriving at the destination (the same situation as in the co–located antenna systems).

The next task is to compute the decaying exponent of $P^s_{2,1D}$. Different from [P8, P14], the probability $P^s_{2,1D}$ cannot be upperbounded by the case, in which the relay decodes a symbol being at the distance $d_{\max}$ from the symbol actually transmitted. The conclusions in [P8, P14] are inherited from transmission scheme of Protocol II and will be explained later.

Proposition 2. *For soft–power scaling and general rectangular QAM constellations, the average probability $P^s_{2,1D}$ is upperbounded as follows:*

$$P^s_{2,1D} \overset{\bar{\gamma}\to\infty}{\lessapprox} E\Bigg\{ \sum_{i\neq j} (\log_2 |\mathbf{S}|) Q(\sqrt{\mu\gamma_{SR}}) \; Q\left(\frac{\left(|a_{SD_1}|^2 + |w_{RD}|^2\right) d_{\min} \pm 2d_{\min}\sqrt{\alpha_1}\mathrm{Re}\{w_{RD}a_{RD}\}}{\sqrt{2N_0\left(|a_{SD_1}|^2 + |w_{RD}|^2\right)}} \right) \Bigg\} \tag{5.26}$$

where the signs $\pm$, respectively, correspond to $d_{ij} \lessgtr 0$ and d_{ij} is the distance between s_i and s_j.

Proof: See Appendix 5.D.

Proposition 2 tells us that when a wrong decision is made at the relay, the error probabilities corresponding to the situation that the destination erroneously chooses the nearest points from the actual transmitted point, are highest.

For BPSK, $\mu = 2$, $d_{ij} = d_{\min} = \tilde{d}_i = 2\sqrt{E_s}$ and (5.26) becomes the exact upper bound on $P^s_{2,1D}$. Then $P^s_{2,1D}$ reduces to probability P_2 and the diversity order is equal to 3 for this case.

For QPSK, the RHS of (5.26) also simplifies to the form identical (within a scale) to P_2 by substituting $\mu = 1$, $d_{ij} = d_{\min} = \tilde{d}_i = \sqrt{2E_s}$. Thus, $P^s_{2,1D}$ also enjoys a diversity order of 3.

For other higher–order rectangular QAM constellations, the expectation in (5.26) becomes intractable but can be obtained by Monte–Carlo simulation. For 16–QAM, simulation results show that the diversity order equals to 2, not 3. This is due to the existence of the term $\mathrm{Re}\{a^*_{\mathrm{SD}_2} a_{\mathrm{RD}}\}$, resulting from
$\mathrm{Re}\{w_{\mathrm{RD}} a_{\mathrm{RD}}\} = \left[\sqrt{\alpha_1}|a_{\mathrm{RD}}|^2 + \mathrm{Re}\{a^*_{\mathrm{SD}_2} a_{\mathrm{RD}}\}\right]$ in (5.26), which is not present in the case of BPSK and QPSK.

As Protocol II is a special case of Protocol I, from (5.71) (See Appendix 5.D) and the fact that $|d_{ij}| \leq d_{\max}$, one can obtain an upper bound on $\tilde{P}_2^{(\text{P-II})}(s_i \to s_j|\gamma_{\mathrm{SR}}, a_{\mathrm{SD}_1}, a_{\mathrm{SD}_2}, a_{\mathrm{RD}})$ in Protocol II by considering the worst case as follows:

$$\tilde{P}_2^{(\text{P-II})}(s_i \to s_j|\gamma_{\mathrm{SR}}, a_{\mathrm{SD}_1}, a_{\mathrm{SD}_2}, a_{\mathrm{RD}}) \leq Q\left(\frac{|a_{\mathrm{SD}_1}|^2 d_{\min} - \alpha_1 |a_{\mathrm{RD}}|^2 (2d_{\max} - d_{\min})}{\sqrt{2N_0\left(|a_{\mathrm{SD}_1}|^2 + \alpha_1 |a_{\mathrm{RD}}|^2\right)}}\right), \ \forall d \tag{5.27}$$

where $w_{\mathrm{RD}} = \sqrt{\alpha_1} a^*_{\mathrm{RD}}$. Thus, (5.27) confirms the corresponding results in [P8, P14], i.e., it is safe to use the worst case to upperbound the error performance when a wrong decoding decision is committed at the relay.

To summarize, the smart relaying system can obtain a diversity order of 2 for BPSK and QPSK with the soft–power scaling factor α_1. For other higher–order rectangular QAM constellations, e.g., 16–QAM, the performance analysis becomes intractable. However, Monte–Carlo evaluation of (5.26) can be carried out to predict the diversity order of the system. In particular, simulation results show that the smart relaying also obtains a diversity order of 2 for 16–QAM modulation.

5.3.2 Hard–Power Scaling

This part examines the diversity analysis with the hard–power scaling given in (5.8). Our analysis covers the analysis in [P14] for Protocol II. But different from

Protocol II, it will be shown that the smart relaying always achieves a diversity order of 2, even for the simplest on–off relaying scheme. This fact can be explained as follows. For Protocol II, in the case of correctly decoding at the relay, i.e., $\hat{s} = s$, there exists a probability that the relay sends nothing, i.e., $\alpha_q(N_q, \theta) = 0$. This means that there is only one signal path from the source to the destination in the first time slot, and hence Protocol II cannot achieve a diversity order of 2, which was indeed proved in [P14]. On the contrary, for Protocol I, such a circumstance can never happen since there is another independent signal version from the source during the second time slot.

To ease the analysis, the hard–power scaling coefficient in (5.8) is rewritten as follows:

$$\alpha_q(N_q, \theta) = \begin{cases} 0, & 0 \le \gamma_{\rm SR} \le \frac{\theta\bar{\gamma}_{\rm RD}}{2(M-1)} \\ \frac{i}{M-1}, & \frac{(2i-1)\theta\bar{\gamma}_{\rm RD}}{2(M-1)} \le \gamma_{\rm SR} \le \frac{(2i+1)\theta\bar{\gamma}_{\rm RD}}{2(M-1)}, i = [1, M-2] \\ 1, & \frac{(2M-3)\theta\bar{\gamma}_{\rm RD}}{2(M-1)} \le \gamma_{\rm SR} \end{cases} \tag{5.28}$$

As pointed out earlier, one has $\alpha_{\text{on–off}} = \alpha_q(1, 2)$ from (5.28).

Consider BPSK. In order to calculate the diversity order of the smart relaying system with hard–power scaling, one can mimic the steps done for BPSK and soft–power scaling by appropriately replacing α_1 by $\alpha_q(N_q, \theta)$.

Proposition 3. *For hard–power scaling and BPSK, the average overall BEP, $P_{b,h}$, can be upperbounded as*

$$P_{b,h} \le \hat{P}_{b,h} \overset{\bar{\gamma}\to\infty}{\approx} (k_h\bar{\gamma})^{-2}, \tag{5.29}$$

where k_h is a nonnegative constant that depends on $(\sigma_{SR}^2, \sigma_{RD}^2, \sigma_{SD}^2)$.

Proof: See Appendix 5.E.

It should be stressed here that the diversity order established in Proposition 3 does not depend on how perfect the feedback of the R–D channel and how exact the quantization process are.

Likewise, the analysis can be straightforwardly extended to QPSK by following the same steps as done in the soft–power scaling case. In summary, for hard–power scaling and QPSK, the smart relaying also achieves a diversity order of 2. For other higher–order rectangular QAM constellations, the analysis becomes intractable and one also needs to resort to computer simulations. As shown in the next section, the smart relaying also achieves a diversity order of 2 for 16–QAM under hard–power scaling.

5.4 Numerical Results

This section presents simulation results of the BEPs for the relaying system under consideration. Three possible scenarios for practical SNRs, i.e., the relay is close to the source, the relay is close to the destination and the three nodes are equidistant, are considered. The three scenarios mentioned above are assumed to correspond to the following three cases: $(\bar{\gamma}_{\rm SR}, \bar{\gamma}_{\rm RD}, \bar{\gamma}_{\rm SD}) = (\bar{\gamma} + 30{\rm dB}, \bar{\gamma}, \bar{\gamma})$, $(\bar{\gamma}, \bar{\gamma} + 30{\rm dB}, \bar{\gamma})$ and $(\bar{\gamma}, \bar{\gamma}, \bar{\gamma})$ (recall that $\bar{\gamma} = E_s/N_0$).

For a fair comparison among different schemes, the total power used in all schemes is fixed to be $\bar{\gamma}_{\rm tot} = \bar{\gamma}(2 + \bar{\alpha})$ where, depending on the power scaling employed, the average power scaling, $\bar{\alpha}$ at the relay is one of the following [P14]:

$$\bar{\alpha} = E[\alpha] = \frac{\bar{\gamma}_{\rm SR}}{\bar{\gamma}_{\rm RD}} \log\left(1 + \frac{\bar{\gamma}_{\rm RD}}{\bar{\gamma}_{\rm SR}}\right) \tag{5.30}$$

$$\bar{\alpha} = E[\alpha_{\text{on–off}}] = \exp\left(-\frac{\bar{\gamma}_{\rm RD}}{\bar{\gamma}_{\rm SR}}\right) \tag{5.31}$$

$$\bar{\alpha} = E[\alpha_q(N_q, \theta)] = \sum_{i=1}^{M-1} \frac{1}{M-1} \exp\left(-\frac{(2i-1)\theta\bar{\gamma}_{\rm RD}}{2(M-1)\bar{\gamma}_{\rm SR}}\right). \tag{5.32}$$

It is noted that

$$\lim_{N_q \to \infty} E[\alpha_q(N_q, 1)] = E[\alpha_1(\theta = 1)] = \frac{\bar{\gamma}_{\rm SR}}{\bar{\gamma}_{\rm RD}} \left[1 - \exp\left(-\frac{\bar{\gamma}_{\rm RD}}{\bar{\gamma}_{\rm SR}}\right)\right], \tag{5.33}$$

which follows from the fact that $\lim_{N_q \to \infty} \alpha_q(N_q, 1) = \alpha_1(\theta = 1)$. For the conventional relaying, the total power $\bar{\gamma}_{\rm tot}$ is equal to $3\bar{\gamma}$.

For BPSK, Fig. 5.3 shows that the smart relaying systems with the *soft* and

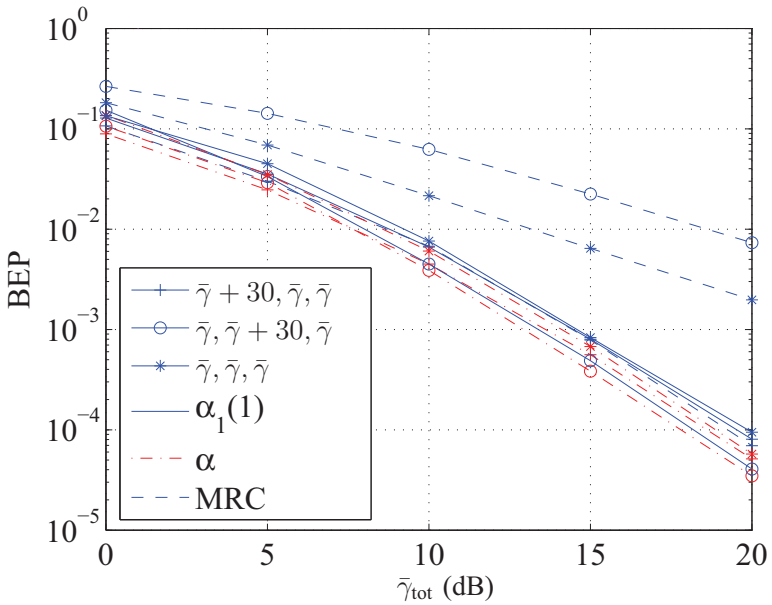

Figure 5.3 Performance of BPSK – Different SNR triples.

instantaneous power scaling, i.e., with $\alpha_1(1)$ and α, respectively, significantly outperform the conventional relaying systems with MRC in two cases of $(\bar{\gamma}, \bar{\gamma}+30\text{dB}, \bar{\gamma})$ and $(\bar{\gamma}, \bar{\gamma}, \bar{\gamma})$. Their performances are almost identical in the remaining case of $(\bar{\gamma}+30\text{dB}, \bar{\gamma}, \bar{\gamma})$. Such results are expected from the analysis in Section 5.3, where it is shown that the smart relaying always achieves a diversity order of 2, while the conventional relaying looses its diversity when the S–R link is not reliable. Moreover, it is observed that the instantaneous–power scaling serves as a lower bound on the performance of the soft–power scaling. This is expected since the former scaling, with the instantaneous R–D channel information available at the relay, can adapt better to the R–D link condition than the latter. However, the price for this performance advantage is the larger bandwidth required for the feedback signals. Further, it might not be possible to track the instantaneous R–D channel information if it changes too fast.

Fig. 5.4 illustrates the impact of feedback channel quality on the overall performance. Since the smart relaying works well regardless of the location of the relay, we only consider the case that three nodes are equidistant. One can see that the BEP curves have identical slopes when imperfect feedback is received at the relay. With

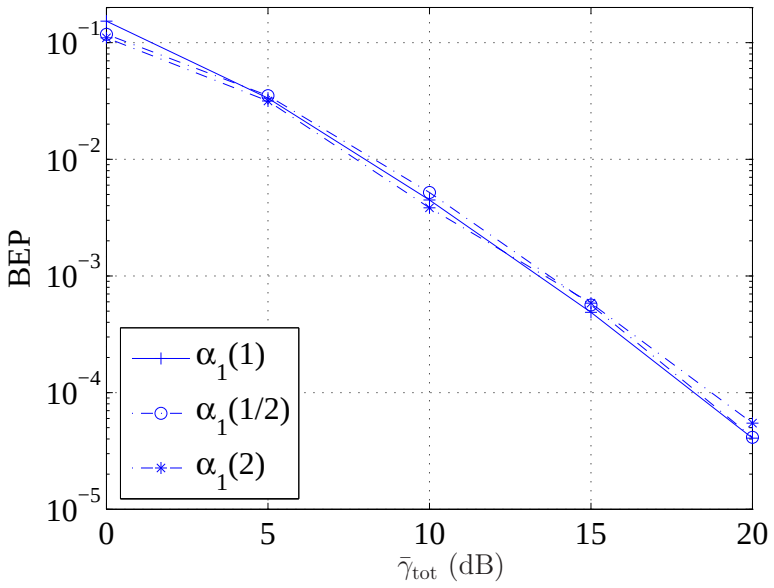

Figure 5.4 Performance of BPSK – Different feedback channel conditions.

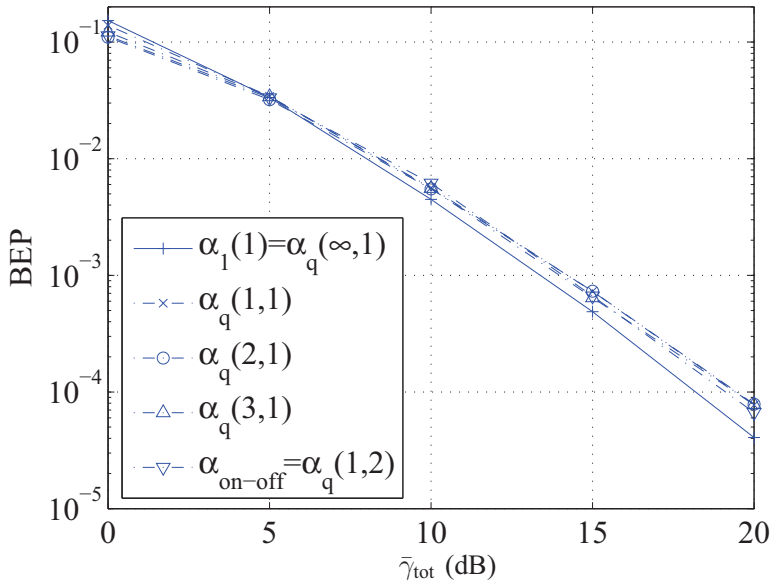

Figure 5.5 Performance of BPSK – Different quantization bits.

two examples, i.e., $\theta = 1/2$ and $\theta = 2$, the loss in error performance is insignificant when compared to the perfect feedback case.

The effect of the quantization error on the achievable diversity order is presented in Fig. 5.5. Different from the corresponding results in [P14] for Protocol II, Protocol

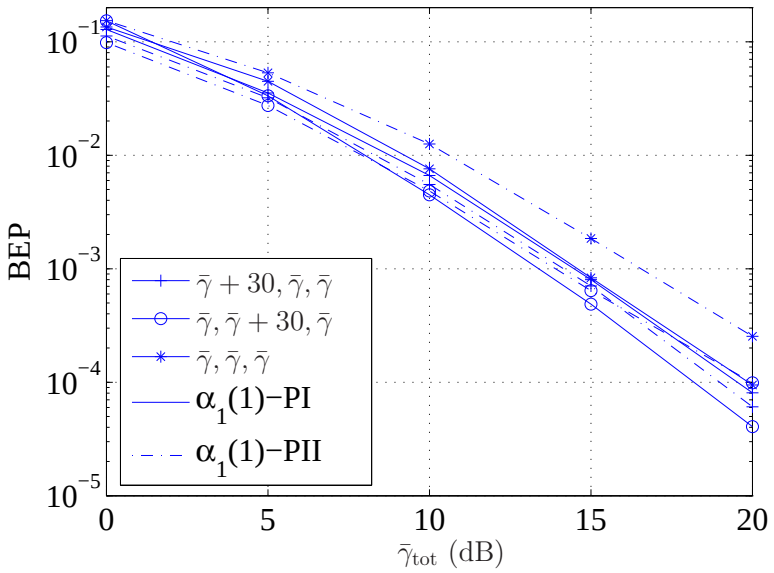

Figure 5.6 Performance of BPSK – Protocols I and II.

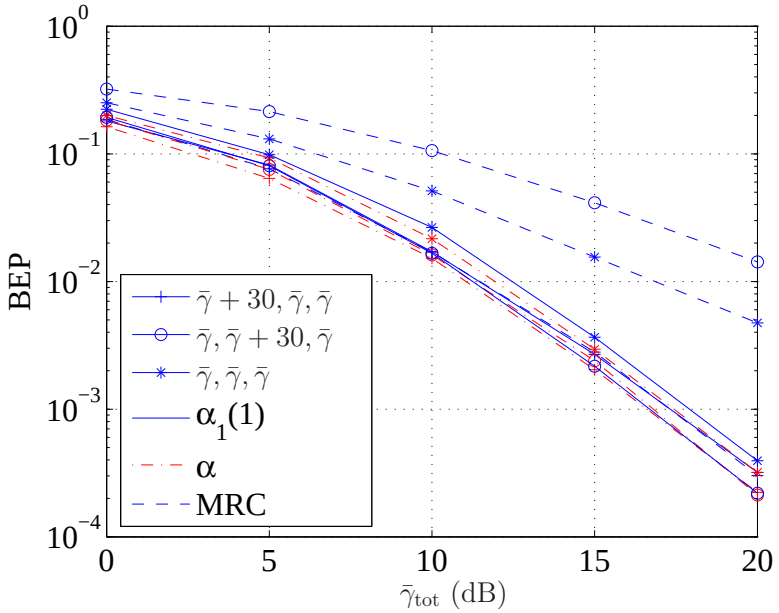

Figure 5.7 Performance of QPSK – Different SNR triples.

I can achieve a diversity order of 2 for all cases of numbers of quantization bits. From the relay's complexity viewpoint, one would use only 1 quantization bit to scale the transmitted power at the relay for simplicity, while the diversity order 2 is still maintained at the destination.

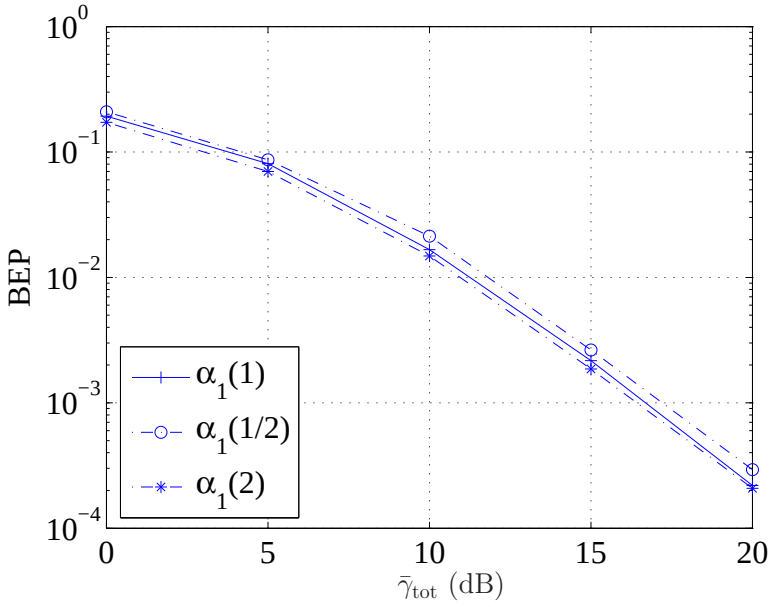

Figure 5.8 Performance of QPSK – Different feedback channel conditions.

To compare the performance of the smart relaying in Protocols I and II, Fig. 5.6 plots the error curves when $\alpha_1(1)$ is used in both protocols. It should be noted that the total power used for Protocol II is now $\bar{\gamma}(1 + E[\alpha_1])$ while it is $\bar{\gamma}(2 + E[\alpha_1])$ for Protocol I. Although the average SNR, $\bar{\gamma}$, for Protocol I is lower than that for Protocol II, Protocol I performs almost the same as Protocol II in the case of $(\bar{\gamma} + 30\text{dB}, \bar{\gamma}, \bar{\gamma})$. It outperforms Protocol II in two other cases of $(\bar{\gamma}, \bar{\gamma} + 30\text{dB}, \bar{\gamma})$ and $(\bar{\gamma}, \bar{\gamma}, \bar{\gamma})$. This observation is due to the fact that when the S–R link is severely unreliable, the received SNR at the destination in the second time slot might be scaled to a very small value in Protocol II, whereas in Protocol I it is still at a high value as there exists another signal from the source.

For QPSK, the same settings for BPSK are adopted in the simulations. As shown in Fig. 5.7, using smart relaying in Protocol I also provides a diversity order of 2, which is in agreement with the analysis done before. In comparison, the performance of conventional relaying with MRC is also presented. As expected, using $\alpha_1(1)$ offers a significant performance improvement over MRC when $(\bar{\gamma}_{\text{SR}}, \bar{\gamma}_{\text{RD}}, \bar{\gamma}_{\text{SD}}) = (\bar{\gamma}, \bar{\gamma} + 30\text{dB}, \bar{\gamma})$ or $(\bar{\gamma}, \bar{\gamma}, \bar{\gamma})$ and it performs virtually identical to MRC for the case of $(\bar{\gamma}_{\text{SR}}, \bar{\gamma}_{\text{RD}}, \bar{\gamma}_{\text{SD}}) = (\bar{\gamma} + 30\text{dB}, \bar{\gamma}, \bar{\gamma})$.

Under the condition that three nodes are equidistant, Figs. 5.8 and 5.9 investigate the system performance when different feedback channel conditions and quantization bits are used, respectively. As shown in Fig. 5.8, the smart relaying is very robust in various feedback channel conditions. Not only a diversity order of 2 is obtained but also there exists only a very small performance loss compared to the perfect feedback case. Fig. 5.9 illustrates that soft–power scaling tightly upperbounds hard power scalings, even for the simple on–off scaling.

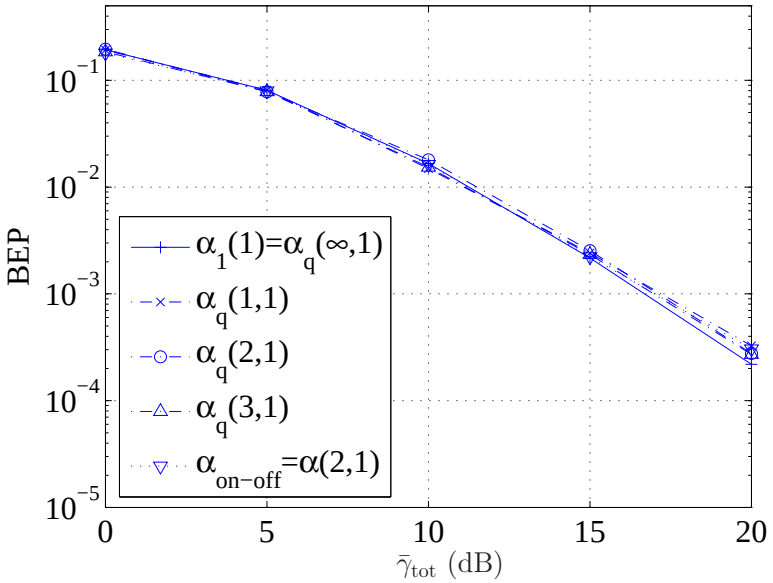

Figure 5.9 Performance of QPSK – Different quantization bits.

Consistently with the observation for BPSK, Fig. 5.10 shows that Protocol I for QPSK offers a gain of 2 dB at BEP $= 10^{-3}$ over Protocol II when S, R and D are equidistant, while the performance of the two protocols are virtually identical for the other two scenarios.

The last investigation studies the smart relaying performance when 16–QAM is used. As shown in Fig. 5.11, using $\alpha_1(1)$ obtains a diversity order of 2 in all cases considered. Moreover, using $\alpha_{\text{on–off}}$ not only achieves the same diversity as using $\alpha_1(1)$ but also outperforms it by about 1 dB at BEP $= 10^{-2}$ under the symmetry condition. As can be predicted, the MRC can achieve a diversity order of 2 provided that the S–R link is reliable. However, the diversity order achieved by the MRC degrades in

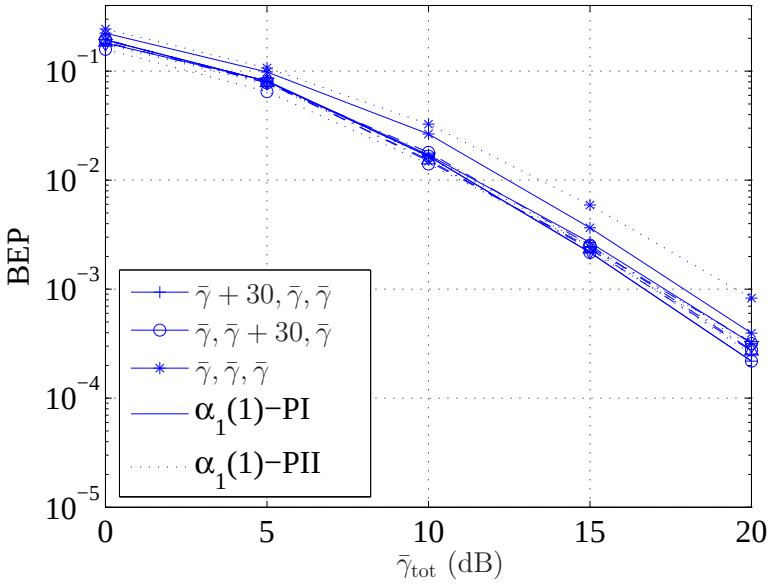

Figure 5.10 Performance of QPSK – Protocols I and II.

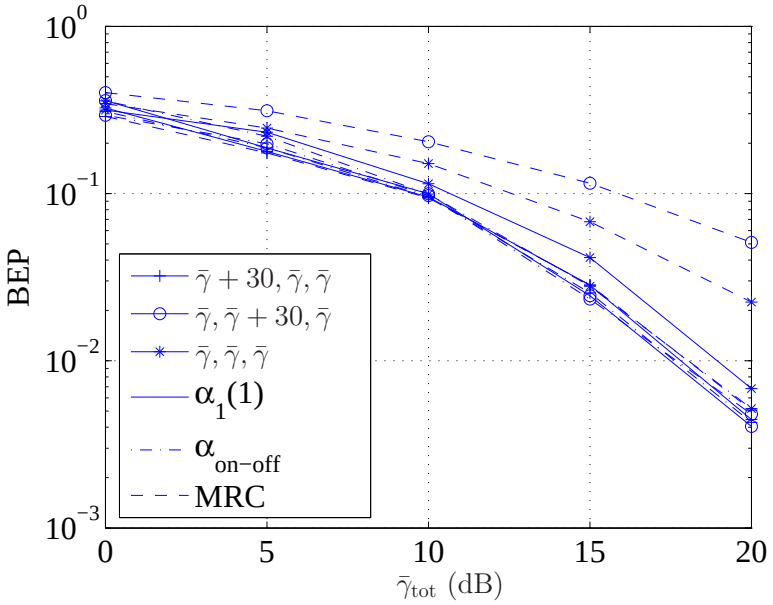

Figure 5.11 Performance of 16–QAM – Different SNR triples.

other cases.

5.5 Conclusions

This paper generalized the smart relaying technique presented in [P14] to Protocol I for uncoded DF systems. It was proved that Protocol I always achieves a diversity order of 2 for not only the soft–power scaling, but also hard–power scaling when BPSK and QPSK are employed. For rectangular 16–QAM constellation, it is also shown by simulations that the smart relaying systems also enjoys the diversity order 2. Since Protocol I includes Protocol II as a special case, the analysis done in this paper subsumes all the corresponding results in [P14]. Moreover it was demonstrated that with smart–relaying in DF, Protocol I offers performance improvement over Protocol II.

5.A Proof of Lemma 1

The conditional probability $P_1(\gamma_{\mathrm{SR}}, a_{\mathrm{SD}_1}, a_{\mathrm{SD}_2}, a_{\mathrm{RD}})$ in (5.16) can be upperbounded as

$$P_1(\gamma_{\mathrm{SR}}, a_{\mathrm{SD}_1}, a_{\mathrm{SD}_2}, a_{\mathrm{RD}}) \leq Q\left(\sqrt{2\bar{\gamma}\left(|a_{\mathrm{SD}_1}|^2 + |\sqrt{\alpha_1}a_{\mathrm{RD}} + a_{\mathrm{SD}_2}|^2\right)}\right), \tag{5.34}$$

Conditioned on $(\gamma_{\mathrm{SR}}, \bar{\gamma}_{\mathrm{RD}})$, $a_1 = (\sqrt{\alpha_1}a_{\mathrm{RD}} + a_{\mathrm{SD}_2})$ is $\mathcal{CN}(0, \sigma_{a_1}^2)$, where

$$\sigma_{a_1}^2 = \alpha_1\sigma_{\mathrm{RD}}^2 + \sigma_{\mathrm{SD}}^2 = \frac{\min(\gamma_{\mathrm{SR}}, \theta\bar{\gamma}_{\mathrm{RD}})}{\theta\bar{\gamma}_{\mathrm{RD}}}\sigma_{\mathrm{RD}}^2 + \sigma_{\mathrm{SD}}^2. \tag{5.35}$$

Then (5.34) becomes

$$P_1(\gamma_{\mathrm{SR}}, a_{\mathrm{SD}_1}, a_{\mathrm{SD}_2}, a_{\mathrm{RD}}) \leq Q\left(\sqrt{2(\gamma_{\mathrm{SD}_1} + \gamma_1)}\right) \leq \frac{1}{2}\exp\left(-(\gamma_{\mathrm{SD}_1} + \gamma_1)\right), \tag{5.36}$$

where the instantaneous SNR $\gamma_1 = |a_1|^2(E_s/N_0) = |a_1|^2\bar{\gamma}$ is an exponential RV with mean $\bar{\gamma}_1 = \sigma_{a_1}^2\bar{\gamma} = \alpha_1\bar{\gamma}_{\mathrm{RD}} + \bar{\gamma}_{\mathrm{SD}}$. Note that the inequality in (5.36) comes from the Chernoff bound that $Q(x) \leq (1/2)\exp(-x^2/2)$ for $x \geq 0$.

The upper bound on the unconditional BEP, P_1, can be calculated as

$$P_1 \leq \int_0^\infty \int_0^\infty \int_0^\infty \frac{1}{2}\exp\left(-(\gamma_{\mathrm{SD}_1} + \gamma_1)\right) p_{\gamma_{\mathrm{SD}_1}}(\gamma_{\mathrm{SD}}) p_{\gamma_1|\gamma_{\mathrm{SR}}}(\gamma_1|\gamma_{\mathrm{SR}}) p_{\gamma_{\mathrm{SR}}}(\gamma_{\mathrm{SR}}) d\gamma_{\mathrm{SD}_1} d\gamma_1 d\gamma_{\mathrm{SR}}, \tag{5.37}$$

where

$$p_{\gamma_1|\gamma_{\rm SR}}(\gamma_1|\gamma_{\rm SR}) = \frac{1}{\bar{\gamma}_1}\exp\left(-\frac{\gamma_1}{\bar{\gamma}_1}\right)$$
$$= \frac{1}{\frac{\min(\gamma_{\rm SR},\theta\bar{\gamma}_{\rm RD})}{\theta\bar{\gamma}_{\rm RD}}\bar{\gamma}_{\rm RD}+\bar{\gamma}_{\rm SD}}\exp\left(-\frac{\gamma_1}{\frac{\min(\gamma_{\rm SR},\theta\bar{\gamma}_{\rm RD})}{\theta\bar{\gamma}_{\rm RD}}\bar{\gamma}_{\rm RD}+\bar{\gamma}_{\rm SD}}\right). \quad (5.38)$$

Since the RV $\gamma_{\rm SD_1}$ is independent of the other RVs, (5.37) can be rewritten as

$$P_1 \le \frac{1}{2}\int_0^\infty \frac{\exp\left(-\gamma_{\rm SD_1}\right)}{\bar{\gamma}_{\rm SD}}\exp\left(-\frac{\gamma_{\rm SD_1}}{\bar{\gamma}_{\rm SD}}\right)d\gamma_{\rm SD_1}\int_0^\infty\left[\int_0^\infty\frac{\exp\left(-\gamma_1\right)}{\bar{\gamma}_1}\exp\left(-\frac{\gamma_1}{\bar{\gamma}_1}\right)d\gamma_1\right]$$
$$p_{\gamma_{\rm SR}}(\gamma_{\rm SR})d\gamma_{\rm SR} \quad (5.39)$$
$$= \frac{1}{2(1+\bar{\gamma}_{\rm SD})}\int_0^\infty\frac{1}{\bar{\gamma}_{\rm SR}(1+\bar{\gamma}_1)}\exp\left(-\frac{\gamma_{\rm SR}}{\bar{\gamma}_{\rm SR}}\right)d\gamma_{\rm SR}. \quad (5.40)$$

By substituting $\bar{\gamma}_1$ into (5.40), the upper bound on P_1 becomes

$$P_1 \le \frac{1}{2(1+\bar{\gamma}_{\rm SD})}\int_0^\infty\frac{1}{\bar{\gamma}_{\rm SR}(1+\alpha_1\bar{\gamma}_{\rm RD}+\bar{\gamma}_{\rm SD})}\exp\left(-\frac{\gamma_{\rm SR}}{\bar{\gamma}_{\rm SR}}\right)d\gamma_{\rm SR} = I_{11}+I_{12}, \quad (5.41)$$

where

$$I_{11} = \frac{1}{2(1+\bar{\gamma}_{\rm SD})}\int_0^{\theta\bar{\gamma}_{\rm RD}}\frac{1}{\bar{\gamma}_{\rm SR}(1+\gamma_{\rm SR}/\theta+\bar{\gamma}_{\rm SD})}\exp\left(-\frac{\gamma_{\rm SR}}{\bar{\gamma}_{\rm SR}}\right)d\gamma_{\rm SR}$$
$$= \frac{\theta}{2\bar{\gamma}_{\rm SR}(1+\bar{\gamma}_{\rm SD})}\exp\left(\frac{(1+\bar{\gamma}_{\rm SD})\theta}{\bar{\gamma}_{\rm SR}}\right)\left[\mathrm{Ei}\left(-\frac{(1+\bar{\gamma}_{\rm RD}+\bar{\gamma}_{\rm SD})\theta}{\bar{\gamma}_{\rm SR}}\right)-\right.$$
$$\left.\mathrm{Ei}\left(-\frac{(1+\bar{\gamma}_{\rm SD})\theta}{\bar{\gamma}_{\rm SR}}\right)\right] \quad (5.42)$$
$$I_{12} = \frac{1}{2(1+\bar{\gamma}_{\rm SD})}\int_{\theta\bar{\gamma}_{\rm RD}}^\infty\frac{1}{\bar{\gamma}_{\rm SR}(1+\bar{\gamma}_{\rm RD}+\bar{\gamma}_{\rm SD})}\exp\left(-\frac{\gamma_{\rm SR}}{\bar{\gamma}_{\rm SR}}\right)d\gamma_{\rm SR}$$
$$= \frac{1}{2(1+\bar{\gamma}_{\rm RD}+\bar{\gamma}_{\rm SD})(1+\bar{\gamma}_{\rm SD})}\exp\left(-\frac{\theta\bar{\gamma}_{\rm RD}}{\bar{\gamma}_{\rm SR}}\right). \quad (5.43)$$

In (5.42), $\mathrm{Ei}(x)$ is the exponential integral function, defined as [P16, pp. 883, Eq. 8.211.1]:

$$\mathrm{Ei}(x) = -\int_{-x}^\infty\frac{\exp(-t)}{t}dt, \quad x<0.$$

Substituting (5.42) and (5.43) into (5.41) proves Lemma 1. It should also be pointed out that for Protocol II, $\bar{\gamma}_1$ simplifies to $\alpha_1\bar{\gamma}_{\rm RD}$ and it can be easily verified that the upper bound on P_1 in (5.41) reduces to [P14, Eq. (29)].

$$P_2(\gamma_{\rm SR}, a_{\rm SD_1}, a_{\rm SD_2}, a_{\rm RD}) \le Q\left(\sqrt{2\gamma_{\rm SR}}\right) Q\left(\frac{\sqrt{2\bar{\gamma}}\left(|a_{\rm SD_1}|^2 + |a_{\rm SD_2}|^2 - \alpha_1 |a_{\rm RD}|^2\right)}{\sqrt{|a_{\rm SD_1}|^2 + 2\alpha_1 |a_{\rm RD}|^2 + 2|a_{\rm SD_2}|^2}}\right)$$
$$\le Q\left(\sqrt{2\gamma_{\rm SR}}\right) Q\left(\frac{\sqrt{2\bar{\gamma}}\left(|a_{\rm SD_1}|^2 + |a_{\rm SD_2}|^2 - \alpha_1 |a_{\rm RD}|^2\right)}{\sqrt{2|a_{\rm SD_1}|^2 + 2\alpha_1 |a_{\rm RD}|^2 + 2|a_{\rm SD_2}|^2}}\right)$$
$$= Q\left(\sqrt{2\gamma_{\rm SR}}\right) Q\left(\frac{\gamma_{\rm SD_1} + \gamma_{\rm SD_2} - \alpha_1 \gamma_{\rm RD}}{\sqrt{\gamma_{\rm SD_1} + \gamma_{\rm SD_2} + \alpha_1 \gamma_{\rm RD}}}\right), \tag{5.44}$$

$$P_A = \int_0^\infty \int_0^\infty \int_{\alpha_2 \gamma_{\rm RD}}^\infty \frac{1}{4} \exp(-\gamma_{\rm SR}) \exp\left(-\frac{\left(\gamma_{\rm SD} - \alpha_2 \gamma_{\rm RD}\right)^2}{2(\gamma_{\rm SD} + \alpha_2 \gamma_{\rm RD})}\right)$$
$$p_{\gamma_{\rm SD}}(\gamma_{\rm SD}) p_{\gamma_{\rm SR}}(\gamma_{\rm SR}) p_{\gamma_{\rm RD}}(\gamma_{\rm RD}) d\gamma_{\rm SD} d\gamma_{\rm SR} d\gamma_{\rm RD} \tag{5.45}$$
$$P_B = \int_0^\infty \int_0^\infty \int_0^{\alpha_2 \gamma_{\rm RD}} \frac{1}{2} \exp(-\gamma_{\rm SR}) p_{\gamma_{\rm SD}}(\gamma_{\rm SD}) p_{\gamma_{\rm RD}}(\gamma_{\rm RD}) p_{\gamma_{\rm SR}}(\gamma_{\rm SR}) d\gamma_{\rm SD} d\gamma_{\rm RD} d\gamma_{\rm SR}, \tag{5.46}$$

5.B Proof of Lemma 2

The second conditional probability $P_2(\gamma_{\rm SR}, a_{\rm SD_1}, a_{\rm SD_2}, a_{\rm RD})$ can be bounded as (5.44), where the first inequality comes from the the fact $|x+y|^2 \le 2|x|^2 + 2|y|^2$.

In (5.44), let $\gamma_{\rm SD} = \gamma_{\rm SD_1} + \gamma_{\rm SD_2}$. The pdf of $\gamma_{\rm SD}$ is $p_{\gamma_{\rm SD}}(\gamma_{\rm SD}) = \frac{\gamma_{\rm SD}}{\bar{\gamma}_{\rm SD}^2} \exp\left(-\frac{\gamma_{\rm SD}}{\bar{\gamma}_{\rm SD}}\right)$, where $\bar{\gamma}_{\rm SD} = \bar{\gamma}\sigma_{\rm SD}^2$. Hence, the inequality (5.44) can be rewritten as

$$P_2(\gamma_{\rm SD}, \gamma_{\rm SR}, \gamma_{\rm RD}) \le Q\left(\sqrt{2\gamma_{\rm SR}}\right) Q\left(\frac{\gamma_{\rm SD} - \alpha_1 \gamma_{\rm RD}}{\sqrt{\gamma_{\rm SD} + \alpha_1 \gamma_{\rm RD}}}\right)$$
$$\le Q\left(\sqrt{2\gamma_{\rm SR}}\right) Q\left(\frac{\gamma_{\rm SD} - \alpha_2 \gamma_{\rm RD}}{\sqrt{\gamma_{\rm SD} + \alpha_2 \gamma_{\rm RD}}}\right). \tag{5.47}$$

The second inequality above comes from the fact that $\alpha_1 \le \alpha_2 = \gamma_{\rm SR}/(\theta\bar{\gamma}_{\rm RD})$. Note also that (5.47) is conditioned on three instantaneous SNRs, namely $\gamma_{\rm SD}$, $\gamma_{\rm SR}$ and $\gamma_{\rm RD}$.

Applying the Chernoff bound, the unconditional probability P_2 can be bounded as $P_2 \le P_A + P_B$, where P_A and P_B are specified by (5.45) and (5.46), respectively.

$$I_{21}(\gamma_{\rm SR},\gamma_{\rm RD}) = \int_0^\infty \exp\left(-\frac{1}{2}\left(\gamma_{\rm SD}+\alpha_2\gamma_{\rm RD}-2\sqrt{\alpha_2\gamma_{\rm RD}\gamma_{\rm SD}}\right)\right) p_{\gamma_{\rm SD}}(\gamma_{\rm SD})d\gamma_{\rm SD}$$
$$\frac{1}{\bar{\gamma}_{\rm SD}^2}\int_0^\infty \gamma_{\rm SD}\exp\left[-\left(\underbrace{\sqrt{\beta_1\gamma_{\rm SD}}-\sqrt{\beta_2\gamma_{\rm eq}}}_{u}\right)^2-\gamma_{\rm eq}(0.5-\beta_2)\right]d\gamma_{\rm SD}, \tag{5.50}$$

The probability P_A can be upperbounded as follows

$$P_A \le \int_0^\infty\int_0^\infty\int_0^\infty \frac{1}{4}\exp(-\gamma_{\rm SR})\exp\left(-\frac{\left(\gamma_{\rm SD}+\alpha_2\gamma_{\rm RD}-2\sqrt{\alpha_2\gamma_{\rm RD}\gamma_{\rm SD}}\right)}{2}\right)p_{\gamma_{\rm SD}}(\gamma_{\rm SD})$$
$$p_{\gamma_{\rm SR}}(\gamma_{\rm SR})p_{\gamma_{\rm RD}}(\gamma_{\rm RD})d\gamma_{\rm SD}d\gamma_{\rm SR}d\gamma_{\rm RD} = I_2, \tag{5.48}$$

where the inequality (5.48) comes from the Cauchy-Schwarz inequality[3] and the fact that $\int_a^\infty f(x)dx \le \int_0^\infty f(x)dx$, $f(x)\ge 0\ \forall x\in[0,\infty\}$, and $a\ge 0$. In the next steps, the RHS of (5.48) is averaged over $\gamma_{\rm SD}$, then $\gamma_{\rm SR}$ and finally $\gamma_{\rm RD}$.

First, I_2 can be calculated as

$$I_2 = \int_0^\infty\int_0^\infty \frac{1}{4}\exp(-\gamma_{\rm SR})p_{\gamma_{\rm SR}}(\gamma_{\rm SR})p_{\gamma_{\rm RD}}(\gamma_{\rm RD})I_{21}(\gamma_{\rm SR},\gamma_{\rm RD})d\gamma_{\rm SR}d\gamma_{\rm RD}, \tag{5.49}$$

where $I_{21}(\gamma_{\rm SR},\gamma_{\rm RD})$ is given in (5.50) with $\beta_1=\frac{2+\bar{\gamma}_{\rm SD}}{2\bar{\gamma}_{\rm SD}}$, $\beta_2=\frac{\bar{\gamma}_{\rm SD}}{2(2+\bar{\gamma}_{\rm SD})}$, $\gamma_{\rm eq}=\alpha_2\gamma_{\rm RD}=\frac{\gamma_{\rm SR}\gamma_{\rm RD}}{\theta\bar{\gamma}_{\rm RD}}$.

By changing the variable $u=\sqrt{\beta_1\gamma_{\rm SD}}-\sqrt{\beta_2\gamma_{\rm eq}}$, $I_{21}(\gamma_{\rm SR},\gamma_{\rm RD})$ can be calculated and bounded as follows:

$$I_{21}(\gamma_{\rm SR},\gamma_{\rm RD}) = \frac{2\exp(-\gamma_{\rm eq}(0.5-\beta_2))}{\bar{\gamma}_{\rm SD}^2\beta_1^2}\int_{-\sqrt{\beta_2\gamma_{\rm eq}}}^\infty \left(u+\sqrt{\beta_2\gamma_{\rm eq}}\right)^3\exp(-u^2)du \tag{5.51}$$
$$\le \frac{\beta_2\gamma_{\rm eq}\exp(-\gamma_{\rm eq}/2)}{\bar{\gamma}_{\rm SD}^2\beta_1^2}+\frac{\exp(-\gamma_{\rm eq}/2)}{\bar{\gamma}_{\rm SD}^2\beta_1^2}+$$
$$\frac{2\exp(-\gamma_{\rm eq}(0.5-\beta_2))}{\bar{\gamma}_{\rm SD}^2\beta_1^2}\left((\beta_2\gamma_{\rm eq})^{1.5}+\frac{3\sqrt{\beta_2\gamma_{\rm eq}}}{2}\right)\sqrt{\pi}, \tag{5.52}$$

[3]The Cauchy-Schwarz inequality states that for two vectors $\mathbf{u}$ and $\mathbf{v}$, one has $\langle\mathbf{u},\mathbf{v}\rangle\le\|\mathbf{u}\|\|\mathbf{v}\|$. Taking $\mathbf{u}=[\sqrt{x},\sqrt{y}]$, $\mathbf{v}=[1,1]$ yields the inequality. However the inequality $x+y\ge 2\sqrt{xy}$, for x, $y\ge 0$, is better recognized as the arithmetic and geometric (AM-GM) bound.

where the inequality (5.52) comes from the fact that
$\int_{-\sqrt{\beta_2\gamma_{\rm eq}}}^{\infty}\exp(-u^2)du \leq \int_{-\infty}^{\infty}\exp(-u^2)du = \sqrt{\pi}$.

Substituting (5.52) to (5.49), I_2 can be upperbounded as

$$I_2 \leq I_{22} + I_{23} + I_{24}, \tag{5.53}$$

in which

$$I_{22} = \int_0^{\infty}\int_0^{\infty}\frac{1}{4}\exp(-\gamma_{\rm SR})\frac{\beta_2\gamma_{\rm eq}\exp(-\gamma_{\rm eq}/2)}{\bar{\gamma}_{\rm SD}^2\beta_1^2}p_{\gamma_{\rm SR}}(\gamma_{\rm SR})p_{\gamma_{\rm RD}}(\gamma_{\rm RD})d\gamma_{\rm SR}d\gamma_{\rm RD}, \tag{5.54}$$

$$I_{23} = \int_0^{\infty}\int_0^{\infty}\frac{1}{4}\exp(-\gamma_{\rm SR})\frac{\exp(-\gamma_{\rm eq}/2)}{\bar{\gamma}_{\rm SD}^2\beta_1^2}p_{\gamma_{\rm SR}}(\gamma_{\rm SR})p_{\gamma_{\rm RD}}(\gamma_{\rm RD})d\gamma_{\rm SR}d\gamma_{\rm RD}, \tag{5.55}$$

$$I_{24} = \int_0^{\infty}\int_0^{\infty}\frac{\sqrt{\pi}}{2}\exp(-\gamma_{\rm SR})\frac{\exp(-\gamma_{\rm eq}(0.5-\beta_2))}{\bar{\gamma}_{\rm SD}^2\beta_1^2} \left[(\beta_2\gamma_{\rm eq})^{1.5} + \frac{3\sqrt{\beta_2\gamma_{\rm eq}}}{2}\right] p_{\gamma_{\rm SR}}(\gamma_{\rm SR})p_{\gamma_{\rm RD}}(\gamma_{\rm RD})d\gamma_{\rm SR}d\gamma_{\rm RD}. \tag{5.56}$$

Averaging over two variables $\gamma_{\rm SR}$ and $\gamma_{\rm RD}$, I_{22} is given as follows:

$$I_{22} = \frac{2\theta\bar{\gamma}_{\rm SD}}{\bar{\gamma}_{\rm SR}(2+\bar{\gamma}_{\rm SD})^3}\int_0^{\infty}\frac{u\exp(-2\theta u)}{\left(1+\frac{1}{\bar{\gamma}_{\rm SR}}+u\right)^2}du \overset{\bar{\gamma}\to\infty}{\approx} (k_{22}\bar{\gamma})^{-3}, \tag{5.57}$$

where k_{22} is a nonnegative constant that depends on $(\sigma_{\rm SR}^2, \sigma_{\rm SD}^2)$. Similarly, I_{23} is bounded as

$$I_{23} \leq \frac{1}{\bar{\gamma}_{\rm SR}(2+\bar{\gamma}_{\rm SD})^2(1+\frac{1}{\bar{\gamma}_{\rm SR}})} \overset{\bar{\gamma}\to\infty}{\approx} (k_{23}\bar{\gamma})^{-3}, \tag{5.58}$$

where k_{23} is a nonnegative constant that depends on $(\sigma_{\rm SR}^2, \sigma_{\rm SD}^2)$. Finally, I_{24} can be bounded as follows:

$$I_{24} \leq \frac{\sqrt{\pi/2}\Gamma^2(2.5)\bar{\gamma}_{\rm SD}^{1.5}}{\theta^{1.5}\bar{\gamma}_{\rm SR}\left(1+\frac{1}{\bar{\gamma}_{\rm SR}}\right)^{2.5}(2+\bar{\gamma}_{\rm SD})^{3.5}} + \frac{3\sqrt{\pi/2}\Gamma^2(1.5)\bar{\gamma}_{\rm SD}^{0.5}}{\theta^{0.5}\bar{\gamma}_{\rm SR}\left(1+\frac{1}{\bar{\gamma}_{\rm SR}}\right)^{1.5}(2+\bar{\gamma}_{\rm SD})^{2.5}} \overset{\bar{\gamma}\to\infty}{\approx} (k_{24}\bar{\gamma})^{-3}, \tag{5.59}$$

where (5.59) comes from [P16, pp. 346, Eq. (3.381.4)] and $\Gamma(z) = \int_0^{\infty}\exp(-t)t^{z-1}dt$ is the gamma function. The constant k_{24} is a nonnegative constant that depends on $(\sigma_{\rm SR}^2, \sigma_{\rm SD}^2)$.

It follows from (5.48), (5.53), (5.57), (5.58) and (5.59) that the BEP P_A is inversely proportional to order three of the average SNR $\bar{\gamma}$, i.e.,

$$P_A \overset{\bar{\gamma}\to\infty}{\leq} (k_A\bar{\gamma})^{-3}, \tag{5.60}$$

where k_A is a nonnegative constant that depends on $(\sigma_{\mathrm{SR}}^2, \sigma_{\mathrm{SD}}^2)$.

To calculate the probability P_B, one can take the expectation over γ_{SD}, then γ_{RD} and finally γ_{SR}. First, $P_B(\gamma_{\mathrm{RD}}, \gamma_{\mathrm{SR}})$ can be computed as follows

$$P_B(\gamma_{\mathrm{RD}},\gamma_{\mathrm{SR}}) = \frac{1}{2}\exp(-\gamma_{\mathrm{SR}})p_{\gamma_{\mathrm{RD}}}(\gamma_{\mathrm{RD}})p_{\gamma_{\mathrm{SR}}}(\gamma_{\mathrm{SR}})\int_0^{\alpha_2\gamma_{\mathrm{RD}}} \frac{\gamma_{\mathrm{SD}}}{\bar{\gamma}_{\mathrm{SD}}^2}\exp\left(-\frac{\gamma_{\mathrm{SD}}}{\bar{\gamma}_{\mathrm{SD}}}\right)d\gamma_{\mathrm{SD}}. \tag{5.61}$$

After some manipulations and with the help of [P16, pp. 885, Eq. (8.215)], the unconditional probability P_B can be evaluated as

$$P_B \approx \frac{1}{\theta^2\bar{\gamma}_{\mathrm{SR}}\bar{\gamma}_{\mathrm{SD}}^2\left(1+\frac{1}{\bar{\gamma}_{\mathrm{SR}}}\right)^3} + O(\bar{\gamma}^{-3}) \overset{\bar{\gamma}\to\infty}{\approx} (k_B\bar{\gamma})^{-3}, \tag{5.62}$$

where the function $O(x)$ satisfies $\lim_{x\to 0} O(x)/x = 0$ and the constant k_B is nonnegative and depends on $(\sigma_{\mathrm{SR}}^2, \sigma_{\mathrm{SD}}^2)$.

Using (5.60) and (5.62) in $P_2 \leq P_A + P_B$ proves Lemma 2.

Note that for Protocol II, the RV γ_{SD} should be replaced by the exponential RV γ_{SD_1} with mean $\bar{\gamma}_{\mathrm{SD}}$. To compute $P_A^{(\text{P-II})}$ in Protocol II, one needs to calculate $I_{21}^{(\text{P-II})}(\gamma_{\mathrm{RD}}, \gamma_{\mathrm{SR}})$ as in (5.50). In Protocol II, (5.51) now becomes

$$I_{21}^{(\text{P-II})}(\gamma_{\mathrm{RD}}, \gamma_{\mathrm{SR}}) = \frac{2\exp(-\gamma_{\mathrm{eq}}(0.5-\beta_2))}{\bar{\gamma}_{\mathrm{SD}}\beta_1}\int_{-\sqrt{\beta_2\gamma_{\mathrm{eq}}}}^{\infty}\left(u+\sqrt{\beta_2\gamma_{\mathrm{eq}}}\right)\exp(-u^2)du. \tag{5.63}$$

For the computation of P_B, (5.61) becomes

$$P_B^{(\text{P-II})}(\gamma_{\mathrm{RD}},\gamma_{\mathrm{SR}}) = \frac{1}{2}\exp(-\gamma_{\mathrm{SR}})p_{\gamma_{\mathrm{RD}}}(\gamma_{\mathrm{RD}})p_{\gamma_{\mathrm{SR}}}(\gamma_{\mathrm{SR}})\int_0^{\alpha_2\gamma_{\mathrm{RD}}} \frac{1}{\bar{\gamma}_{\mathrm{SD}}}\exp\left(-\frac{\gamma_{\mathrm{SD}}}{\bar{\gamma}_{\mathrm{SD}}}\right)d\gamma_{\mathrm{SD}}. \tag{5.64}$$

One can follow the same steps as done for P_A and P_B to calculate the upperbounds on $P_A^{(\text{P-II})}$ and $P_B^{(\text{P-II})}$, respectively. Due to the space limit, the calculations are omitted here. It can be proved that $P_2^{(\text{P-II})}$ does not achieve the diversity order of 3, but 2 in Protocol II.

5.C Proof of Proposition 1

Applying the union bound, $P^s_{1,1D}$ can be bounded as

$$P^s_{1,1D} \leq [1 - P^s_{\mathrm{SR}}(\gamma_{\mathrm{SR}})] \sum_{i \neq j} P_1(s_i \to s_j) \leq \sum_{i \neq j} P_1(s_i \to s_j), \tag{5.65}$$

where the average pairwise error probability (PEP) $P_1(s_i \to s_j)$ is the probability of decoding to s_j while s_i is transmitted in one dimensional space, provided that a correct decoding decision was made at the relay.

Without loss of generality, it can be assumed that the symbol s_i was transmitted and the relay correctly decoded and resent s_i to the destination. Hence, the conditional PEP $P_1(s_i \to s_j | \gamma_{\mathrm{SR}}, a_{\mathrm{SD}_1}, a_{\mathrm{SD}_2}, a_{\mathrm{RD}})$ is equal to the probability of the event that the destination, instead of s_i, wrongly decodes to $s_j = s_i + d_{ij}$, $d_{ij} \in \Re$, $|d_{ij}| \geq d_{\min}$. This event is expressed as follows:

$$\mathrm{Re}\{z\} \quad \geq \quad \left(|a_{\mathrm{SD}_1}|^2 + |w_{\mathrm{RD}}|^2\right) |d_{ij}|/2. \tag{5.66}$$

Here w_{RD} is given in (5.12) and $z = a^*_{\mathrm{SD}_1} z_{\mathrm{D}}[1] + w_{\mathrm{RD}} z_{\mathrm{D}}[2]$ is the noise at the output of the demodulator. Since $\mathrm{Re}\{z\}$ is a real Gaussian RV with zero mean and variance $\sigma^2 = \left(|a_{\mathrm{SD}_1}|^2 + |w_{\mathrm{RD}}|^2\right) N_0/2$, $P_1(s_i \to s_j | \gamma_{\mathrm{SR}}, a_{\mathrm{SD}_1}, a_{\mathrm{SD}_2}, a_{\mathrm{RD}})$ is bounded as

$$P_1(s_i \to s_j | \gamma_{\mathrm{SR}}, a_{\mathrm{SD}_1}, a_{\mathrm{SD}_2}, a_{\mathrm{RD}}) \leq Q\left(\sqrt{\eta\bar{\gamma}\left(|a_{\mathrm{SD}_1}|^2 + |\sqrt{\alpha_1} a_{\mathrm{RD}} + a_{\mathrm{SD}_2}|^2\right)}\right), \tag{5.67}$$

where $\eta\bar{\gamma} = d^2_{\min}/N_0$ and the constant η depends on the specific constellation.

Observe that the RHS of (5.67) only differs from the RHS of (5.34) by the constant η. Since the high SNR behavior is not affected by the constant η, the diversity performance claimed for P_1 in (5.21) is still valid for any $P_1(s_i \to s_j)$, $i \neq j$. Therefore, Proposition 1 is proved.

5.D Proof of Proposition 2

The union bound is again used to bound $P^s_{2,1D}$ as

$$P^s_{2,1D} \quad \leq \quad P^s_{\mathrm{SR}}(\gamma_{\mathrm{SR}}) \sum_{i \neq j} \tilde{P}_2(s_i \to s_j), \tag{5.68}$$

$$
\begin{aligned}
& d_{ij}\left(2s_i + d_{ij}\right)\left(\left|a_{\mathrm{SD}_1}\right|^2 + \left|w_{\mathrm{RD}}\right|^2\right) - 2d_{ij}\mathrm{Re}\{a^*_{\mathrm{SD}_1} y_{\mathrm{D}}[1] + w_{\mathrm{RD}} y_{\mathrm{D}}[2]\} \le 0 \\
\Leftrightarrow \quad & \begin{cases} \mathrm{Re}\{z\} \ge \frac{1}{2}\Big(\left(\left|a_{\mathrm{SD}_1}\right|^2 + \left|w_{\mathrm{RD}}\right|^2\right)|d_{ij}| - 2\tilde{d}_i\sqrt{\alpha_1}\mathrm{Re}\{w_{\mathrm{RD}}a_{\mathrm{RD}}\}\Big), & d_{ij} \ge 0 \\ \mathrm{Re}\{z\} \le -\frac{1}{2}\Big(\left(\left|a_{\mathrm{SD}_1}\right|^2 + \left|w_{\mathrm{RD}}\right|^2\right)|d_{ij}| + 2\tilde{d}_i\sqrt{\alpha_1}\mathrm{Re}\{w_{\mathrm{RD}}a_{\mathrm{RD}}\}\Big), & d_{ij} < 0 \end{cases}
\end{aligned} \tag{5.70}
$$

$$
\tilde{P}_2(s_i \to s_j|\gamma_{\mathrm{SR}}, a_{\mathrm{SD}_1}, a_{\mathrm{SD}_2}, a_{\mathrm{RD}}) \le \begin{cases} Q\left(\dfrac{\left(\left|a_{\mathrm{SD}_1}\right|^2+|w_{\mathrm{RD}}|^2\right)d_{\min} - 2\tilde{d}_i\sqrt{\alpha_1}\mathrm{Re}\{w_{\mathrm{RD}}a_{\mathrm{RD}}\}}{\sqrt{2N_0\left(\left|a_{\mathrm{SD}_1}\right|^2+\left|\sqrt{\alpha_1}a_{\mathrm{RD}}+a_{\mathrm{SD}_2}\right|^2\right)}}\right), & d_{ij} \ge 0 \\ Q\left(\dfrac{\left(\left|a_{\mathrm{SD}_1}\right|^2+|w_{\mathrm{RD}}|^2\right)d_{\min} + 2\tilde{d}_i\sqrt{\alpha_1}\mathrm{Re}\{w_{\mathrm{RD}}a_{\mathrm{RD}}\}}{\sqrt{2N_0\left(\left|a_{\mathrm{SD}_1}\right|^2+|w_{\mathrm{RD}}|^2\right)}}\right), & d_{ij} < 0 \end{cases} \tag{5.71}
$$

---

in which the average PEP $\tilde{P}_2(s_i \to s_j)$ is the probability of decoding to s_j while s_i was actually transmitted and provided that a wrong decoding decision was made at the relay. Using the same assumptions for $P^s_{1,1D}$, except that the decoded symbol at the relay now is

$$
\tilde{s}_i = s_i + \tilde{d}_i, \quad \tilde{d}_i \in \Re, \quad d_{\min} \le |\tilde{d}_i| \le d_{\max}, \tag{5.69}
$$

the conditional PEP $\tilde{P}_2(s_i \to s_j|\gamma_{\mathrm{SR}}, a_{\mathrm{SD}_1}, a_{\mathrm{SD}_2}, a_{\mathrm{RD}})$ is the probability of the event in (5.70). Therefore, the conditional PEP $\tilde{P}_2(s_i \to s_j|\gamma_{\mathrm{SR}}, a_{\mathrm{SD}_1}, a_{\mathrm{SD}_2}, a_{\mathrm{RD}})$ can be bounded by (5.71).

To assess the diversity order of $P^s_{2,1D}$, one has to average the RHS of (5.68) with the aid of the upper bound on $\tilde{P}_2(s_i \to s_j|\gamma_{\mathrm{SR}}, a_{\mathrm{SD}_1}, a_{\mathrm{SD}_2}, a_{\mathrm{RD}})$ given in (5.71).

The inequality (5.71) shows that, different from Protocol II in [P8, P14], $\tilde{P}_2(s_i \to s_j)$ in Protocol I can not be upperbounded by the worst case performance at the relay, i.e., $\tilde{d}_i = d_{\max}$. This is because the RHS of (5.71) depends on the sign of $\mathrm{Re}\{a^*_{\mathrm{SD}_2}a_{\mathrm{RD}}\}$, which results from $\mathrm{Re}\{w_{\mathrm{RD}}a_{\mathrm{RD}}\} = \left[\sqrt{\alpha_1}|a_{\mathrm{RD}}|^2 + \mathrm{Re}\{a^*_{\mathrm{SD}_2}a_{\mathrm{RD}}\}\right]$.

At very high SNR, it is reasonable to assume that the relay mostly decodes to the symbol nearest to the one actually sent from the source, i.e., $\tilde{d}_i \approx d_{\min}$, $\forall i$. Then applying (5.71) and (5.24) to (5.68), one arrives at Proposition 2.

5.E Proof of Proposition 3

Let $P_{b,h}$, $P_{1,h}$ and $P_{2,h}$ in hard–power scaling correspond to P_b, P_1 and P_2 in soft–power scaling, respectively. To show that the decaying exponent of $P_{b,h}$ is 2, one needs to show that the lowest decaying exponent of $P_{1,h}$ and $P_{2,h}$ is 2.

For $P_{1,h}$, the following upper bound on $P_{1,h}$, similar to the bound given in (5.41), can be obtained:

$$P_{1,h} \leq \frac{1}{2(1+\bar{\gamma}_{\mathrm{SD}})} \int_0^\infty \frac{1}{\bar{\gamma}_{\mathrm{SR}}(1+\alpha_q(N_q,\theta)\bar{\gamma}_{\mathrm{RD}}+\bar{\gamma}_{\mathrm{SD}})} \exp\left(-\frac{\gamma_{\mathrm{SR}}}{\bar{\gamma}_{\mathrm{SR}}}\right) d\gamma_{\mathrm{SR}}. \tag{5.72}$$

Note that, for Protocol II, the above bound becomes

$$P_{1,h} \leq \frac{1}{2(1+\bar{\gamma}_{\mathrm{SD}})} \int_0^\infty \frac{1}{\bar{\gamma}_{\mathrm{SR}}(1+\alpha_q(N_q,\theta)\bar{\gamma}_{\mathrm{RD}})} \exp\left(-\frac{\gamma_{\mathrm{SR}}}{\bar{\gamma}_{\mathrm{SR}}}\right) d\gamma_{\mathrm{SR}}. \tag{5.73}$$

As seen in (5.73), $P_{1,h}$ cannot provide a diversity order of 2 when $\alpha_q(N_q,\theta) = 0$ for some regions of γ_{SR}. Therefore, the result quantifies our previous discussion on the obtainable diversity order of the smart relaying for Protocol II in the case of hard–power scaling.

For Protocol I, the upperbound on $P_{1,h}$ can be computed as

$$\begin{aligned} P_{1,h} \leq \frac{1}{2(1+\bar{\gamma}_{\mathrm{SD}})} \Bigg[& \frac{1-\exp\left(-\frac{-\theta\bar{\gamma}_{\mathrm{RD}}}{2(M-1)\bar{\gamma}_{\mathrm{SR}}}\right)}{(1+\bar{\gamma}_{\mathrm{SD}})} + \frac{\exp\left(-\frac{(2M-3)\theta\bar{\gamma}_{\mathrm{RD}}}{2(M-1)\bar{\gamma}_{\mathrm{SR}}}\right)}{1+\bar{\gamma}_{\mathrm{RD}}+\bar{\gamma}_{\mathrm{SD}}} \\ & + \sum_{i=1}^{M-2} \frac{\exp\left(-\frac{(2i-1)\theta\bar{\gamma}_{\mathrm{RD}}}{2(M-1)\bar{\gamma}_{\mathrm{SR}}}\right) - \exp\left(-\frac{(2i+1)\theta\bar{\gamma}_{\mathrm{RD}}}{2(M-1)\bar{\gamma}_{\mathrm{SR}}}\right)}{1+i\bar{\gamma}_{\mathrm{RD}}/(M-1)} \Bigg] \overset{\bar{\gamma}\to\infty}{\approx} (k_{1,h}\bar{\gamma})^{-2}, \end{aligned} \tag{5.74}$$

where $k_{1,h}$ is a nonnegative constant that depends on $(\sigma^2_{\mathrm{SR}}, \sigma^2_{\mathrm{RD}}, \sigma^2_{\mathrm{SD}})$.

For the case of wrong decoding at the relay, one has the upperbound on the unconditional probability $P_{2,h}$ as $P_{2,h} \leq P_{A,h} + P_{B,h}$, where $P_{A,h}$ and $P_{B,h}$ are given in (5.45) and (5.46), respectively. To compute $P_{A,h}$, one can mimic the steps done in

$$I_{22,h} = \frac{\bar{\gamma}_{\mathrm{SD}}}{2\bar{\gamma}_{\mathrm{SR}}(2+\bar{\gamma}_{\mathrm{SD}})^3} \left[\sum_{i=1}^{M-2} \frac{i\left[\exp\left(-\left(1+\frac{1}{\bar{\gamma}_{\mathrm{SR}}}\right)\frac{(2i-1)\theta\bar{\gamma}_{\mathrm{RD}}}{2(M-1)}\right) - \exp\left(-\left(1+\frac{1}{\bar{\gamma}_{\mathrm{SR}}}\right)\frac{(2i+1)\theta\bar{\gamma}_{\mathrm{RD}}}{2(M-1)}\right)\right]}{(M-1)\bar{\gamma}_{\mathrm{RD}}\left(1+\frac{1}{\bar{\gamma}_{\mathrm{SR}}}\right)\left(\frac{1}{\bar{\gamma}_{\mathrm{RD}}}+\frac{i}{2(M-1)}\right)^2} + \frac{\exp\left(-\left(1+\frac{1}{\bar{\gamma}_{\mathrm{SR}}}\right)\frac{(2M-3)\theta\bar{\gamma}_{\mathrm{RD}}}{2(M-1)}\right)}{\bar{\gamma}_{\mathrm{RD}}\left(1+\frac{1}{\bar{\gamma}_{\mathrm{SR}}}\right)\left(\frac{1}{2}+\frac{1}{\bar{\gamma}_{\mathrm{RD}}}\right)^2} \right]. \tag{5.75}$$

$$I_{23,h} = \frac{1}{\bar{\gamma}_{\mathrm{SR}}(2+\bar{\gamma}_{\mathrm{SD}})^2} \left[\frac{1-\exp\left(-\left(1+\frac{1}{\bar{\gamma}_{\mathrm{SR}}}\right)\frac{\theta\bar{\gamma}_{\mathrm{RD}}}{2(M-1)}\right)}{\left(1+\frac{1}{\bar{\gamma}_{\mathrm{SR}}}\right)} + \frac{\exp\left(-\left(1+\frac{1}{\bar{\gamma}_{\mathrm{SR}}}\right)\frac{(2M-3)\theta\bar{\gamma}_{\mathrm{RD}}}{2(M-1)}\right)}{\bar{\gamma}_{\mathrm{RD}}\left(1+\frac{1}{\bar{\gamma}_{\mathrm{SR}}}\right)\left(\frac{1}{2}+\frac{1}{\bar{\gamma}_{\mathrm{RD}}}\right)} + \sum_{i=1}^{M-2} \frac{\left[\exp\left(-\left(1+\frac{1}{\bar{\gamma}_{\mathrm{SR}}}\right)\frac{(2i-1)\theta\bar{\gamma}_{\mathrm{RD}}}{2(M-1)}\right) - \exp\left(-\left(1+\frac{1}{\bar{\gamma}_{\mathrm{SR}}}\right)\frac{(2i+1)\theta\bar{\gamma}_{\mathrm{RD}}}{2(M-1)}\right)\right]}{\bar{\gamma}_{\mathrm{RD}}\left(1+\frac{1}{\bar{\gamma}_{\mathrm{SR}}}\right)\left(\frac{1}{\bar{\gamma}_{\mathrm{RD}}}+\frac{i}{2(M-1)}\right)} \right]. \tag{5.76}$$

$$\begin{aligned} I_{24,h} = & \frac{\sqrt{\pi/2}\bar{\gamma}_{\mathrm{SD}}^{1.5}}{\bar{\gamma}_{\mathrm{SR}}(2+\bar{\gamma}_{\mathrm{SD}})^{3.5}} \left[\frac{\Gamma(2.5)\exp\left(-\left(1+\frac{1}{\bar{\gamma}_{\mathrm{SR}}}\right)\frac{(2M-3)\theta\bar{\gamma}_{\mathrm{RD}}}{2(M-1)}\right)}{\bar{\gamma}_{\mathrm{RD}}\left(1+\frac{1}{\bar{\gamma}_{\mathrm{SR}}}\right)\left(\frac{1}{\bar{\gamma}_{\mathrm{RD}}}+\frac{1}{2+\bar{\gamma}_{\mathrm{SD}}}\right)^{2.5}} \right. \\ & \left. + \sum_{i=1}^{M-2} \frac{i^{1.5}\Gamma(2.5)\left[\exp\left(-\left(1+\frac{1}{\bar{\gamma}_{\mathrm{SR}}}\right)\frac{(2i-1)\theta\bar{\gamma}_{\mathrm{RD}}}{2(M-1)}\right) - \exp\left(-\left(1+\frac{1}{\bar{\gamma}_{\mathrm{SR}}}\right)\frac{(2i+1)\theta\bar{\gamma}_{\mathrm{RD}}}{2(M-1)}\right)\right]}{(M-1)^{1.5}\bar{\gamma}_{\mathrm{RD}}\left(1+\frac{1}{\bar{\gamma}_{\mathrm{SR}}}\right)\left(\frac{1}{\bar{\gamma}_{\mathrm{RD}}}+\frac{i}{(M-1)(2+\bar{\gamma}_{\mathrm{RD}})}\right)^{2.5}} \right] \\ & + \frac{3\sqrt{\pi\bar{\gamma}_{\mathrm{SD}}}}{\sqrt{2}\bar{\gamma}_{\mathrm{SR}}(2+\bar{\gamma}_{\mathrm{SD}})^{2.5}} \left[\frac{\Gamma(1.5)\exp\left(-\left(1+\frac{1}{\bar{\gamma}_{\mathrm{SR}}}\right)\frac{(2M-3)\theta\bar{\gamma}_{\mathrm{RD}}}{2(M-1)}\right)}{\bar{\gamma}_{\mathrm{RD}}\left(1+\frac{1}{\bar{\gamma}_{\mathrm{SR}}}\right)\left(\frac{1}{\bar{\gamma}_{\mathrm{RD}}}+\frac{1}{2+\bar{\gamma}_{\mathrm{SD}}}\right)^{1.5}} \right. \\ & \left. + \sum_{i=1}^{M-2} \frac{\sqrt{i}\Gamma(1.5)\left[\exp\left(-\left(1+\frac{1}{\bar{\gamma}_{\mathrm{SR}}}\right)\frac{(2i-1)\theta\bar{\gamma}_{\mathrm{RD}}}{2(M-1)}\right) - \exp\left(-\left(1+\frac{1}{\bar{\gamma}_{\mathrm{SR}}}\right)\frac{(2i+1)\theta\bar{\gamma}_{\mathrm{RD}}}{2(M-1)}\right)\right]}{\sqrt{M-1}\bar{\gamma}_{\mathrm{RD}}\left(1+\frac{1}{\bar{\gamma}_{\mathrm{SR}}}\right)\left(\frac{1}{\bar{\gamma}_{\mathrm{RD}}}+\frac{i}{(M-1)(2+\bar{\gamma}_{\mathrm{RD}})}\right)^{1.5}} \right]. \end{aligned} \tag{5.77}$$

(5.48) and (5.53) for its counterpart P_A in the soft–power scaling case. In particular, $P_{A,h} \leq I_{22,h} + I_{23,h} + I_{24,h}$, where $I_{22,h}$, $I_{23,h}$ and $I_{24,h}$ are, respectively, given as in (5.54), (5.55) and (5.56). Note that the parameters β_1 and β_2 are the same as in the case of soft–power scaling. However, γ_{eq} is now set to $\alpha_q(N_q, \theta)\gamma_{\mathrm{RD}}$.

The integrals $I_{22,h}$, $I_{23,h}$ and $I_{24,h}$ are found in (5.75), (5.76) and (5.77), respectively.

Recognize that the lowest decaying exponent among $I_{22,h}$, $I_{23,h}$ and $I_{24,h}$ is deter-

mined by that of $I_{23,h}$, which is 3 at high SNR region. Therefore one concludes that $P_{A,h}$ also decays with the exponent of 3 at high SNR, i.e.,

$$P_{A,h} \overset{\bar{\gamma}\to\infty}{\leq} (k_{A,h}\bar{\gamma})^{-3}, \tag{5.78}$$

where $k_{A,h}$ is a nonnegative constant that depends on $(\sigma^2_{\mathrm{SR}}, \sigma^2_{\mathrm{RD}}, \sigma^2_{\mathrm{SD}})$.

The computation of $P_{B,h}$ can be carried out by following the same procedure done for P_B, i.e., averaging $P_{B,h}$ over γ_{SD}, then γ_{RD} and finally γ_{SR}. It can be evaluated as $P_{B,h} = I_{31,h} - I_{32,h} - I_{33,h}$, where

$$I_{31,h} = \int_0^\infty \int_0^\infty \frac{\exp(-\gamma_{\mathrm{SR}})}{2} p_{\gamma_{\mathrm{RD}}}(\gamma_{\mathrm{RD}}) p_{\gamma_{\mathrm{SR}}}(\gamma_{\mathrm{SR}}) d\gamma_{\mathrm{RD}} d\gamma_{\mathrm{SR}} = \frac{1}{2\bar{\gamma}_{\mathrm{SR}}\left(1+\frac{1}{\bar{\gamma}_{\mathrm{SR}}}\right)}. \tag{5.79}$$

$$\begin{aligned} I_{32,h} =& \int_0^\infty \frac{\exp\left[-\left(1+\frac{1}{\bar{\gamma}_{\mathrm{SR}}}\right)\gamma_{\mathrm{SR}}\right] d\gamma_{\mathrm{SR}}}{2\bar{\gamma}_{\mathrm{RD}}\bar{\gamma}_{\mathrm{SR}}\left(\frac{\alpha_q(N_q,\theta)}{\bar{\gamma}_{\mathrm{SD}}}+\frac{1}{\bar{\gamma}_{\mathrm{RD}}}\right)} \\ =& \frac{1}{2\bar{\gamma}_{\mathrm{SR}}\left(1+\frac{1}{\bar{\gamma}_{\mathrm{SR}}}\right)}\left(1-\exp\left[-\frac{\theta\bar{\gamma}_{\mathrm{RD}}}{2(M-1)}\left(1+\frac{1}{\bar{\gamma}_{\mathrm{SR}}}\right)\right]\right) \\ &+ \sum_{i=1}^{M-2} \int_{\frac{(2i-1)\theta\bar{\gamma}_{\mathrm{RD}}}{2(M-1)}}^{\frac{(2i+1)\theta\bar{\gamma}_{\mathrm{RD}}}{2(M-1)}} \frac{\exp\left[-\left(1+\frac{1}{\bar{\gamma}_{\mathrm{SR}}}\right)\gamma_{\mathrm{SR}}\right] d\gamma_{\mathrm{SR}}}{2\bar{\gamma}_{\mathrm{RD}}\bar{\gamma}_{\mathrm{SR}}\left(\frac{i}{(M-1)\bar{\gamma}_{\mathrm{SD}}}+\frac{1}{\bar{\gamma}_{\mathrm{RD}}}\right)} \\ &+ \int_{\frac{(2M-3)\theta\bar{\gamma}_{\mathrm{RD}}}{2(M-1)}}^{\infty} \frac{\exp\left[-\left(1+\frac{1}{\bar{\gamma}_{\mathrm{SR}}}\right)\gamma_{\mathrm{SR}}\right] d\gamma_{\mathrm{SR}}}{2\bar{\gamma}_{\mathrm{RD}}\bar{\gamma}_{\mathrm{SR}}\left(\frac{i}{(M-1)\bar{\gamma}_{\mathrm{SD}}}+\frac{1}{\bar{\gamma}_{\mathrm{RD}}}\right)}. \end{aligned} \tag{5.80}$$

Excluding $I_{33,h}$ and the last two terms of $I_{32,h}$ in the expression $P_{B,h} = I_{31,h} - I_{32,h} - I_{33,h}$ results in the following upperbound on $P_{B,h}$:

$$\begin{aligned} P_{B,h} \leq& \frac{1}{2\bar{\gamma}_{\mathrm{SR}}\left(1+\frac{1}{\bar{\gamma}_{\mathrm{SR}}}\right)} \exp\left[-\frac{\theta\bar{\gamma}_{\mathrm{RD}}}{2(M-1)}\left(1+\frac{1}{\bar{\gamma}_{\mathrm{SR}}}\right)\right] \\ \overset{\bar{\gamma}\to\infty}{<}& \frac{1}{2\bar{\gamma}_{\mathrm{SR}}\left(1+\frac{1}{\bar{\gamma}_{\mathrm{SR}}}\right)\left[\frac{\theta\bar{\gamma}_{\mathrm{RD}}}{2(M-1)}\left(1+\frac{1}{\bar{\gamma}_{\mathrm{SR}}}\right)\right]^2} \overset{\bar{\gamma}\to\infty}{\approx} (k_{B,h}\bar{\gamma})^{-3}, \end{aligned} \tag{5.81}$$

where $k_{B,h}$ is a nonnegative constant that depends on $(\sigma^2_{\mathrm{SR}}, \sigma^2_{\mathrm{RD}})$. Note that the second inequality in (5.81) follows from the inequality: $\exp(-x) \overset{x\to\infty}{<} 1/x^2$, $x > 0$.

Finally, combining (5.74), (5.78) and (5.81) proves Proposition 3.

Acknowledgment

The authors would like to thank the anonymous reviewers for their helpful comments, which significantly improved the accuracy and clarity of the paper.

REFERENCES

[P1] A. Sendonaris, E. Erkip, and B. Aazhang, "User cooperation diversity – part 1: System description," *IEEE Trans. Commun.*, vol. 51, pp. 1927–1938, Nov. 2003.

[P2] A. Sendonaris, E. Erkip, and B. Aazhang, "User cooperation diversity – part 2: Implementation aspects and performance analysis," *IEEE Trans. Commun.*, vol. 51, pp. 1939–1948, Nov. 2003.

[P3] J. N. Laneman and G. W. Wornell, "Distributed space–time–coded protocol for exploiting cooperative diversity," *IEEE Trans. Inform. Theory*, vol. 49, pp. 2415–2425, Oct. 2003.

[P4] J. N. Laneman, D. N. C. Tse, and G. W. Wornell, "Cooperative diversity in the wireles networks: Efficient protocols and outage behavior," *IEEE Trans. Inform. Theory*, vol. 49, pp. 3062–3080, Dec. 2004.

[P5] D. Michalopoulos and G. Karagiannidis, "PHY-layer fairness in amplify and forward cooperative diversity systems," *IEEE Trans. on Wireless Commun.*, vol. 7, pp. 1073–1082, March 2008.

[P6] D. Michalopoulos, G. Karagiannidis, T. Tsiftsis, and R. Mallik, "Distributed transmit antenna selection (DTAS) under performance or energy consumption constraints," *IEEE Trans. on Wireless Commun.*, vol. 7, pp. 1168 – 1173, April 2008.

[P7] "Special issue on cooperative communications," *IEEE Trans. on Wireless Commun.*, vol. 7, no. 5, May 2008.

[P8] T. Wang, A. Cano, G. B. Giannakis, and J. N. Laneman, "High–performance

cooperative demodulation with decode–and–forward relays," *IEEE Trans. Commun.*, vol. 55, pp. 1427–1438, July 2007.

[P9] R. U. Nabar, H. Bolcskei, and F. W. Kneubhler, "Fading relay channels: performance limits and space–time signal design," *IEEE J. Select. Areas in Commun.*, vol. 22, pp. 1099–1109, Aug. 2004.

[P10] A. Ribeiro, X. Cai, and G. Giannakis, "Symbol error probabilities for general cooperative links," *IEEE Trans. on Wireless Commun.*, vol. 4, pp. 1264–1273, May 2005.

[P11] J. Adeane, M. R. D. Rodrigues, and I. J. Wassell, "Characterisation of the performance of cooperative networks in Ricean fading channels," in *Proc. of the International Conf. on Telecommunications*, (Cape Town, South Africa), May 2005.

[P12] D. Chen and J. N. Laneman, "Modulation and demodulation for cooperative diversity in wireless systems," *IEEE Trans. on Wireless Commun.*, vol. 5, pp. 1785–1794, July 2006.

[P13] T. Wang, R. Wang, and G. B. Giannakis, "Smart regenerative relays for link–adaptive cooperative communications," in *40th Annual Conference on Information Sciences and Systems*, pp. 1038–1043, Mar. 2006.

[P14] T. Wang, R. Wang, and G. B. Giannakis, "Smart regenerative relays for link–adaptive cooperative communications," to appear in *IEEE Trans. Commun.*

[P15] Y. Ding, J.-K. Zhang, and K. M. Wong, "The amplify-and-forward half-duplex cooperative system: Pairwise error probability and precoder design," *IEEE Trans. Signal Process.*, vol. 55, pp. 605–617, Feb. 2007.

[P16] L. S. Gradshteyn and L. M. Ryzhik, *Tables of Integrals, Series and Products.* Academic Press, 6th ed., 2000.

6. Performance Analysis of Fixed-Gain Amplified-and-Forward Relaying with MRC

Published as:

N. H. Vien and H. H. Nguyen, "Performance analysis of fixed-gain amplified-and-forward relaying with MRC," to appear in *IEEE Trans. Veh. Technol.*[1]

As discussed in Chapter 2, there are two main signal processing methods, i.e., DF and AF, for relay communications. The manuscripts in Chapters 3, 4 and 5 have considered the relaying systems under various scenarios of interests for DF. With the DF method, the relay decodes the source's signals, makes hard decisions and then forwards the decoded/demodulated signals to the destination. Since no signal regeneration is performed at the relay, the AF method reduces relay complexity when compared to that of the DF method. Furthermore, to maintain a long-term average transmit power at each relay, the fixed-gain AF relaying does not require the instantaneous CSI at the relay(s) but uses a fixed gain based on only the second-order statistics of the source-relay fading channels. Therefore, the system complexity can be even lowered. Motivated by the above observations, the manuscript included in this chapter studies performance of a fixed-gain AF multiple-relay system with the optimal MRC implemented at the destination.

To be more specific, the system model in the manuscript is a multiple-relay version of the fixed-gain AF single-relay system under Nakagami fading channels considered in Chapter 2. A tight upperbound on the error performance is first obtained. The

[1]This paper is included with the expressed permission of the journal's publisher.

tightness of the obtained bound is illustrated over a wide range of channel settings. Similar to the cases of Smart MRC and Smart EGC in Chapters 3 and 4, respectively, here the AF relaying system with MRC is shown to achieve the maximal diversity under Nakagami fading channels. To improve the error performance, a power allocation (PA) scheme is also investigated by minimizing the obtained bound. More specifically, the statistics of all the channels are assumed to be available at the destination. Based on this assumption, the proposed power allocation coefficients are easily calculated at the destination and then fed back to the source and relays via low-rate channels during a startup phase. It is demonstrated that the proposed PA obtained based on the bound works very well.

Performance Analysis of Fixed-Gain Amplified-and-Forward Relaying with MRC

Nam H. Vien*, *Student Member, IEEE* and Ha H. Nguyen, *Senior Member, IEEE*

Abstract

Relay transmission has recently attracted much attention since it can offer spatial diversity with single antenna terminals. This paper addresses the performance of a multiple-relay system with fixed-gain amplify-and-forward (AF) relaying in Nakagami-m fading. A tight upperbound on the average symbol error probability (SEP) is obtained for a system with K relays and when the maximal ratio combining (MRC) is used at the destination. Based on the obtained bound, a maximum diversity order of $m(K+1)$, where m is the fading parameter, is shown. Moreover, the problem of power allocation to minimize the SEP upperbound is investigated. Numerical results illustrate significant gains provided by the proposed power allocation over equal power allocation (EPA) under various channel conditions.

Index terms

Relay communications, amplify-and-forward protocol, performance analysis, power allocation, diversity order, maximum ratio combining, Nakagami-m fading.

6.1 Introduction

Recently, relay communication attracts a lot of research interests due to its ability to offer spatial diversity while still satisfying size and power constraints of mobile devices [P1–P9]. The benefit comes from the cooperation of relays in a network in order to assist transmission from the source to destination. This is because with the assistance of relays, the transmission from the source to destination can be performed over a virtual antenna array [P3, P4].

Nam H. Vien (*contact author) and Ha H. Nguyen are with the Department of Electrical & Computer Engineering, University of Saskatchewan, 57 Campus Dr., Saskatoon, SK, Canada S7N 5A9. Emails: nam.vien@usask.ca, ha.nguyen@usask.ca. This work was supported by an NSERC Discovery Grant.

The most popular signal processing methods at relays are decode-and-forward (DF) and amplify-and-forward (AF). For DF, cooperative relays first try to decode the received information and then re-generate a new version to transmit to the destination [P3,P10–P12]. On the other hand, for AF, the relays retransmit scaled versions of the received information to the destination without decoding them. Therefore, AF does not need any sophisticated processing at the relays or the destination [P3, P5, P13]. In order to limit the transmit power at the relays, the received signal at each relay can be amplified with a varying or fixed gain. The varying-gain relaying scheme maintains the constant transmit power at the relays at all times, but it requires the knowledge of the instantaneous channel gains of all the source-relay links. To reduce the complexity at the relays, the fixed-gain relaying scheme has been proposed, which maintains the long-term average transmit power at each relay [P6].

For AF relaying, the optimal maximal ratio combining (MRC) has been considered in [P4, P6, P14–P16]. In [P14, P15], the performance of a single-relay system with a multiple-antenna destination is considered. In [P14], under Rayleigh fading, the maximum diversity orders with varying and fixed gains are shown to be $2N$ and $N + 1$, respectively, where N is the number of antennas at the destination. For Nakagami-m fading, the exact MRC performance for the fixed-gain relay system is derived with the help of the Kampe de Feriet's function in [P15]. For the multiple-relay systems with single antenna in both transmitter and receiver, the work in [P4] investigates the symbol error probability (SEP) for AF with the varying gains at relays and MRC at the destination. In [P16], the performance of relay systems with fixed-gain relays over generalized fading channels is determined by using the geometric-mean (G-M) bound on the instantaneous signal-to-noise ratio (SNR). This bound is then used to evaluate the outage and error probabilities by using the well-known moment generating function (MGF) approach. Using the same technique as in [P4], the authors in [P6] consider the outage probability behaviors of the relay systems with both varying and fixed gains in Nakagami-m fading at the high SNR region. The work shows that when the fading severity difference between the source-to-relay and the

relay-to-destination channels exists, both strategies can achieve the same diversity gain whereas the fixed-gain AF relaying strictly looses some coding gains. However, the limitation of the method used in [P4,P6] is that it can only predict the asymptotic performance of the systems at the high SNR region while in some applications, the performance at low and medium SNRs might be more important [P17].

It should be pointed out that the above works on AF relay systems assume that the total transmit power is uniformly allocated over the source and the relays, i.e., equal power allocation (EPA). Obviously, the performance of such AF systems with EPA is inferior to that with optimal power allocation (OPA) among the source and all the cooperating relays [P18]. Such OPA schemes have been recently considered in [P18–P22]. However, all the previously proposed OPA schemes are restricted to Rayleigh fading channels. It is well-known that the Nakagami-m distribution provides a much better fitting for the fading channel distributions than the Rayleigh distribution in many scenarios [P23]. In fact, it includes the Rayleigh distribution ($m = 1$) as a special case [P23].

Motivated by the above observations, this paper first obtains a tight upperbound on the SEP for fixed-gain AF multiple-relay systems with MRC at the destination. It is illustrated that the obtained bound is effective over a wide range of channel settings. It is also shown that MRC can achieve the maximum diversity order of $m(K+1)$. Based on the minimization of the obtained bound on the SEP performance, a novel power allocation (PA) scheme is proposed. In particular, under the assumption that all the channel statistics are available at the destination, the proposed power allocation coefficients can be calculated easily at the destination and then fed back to the source and the relays during a startup phase. The proposed PA demonstrates significant performance gains over EPA.

The rest of the paper is organized as follows. Section 6.2 describes the system model under consideration. The upperbound on the overall SEP is derived in Section 6.3. The proposed power allocation is described in Section 6.4. Conclusions are given in Section 6.5.

Notation: x^* is the complex conjugate of x, $\mathrm{Re}(x)$ takes the real part of complex number x. For a random variable (RV) X, $p_X(\cdot)$ denotes its probability density function (pdf), $E\{X\}$ its expectation. The circularly symmetric complex Gaussian RV with variance σ^2 is denoted by $\mathcal{CN}(0,\sigma^2)$. The Q-function is defined as $Q(x) = (1/\sqrt{2\pi})\int_x^\infty \exp(-t^2/2)dt$. The notation $E_1(x)$ is used to denote the exponential integral, i.e., $E_1(x) = \int_x^\infty (\exp(-t)/t)dt$. $\Gamma(x)$ represents the gamma function, i.e., $\Gamma(x) = \int_0^\infty \exp(-t)t^{x-1}dt$, $\mathrm{Re}(x) > 0$. The incomplete gamma function is denoted by $\gamma(\alpha, x)$, i.e., $\gamma(\alpha, x) = \int_0^x \exp(-t)t^{\alpha-1}dt$, $\mathrm{Re}(\alpha) > 0$.

6.2 System Model

Consider a multi-relay system with a source S, K relays $(\mathrm{R}_k)_{k=1}^K$ and a destination D. All nodes are equipped with single-antenna transmitter and receiver. Information is sent from S to D with the help of $(\mathrm{R}_k)_{k=1}^K$. The system is half-duplex, in which $(\mathrm{R}_k)_{k=1}^K$ cannot transmit and receive at the same time. Frequency-flat slow fading is assumed throughout the paper. The channel coefficients $(a_{\mathrm{SR}_k})_{k=1}^K$, $(a_{\mathrm{R}_k\mathrm{D}})_{k=1}^K$ and a_{SD} represent independent Nakagami-m fading with mean-square values $(\Omega_{\mathrm{SR}_k})_{k=1}^K$, $(\Omega_{\mathrm{R}_k\mathrm{D}})_{k=1}^K$ and Ω_{SD}, respectively. Therefore, the normalized received SNR of the PQ link without power scaling, i.e., $\gamma_{\mathrm{PQ}} = \bar{\gamma}|a_{\mathrm{PQ}}|^2$, $(\mathrm{PQ}) \in \{(\mathrm{SR}_k)_{k=1}^K, (\mathrm{R}_k\mathrm{D})_{k=1}^K, \mathrm{SD}\}$ with $\bar{\gamma} = E_s/N_0$, has the following pdf [P24, Eq. (14.4-35)]

$$p_{\gamma_{\mathrm{PQ}}}(\gamma_{\mathrm{PQ}}) = m^m \gamma_{\mathrm{PQ}}^{m-1}/(\bar{\gamma}_{\mathrm{PQ}}^m \Gamma(m)) \exp\left(-m\gamma_{\mathrm{PQ}}/(\bar{\gamma}_{\mathrm{PQ}})\right), \tag{6.1}$$

where m is the Nakagami-m fading parameter and assumed to be integer[2]. The average SNR of the PQ link, i.e., $\bar{\gamma}_{\mathrm{PQ}}$, is equal to $\bar{\gamma}\Omega_{\mathrm{PQ}}$.

Transmission to D is done in $(K+1)$ time slots. In the first time slot, S broadcasts the signal s with the average transmitted power $\sqrt{\varepsilon_s E_s}$ to $(\mathrm{R}_k)_{k=1}^K$ and D, where $0 \le \varepsilon_s \le K+1$, is the scaling power coefficient at S. The received signals at R_k, y_{SR_k},

[2]For simplicity of analysis and presentation, it is assumed that the Nakagami fading parameter, m, is the same for all links. The analysis method in this paper, however, can be extended to the case where all the links have unequal fading parameters.

and at D, y_{SD}, are respectively given as

$$y_{\mathrm{SR}_k} = \sqrt{\varepsilon_s E_s} a_{\mathrm{SR}_k} s + z_{\mathrm{SR}_k} \tag{6.2}$$

$$y_{\mathrm{SD}} = \sqrt{\varepsilon_s E_s} a_{\mathrm{SD}} s + z_{\mathrm{SD}}, \tag{6.3}$$

where z_{SR_k} and z_{SD} represent additive white Gaussian noise (AWGN) and are modeled as independent and identically distributed (i.i.d) $\mathcal{CN}(0, N_0)$ random variables.

For AF with fixed-gain relays, R_k applies a fixed scaling to the received signal from S, regardless of the fading amplitude of the first hop in order to maintain the long-term average transmitted power at R_k. The received signals, $y_{\mathrm{R}_k\mathrm{D}}$, at D from time slot 2 to time slot $(K+1)$ are given as

$$y_{\mathrm{R}_k\mathrm{D}} = G_k a_{\mathrm{R}_k\mathrm{D}} (\sqrt{\varepsilon_s E_s} a_{\mathrm{SR}_k} s + z_{\mathrm{SR}_k}) + z_{\mathrm{R}_k\mathrm{D}}, \quad k = 1, \ldots, K, \tag{6.4}$$

where $z_{\mathrm{R}_k\mathrm{D}}$ is $\mathcal{CN}(0, N_0)$ and represents AWGN at D. The fixed gain G_k can be expressed as [P13]:

$$G_k^2 = \varepsilon_k E_s / (\varepsilon_s E_s \Omega_{\mathrm{SR}_k} + N_0) = \varepsilon_k \bar{\gamma} / (\varepsilon_s \bar{\gamma}_{\mathrm{SR}_k} + 1), \tag{6.5}$$

which makes the long-term average SNR at R_k to be $\varepsilon_k \bar{\gamma}$, where $0 \leq \varepsilon_k \leq K+1$, is the power scaling coefficient at R_k. Therefore, the total power, E_{tot}, used in the system is computed as

$$E_{\mathrm{tot}} = \left(\varepsilon_s + \sum_{k=1}^{K} \varepsilon_k \right) E_s. \tag{6.6}$$

For convenience, the corresponding signal-to-noise ratio is defined as $\bar{\gamma}_{\mathrm{tot}} = E_{\mathrm{tot}}/N_0$. Let us normalize $\left(\varepsilon_s + \sum_{k=1}^{K} \varepsilon_k\right)$ to be $(K+1)$ so that the total power equals to $(K+1)E_s$, the same as that in equal power allocation (EPA) in which all the source and relays transmit at the same power E_s.

The destination implements the optimal MRC detector as in [P14, P21, P22]. The corresponding SNR at the output of the detector is

$$\gamma = \varepsilon_s \gamma_{\mathrm{SD}} + \sum_{k=1}^{K} G_k^2 \varepsilon_s \gamma_{\mathrm{SR}_k} \gamma_{\mathrm{R}_k\mathrm{D}} \Big/ \left(\bar{\gamma} + G_k^2 \gamma_{\mathrm{R}_k\mathrm{D}} \right). \tag{6.7}$$

6.3 Error Performance Analysis

For simplicity of presentation, the following analysis considers M-PSK constellation. However the method and main results can be easily generalized to an arbitrary two-dimensional constellation (such as M-QAM). The average SEP for M-PSK is given by [P23, Eq. (8.22)]

$$P_s = \frac{1}{\pi}\int_0^{(M-1)\pi/M} \mathcal{M}_\gamma\left(-\sin^2(\pi/M)/\sin^2\theta\right) d\theta, \tag{6.8}$$

in which

$$\mathcal{M}_\gamma(-t) = E_\gamma\left\{\exp(-t\gamma)\right\}, \tag{6.9}$$

is the MGF of the instantaneous received SNR at D given in (6.7). To calculate P_s as in (6.8), one needs to take the expectation of $\exp(-t\gamma)$ over all the channel signal-to-noise ratios (SNRs), i.e., γ_{SD}, $(\gamma_{\mathrm{SR}_k})_{k=1}^K$ and $(\gamma_{\mathrm{R}_k\mathrm{D}})_{k=1}^K$, and then compute the integral (6.8) over finite limits. Due to the complexity of such an exact computation, the interest here is to obtain a tight upperbound on the SEP. It is given in the following Lemma.

Lemma 1. *For the K-relay system with the received SNR at D, γ, given in* (6.7)*, M-PSK modulation and Nakagami-m fading, the average SEP, P_s, is upperbounded as*

$$P_s \le \frac{1}{\pi}\int_0^{\frac{(M-1)\pi}{M}} \left[\frac{1}{(t\varepsilon_s\bar{\gamma}_{SD}/m+1)^m}\prod_{k=1}^{K}\left(A_{k,1}(t)-A_{k,2}(t)+B_{k,1}(t)\right)\right]_{t=\sin^2(\pi/M)/\sin^2\theta} d\theta, \tag{6.10}$$

where $A_{k,1}(t)$, $A_{k,2}(t)$ and $B_{k,1}(t)$ are given in (6.11), (6.12) *and* (6.13)*, respectively, at the top of next page.*

Proof: See Appendix 6.A.

A closed-form expression for the upperbound in (6.10) seems hard to obtain. However, for the simplest case when there is only 1 relay R with BPSK modulation

$$A_{k,1}(t) = \frac{1}{\Gamma(m)} \left(\frac{2m^2\bar{\gamma}}{tG_k^2\varepsilon_s\bar{\gamma}_{\mathrm{SR}_k}\bar{\gamma}_{\mathrm{R}_k\mathrm{D}}} \right)^m \left\{ \left(-\frac{2m\bar{\gamma}}{tG_k^2\varepsilon_s\bar{\gamma}_{\mathrm{R}_k\mathrm{D}}} \right)^{m-1} \exp\left(\frac{2m^2\bar{\gamma}}{tG_k^2\varepsilon_s\bar{\gamma}_{\mathrm{SR}_k}\bar{\gamma}_{\mathrm{R}_k\mathrm{D}}} \right) \right.$$
$$\mathrm{E}_1\left(\frac{2m^2\bar{\gamma}}{tG_k^2\varepsilon_s\bar{\gamma}_{\mathrm{SR}_k}\bar{\gamma}_{\mathrm{R}_k\mathrm{D}}} \right) + \sum_{l=1}^{m-1} \left(-\frac{2m\bar{\gamma}}{tG_k^2\varepsilon_s\bar{\gamma}_{\mathrm{R}_k\mathrm{D}}} \right)^{m-1-l} \binom{m-1}{l} \left[\frac{1}{l!} \sum_{p=1}^{l} (p-1)! \left(-\frac{m}{\bar{\gamma}_{\mathrm{SR}_k}} \right)^{l-p} \right.$$
$$\left. \left. \left(\frac{2m^2\bar{\gamma}}{tG_k^2\varepsilon_s\bar{\gamma}_{\mathrm{R}_k\mathrm{D}}} \right)^{-p} + \frac{(-m/\bar{\gamma}_{\mathrm{SR}_k})^l}{l!} \exp\left(\frac{2m^2\bar{\gamma}}{tG_k^2\varepsilon_s\bar{\gamma}_{\mathrm{SR}_k}\bar{\gamma}_{\mathrm{R}_k\mathrm{D}}} \right) \mathrm{E}_1\left(\frac{2m^2\bar{\gamma}}{tG_k^2\varepsilon_s\bar{\gamma}_{\mathrm{SR}_k}\bar{\gamma}_{\mathrm{R}_k\mathrm{D}}} \right) \right] \right\}, \tag{6.11}$$

$$A_{k,2}(t) = \frac{\exp\left(-\frac{m\bar{\gamma}}{G_k^2\bar{\gamma}_{\mathrm{R}_k\mathrm{D}}} \right)}{\Gamma^2(m)} \left(\frac{m^2}{\bar{\gamma}_{\mathrm{SR}_k}\bar{\gamma}_{\mathrm{R}_k\mathrm{D}}} \right)^m \sum_{l=0}^{m-1} \frac{(\bar{\gamma}/G_k^2)^l}{l!} \left(\frac{2\bar{\gamma}}{tG_k^2\varepsilon_s} \right)^{m-l} \left\{ \sum_{\substack{p=0 \\ p\geq m-l}}^{m-1} \binom{m-1}{p} \right.$$
$$\left(-\frac{2m\bar{\gamma}}{tG_k^2\varepsilon_s\bar{\gamma}_{\mathrm{R}_k\mathrm{D}}} \right)^{m-1-p} \sum_{q=0}^{p+l-m} \binom{p+l-m}{q} \left(\frac{2m\bar{\gamma}}{tG_k^2\varepsilon_s\bar{\gamma}_{\mathrm{R}_k\mathrm{D}}} \right)^{p+l-m-q} \frac{q!}{\left(\frac{t\varepsilon_s}{2} + \frac{m}{\bar{\gamma}_{\mathrm{SR}_k}} \right)^{q+1}}$$
$$\sum_{\substack{p=0 \\ p=m-l-1}}^{m-1} \binom{m-1}{p} \left(-\frac{2m\bar{\gamma}}{tG_k^2\varepsilon_s\bar{\gamma}_{\mathrm{R}_k\mathrm{D}}} \right)^{m-1-p} \exp\left(\left(\frac{t\varepsilon_s}{2} + \frac{m}{\bar{\gamma}_{\mathrm{SR}_k}} \right) \frac{2m\bar{\gamma}}{tG_k^2\varepsilon_s\bar{\gamma}_{\mathrm{R}_k\mathrm{D}}} \right)$$
$$\mathrm{E}_1\left(\left(\frac{t\varepsilon_s}{2} + \frac{m}{\bar{\gamma}_{\mathrm{SR}_k}} \right) \frac{2m\bar{\gamma}}{tG_k^2\varepsilon_s\bar{\gamma}_{\mathrm{R}_k\mathrm{D}}} \right) + \sum_{\substack{p=0 \\ p\leq m-l-2}}^{m-1} \binom{m-1}{p} \left(-\frac{2m\bar{\gamma}}{tG_k^2\varepsilon_s\bar{\gamma}_{\mathrm{R}_k\mathrm{D}}} \right)^{m-1-p}$$
$$\left[\frac{1}{(m-p-l-1)!} \sum_{q=0}^{m-p-l-1} (q-1)! \left(-\frac{t\varepsilon_s}{2} - \frac{m}{\bar{\gamma}_{\mathrm{SR}_k}} \right)^{m-p-l-q-1} \left(\frac{2m\bar{\gamma}}{tG_k^2\varepsilon_s\bar{\gamma}_{\mathrm{R}_k\mathrm{D}}} \right)^{-q} \right.$$
$$\left. + \frac{\left(-\frac{t\varepsilon_s}{2} - \frac{m}{\bar{\gamma}_{\mathrm{SR}_k}} \right)^{m-p-l-1}}{(m-p-l-1)!} \exp\left(\left(\frac{t\varepsilon_s}{2} + \frac{m}{\bar{\gamma}_{\mathrm{SR}_k}} \right) \frac{2m\bar{\gamma}}{tG_k^2\varepsilon_s\bar{\gamma}_{\mathrm{R}_k\mathrm{D}}} \right) \right.$$
$$\left. \left. \mathrm{E}_1\left(\left(\frac{t\varepsilon_s}{2} + \frac{m}{\bar{\gamma}_{\mathrm{SR}_k}} \right) \frac{2m\bar{\gamma}}{tG_k^2\varepsilon_s\bar{\gamma}_{\mathrm{R}_k\mathrm{D}}} \right) \right] \right\}, \tag{6.12}$$

$$B_{k,1}(t) = \left[m \Big/ \left(\bar{\gamma}_{\mathrm{SR}_k} \left(\frac{t\varepsilon_s}{2} + \frac{m}{\bar{\gamma}_{\mathrm{SR}_k}} \right) \right) \right]^m \frac{\Gamma(m, m\bar{\gamma}/(G_k^2\bar{\gamma}_{\mathrm{R}_k\mathrm{D}}))}{\Gamma(m)}. \tag{6.13}$$

---

and Rayleigh fading ($m = 1$), the bound can be simplified by using the Chernoff

bound as follows:

$$P_s \leq \frac{1}{2}\Bigg\{\frac{2\bar{\gamma}}{G^2\varepsilon_s\bar{\gamma}_{\mathrm{RD}}\bar{\gamma}_{\mathrm{SR}}}\exp\left(\frac{2\bar{\gamma}}{G^2\varepsilon_s\bar{\gamma}_{\mathrm{RD}}\bar{\gamma}_{\mathrm{SR}}}\right)\mathrm{E}_1\left(\frac{2\bar{\gamma}}{G^2\varepsilon_s\bar{\gamma}_{\mathrm{RD}}\bar{\gamma}_{\mathrm{SR}}}\right) - \frac{2\bar{\gamma}\exp\left(-\frac{\bar{\gamma}}{G^2\bar{\gamma}_{\mathrm{RD}}}\right)}{G^2\varepsilon_s\bar{\gamma}_{\mathrm{SR}}\bar{\gamma}_{\mathrm{RD}}}$$
$$\exp\left(\left(\frac{\varepsilon_s}{2}+\frac{1}{\bar{\gamma}_{\mathrm{SR}}}\right)\frac{2\bar{\gamma}}{G^2\varepsilon_s\bar{\gamma}_{\mathrm{RD}}}\right)\mathrm{E}_1\left(\left(\frac{\varepsilon_s}{2}+\frac{1}{\bar{\gamma}_{\mathrm{SR}}}\right)\frac{2\bar{\gamma}}{G^2\varepsilon_s\bar{\gamma}_{\mathrm{RD}}}\right) + \frac{\exp\left(-\frac{\bar{\gamma}}{G^2\bar{\gamma}_{\mathrm{RD}}}\right)}{\left(1+\frac{\varepsilon_s\bar{\gamma}_{\mathrm{SR}}}{2}\right)}\Bigg\}$$
$$\frac{1}{\left(1+\frac{\varepsilon_s\bar{\gamma}_{\mathrm{SD}}}{2}\right)}. \tag{6.14}$$

The fixed-gain G is computed as $G = \varepsilon_1\bar{\gamma}/(\varepsilon_s\bar{\gamma}_{\mathrm{SR}}+1)$ where ε_s and ε_1 are the scaling coefficients at S and R, respectively. Note that symbol error probability is identical with bit error probability (BEP) for the case of BPSK.

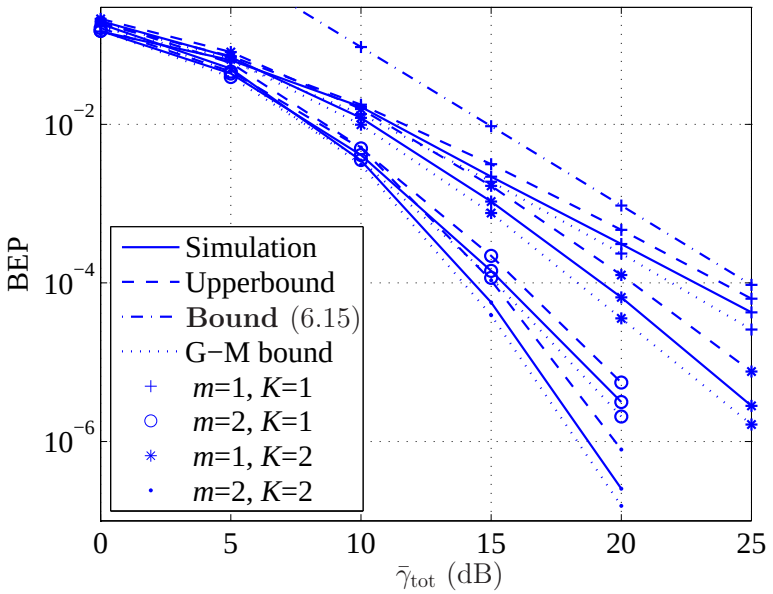

Figure 6.1 Simulation results, upperbounds and G-M lowerbounds on the SEP performance: $(\Omega_{\mathrm{SR}}, \Omega_{\mathrm{RD}}, \Omega_{\mathrm{SD}}) = (0,0,0)$dB.

For the case of EPA, i.e., $\varepsilon_s = \varepsilon_1 = 1$, and in the high SNR region, (6.14) can be

further approximated as

$$P_s \overset{\bar{\gamma}\to\infty}{\lessapprox} \frac{1}{2}\Bigg\{ \frac{2\bar{\gamma}}{\frac{\bar{\gamma}}{\bar{\gamma}_{\mathrm{SR}}}\bar{\gamma}_{\mathrm{RD}}\bar{\gamma}_{\mathrm{SR}}} \frac{1}{\left(\eta + \frac{2\bar{\gamma}}{\frac{\bar{\gamma}}{\bar{\gamma}_{\mathrm{SR}}}\bar{\gamma}_{\mathrm{RD}}\bar{\gamma}_{\mathrm{SR}}}\right)} - \frac{2\bar{\gamma}\exp\left(-\bar{\gamma}/(\frac{\bar{\gamma}}{\bar{\gamma}_{\mathrm{SR}}}\bar{\gamma}_{\mathrm{RD}})\right)}{\frac{\bar{\gamma}}{\bar{\gamma}_{\mathrm{SR}}}\bar{\gamma}_{\mathrm{RD}}\bar{\gamma}_{\mathrm{SR}}} \frac{1}{1+\left(\frac{1}{2}+\frac{1}{\bar{\gamma}_{\mathrm{SR}}}\right)\frac{2\bar{\gamma}}{\frac{\bar{\gamma}}{\bar{\gamma}_{\mathrm{SR}}}\bar{\gamma}_{\mathrm{RD}}}}}$$
$$+ \frac{\exp\left(-\bar{\gamma}/(\frac{\bar{\gamma}}{\bar{\gamma}_{\mathrm{SR}}}\bar{\gamma}_{\mathrm{RD}})\right)}{1+\frac{\bar{\gamma}_{\mathrm{SR}}}{2}}\Bigg\} \frac{1}{\left(1+\frac{\bar{\gamma}_{\mathrm{SD}}}{2}\right)} \overset{\bar{\gamma}\to\infty}{\approx} \frac{2}{\bar{\gamma}_{\mathrm{SD}}}\left(\frac{1}{\bar{\gamma}_{\mathrm{RD}}} + \frac{\exp(-\bar{\gamma}_{\mathrm{SR}}/\bar{\gamma}_{\mathrm{RD}})\bar{\gamma}_{\mathrm{RD}}}{\bar{\gamma}_{\mathrm{SR}}(\bar{\gamma}_{\mathrm{SR}}+\bar{\gamma}_{\mathrm{RD}})}\right), \tag{6.15}$$

where the inequality $1/(1+x) < \exp(x)\mathrm{E}_1(x) \leq 1/(\eta+x)$, $\forall x > 0$, $0 < \eta < 1$ [P25] has been used. The approximated bound in (6.15) is strikingly simple when compared to the original one in (6.10) while still maintaining its tightness (as seen later in Figs. 6.1 and 6.2). It can be clearly seen from the bound in (6.15) that the overall performance slope decays with the exponent of 2 in the log–log scale. The expression also shows how the channel qualities, i.e., $\bar{\gamma}_{\mathrm{SR}}$, $\bar{\gamma}_{\mathrm{RD}}$ and $\bar{\gamma}_{\mathrm{SD}}$, contribute to the overall performance in this special case.

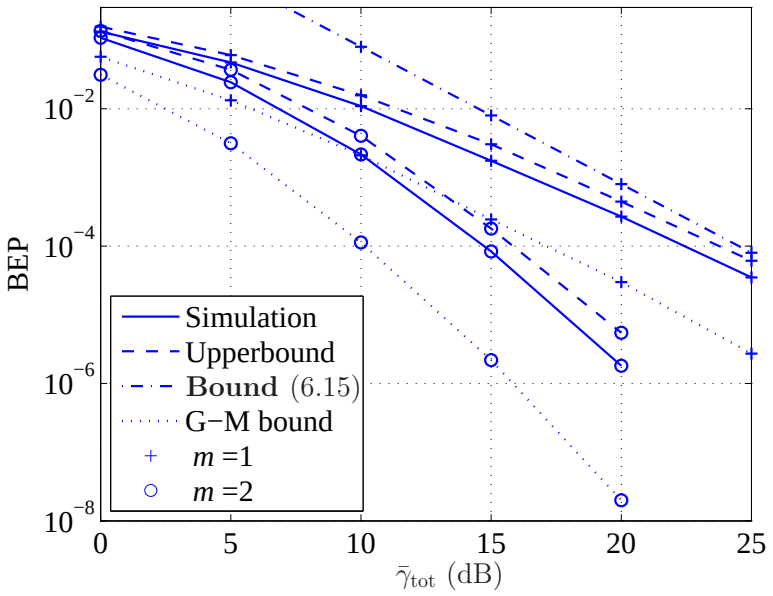

Figure 6.2 Simulation results, upperbounds and G-M lowerbounds on the SEP performance for 1 relay: $(\Omega_{\mathrm{SR}}, \Omega_{\mathrm{RD}}, \Omega_{\mathrm{SD}}) = (20, 0, 0)$dB.

For the general case, the upperbound can be easily calculated by numerical integration techniques since the RHS of (6.10) involves only a single integral with finite

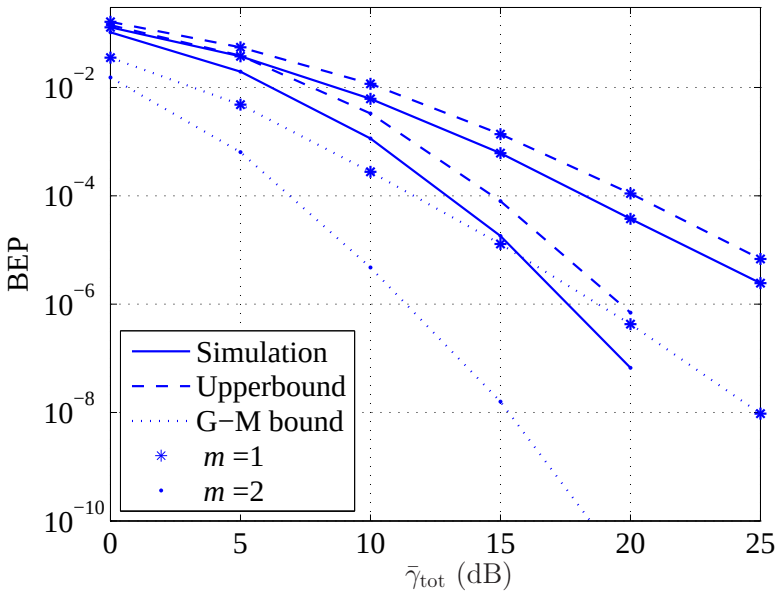

Figure 6.3 Simulation results, upperbounds and G-M lowerbounds on the SEP performance for 2 relays: $(\Omega_{\rm SR}, \Omega_{\rm RD}, \Omega_{\rm SD}) = (20, 0, 0)$dB.

limits. Figs. 6.1, 6.2 and 6.3 show the tightness of the derived bound on the performance of MRC with binary phase-shift keying (BPSK) modulation[3]. The total power $\bar{\gamma}_{\rm tot}$ is equally distributed among the source and relays in these special cases. For the case that $(\Omega_{\rm SR}, \Omega_{\rm RD}, \Omega_{\rm SD}) = (0, 0, 0)$dB, Fig. 6.1 reveals that the derived bound and its simplified version (for the case of $(m = 1, K = 1)$) are reasonably tight when compared to the simulation results. For all the four cases of $(m = 1, K = 1)$, $(m = 2, K = 1)$, $(m = 1, K = 2)$ and $(m = 2, K = 2)$, all the corresponding bounds lie within 0.7dB of the simulation curves. Fig.6.1 also plots the geometric-mean (G-M) lowerbound obtained in [P16]. It can be seen that the G-M lowerbound is also quite tight over the whole range of SNR. The tightness of the G-M lowerbound in this case is a consequence of the fact that the equality condition of the G-M lowerbound holds when $\gamma_{{\rm SR}_i} = \gamma_{{\rm R}_i{\rm D}}$, $i = 1, \ldots, K$, i.e., balanced channels. However, the G-M lower bound becomes very loose when the channels are unbalanced, i.e., $\Omega_{{\rm SR}_i} \neq \Omega_{{\rm R}_i{\rm D}}$, $i = 1, \ldots, K$, as can be clearly observed in Figs. 6.2 and 6.3. In contrast, our derived bound can maintain its tightness over a wide range of channel settings. As shown

[3]For $K = 2$, it is assumed that $\Omega_{{\rm SR}_1} = \Omega_{{\rm SR}_2} = \Omega_{\rm SR}$ and $\Omega_{{\rm R}_1{\rm D}} = \Omega_{{\rm R}_2{\rm D}} = \Omega_{\rm RD}$.

in Figs. 6.2 and 6.3, the proposed bounds and its simplified version (for the case of $(m = 1, K = 1)$) still lie within about 1.5dB of the simulation results for all the four cases of $(m = 1, K = 1)$, $(m = 2, K = 1)$, $(m = 1, K = 2)$ and $(m = 2, K = 2)$ when $(\Omega_{\rm SR}, \Omega_{\rm RD}, \Omega_{\rm SD}) = (20, 0, 0)$dB.[4]

To give an insight into the SEP performance, the following proposition establishes the achievable diversity order of the relay system by further examining its bound in Lemma 1.

Proposition 1. *For the K-relay system with the received SNR at D, γ, given in* (6.7)*, M-PSK modulation and Nakagami-m fading, the average SEP, P_s, is bounded as*

$$(\underline{k}_s\bar{\gamma})^{-m(K+1)} \overset{\bar{\gamma}\to\infty}{\lessapprox} P_s \overset{\bar{\gamma}\to\infty}{\lessapprox} (\bar{k}_s\bar{\gamma})^{-m(K+1)} \tag{6.16}$$

where $\bar{k}_s$ and $\underline{k}_s$ are nonnegative constants that depend on $(\Omega_{SR_k}, \Omega_{R_kD})_{k=1}^K$ and Ω_{SD}.

Proof: See Appendix 6.B.

Since both the upper and lower bounds in Proposition 1 are proportional with $(1/\bar{\gamma})^{m(K+1)}$, one can conclude that MRC with fixed-gain relays can offer the maximum diversity order of $m(K+1)$ in the high SNR region. Furthermore, the achievable diversity order does not depend on the locations of $(\mathrm{R}_k)_{k=1}^K$.

6.4 Power Allocation and Illustrative Results

Exercising power allocation to optimize the performance (such as error or outage probabilities) of relaying systems has been studied extensively in the literature (see, e.g., [P10, P18, P19, P21, P22]). In most cases using the *exact* performance analysis as the optimization objective for the power allocation problem is not tractable. As such it is common to rely on the performance bounds, e.g., upperbounds on the average symbol error probability [P10] or on the pairwise error probability [P19, P21] as they

[4]The tightness of the proposed bound can also be seen with other channel conditions, such as $(\Omega_{\rm SR}, \Omega_{\rm RD}, \Omega_{\rm SD}) = (0, 20, 0)$dB. However, due to space limit, the figures are omitted.

are more favorable to analyze. Given the tightness of the bounds, it is expected that the power allocation obtained based on the bounds works well for the actual performance as well.

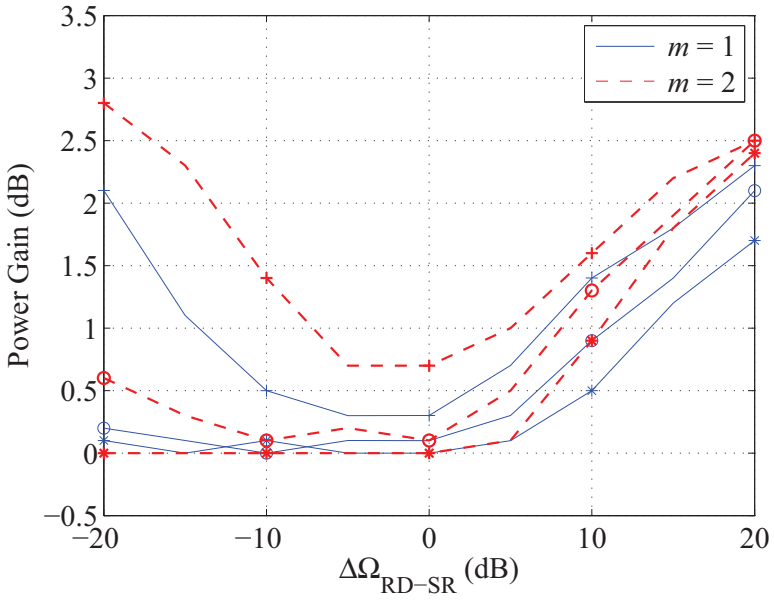

Figure 6.4 Power gains of proposed PA over EPA for 1 relay (predicted by the SEP bound). Three cases of $\Omega_{\mathrm{SR}} = \{-20, 0, 20\}$dB correspond to the (+,o,*) markers, respectively.

This section investigates the effects of power allocation on the SEP performance of the relay system under consideration. Here the goal is to minimize the SEP upperbound, which is given in (6.10). The proposed power allocation scheme only requires that the destination knows the channel statistics, i.e., $(\Omega_{\mathrm{SR}_k})_{k=1}^{K}$, $(\Omega_{\mathrm{R}_k\mathrm{D}})_{k=1}^{K}$ and Ω_{SD}, to compute the SEP upperbound. Having all the needed information, the destination then computes the power coefficients for the source and relays, and notifies all the nodes of their transmission powers via low rate feedback channels. The optimization problem is formulated as follows.

Problem Statement 1. *For given channel statistics,* $(\Omega_{SR_k})_{k=1}^{K}$, $(\Omega_{R_kD})_{k=1}^{K}$ *and* Ω_{SD}, *and the total power constraint* E_{tot}, *determine the power allocation coefficients* $\left(\varepsilon_s^{OPA}, (\varepsilon_k^{OPA})_{k=1}^{K}\right)$ *to minimize the upperbound on* P_s *given in Eq.* (6.10) *while satisfying the total power constraint,* $E_{tot} = \left(\varepsilon_s^{OPA} + \sum_{k=1}^{K} \varepsilon_k^{OPA}\right) E_s = (K+1)\, E_s$.

Table 6.1 Power allocation coefficients ($\varepsilon_s^{OPA}/\varepsilon_1^{OPA}$ and $\varepsilon_s^{OPA}/\varepsilon_1^{OPA}/\varepsilon_2^{OPA}$ for $K = 1$ and 2, respectively).

(a) $\Delta\Omega_{\text{RD-SR}} = 20\text{dB}$

Ω_{SR}	$K=1$		$K=2$	
dB	$m=1$	$m=2$	$m=1$	$m=2$
-20	1.77/0.23	1.86/0.14	2.46/0.27/0.27	2.78/0.11/0.11
0	1.69/0.31	1.81/0.19	2.28/0.36/0.36	2.64/0.18/0.18
20	1.63/0.37	1.78/0.22	2.18/0.41/0.41	2.52/0.24/0.24

b) $\Delta\Omega_{\text{RD-SR}} = -20\text{dB}$

Ω_{SR}	$K=1$		$K=2$	
dB	$m=1$	$m=2$	$m=1$	$m=2$
-20	1.81/0.19	1.90/0.10	2.32/0.34/0.34	2.80/0.10/0.10

Unfortunately, an analytical solution for the above power allocation problem appears to be intractable, even with high SNR approximations. Here we resort to numerical search based on the SEP upperbound obtained in Lemma 1. It should be emphasized that the bound contains simple non-linear functions, i.e., the gamma function $\Gamma(x)$ and exponential integral function $E_1(x)$, which are readily available in many computing softwares (e.g. Matlab). Common computing softwares (e.g. Matlab) provide both Gaussian quadrature and the simple techniques such as the Newton-Cotes formula as well. These techniques can be readily adapted to calculate the integral expression in Lemma 1. Once the SEP upperbound is computed, the numerical search for the optimal power allocation can be easily carried out. For the simplest case of 1-relay system, the line search method [P26] is used to find the optimal values numerically. However, when there are more than 1 relay in the system, we rely on the brute-force search to find out the optimal power coefficients for S and $(\text{R}_k)_{k=1}^K$, i.e., $\varepsilon_s^{\text{OPA}}$ and $(\varepsilon_k^{\text{OPA}})_{k=1}^K$. Furthermore, in practical implementation the optimal power allocation coefficients can be obtained in advance for typical channel statistics $(\Omega_{\text{SR}_k})_{k=1}^K$, $(\Omega_{\text{R}_k\text{D}})_{k=1}^K$ and Ω_{SD} and then built into a lookup table.

As a first example, consider a single-relay system, i.e., $K = 1$. To cover a wide

range of possible channel settings, i.e., the triple mean-squared values $(\Omega_{\text{SR}}, \Omega_{\text{RD}}, \Omega_{\text{SD}})$, we first normalize Ω_{SD} to be 0dB. For the SR link, three possible cases are: R is farther to S than D; R and D are equidistant to S; and R is closer to S than D. These three settings are assumed to correspond to $\Omega_{\text{SR}} = -20$, 0 and 20dB, respectively. For each value of Ω_{SR}, a range of Ω_{RD}, i.e., $\Omega_{\text{RD}} \in (\Omega_{\text{SR}} - 20\text{dB}, \Omega_{\text{SR}} + 20\text{dB})$, is investigated.[5] Figs. 6.4 shows the power gains of the proposed PA over EPA for $m = 1$ and 2, respectively, under the target BEP of 10^{-4}. For a wide range of the relative gap between Ω_{RD} and Ω_{SR}, i.e., $\Delta\Omega_{\text{RD-SR}} = (\Omega_{\text{RD}} - \Omega_{\text{SR}})$dB, the predictable gains are promising, up to 2.3dB for $m = 1$ and 2.7dB for $m = 2$. When the RD link is better than the SR link, i.e., $\Delta\Omega_{\text{RD-SR}} = 20$dB, the proposed PA can offer gains of at least 1.5 and 2.3dB for $m = 1$ and 2, respectively. As shown in Fig. 6.4, the proposed PA also provides power gains when Ω_{SR} is -20dB and $\Delta\Omega_{\text{RD-SR}}$ is low, say $\Delta\Omega_{\text{RD-SR}} = -20$dB. This is explained as follows. Due to the very poor quality of the indirect channels when compared to that of the direct link ($\Omega_{\text{SD}} = 0$dB here), it is helpful to assign large amount of power to the source in the first time slot rather than distribute power equally between the source and relays. The overall performance is then mainly determined by the direct transmission during the first time slot. As a result, the performance gain offered by the proposed PA over EPA can be large. On the other hand, when the indirect links are getting better (say $\Delta\Omega_{\text{RD-SR}} = 0$dB), the imbalance between the indirect and direct channels' qualities is decreasing. The proposed PA tends to converge to EPA and consequently there is not much performance improvement when using the proposed PA instead of EPA. Similar explanation applies for the other cases that Ω_{SR} is 0 or 20dB.

Similarly, for the 2-relay system, i.e., $K = 2$, our results[6] also show that the proposed PA can offer even more power gains over EPA when compared to the single-

[5]Other settings reported in [P7, P10, P21] only consider the case that three nodes S, R and D are in a 2-dimensional space, which puts a constraint on the set $(\Omega_{\text{SR}}, \Omega_{\text{RD}}, \Omega_{\text{SD}})$, for example, Eq. (22) in [P7]. On the other hand we study in this paper the more general case, i.e., 3 nodes are in a 3-dimensional space, which has no constraint on the set $(\Omega_{\text{SR}}, \Omega_{\text{RD}}, \Omega_{\text{SD}})$.

[6]Due to the space limit, the figure is omitted.

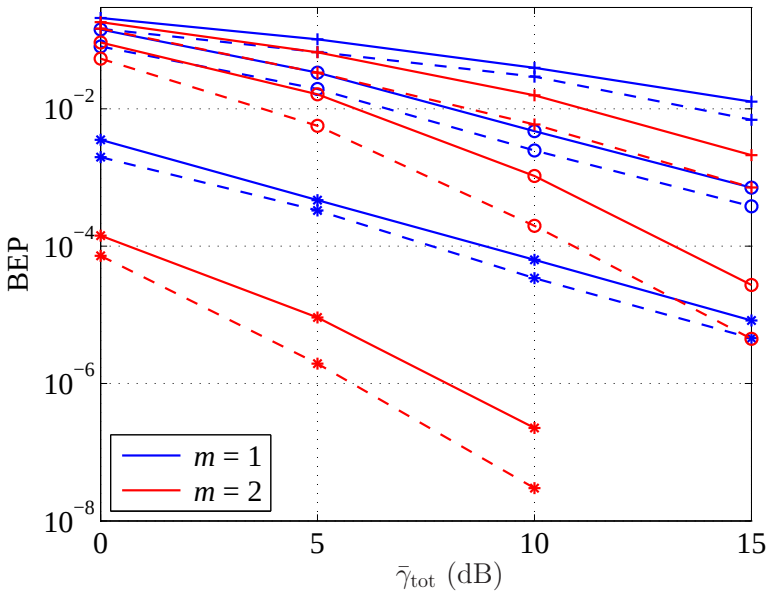

Figure 6.5 Performance comparison of 1 relay with proposed PA (dashed line) and EPA (solid line): $\Delta\Omega_{\text{RD-SR}} = 20$dB. The cases of $\Omega_{\text{SR}} = (-20, 0, 20)$dB correspond to the (+,o,*) markers, respectively.

relay systems, e.g., 3.5 and 4.5dB for $m = 1$ and $m = 2$, respectively. Such larger gains are reasonable since with more relays in the system, there is more freedom to allocate power between the relays and source.

Next, simulation results are provided to confirm the power gains predicted by the bound (presented in Fig. 6.4). For each specific value of Ω_{SR}, various values of $\Delta\Omega_{\text{RD-SR}}$ are investigated. The particularly important values are those corresponding to the boundary and middle ones, i.e., $\Delta\Omega_{\text{RD-SR}} = -20$, 0 and 20dB. Therefore, the following simulation results shall focus to validate the performance gains at these values.

For the single- and 2-relay systems, Figs. 6.5 and 6.6 compare the performance of EPA and proposed PA for the two values of m when the RD channel is better than the SR channel ($\Delta\Omega_{\text{RD-SR}} = 20$dB). The optimal power allocation coefficients for the source and relays are presented in Table 6.1-(a). For the single-relay system under the Rayleigh fading, i.e., $m = 1$, and in the three cases that $\Omega_{\text{SR}} = 20$, 0 and -20dB,

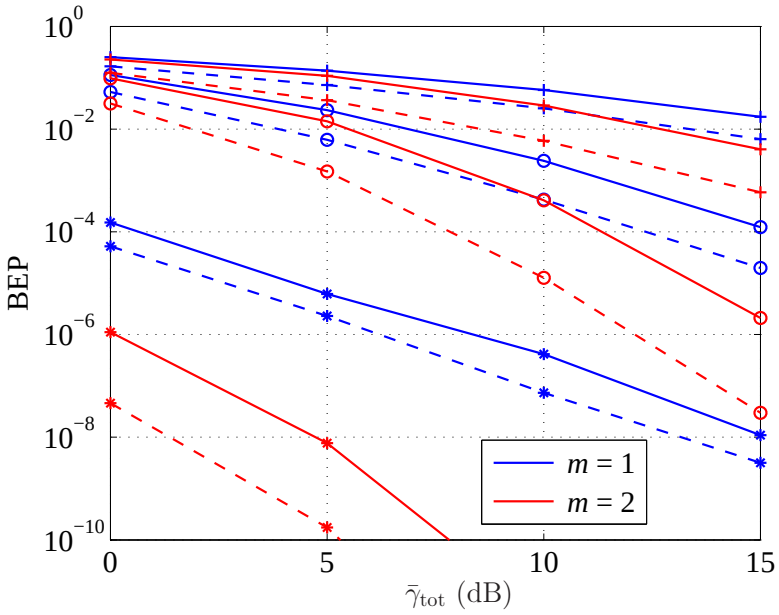

Figure 6.6 Performance comparison of 2 relays with proposed PA (dashed line) and EPA (solid line): $\Delta\Omega_{\text{RD-SR}} = 20$dB. The cases of $\Omega_{\text{SR}} = (-20, 0, 20)$dB correspond to the (+,o,*) markers, respectively.

the proposed PA can offer gains of about 2, 1.6 and 1.2dB, respectively, over the EPA. These gains are in good agreement with the gains predicted in Fig. 6.4 (based on the bound). For $m = 2$, the improvement of the proposed PA over EPA is also very promising, about 2.5, 2 and 1.8dB for $\Omega_{\text{SR}} = 20$, 0 and -20dB, respectively, similar to what predicted in Fig. 6.4. For the 2-relay system, the benefits of the proposed power allocation are illustrated in Fig. 6.6. As can be seen from Fig. 6.6, for both values of m, the gains are at least 3dB as predicted.

Fig. 6.7 demonstrates the performance gains by the proposed PA when $\Omega_{\text{SR}} = -20$dB and $\Delta\Omega_{\text{RD-SR}} = -20$dB. The optimal power coefficients for the sources and relays are given in Table 6.1-(b). The channel settings investigated in Fig. 6.7 represent the case that the RD and SR fading channels are very poor when compared to the direct link SD. However, one can still obtain significant gains of about 2.5, 2.8, 3 and 4.5dB for $(K = 1, m = 1)$, $(K = 1, m = 2)$, $(K = 2, m = 1)$ and $(K = 2, m = 2)$, respectively. These gains also agree with what predicted based on the SEP bound

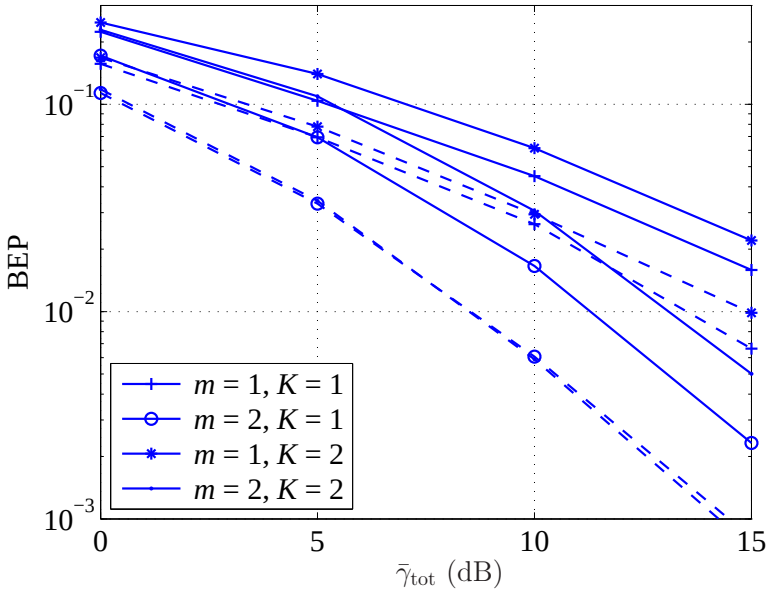

Figure 6.7 Performance comparison of SEP performance between proposed PA (dashed line) and EPA (solid line): $\Omega_{\text{SR}} = -20\text{dB}$ and $\Delta\Omega_{\text{RD-SR}} = -20\text{dB}$.

(Fig. 6.4). It is worthwhile to point out that the cases of $(m = 2, K = 1)$ and $(m = 2, K = 2)$ have almost the same performance with the proposed PA in the SNR range shown in Fig. 6.7. It can be verified that at the *very high* SNR region the two curves depart and have their decaying exponents to be 4 and 8, respectively, as proven in Proposition 1.

Finally, Fig. 6.8 compares the performance of the "optimal" PA proposed by Zhao et al. [P22] with our proposed PA. It should be noted that the authors in [P22] consider the varying-gain relay system where the transmit power at the relays is maintained constant at all time. The varying gain requires the relays to know the instantaneous channel gains of all the source-relay links, whereas the fixed gain requires only the source-relay statistics available at the relays. Since the OPA algorithm in [P22] predetermines the power for S, i.e., $\varepsilon_s E_s$, in the first time slot, the comparison only makes sense if the system has more than 1 relay and the relays are at different locations, i.e., $K > 1$, $\Omega_{\text{SR}_i} \neq \Omega_{\text{SR}_j}$ or $\Omega_{\text{R}_i\text{D}} \neq \Omega_{\text{R}_j\text{D}}$ where $i \neq j$ and $i, j = 1, \ldots, K$. For the 2-relay system, consider the case that R_1 is closer to S than D, while R_2 is closer to D than S.

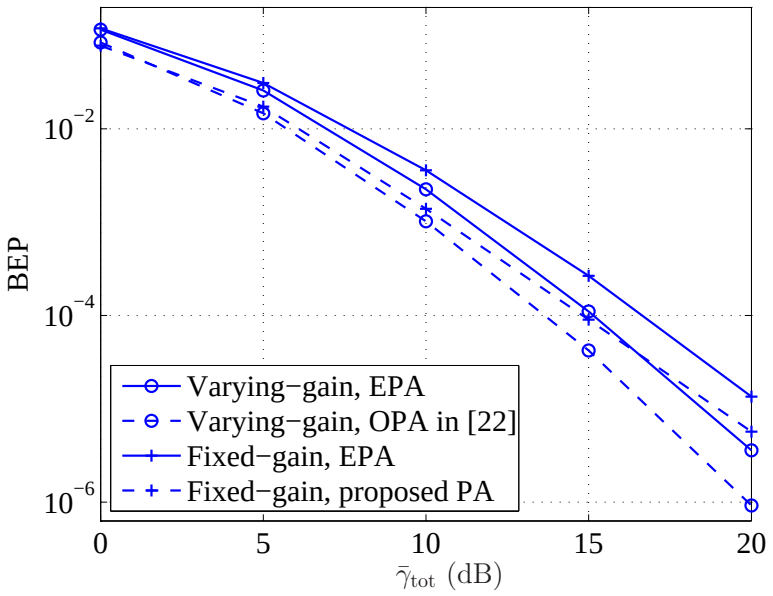

Figure 6.8 Performance comparison of SEP performance between varying- and fixed-gain relaying systems.

The case is assumed to correspond to $\Omega_{\text{SR}_1} = \Omega_{\text{R}_2\text{D}} = 0$dB and $\Omega_{\text{SR}_2} = \Omega_{\text{R}_1\text{D}} = 20$dB. The optimal power allocation coefficients, i.e., $\varepsilon_s^{\text{OPA}}/\varepsilon_1^{\text{OPA}}/\varepsilon_2^{\text{OPA}}$, are found to be[7] 1.8/0.1305/1.0695 and 1.8/0.3/0.9 for the varying- and fixed-gain relay systems, respectively. Fig. 6.8 shows that, in this setting, the varying-gain system performs better than the fixed-gain as expected. It is interesting to see that at BEP $= 10^{-3}$, the gains offered by our algorithm and the one by Zhao et al. over the EPA are the same, about 0.5dB. It should be noted that the performance gains depend on the channel setting. When the channels from S to R_1 and R_2 to D are worse, the performance of the fixed-gain relaying approaches that of the varying-gain relaying. Both algorithms tell us that less power should be allocated to R_1 and more power to R_2. For example, for the case[8] of $\Omega_{\text{SR}_1} = \Omega_{\text{R}_2\text{D}} = -20$dB and $\Omega_{\text{SR}_2} = \Omega_{\text{R}_1\text{D}} = 20$dB, one

[7] Note that the performance of the OPA in [P22] depends on the predetermined power coefficient, ε_s, at the source. However the issue of optimizing ε_s is not addressed in [P22]. As such, in the comparison between the OPA in [P22] and our proposed PA, the same power allocation obtained from our proposed PA is also applied for the case of OPA.

[8] Again, due to space limit, the figure for such a channel setting is omitted.

obtains $\varepsilon_s^{\mathrm{OPA}}/\varepsilon_1^{\mathrm{OPA}}/\varepsilon_2^{\mathrm{OPA}} = 2.1/0.0135/0.8865$ and $2.1/0.1/0.8$ for the varying- and fixed-gain relaying, respectively. Both varying- and fixed-gain relaying performance curves are almost identical and the gain over the EPA is about 2dB at BER $= 10^{-3}$.

6.5 Conclusions

In this paper, an upperbound on the SEP was derived for the multiple-relay systems with fixed-gain AF relaying and MRC. It was shown that the tightness of the bound is maintained over a wide range of channel settings even when the source-relay and relay-destination channels are unbalanced. The bound also shows that MRC can achieve the maximum diversity order of $m(K+1)$. Based on the obtained bound, a novel PA scheme was proposed. Extensive simulation was conducted and the results are in good agreement with the gains predicted based on the bound and shown to provide a significant saving of total transmitted power.

6.A Proof of Lemma 1

To calculate the upperbound on the average SEP P_s, one needs to evaluate the moment generating function $\mathcal{M}_\gamma(-t)$ first. Then the resulting MGF can be applied into (6.8). The MGF $\mathcal{M}_\gamma(-t)$ is computed as

$$\begin{aligned}\mathcal{M}_\gamma(-t) =& E_{\gamma_{\mathrm{SD}}}\left\{\exp\left(-t\varepsilon_s\gamma_{\mathrm{SD}}\right)\right\}\prod_{k=1}^{K} E_{\gamma_{\mathrm{SR}_k},\gamma_{\mathrm{R}_k\mathrm{D}}}\left\{\exp\left[-tG_k^2\varepsilon_s\gamma_{\mathrm{SR}_k}\gamma_{\mathrm{R}_k\mathrm{D}}\Big/\left(\bar{\gamma}+G_k^2\gamma_{\mathrm{R}_k\mathrm{D}}\right)\right]\right\}\\ =& \prod_{k=1}^{K}\left(A_k(t)+B_k(t)\right)\Big/\left[t\varepsilon_s\bar{\gamma}_{\mathrm{SD}}/m+1\right]^m. \qquad (6.17)\end{aligned}$$

The term $A_k(t)$ in the RHS of (6.17) is calculated as

$$A_k(t) = \int_0^\infty \int_0^{\bar{\gamma}/G_k^2} \exp\left[-\frac{tG_k^2\varepsilon_s\gamma_{\mathrm{SR}_k}\gamma_{\mathrm{R}_k\mathrm{D}}}{(\bar{\gamma}+G_k^2\gamma_{\mathrm{R}_k\mathrm{D}})}\right] p_{\gamma_{\mathrm{R}_k\mathrm{D}}}(\gamma_{\mathrm{R}_k\mathrm{D}}) p_{\gamma_{\mathrm{SR}_k}}(\gamma_{\mathrm{SR}_k}) d\gamma_{\mathrm{R}_k\mathrm{D}} d\gamma_{\mathrm{SR}_k} \tag{6.18}$$

$$\leq \int_0^\infty \int_0^{\bar{\gamma}/G_k^2} \exp\left[-tG_k^2\varepsilon_s\gamma_{\mathrm{SR}_k}\gamma_{\mathrm{R}_k\mathrm{D}}/(2\bar{\gamma})\right] p_{\gamma_{\mathrm{R}_k\mathrm{D}}}(\gamma_{\mathrm{R}_k\mathrm{D}}) p_{\gamma_{\mathrm{SR}_k}}(\gamma_{\mathrm{SR}_k}) d\gamma_{\mathrm{R}_k\mathrm{D}} d\gamma_{\mathrm{SR}_k} \tag{6.19}$$

$$= \int_0^\infty \frac{m^m}{\Gamma(m)\bar{\gamma}_{\mathrm{R}_k\mathrm{D}}^m}\left[\frac{\Gamma(m)}{\left(tG_k^2\varepsilon_s\gamma_{\mathrm{SR}_k}/(2\bar{\gamma})+m/(\bar{\gamma}_{\mathrm{R}_k\mathrm{D}})\right)^m} - \exp\left(-\frac{\bar{\gamma}}{G_k^2}\left(\frac{tG_k^2\varepsilon_s\gamma_{\mathrm{SR}_k}}{2\bar{\gamma}}+\frac{m}{\bar{\gamma}_{\mathrm{R}_k\mathrm{D}}}\right)\right)\right.$$
$$\left.\sum_{l=0}^{m-1}\frac{\Gamma(m)(\bar{\gamma}/G_k^2)^l}{\Gamma(l+1)\left(tG_k^2\varepsilon_s\gamma_{\mathrm{SR}_k}/(2\bar{\gamma})+m/\bar{\gamma}_{\mathrm{R}_k\mathrm{D}}\right)^{m-l}}\right] p_{\gamma_{\mathrm{SR}_k}}(\gamma_{\mathrm{SR}_k}) d\gamma_{\mathrm{SR}_k} \tag{6.20}$$

$$= A_{k,1}(t) - A_{k,2}(t). \tag{6.21}$$

After some manipulations on the RHS of (6.20), $A_k(t)$ can be bounded as

$$A_k(t) \leq A_{k,1}(t) - A_{k,2}(t), \tag{6.22}$$

where $A_{k,1}(t)$ and $A_{k,2}(t)$ are specified in (6.11) and (6.12), respectively. To arrive at (6.22), one can use [P27, Eqs. (3.351.1), (3.351.3), (3.352.4) and (3.353.2)].

The term $B_k(t)$ in (6.17) is expressed as

$$B_k(t) = \int_0^\infty \int_{\bar{\gamma}/G_k^2}^\infty \exp\left[-\frac{tG_k^2\varepsilon_s\gamma_{\mathrm{SR}_k}\gamma_{\mathrm{R}_k\mathrm{D}}}{(\bar{\gamma}+G_k^2\gamma_{\mathrm{R}_k\mathrm{D}})}\right] p_{\gamma_{\mathrm{R}_k\mathrm{D}}}(\gamma_{\mathrm{R}_k\mathrm{D}}) p_{\gamma_{\mathrm{SR}_k}}(\gamma_{\mathrm{SR}_k}) d\gamma_{\mathrm{R}_k\mathrm{D}} d\gamma_{\mathrm{SR}_k} \tag{6.23}$$

$$\leq \int_0^\infty \int_{\bar{\gamma}/G_k^2}^\infty \exp\left(-t\varepsilon_s\gamma_{\mathrm{SR}_k}/2\right) p_{\gamma_{\mathrm{R}_k\mathrm{D}}}(\gamma_{\mathrm{R}_k\mathrm{D}}) p_{\gamma_{\mathrm{SR}_k}}(\gamma_{\mathrm{SR}_k}) d\gamma_{\mathrm{R}_k\mathrm{D}} d\gamma_{\mathrm{SR}_k}$$

$$= \left[m\Big/\left(\bar{\gamma}_{\mathrm{SR}_k}\left(t\varepsilon_s/2+m/\bar{\gamma}_{\mathrm{SR}_k}\right)\right)\right]^m \Gamma(m, m\bar{\gamma}/(G_k^2\bar{\gamma}_{\mathrm{R}_k\mathrm{D}}))/\Gamma(m) = B_{k,1}(t), \tag{6.24}$$

where (6.24) is computed with the aid of [P27, Eq. (3.351.2)] and [P27, Eq. (3.351.3)].

Substituting (6.17), (6.22) and (6.24) into (6.8) completes the proof of Lemma 1.

6.B Proof of Proposition 1

The Chernoff bound can be used to upperbound the probability P_s by setting θ in (6.10) to $\pi/2$ as follows:

$$P_s \leq \frac{M-1}{M\left(\sin^2(\pi/M)\varepsilon_s\bar{\gamma}_{\mathrm{SD}}/m+1\right)^m}\Big[\prod_{k=1}^{K}(A_{k,1}(t)-A_{k,2}(t)+B_{k,1}(t))\Big]_{t=\sin^2(\pi/M)} \tag{6.25}$$

$$\leq \frac{M-1}{M\left(\sin^2(\pi/M)\varepsilon_s\bar{\gamma}_{\mathrm{SD}}/m+1\right)^m}\Big[\prod_{k=1}^{K}(A_{k,1}(t)+B_{k,1}(t))\Big]_{t=\sin^2(\pi/M)}. \tag{6.26}$$

The term $A_{k,1}(t)$ in (6.21) can be calculated and bounded as

$$A_{k,1}(t) = \frac{m^{2m}}{\Gamma(m)\bar{\gamma}_{\mathrm{SR}_k}^m\bar{\gamma}_{\mathrm{R}_k\mathrm{D}}^m}\left(\frac{2\bar{\gamma}}{tG_k^2\varepsilon_s}\right)^m\int_0^\infty\frac{\gamma_{\mathrm{SR}_k}^{m-1}}{\left(\gamma_{\mathrm{SR}_k}+\frac{2m\bar{\gamma}}{tG_k^2\varepsilon_s\bar{\gamma}_{\mathrm{R}_k\mathrm{D}}}\right)^m}\exp\left(-\frac{m\gamma_{\mathrm{SR}_k}}{\bar{\gamma}_{\mathrm{SR}_k}}\right)d\gamma_{\mathrm{SR}_k} \tag{6.27}$$

$$< \frac{m^{2m}}{\Gamma(m)\bar{\gamma}_{\mathrm{SR}_k}^m\bar{\gamma}_{\mathrm{R}_k\mathrm{D}}^m}\left(\frac{2\bar{\gamma}}{tG_k^2\varepsilon_s}\right)^m\int_0^\infty\frac{1}{\left(\gamma_{\mathrm{SR}_k}+\frac{2m\bar{\gamma}}{tG_k^2\varepsilon_s\bar{\gamma}_{\mathrm{R}_k\mathrm{D}}}\right)}\exp\left(-\frac{m\gamma_{\mathrm{SR}_k}}{\bar{\gamma}_{\mathrm{SR}_k}}\right)d\gamma_{\mathrm{SR}_k} \tag{6.28}$$

$$= \frac{1}{\Gamma(m)}\left(\frac{2m^2\bar{\gamma}}{tG_k^2\varepsilon_s\bar{\gamma}_{\mathrm{SR}_k}\bar{\gamma}_{\mathrm{R}_k\mathrm{D}}}\right)^m\exp\left(\frac{2m^2\bar{\gamma}}{tG_k^2\varepsilon_s\bar{\gamma}_{\mathrm{SR}_k}\bar{\gamma}_{\mathrm{R}_k\mathrm{D}}}\right)\mathrm{E}_1\left(\frac{2m^2\bar{\gamma}}{tG_k^2\varepsilon_s\bar{\gamma}_{\mathrm{SR}_k}\bar{\gamma}_{\mathrm{R}_k\mathrm{D}}}\right) \tag{6.29}$$

$$< \frac{1}{\Gamma(m)}\left(\frac{2m^2\bar{\gamma}}{tG_k^2\varepsilon_s\bar{\gamma}_{\mathrm{SR}_k}\bar{\gamma}_{\mathrm{R}_k\mathrm{D}}}\right)^m\frac{tG_k^2\varepsilon_s\bar{\gamma}_{\mathrm{SR}_k}\bar{\gamma}_{\mathrm{R}_k\mathrm{D}}}{2m^2\bar{\gamma}/+\eta tG_k^2\varepsilon_s\bar{\gamma}_{\mathrm{SR}_k}\bar{\gamma}_{\mathrm{R}_k\mathrm{D}}}, \tag{6.30}$$

where the inequality (6.28) follows from the fact that

$$\frac{\gamma_{\mathrm{SR}_k}^{m-1}}{\left(\gamma_{\mathrm{SR}_k}+\frac{2m\bar{\gamma}}{tG_k^2\varepsilon_s\bar{\gamma}_{\mathrm{R}_k\mathrm{D}}}\right)^m} < \frac{\left(\gamma_{\mathrm{SR}_k}+\frac{2m\bar{\gamma}}{tG_k^2\varepsilon_s\bar{\gamma}_{\mathrm{R}_k\mathrm{D}}}\right)^{m-1}}{\left(\gamma_{\mathrm{SR}_k}+\frac{2m\bar{\gamma}}{tG_k^2\varepsilon_s\bar{\gamma}_{\mathrm{R}_k\mathrm{D}}}\right)^m} = \frac{1}{\left(\gamma_{\mathrm{SR}_k}+\frac{2m\bar{\gamma}}{tG_k^2\varepsilon_s\bar{\gamma}_{\mathrm{R}_k\mathrm{D}}}\right)}. \tag{6.31}$$

The equality (6.29) is evaluated with the help of [P27, Eq. 3.532.4] and (6.30) comes from the following inequality: $1/(1+x) < \exp(x)\mathrm{E}_1(x) \leq 1/(\eta+x)$, $\forall x>0$, $0<\eta<1$ [P25].

Substituting $B_{k,1}(t)$ and the upperbound on $A_{k,1}(t)$ in (6.24) and (6.30), respectively, to (6.26) results in (6.16) in Proposition 1.

For the lower bound, one also needs to evaluate the moment generating function $M_\gamma(-t)$ then applies the resulting MGF into (6.8). Using the result in (6.17), the

MGF $M_\gamma(-t)$ is calculated and lowerbounded as

$$\begin{aligned}\mathcal{M}_\gamma(-t) =& E_{\gamma_{\mathrm{SD}}}\left\{\exp\left(-t\varepsilon_s\gamma_{\mathrm{SD}}\right)\right\}\prod_{k=1}^{K} E_{\gamma_{\mathrm{SR}_k},\gamma_{\mathrm{R}_k\mathrm{D}}}\left\{\exp\left[-tG_k^2\varepsilon_s\gamma_{\mathrm{SR}_k}\gamma_{\mathrm{R}_k\mathrm{D}}\Big/\left(\bar{\gamma}+G_k^2\gamma_{\mathrm{R}_k\mathrm{D}}\right)\right]\right\}\\ =& \prod_{k=1}^{K}\left[A_k(t)+B_k(t)\right]\Big/\left[t\varepsilon_s\bar{\gamma}_{\mathrm{SD}}/m+1\right]^m \geq \prod_{k=1}^{K} A_k(t)\Big/\left[t\varepsilon_s\bar{\gamma}_{\mathrm{SD}}/m+1\right]^m,\end{aligned} \tag{6.32}$$

where $A_k(t)$ and $B_k(t)$ are given in (6.18) and (6.23), respectively. The inequality (6.32) is due to the fact that $B_k(t) \geq 0$.

The term $A_k(t)$ is then lowerbounded as

$$\begin{aligned}A_k(t) \geq& \int_0^\infty\int_0^{\bar{\gamma}/G_k^2}\exp\left(-t\varepsilon_s\gamma_{\mathrm{SR}_k}/2\right)p_{\gamma_{\mathrm{R}_k\mathrm{D}}}(\gamma_{\mathrm{R}_k\mathrm{D}})p_{\gamma_{\mathrm{SR}_k}}(\gamma_{\mathrm{SR}_k})d\gamma_{\mathrm{R}_k\mathrm{D}}d\gamma_{\mathrm{SR}_k}\\ =& \int_0^\infty\frac{\exp\left(-t\varepsilon_s\gamma_{\mathrm{SR}_k}/2\right)}{\Gamma(m)}\gamma\left(m,\frac{m\bar{\gamma}}{G_k^2\bar{\gamma}_{\mathrm{R}_k\mathrm{D}}}\right)\frac{m^m\gamma_{\mathrm{SR}_k}^{m-1}}{\bar{\gamma}_{\mathrm{SR}_k}^m\Gamma(m)}\exp\left(-\frac{m\gamma_{\mathrm{SR}_k}}{\bar{\gamma}_{\mathrm{SR}_k}}\right)d\gamma_{\mathrm{SR}_k}\end{aligned} \tag{6.33}$$

$$= \frac{m^m}{\Gamma(m)\bar{\gamma}_{\mathrm{SR}_k}^m}\gamma\left(m,\frac{m\bar{\gamma}}{G_k^2\bar{\gamma}_{\mathrm{R}_k\mathrm{D}}}\right)\left(\frac{t\varepsilon_s}{2}+\frac{m}{\bar{\gamma}_{\mathrm{SR}_k}}\right)^{-m}, \tag{6.34}$$

where (6.33) and (6.34) are computed with the help of [P27, Eq. 3.531.1] and [P27, Eq. 3.531.3], respectively.

Substituting (6.34) and (6.32) into (6.8), one has the lowerbound on the average SEP for M-PSK as follows:

$$\begin{aligned}P_s \geq& \frac{m^{m(K+1)}}{\pi[\Gamma(m)]^K\bar{\gamma}_{\mathrm{SD}}^m}\prod_{k=1}^{K}\frac{\gamma\left(m,\frac{m\bar{\gamma}}{G_k^2\bar{\gamma}_{\mathrm{R}_k\mathrm{D}}}\right)}{\bar{\gamma}_{\mathrm{SR}_k}^m}\\ &\int_0^{\frac{(M-1)\pi}{M}}\left[\frac{1}{\left(t\varepsilon_s+\frac{m}{\bar{\gamma}_{\mathrm{SD}}}\right)^m}\prod_{k=1}^{K}\frac{1}{\left(\frac{t\varepsilon_s}{2}+\frac{m}{\bar{\gamma}_{\mathrm{SR}_k}}\right)^m}\right]_{t=\frac{\sin^2(\pi/M)}{\sin^2\theta}}d\theta.\end{aligned} \tag{6.35}$$

As clearly seen in (6.35), one can conclude that the lowerbound on P_s is proportional to $(1/\bar{\gamma})^{m(K+1)}$ in the high SNR region. Therefore the proof of the lower bound in (6.16) is completed.

REFERENCES

[P1] A. Sendonaris, E. Erkip, and B. Aazhang, "User cooperation diversity – part 1: System description," *IEEE Trans. Commun.*, vol. 51, pp. 1927–1938, Nov. 2003.

[P2] J. N. Laneman and G. W. Wornell, "Distributed space–time–coded protocol for exploiting cooperative diversity," *IEEE Trans. Inform. Theory*, vol. 49, pp. 2415–2425, Oct. 2003.

[P3] J. N. Laneman, D. N. C. Tse, and G. W. Wornell, "Cooperative diversity in the wireles networks: Efficient protocols and outage behavior," *IEEE Trans. Inform. Theory*, vol. 49, pp. 3062–3080, Dec. 2004.

[P4] A. Ribeiro, X. Cai, and G. Giannakis, "Symbol error probabilities for general cooperative links," *IEEE Trans. on Wireless Commun.*, vol. 4, pp. 1264–1273, May 2005.

[P5] D. Chen and J. N. Laneman, "Modulation and demodulation for cooperative diversity in wireless systems," *IEEE Trans. on Wireless Commun.*, vol. 5, pp. 1785–1794, July 2006.

[P6] Y. Li and S. Kishore, "Asymptotic analysis of amplify-and-forward relaying in Nakagami fading environments," *IEEE Trans. on Wireless Commun.*, vol. 6, pp. 4256–4262, December 2007.

[P7] W. Cho, R. Cao, and L. Yang, "Optimum resource allocation for amplify-and-forward relay networks with differential modulation," *IEEE Trans. Signal Process.*, vol. 56, pp. 5680–5691, Nov. 2008.

[P8] "Special issue on cooperative communications," *IEEE Trans. on Wireless Commun.*, vol. 7, no. 5, May 2008.

[P9] D. S. Michalopoulos, G. K. Karagiannidis, and G. S. Tombras, "Symbol error probability of decode and forward cooperative diversity in Nakagami-m fading channels," *Journal of the Franklin Institute*, vol. 345, no. 7, pp. 723 – 728, 2008.

[P10] W. Cho and L. Yang, "Optimum resource allocation for relay networks with differential modulation," *IEEE Trans. Commun.*, vol. 56, pp. 531–534, April 2008.

[P11] T. Wang, G. Giannakis, and R. Wang, "Smart regenerative relays for link-adaptive cooperative communications," *IEEE Trans. Commun.*, vol. 56, pp. 1950–1960, Nov. 2008.

[P12] N. Vien, H. Nguyen, and T. Le-Ngoc, "Diversity analysis of smart relaying," *IEEE Trans. Veh. Technol.*, vol. 58, pp. 2849–2862, July 2009.

[P13] R. U. Nabar, H. Bolcskei, and F. W. Kneubhler, "Fading relay channels: Performance limits and space–time signal design," *IEEE J. Select. Areas in Commun.*, vol. 22, pp. 1099–1109, Aug. 2004.

[P14] H. Mheidat and M. Uysal, "Impact of receive diversity on the performance of amplify-and-forward relaying under APS and IPS power constraints," *IEEE Commun. Letters*, vol. 10, pp. 468–470, June 2006.

[P15] H. Shin and J. Song, "MRC analysis of cooperative diversity with fixed-gain relays in Nakagami-m fading channels," *IEEE Trans. on Wireless Commun.*, vol. 7, pp. 2069–2074, June 2008.

[P16] G. Karagiannidis, "Performance bounds of multihop wireless communications with blind relays over generalized fading channels," *IEEE Trans. on Wireless Commun.*, vol. 5, pp. 498–503, March 2006.

[P17] A. Avestimehr and D. Tse, "Outage capacity of the fading relay channel in the low-SNR regime," *IEEE Trans. Inform. Theory*, vol. 53, pp. 1401–1415, April 2007.

[P18] A. Host-Madsen and J. Zhang, "Capacity bounds and power allocation for wireless relay channels," *IEEE Trans. Inform. Theory*, vol. 51, pp. 2020–2040, June 2005.

[P19] Y. Jing and B. Hassibi, "Distributed space-time coding in wireless relay networks," *IEEE Trans. on Wireless Commun.*, vol. 5, pp. 3524–3536, December 2006.

[P20] Y. Yao, X. Cai, and G. Giannakis, "On energy efficiency and optimum resource allocation of relay transmissions in the low-power regime," *IEEE Trans. on Wireless Commun.*, vol. 4, pp. 2917–2927, Nov. 2005.

[P21] M. Fareed and M. Uysal, "BER-optimized power allocation for fading relay channels," *IEEE Trans. on Wireless Commun.*, vol. 7, pp. 2350–2359, June 2008.

[P22] Y. Zhao, R. Adve, and T. Lim, "Improving amplify-and-forward relay networks: Optimal power allocation versus selection," *IEEE Trans. on Wireless Commun.*, vol. 6, pp. 3114–3123, August 2007.

[P23] M. K. Simon and M.-S. Alouini, *Digital Communication over Fading Channels.* Wiley-IEEE Press, 1th ed., 2000.

[P24] J. G. Proakis, *Digital Communications.* McGraw-Hill, 4th ed., 2001.

[P25] T. Wang, A. Cano, and G. B. Giannakis, "Link–adaptive cooperative communications without channel state information," in *Proc. IEEE Military Commun. Conf.*, pp. 1–7, Oct. 2006.

[P26] S. Boyd and L. Vandenberghe, *Convex Optimization.* Cambridge University Press, March 2004.

[P27] L. S. Gradshteyn and L. M. Ryzhik, *Tables of Integrals, Series and Products.* Academic Press, 7th ed., 2007.

7. Conclusions and Suggestions for Further Study

7.1 Conclusions

This dissertation was mainly devoted to the performance analysis of relay communication systems under different fading channels and how to improve the error performance by utilizing the systems' resources effectively. Two major signal processing methods, i.e., decode-and-forward (DF) and amplify-and-forward (AF), are considered for the relaying systems. Specifically, the main contributions of this dissertation are summarized as follows:

- For DF in Protocol II, diversity analysis for Smart MRC under Nakagami and Hoyt fading channels has been investigated in Chapter 3. It is shown that Smart MRC can always achieve the maximal diversity orders under these channel models when BPSK modulation is used. As Rayleigh distribution is a special case of Nakagami and Hoyt distributions, our analysis subsumes all the corresponding analytical results reported in [R1].

- In order to reduce the system complexity of Smart MRC, Smart EGC was proposed by integrating EGC with smart relaying for DF in Chapter 4. Similar to the case of Smart MRC, it has been shown that Smart EGC can always achieve the maximal diversity under Nakagami and Hoyt fading channels. It should be noted that only the phases of the channels coefficients are required at the destination due to the use of EGC detection rule.

- For DF in Protocol I, a single-relay system with smart relaying under Rayleigh fading channel was studied in Chapter 5. For BPSK and QPSK, the system

can achieve the diversity order of 2 when the statistical information of the relay-to-destination is fed back to the relay. For the more general case when higher-order rectangular QAM constellations are used, the diversity orders can be numerically obtained with the help of a derived upperbound on the system performance. The analytical results also show that the achieved diversity orders are robust to not only the feedback channel quality but also the accuracy of the quantization of the power scaling used at the relay.

- For AF, a fixed-gain multiple-relay system under Nakagami fading channels was examined in Chapter 6. A tight performance upperbound has been derived and its tightness was demonstrated over a wide range of channel settings. Along with the upperbound, a lowerbound was also presented. Based on the bounds, it was unfolded that the system can obtained the maximal diversity under Nakagami fading channels. A novel power allocation was then proposed by numerically minimizing the upperbound. Simulation results show that the proposed PA scheme significantly outperforms the equal PA scheme under various channel conditions as predicted by the upperbound.

7.2 Suggestions for Further Study

A large number of research areas on relay communications and related topics deserve to be investigated further. Following are some of the major important directions:

- As presented in Chapter 4, the Smart EGC scheme is proposed by incorporating EGC technique with DF to achieve the maximal diversity. In particular, the proposed system assumes that the phases of the received signals are available at the destination. In some situations, it may be preferable to bypass the channel estimation altogether [R50]. In such situations, wireless relay systems must rely on differential modulation techniques, e.g., differential phase shift keying (DPSK), or noncoherent detection techniques, e.g., envelop or square law detection of frequency shift keying (FSK) modulation. Thus, one of the

potential research direction is to design and investigate wireless relay systems with differential/noncoherent detection techniques. In particular, specific topics are:

  - Design DF relay systems with differential/noncoherent detection techniques when imperfect detection at the relays happens.
  - Design AF relay systems with differential/noncoherent detection techniques. Optimal power allocation scheme should also be found in order to improve the performance of the networks.

- In broadband wireless communications, multipath fading introduces frequency selectivity, resulting in inter-symbol interference that might severely degrade the system performance. To deal with inter-symbol interference, OFDM is a promising technique due to its low implementation complexity and high spectral efficiency. In a frequency-selective fading channel, there is an extra source of diversity, multipath diversity, that can be exploited to improve the performance of the system. The work in [R51] shows that the maximal multipath diversity can be achieved in an OFDM-based AF relaying system. However, the scheme only focuses on AF signal processing method at the relays. Unfortunately, AF requires expensive radio frequency chains to mitigate the existing coupling effects which is not preferable in some applications [R17]. Therefore, it is important to comprehensively study OFDM-based DF relay systems wherein decoding error at the relays is taken into account.

- In general, all of the relaying systems studied in this dissertation are repetition-based schemes, i.e., $(K+1)$ orthogonal channels are required to offer the spatial diversity order of $(K+1)$ for a system with K relays. To further improve the spectral efficiency, distributed space time coding could be used to provide diversity without a significant loss in spectral efficiency. A major challenge in distributed relay communications is to find a strategy to coordinate the relay transmissions. This approach is undesirable since it increases the system

complexity and degrades the performance in terms of transmission rate. In addition, in large-scale distributed relaying systems, the number of involved relays is unknown and random. To overcome this problem, several studies have been conducted [R11, R52, R53] for DF relaying systems, in which, the randomized space time coding (RSTC) is used to achieve diversity. It was shown that RSTC is capable to decentralize the relay transmission and yet obtains diversity and coding gains. To do so, RSTC must assume error-free detection at the relays. Obviously, it is an impractical assumption. Therefore, it is important to study applications of RSTC under imperfect detection at the relays.

A. Copyright Permission

This appendix documents the copyright holders' permissions to include the published/accepted papers in this dissertation.

A.1 Diversity Analysis of Smart Relaying over Nakagami and Hoyt Generalized Fading Channels - Chapter 3

Date: Thu, 25 Feb 2010 14:00:57 +0000

From: "Mitchell,Jade" <Jademitchell@theiet.org>

To: "nav730@mail.usask.ca" <nav730@mail.usask.ca>

Subject: RE: Decision on your Revised Paper - COM-2008-0354.R1

Dear Nam,

Many thanks for your email.

Permission to reproduce as requested is given, provided that the source of the material including the author, title, date, and publisher is acknowledged.

A reproduction fee is not due to the IET on this occasion as the original work was your own and it is for educational purposes.

Thank you for your enquiry. Please do not hesitate to contact me should you require any further information.

Kind Regards,

Jade.

Jade Mitchell

Editorial Assistant

The IET

——Original Message——

From: Nam Vien [mailto:nav730@mail.usask.ca]

Sent: 19 February 2010 20:24

To: iet_com

Cc: Nam Vien Hoai

Subject: Re: Decision on your Revised Paper - COM-2008-0354.R1

Dear Dr. Paul Rowley,

I am Nam Vien, the first author of the paper 'Diversity Analysis of Smart Relaying over Nakagami and Hoyt Generalized Fading Channels,' IET Commun., vol. 3, pp. 1778-1789, November 2009. I am writing my Ph.D. dissertation. Could you give me the permission to include this paper in my thesis? I will appreciate it very much.

Many thanks

Best regards,

Nam Vien

A.2 Diversity Analysis of Smart Relaying - Chapter 5

From: "Weihua Zhuang" <wzhuang@bbcr.uwaterloo.ca>

To: "Nam Vien" <nav730@mail.usask.ca>

Subject: RE: IEEE TVT - Final file submission confirmation for Paper VT-2008-00199.R1

Dear Nam,

The contents of the paper can be included in your thesis. But I do not suggest that you include the TVT paper (identical format) in the thesis as the IEEE owns the copyright of the paper.

Best wishes,

Weihua Zhuang

—Original Message—

From: Nam Vien [mailto:nav730@mail.usask.ca]

Sent: Friday, February 19, 2010 3:14 PM

To: ieeetvt@ecemail.uwaterloo.ca; wzhuang@uwaterloo.ca

Cc: Nam Vien Hoai

Subject: Re: IEEE TVT - Final file submission confirmation for Paper VT-2008-00199.R1

Dear Dr. Zhuang,

I am Nam Vien, the first author of the paper entitled "Diversity Analysis of Smart Relaying" /IEEE Trans. Veh. Technol./, vol. 58, pp. 2849-2862, July 2009. I am writing my Ph.D. dissertation. Could you give me the permission to include this paper in my thesis? I will appreciate it very much.

Many thanks

Best regards,

Nam Vien

A.3 Performance Analysis of Fixed-Gain Amplified-and-Forward Relaying with MRC - Chapter 6

From: "Weihua Zhuang" <wzhuang@bbcr.uwaterloo.ca<

To: "Nam Vien" <nav730@mail.usask.ca<

Subject: RE: IEEE TVT - Final file submission confirmation for Paper VT-2009-00590.R2

Dear Nam,

The contents of the paper can be included in your thesis. But I do not suggest that you include the TVT paper (identical format) in the thesis as the IEEE owns the copyright of the paper.

Best wishes,

Weihua Zhuang

—Original Message—

From: Nam Vien [mailto:nav730@mail.usask.ca]

Sent: Friday, February 19, 2010 3:13 PM

To: ieeetvt@ecemail.uwaterloo.ca; wzhuang@uwaterloo.ca

Cc: Nam Vien Hoai

Subject: Re: IEEE TVT - Final file submission confirmation for Paper VT-2009-00590.R2

Dear Dr. Zhuang,

I am Nam Vien, the first author of Paper VT-2009-00590.R2 entitled "Performance Analysis of Fixed-Gain Amplified-and-Forward Relaying with MRC" to appear in /IEEE Trans. Veh. Technol./. I am writing my Ph.D. dissertation. Could you give me the permission to include this paper in my thesis? I will appreciate it very much.

Many thanks

Best regards,

Nam Vien

References

[R1] T. Wang, G. Giannakis, and R. Wang, "Smart regenerative relays for link-adaptive cooperative communications," *IEEE Trans. Commun.*, vol. 56, pp. 1950–1960, Nov. 2008.

[R2] D. Tse and P. Viswanath, *Fundamentals of Wireless Communication*. Cambridge University Press, 2005.

[R3] J. G. Proakis, *Digital Communications*. McGraw-Hill, 4th ed., 2001.

[R4] A. Goldsmith, *Wireless Communications*. Cambridge University Press, 2005.

[R5] B. Vucetic and J. Yuan, *Space-Time Coding*. John Wiley & Sons, 2003.

[R6] H. Jafarkhani, *Space-Time Coding: Theory and Practice*. Cambridge University Press, 2005.

[R7] N. H. Vien, H. H. Nguyen, and T. Le-Ngoc, "Diversity analysis of smart relaying," *IEEE Trans. Veh. Technol.*, vol. 58, pp. 2849–2862, July 2009.

[R8] N. H. Vien, H. H. Nguyen, and T. Le-Ngoc, "Diversity analysis of smart relaying over Nakagami and Hoyt generalised fading channels," *IET Commun.*, vol. 3, pp. 1778–1789, November 2009.

[R9] R. U. Nabar, H. Bolcskei, and F. W. Kneubhler, "Fading relay channels: performance limits and space–time signal design," *IEEE J. Select. Areas in Commun.*, vol. 22, pp. 1099–1109, Aug. 2004.

[R10] J. N. Laneman and G. W. Wornell, "Distributed space–time–coded protocol for exploiting cooperative diversity," *IEEE Trans. Inform. Theory*, vol. 49, pp. 2415–2425, Oct. 2003.

[R11] B. Sirkeci-Mergen and A. Scaglione, "Randomized space-time coding for distributed cooperative communication," *IEEE Trans. Signal Process.*, vol. 55, pp. 5003–5017, Oct. 2007.

[R12] J. N. Laneman, G. W. Wornell, and D. Tse, "An efficient protocol for realiazing cooperative diversity in wireless networks," in *Proc. IEEE Int. Symp. Inform. Theory*, p. 294, June 2001.

[R13] A. Sendonaris, E. Erkip, and B. Aazhang, "User cooperation diversity – part 1: System description," *IEEE Trans. Commun.*, vol. 51, pp. 1927–1938, Nov. 2003.

[R14] A. Ribeiro, X. Cai, and G. Giannakis, "Symbol error probabilities for general cooperative links," *IEEE Trans. on Wireless Commun.*, vol. 4, pp. 1264–1273, May 2005.

[R15] Y. Li and S. Kishore, "Asymptotic analysis of amplify-and-forward relaying in Nakagami-fading environments," *IEEE Trans. on Wireless Commun.*, vol. 6, pp. 4256–4262, December 2007.

[R16] D. Chen and J. N. Laneman, "Modulation and demodulation for cooperative diversity in wireless systems," *IEEE Trans. on Wireless Commun.*, vol. 5, pp. 1785–1794, July 2006.

[R17] T. Wang, A. Cano, G. B. Giannakis, and J. N. Laneman, "High–performance cooperative demodulation with decode–and–forward relays," *IEEE Trans. Commun.*, vol. 55, pp. 1427–1438, July 2007.

[R18] J. C. H. Lin and A. Stefanov, "Coded cooperation for OFDM systems," in *Proc. IEEE Wireless Networks, Communications and Mobile Computing*, vol. 1, pp. 13–16, June 2005.

[R19] D. Michalopoulos and G. Karagiannidis, "Phy-layer fairness in amplify and forward cooperative diversity systems," *IEEE Trans. on Wireless Commun.*, vol. 7, no. 3, pp. 1073–1082, March 2008.

[R20] J. N. Laneman, *Cooperative Diversity in Wireless Network: Algorithms and Architectures*. PhD thesis, MIT, Cambridge, MA, 2002.

[R21] M. K. Simon and M.-S. Alouini, *Digital Communication over Fading Channels*. Wiley-IEEE Press, 2000.

[R22] L. S. Gradshteyn and L. M. Ryzhik, *Tables of Integrals, Series and Products*. Academic Press, 6th ed., 2000.

[R23] J. Boutros and E. Viterbo, "Signal space diversity: a power- and bandwidth-efficient diversity technique for the rayleigh fading channel," *IEEE Trans. Inform. Theory*, vol. 44, pp. 1453–1467, Jul 1998.

[R24] Z. Liu, G. B. Giannakis, S. Zhuo, and B. Muquet, "Space-time coding for broadband wireless communications," *Wireless Commun. and Mobile Computing*, vol. 1, pp. 35–53, Jan. 2001.

[R25] M. Schwartz, W. R. Bennett, and S. Stein, *Communication Systems and Techniques*. McGraw-Hill, 1966.

[R26] S. Alamouti, "A simple transmit diversity technique for wireless communications," *IEEE J. Select. Areas in Commun.*, vol. 16, pp. 1451–1458, Oct 1998.

[R27] V. Tarokh, N. Seshadri, and A. Calderbank, "Space-time codes for high data rate wireless communication: Performance criterion and code construction," *IEEE Trans. Inform. Theory*, vol. 44, pp. 744–765, Mar 1998.

[R28] V. Tarokh, H. Jafarkhani, and A. Calderbank, "Space-time block codes from orthogonal designs," *IEEE Trans. Inform. Theory*, vol. 45, pp. 1456–1467, Jul 1999.

[R29] N. Seshadri and J. Winters, "Two signaling schemes for improving the error performance of frequency-division-duplex (fdd) transmission systems using transmitter antenna diversity," *Proc. IEEE Veh. Technol. Conf.*, pp. 508–511, May 1993.

[R30] J. Winters, "The diversity gain of transmit diversity in wireless systems with Rayleigh fading," *IEEE Trans. Veh. Technol.*, vol. 47, pp. 119–123, Feb 1998.

[R31] D. Falconer, S. Ariyavisitakul, A. Benyamin-Seeyar, and B. Eidson, "Frequency domain equalization for single-carrier broadband wireless systems," *IEEE Commun. Mag.*, vol. 40, pp. 58–66, Apr 2002.

[R32] A. J. Viterbi, *CDMA: Principles of Spread Spectrum Communication*. Addison-Wesley Wireless Communications, 1995.

[R33] R. Pickholtz, D. Schilling, and L. Milstein, "Theory of spread-spectrum communications–a tutorial," *IEEE Trans. Commun.*, vol. 30, pp. 855–884, May 1982.

[R34] R. Chang, "Synthesis of band-limited orthogonal signals for multichannel data transmission," *Bell System Tech. J.*, vol. 45, pp. 1775–1796, 1966.

[R35] B. Saltzberg, "Performance of an efficient parallel data transmission system," *IEEE Trans. Commun. Technol.*, vol. 15, pp. 805–811, December 1967.

[R36] A. Bletsas, A. Khisti, D. Reed, and A. Lippman, "A simple cooperative diversity method based on network path selection," *IEEE J. Select. Areas in Commun.*, vol. 24, pp. 659–672, March 2006.

[R37] Y. Zhao, R. Adve, and T. Lim, "Improving amplify-and-forward relay networks: Optimal power allocation versus selection," *IEEE Trans. on Wireless Commun.*, vol. 6, pp. 3114–3123, August 2007.

[R38] Y. Jing and B. Hassibi, "Distributed space-time coding in wireless relay networks," *IEEE Trans. on Wireless Commun.*, vol. 5, pp. 3524–3536, December 2006.

[R39] Y. Jing and H. Jafarkhani, "Using orthogonal and quasi-orthogonal designs in wireless relay networks," *IEEE Trans. Inform. Theory*, vol. 53, pp. 4106–4118, Nov. 2007.

[R40] Z. Yi and I.-M. Kim, "Single-symbol ML decodable distributed STBCs for cooperative networks," *IEEE Trans. Inform. Theory*, vol. 53, pp. 2977–2985, Aug. 2007.

[R41] T. Himsoon, W. P. Siriwongpairat, W. Su, and K. J. R. Liu, "Differential modulation with threshold–based decision combining for cooperative communications," *IEEE Trans. Signal Process.*, vol. 55, pp. 3905–3923, July 2007.

[R42] F. Onat, A. Adinoyi, Y. Fan, H. Yanikomeroglu, J. Thompson, and I. Marsland, "Threshold selection for snr-based selective digital relaying in cooperative wireless networks," *IEEE Trans. on Wireless Commun.*, vol. 7, pp. 4226–4237, November 2008.

[R43] H. Mheidat and M. Uysal, "Impact of receive diversity on the performance of amplify-and-forward relaying under APS and IPS power constraints," *IEEE Commun. Letters*, vol. 10, pp. 468–470, June 2006.

[R44] H. Shin and J. Song, "MRC analysis of cooperative diversity with fixed-gain relays in Nakagami-m fading channels," *IEEE Trans. on Wireless Commun.*, vol. 7, pp. 2069–2074, June 2008.

[R45] G. Stuber, *Principles of Mobile Communication*. Kluwer Academic Publishers, 2nd ed., 2001.

[R46] R. Mallik and G. Karagiannidis, "Equal-gain combining with unequal energy constellations," *IEEE Trans. on Wireless Commun.*, vol. 6, pp. 1125 –1132, March 2007.

[R47] J. N. Laneman, D. N. C. Tse, and G. W. Wornell, "Cooperative diversity in the wireless networks: Efficient protocols and outage behavior," *IEEE Trans. Inform. Theory*, vol. 49, pp. 3062–3080, Dec. 2004.

[R48] A. Sendonaris, E. Erkip, and B. Aazhang, "User cooperation diversity – part 2: Implementation aspects and performance analysis," *IEEE Trans. Commun.*, vol. 51, pp. 1939–1948, Nov. 2003.

[R49] J. Adeane, M. R. D. Rodrigues, and I. J. Wassell, "Characterisation of the performance of cooperative networks in Ricean fading channels," in *Proc. of the Int. Conf. on Telecomm.*, (Cape Town, South Africa), May 2005.

[R50] T. Wang, Y. Yao, and G. Giannakis, "Non-coherent distributed space-time processing for multiuser cooperative transmissions," *IEEE Trans. on Wireless Commun.*, vol. 5, pp. 3339 –3343, december 2006.

[R51] H. Mheidat, M. Uysal, and N. Al-Dhahir, "Distributed space–time block coded OFDM for relay–assisted transmission," *IEEE Trans. Signal Process.*, vol. 55, pp. 1839–1852, May 2007.

[R52] B. Mergen and A. Scaglione, "Randomized space-time coding for distributed cooperative communication: Fractional diversity," *IEEE Int. Conf. on Acoustics, Speech and Signal Processing, 2006.*, vol. 4, May 2006.

[R53] S. Choi, J.-H. Park, and D.-J. Park, "Randomized cyclic delay code for cooperative communication systems," *IEEE Commun. Letters*, vol. 12, pp. 271–273, April 2008.